LIGHT TRANSMISSION AND SCATTERING BY RED BLOOD CELL SUSPENSIONS

Naomi M. Anderson
Department of Physiology

LIGHT TRANSMISSION AND SCATTERING PROPERTIES OF FLOWING SUSPENSIONS WITH PARTICULAR REFERENCE TO RED BLOOD CELLS

by

Naomi M. Anderson

A thesis submitted to the Faculty of Graduate Studies and Research in partial fulfilment of the requirements for the degree of Doctor of Philosophy

Department of Physiology
McGill University
Montreal, Quebec

March, 1966

ACKNOWLEDGMENTS

This project was carried out in the laboratories of the Joint Cardio-Respiratory Service of the Royal Victoria Hospital and the Montreal Children's Hospital under the direction of Dr. P. Sekelj, to whom I wish to express my thanks and appreciation. I am also indebted to Dr. M. McGregor for his continued interest and encouragement, and to Dr. D. V. Bates whose encouragement initiated this project.

I wish to extend my thanks to Mr. L. D. Pengelly for his many valuable suggestions and for designing some of the equipment used in this study. I am grateful for technical assistance to Miss J. Doman who performed the Van Slyke analyses and to Mr. L. S. Bartlett who prepared some of the illustrations.

I wish to acknowledge assistance from the Electronics and Mechanical Workshop, and the Biophysics Laboratory of the Montreal Children's Hospital, and from the Radiation Laboratory and the Electrical Engineering Department of McGill University for the construction of equipment used in this study.

Financial support was received from grants from the John A. Hartford Foundation and the Medical Research Council of Canada (MT 1241).

CONTENTS

NOMENCLATURE

I light intensity

I_o incident light intensity

λ wavelength, in Angstroms (A)

D particle diameter

r particle radius

m refractive index

N number of particles per milliliter

c concentration, in millimoles per liter (mM/l)

c_1 relative concentration of oxygenated hemoglobin (except in Chapter VIII where c_1 is an empirical constant)

c_2 relative concentration of reduced hemoglobin (except in Chapter VIII where c_2 is an empirical constant)

ϵ_{mM}^{cm} extinction coefficient (d = 1 cm, c = 1 mM)

ϵ_1 extinction coefficient for hemoglobin at a differential wavelength

ϵ_2 extinction coefficient for hemoglobin at an isobestic wavelength

ϵ_o extinction coefficient for oxygenated hemoglobin

ϵ_r extinction coefficient for reduced hemoglobin (except in Chapter X where ϵ_r is the extinction coefficient for melanin in the red spectral band)

ϵ_{ir} extinction coefficient for melanin in the infrared spectral band

OD optical density = $\log (I_o/I)$

OD_x optical density of blood of unknown oxygen saturation

$OD_{100\%}$ optical density of fully oxygenated blood

a empirical constant in equation 4.2

b empirical constant in equation 4.2 (in Chapter VII, b also refers to a length factor of a scattering particle)

a_1, b_1 empirical constants of equation 4.2 for oxygenated nonhemolyzed blood at a differential wavelength

a_2, b_2 empirical constants of equation 4.2 for reduced nonhemolyzed blood at a differential wavelength

a_3, b_3 empirical constants of equation 4.2 for nonhemolyzed blood at an isobestic wavelength

ς particle density, or number of scatterers per unit volume

σ total attenuation cross section for one scatterer

σ_a absorption cross section for one scatterer

σ_s scattering cross section for one scatterer

$q(\delta)$ fraction of the total scattering cross section of one scatterer in free space received by the detector

H fractional volume occupied by scattering particles

T_1 transmittance in the red spectral region = I/I_o

T_2 transmittance in the infrared spectral region = I/I_o

R reflectance (except in Chapter X where R is the light transmittance of the "bloodless ear" in the red spectral band)

IR light transmittance of the"bloodless ear" in the infrared spectral band

d sample depth

I. INTRODUCTION

For many years, measurements of the light transmitted by thin films of nonhemolyzed whole blood have been used for estimating oxygen saturation. More recently, reflectance measurements of thick layers of nonhemolyzed blood have been used for the same purpose. The lack of precision of these empirical techniques suggested to us that more basic work was required to investigate the light scattering and absorbing properties of nonhemolyzed blood.

Spectral analyses of dilute hemoglobin solutions have been performed since 1862 and concentrated hemoglobin solutions have been studied since 1933. These studies have repeatedly demonstrated that Beer's law is obeyed by hemoglobin solutions and by hemolyzed blood.

Fundamental studies to investigate the scattering properties of nonhemolyzed red blood cells have been few. Empirical observations have shown that light transmission by nonhemolyzed blood deviates from Beer's law. However, the theoretical nature of the absorption and scattering of light by nonhemolyzed blood has not been elucidated.

The investigation of the scattering and absorbing properties of nonhemolyzed blood has been hindered by the inability of conventional measuring techniques to yield

absolute measurements in the study of scattering materials. It is known that the geometrical arrangement of the spectrophotometric system used to measure light transmission or reflection influences to a large extent the measured value. Other factors influencing optical density are cell or particle size and relative refractive index. The extent of the dependence of optical density on these factors has not been adequately demonstrated.

Using both conventional spectrophotometric techniques, and techniques designed to integrate the scattered light, we sought to clarify the nature of the relationship of optical density to particle concentration, sample depth, and pigment changes, and to demonstrate the dependence of optical density values on the geometry of the measuring system. Our chief aim was to study the light absorbing and scattering properties of undiluted nonhemolyzed blood with the hope of explaining these properties in terms of a light scattering theory. An understanding of the basic absorbing and scattering properties of blood might provide a basis for a precise technique for estimating oxygen saturation, or would serve to explain the lack of reliability of present oximetric techniques.

In addition to experiments on red blood cells, the present study includes observations on both absorbing and

nonabsorbing emulsions, and on dyes in the presence of light scattering particles - red blood cells and nonabsorbing emulsified particles.

II. HISTORICAL REVIEW

A. Spectrophotometry

The practice of photometry was founded by Bouguer. His publication in 1729, "Essai d'optique sur la gradation de la lumière," contains a description of the first photometer, an instrument for comparing the luminous intensities of two sources of light using the eye as a null indicator (18). Bouguer realized that the eye is an adequate instrument for making comparisons but cannot be used as a meter for making quantitative measurements. Bouguer's instrument depended on the comparison of the brightness of the two halves of a surface which were respectively illuminated by the two sources to be compared. By varying the distances of the sources from the screen the two halves were made to appear equally bright. He obtained the ratio of the intensities of the two sources by employing a law first clearly enunciated by Kepler - the law of inverse squares.

In the "Essai" Bouguer also showed that the change in the intensity of a collimated beam passing through various thicknesses of a homogeneous absorbing material is an exponential function of its path length in the medium.

If dx represents an infinitesimal thickness of a layer of a homogeneous absorbing medium, I represents the inten-

sity at any point of the path, and α represents the fraction by which absorption reduces the intensity in unit length of path, then

$$dI/dx = - \alpha I \qquad 2.1$$

Equation 2.1 is integrated over the total thickness.

$$\int_{I_o}^{I_x} (dI/I) = - \alpha \int_0^x dx \qquad 2.2$$

If I_o is the incident intensity and I_x is the transmitted intensity through thickness x, then

$$\ln (I_x/I_o) = - \alpha x \qquad 2.3$$

Equation 2.3 may be expressed in the exponential form

$$I_x = I_o e^{-\alpha x} \qquad 2.4$$

where α is a constant, usually referred to as the absorption coefficient.

Lambert (138) arrived at the law independently at a later date. Consequently, it is sometimes referred to as the Bouguer-Lambert law. Middleton (19), in the introduction to his translation of Bouguer's "Traité d'optique," credits Lambert with performing the "essential service of developing a system of photometric units and setting down the laws of photometry."

In 1851, Beer (14) demonstrated that for a given sample thickness light transmission was an exponential function of the concentration of the absorbing substance in a solution - that is, the absorption coefficient introduced by Bouguer and by Lambert was directly proportional to concentration. Therefore,

$$\alpha = kc \qquad 2.5$$

where k is a constant depending upon the nature of the absorbing material per unit concentration at a specified wavelength, and c is the concentration. Substitution of equation 2.5 into equation 2.3 gives the expression commonly referred to as "Beer's law:"

$$\ln (I_x/I_o) = -kcx \qquad 2.6$$

Beer's law applies only if monochromatic radiation is used. This law is strictly true only for the intensity of individual frequencies within a beam of light, but it will be invalid for the total intensity of a band of frequencies.

In 1519 Leonardo da Vinci used colored glasses in the study of his paints - an early example of the separation of light into bands of wavelengths to study absorbing species (240). Newton (173), in 1666, separated sunlight into a ten inch continuous spectrum using a prism and a lens. A

spectrum is defined as the ordered arrangement of radiation according to wavelengths. Spectral lines - which are images of a narrow slit, each of which contains light of a very narrow band of frequencies - were first observed independently by Wollaston (248) in 1802 and by Fraunhofer (68) in 1814.

There is no single device which is capable of separating the entire electromagnetic spectrum into its component wavelengths, nor is any single receiver capable of detecting every region of the spectrum. The term spectroscopy usually implies the range of electromagnetic waves which can be dispersed into individual components by means of prisms, optical gratings or optical interferometers. The first practical application of the prism and the diffraction grating have been credited to Newton and to Fraunhofer, respectively (88). In 1859, Bunsen and Kirchoff (26) developed a practical instrument for producing a spectrum.

The range of wavelengths used in spectroscopy has been subdivided into various regions. Fig. 2.1 shows individual spectral regions, means of dispersion, and detectors used in the subdivisions.

Since the eye is an excellent detector of wavelengths from 4000 A to 7500 A, the first region studied was the visible. The infrared region was first described in 1800 by

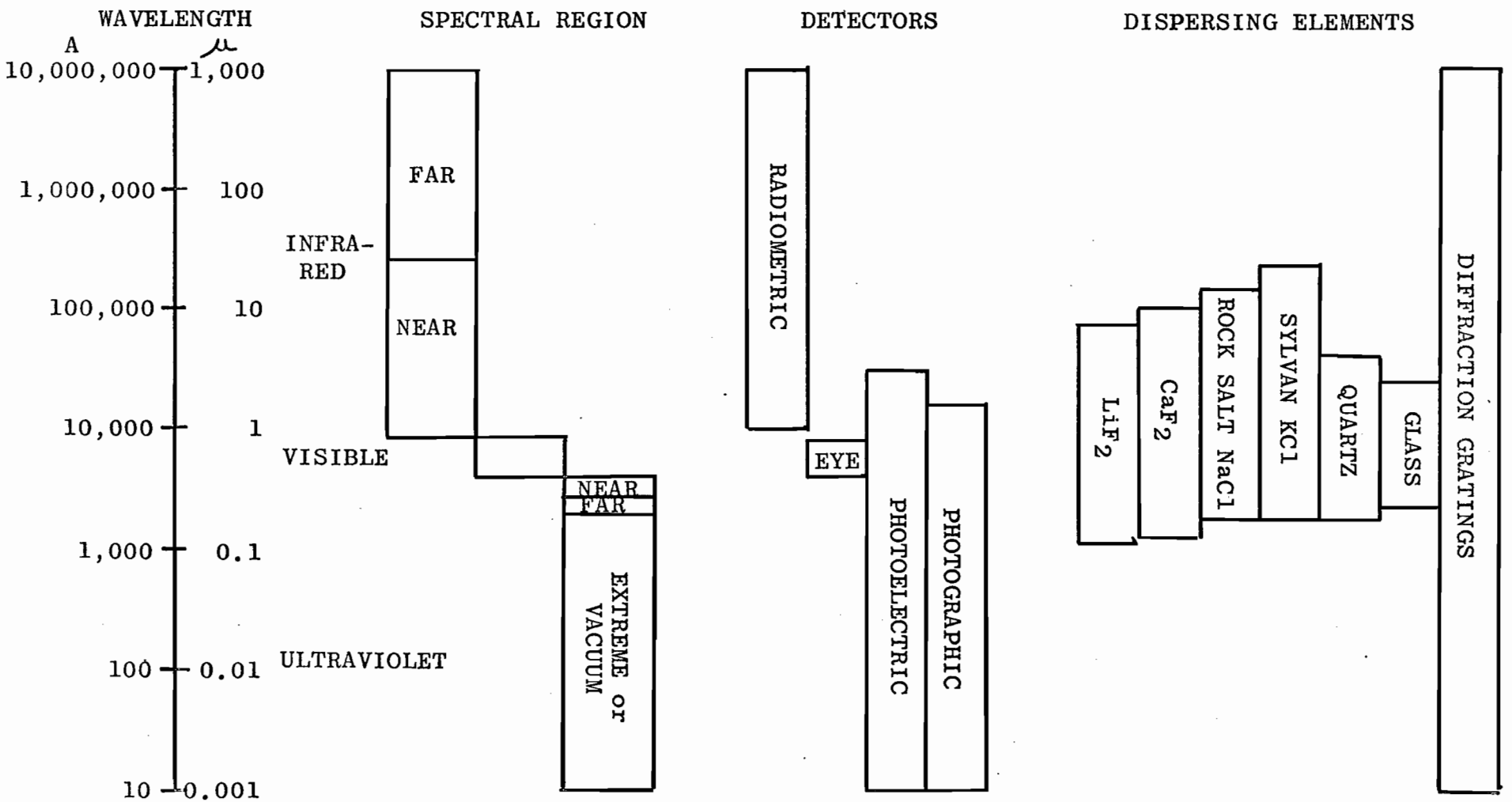

Fig. 2.1. Subdivision of the electromagnetic spectrum into regions used in spectroscopy; wavelength limits of detectors and dispersing elements used in the various spectral regions.

Herschel (95) who used a thermometer to measure the heating power of the various colors in the spectrum of sunlight. In 1801, Ritter (188) made measurements in the ultraviolet by studying the relative efficiencies of rays in different portions of the spectrum in blackening silver chloride.

Bouguer's method, in which the eye is used as the detector, is called subjective photometry. By contrast, the utilization of physical detectors such as radiometers, photoelectric cells, or photographic plates characterizes objective photometry. Strictly speaking, the term photometry should be applied only to the visible region of the spectrum, 4000 A to 7500 A, that is, light. Light was defined by Crittenden (43) in 1923 as "radiant energy evaluated in porportion to its ability to stimulate our sense of sight." The infrared and ultraviolet radiations are properly referred to as sources of radiant energy. Radiometric and photometric units are related numerically by a quantity "K," the "luminosity" or "luminous efficiency" of the radiation involved. K is measured in lumens per watt. Radiometric and photometric units have been compiled by Middleton (162).

B. Spectrophotometry of Hemoglobin Solutions

The first spectral analysis of the pigment hemoglobin was a qualitative study by Hoppe-Seyler (101) in 1862. He

described the absorption bands of oxyhemoglobin at 5750 A and 5400 A (the alpha and beta absorption bands) in the visible region. Vierordt (239), in 1876, carried out quantitative measurements of the absorption of hemoglobin throughout the visible spectrum. Hari (87) has provided a comprehensive survey of the many papers published between 1879 and 1917.

The spectrophotometric constant used by the early workers was introduced by Vierordt (238). The expression was derived from Beer's law and referred to as the "absorption ratio" or "absorption constant," A:

$$A = (c/O.D.) \qquad 2.7$$

where c represents the concentration of hemoglobin in grams per milliliter, and optical density is referred to as O.D.

Drabkin (49) introduced the notation $\epsilon^{cm}_{mM} = (O.D.)/(cd)$ where ϵ^{cm}_{mM} is called the extinction coefficient, c is the concentration in millimoles per liter, d is the sample depth in cm, and O.D. is the optical density using 10 rather than e as the base of the logarithm. Table 2.1 shows extinction coefficients for oxyhemoglobin determined over the period from 1879 to 1943. Since the spectrophotometric constants of the earlier workers were expressed in terms of absorption ratios, it was necessary to convert these into extinction

TABLE 2.1. Extinction coefficients for oxygenated hemoglobin

Author	Year	Wavelength (A)	ϵ^{cm}_{mM}	Wavelength (A)	ϵ^{cm}_{mM}
Hüfner (104)	1879	5380-5470	15.32	5530-5670	11.52
von Noorden (178)	1880	5350-5470	16.70	5530-5670	12.65
Otto (179)	1882	5350-5470	16.53	5530-5670	12.46
	1883	5350-5470	11.93	5530-5670	8.80
	1885	5350-5470	11.93	5530-5670	8.88
	1885	5350-5470	15.46	5530-5670	11.60
Krüger (136)	1888	5360-5530	12.85	. .	. .
	1890	5360-5530	13.05	. .	. .
Cherbuliez (38)	1890	5360-5410	12.59	5530-5580	8.19
Hüfner (105)	1894	5320-5420	12.75	5540-5650	8.07
de Saint Martin (195)	1898	5380-5490	12.56	5570-5680	7.76
Aron and Müller (6)	1906	5340-5460	11.44	5570-5690	8.35
		5340-5460	13.36	5570-5690	8.88
Bardachzi (10)	1906	5320-5420	12.52	5540-5650	7.98
Butterfield (31)	1909	5340-5420	14.15	5560-5650	8.93
Letsche (143)	1911	5340-5420	12.65	5560-5640	8.03
Butterfield (33)	1913	5460	13.36	. .	. .
Hari (87)	1917	5330-5420	14.30	5560-5660	8.86
Newcomer (172)	1919	5390-5430	14.65	5580-5620	8.93
Welker (245)	1920	5340-5420	14.16	5530-5570	9.02
Kennedy (122)	1926	5400	14.35	5600	8.77
Drabkin (48)	1932	5400	15.18	5600	9.60
(49)	1935	5400	15.29	5600	9.43
Horecker (102)	1943	5400	15.00	5600	8.87

coefficients in order to make a valid comparison. The early measurements show considerable variation due to wide spectral bands and inadequate instrumentation.

Until the work of Newcomer (172), the studies on hemoglobin suffered from the disadvantage that crystalline hemoglobin was used for the determinations. Concentration was established by dissolving weighed amounts of crystals in known volumes of water. As Kennedy pointed out (122), the method was inherently inaccurate due to the unknown water content of the crystals. Hüfner (105) and Butterfield (31, 33) checked hemoglobin concentration concentration by measuring carbon monoxide capacity; Butterfield also established the hemoglobin concentration on the basis of iron analyses.

The development of precise gasometric techniques led to the use of the oxygen capacity technique of Van Slyke (234) for establishing hemoglobin concentration much more accurately. The first study employing oxygen capacity measurements was made by Newcomer (172), in 1919. However, the accuracy of this study is doubtful since his optical density measurements were made using a quartz spectrograph with very low dispersion. In 1926, Kennedy, using a Bausch and Lomb spectrophotometer of the König-Martens type, made the first study using precise instrumentation and accurate determinations of hemoglobin concentration based on oxygen capacity

measurements (122).

All the studies mentioned were performed using dilute hemoglobin solutions. It was not until Kramer's study in 1933 (127) and Drabkin's study in 1935 (50) that Beer's law was validated for concentrated hemoglobin solutions. Drabkin used hemolyzed, undiluted, whole blood and crystallized hemoglobin solutions in concentrations as high as those found in red blood cells. The study also validated the assumption that hemoglobin forms a pure solution rather than molecular aggregates. Drabkin and his associates (7, 48, 49) made precise determinations of the extinction coefficients of oxyhemoglobin, as well as various hemoglobin derivatives for the entire visible region of the spectrum.

The first investigator to study the absorption spectrum of hemoglobin in the ultraviolet was Soret (214). In 1878, using a fluorescing eyepiece, he observed a highly absorbing band (which has been named after him) in the ultraviolet, centered at 4300 A. Gamgee (70) continued this investigation in 1895. In 1964, Benesch, Benesch, and Macduff (15) made a thorough investigation of the absorption of reduced hemoglobin in the Soret region and found that former values obtained had been in error due to the presence of methemoglobin.

The absorption characteristics in the near infrared were not studied until 1914 when Hartridge and Hill (92) showed

qualitatively that there was an oxyhemoglobin band in this region. Merkelbach (160), in 1935, showed that oxyhemoglobin had a broad absorption band with a maximum around 9100 A. Carboxyhemoglobin had practically no absorption in the infrared. Sidwell et al (208), in 1938, described the near infrared up to 7700 A and reported an absorption band for reduced hemoglobin at 7550 A. In 1943, Horecker (102) extended the study of hemoglobin in the near infrared up to 10000 A. Horecker pointed out that the question of the presence of impurities had been neglected in previous studies. He compared the extinction coefficients for oxyhemoglobin, reduced hemoglobin, carboxyhemoglobin, methemoglobin, and cyanmethemoglobin, obtained from whole hemolyzed blood with those obtained from solutions of pure hemoglobin. He found no differences in the visible region and concluded that other blood constituents make a negligible contribution to the light absorption of hemolyzed whole blood in this region.

A point which was of interest to several workers was the question of the identity of extinction coefficients for different mammalian species. Reichert and Brown (187) in 1909, Barcroft (9) in 1928, and Winegarden and Borsook (246) in 1933 showed that interspecies differences existed. However, Drabkin and colleagues (48) as well as Horecker (102) could not demonstrate species differences.

The effect of pH on the extinction coefficient of hemoglobin and its derivatives was studied by Drabkin (7, 48), who showed that only that of methemoglobin depended on pH.

C. Measurement of Oxygen Saturation

1. Hemolyzed Blood

The observation that various hemoglobin derivatives exhibit different absorption spectra led to the development of methods for quantitating the individual components in a single solution containing a mixture of two or more pigments. The major problem to which the spectrophotometric technique was first applied was the determination of the oxygen saturation of blood. Until the introduction of spectrophotometric techniques, the standard method of measuring oxygen content and capacity was the manometric technique of Van Slyke and Neill (237).

The analysis of blood for oxygen saturation by optical means was pursued simultaneously along the following lines: in vitro studies on hemolyzed blood and on nonhemolyzed blood; in vivo studies based on transillumination of or reflection from living, perfused tissue.

Bürker in 1911 (28) and Hartridge in 1912 (91) described an instrument called a "microspectroscopic comparator" for measuring the oxygen saturation of hemoglobin solutions.

This instrument was used by Krogh and Leitch in 1919 (135) to study the hemoglobin dissociation in fish blood at low temperatures, and again by Hall in 1934 (80) and in 1939 (81) for measuring the oxygen saturation of human blood. In this technique colorimeter cups containing hemoglobin solutions of 0% and 100% oxygen saturation were arranged in series in the light path. The spectrum of hemoglobin representing any degree of oxygenation could be obtained by varying the relative depths of the solutions in the two cups. The ratio of the depths of the two hemoglobin solutions to one another was read on a vernier scale. A sample of unknown saturation was placed beside the reference samples and by matching the colors the degree of oxygen saturation could be determined. Comparison with the Van Slyke method showed a standard deviation of the differences of $\pm$1.3%, which, considering the rather simple technique, is remarkably good agreement.

A method bearing some resemblance to the microspectrocomparator technique was described by Millikan in 1933 (164). This was an empirical bichromatic technique using a mercury arc as a light source. A Wratten D filter transmitted the 4360 A line in the violet, and a yellow Wratten G filter transmitted the 5790 A, 5760 A, and 5460 A lines. A differential photocell measured directly the difference in the amount of light transmitted through the D and G filters.

Calibration lines for each hemoglobin concentration were obtained from readings on fully oxygenated and fully reduced hemoglobin. In addition to the limited accuracy yielded by this technique, it was also necessary to dilute the blood two hundred times.

A more direct and theoretically sound method for quantitating two or more components present simultaneously in a single solution was described by Vierordt in 1876 (239). The rationale of this method was the use of optical density ratios of mixtures of pigments at discrete wavelengths.

This concept led eventually to many useful techniques: the quantitation of extinction coefficients of hemoglobin derivatives which cannot be isolated, such as sulfhemoglobin; the analysis of blood for oxygenated hemoglobin; the quantitation of the concentration of indicator substances in blood used in the determination of cardiac output by dilution techniques.

a) <u>One Wavelength Methods for Estimating Oxygen Saturation</u>

Vierordt's method is based on the fact that if a solution obeys Beer's law and monochromatic light is used, the extinctions due to different pigments are additive.

Let ϵ_o = extinction coefficient of oxygenated hemoglobin

ϵ_r = extinction coefficient of reduced hemoglobin

c_1 = concentration of oxygenated hemoglobin

c_2 = concentration of reduced hemoglobin

c = total hemoglobin concentration = $c_1 + c_2$

Then

$$OD = (\epsilon_o c_1 + \epsilon_r c_2)d \qquad 2.8$$

and oxygen saturation may be expressed as

$$(c_1/c)(100) = \%O_2 \qquad 2.9$$

From equation 2.8 it can be shown that

$$\%O_2 = (c_1/c)(100) = \left[\frac{-OD}{c(\epsilon_r - \epsilon_o)d} + \frac{\epsilon_r}{(\epsilon_r - \epsilon_o)}\right](100) \qquad 2.10$$

Equation 2.10 shows that percent oxygen saturation is a linear function of optical density. The validity of this relationship was demonstrated by Kramer (128) in 1934, using hemolyzed blood with total hemoglobin concentrations up to 16 gm/100 ml, and a sample depth of 0.22 cm. Kramer's measurements were made in the red region of the spectrum using a Zeiss red filter. Further experiments in 1951 (131) demonstrated the same linear relationship between oxygen saturation and optical density in the near infrared.

Kramer (128) developed a method for determining oxygen saturation based on equation 2.10. In addition to the optical density of the hemolyzed blood sample, the total hemoglobin concentration must be determined. Kramer obtained

the total hemoglobin concentration from the optical density of a fully oxygenated sample.

Other one wavelength methods were described by Brinkman and Wildschut (21) and Jonxis (112, 113) between 1938 and 1943. These authors estimated total hemoglobin concentration by reducing the sample with sodium dithionite and measuring the optical density of the reduced sample.

In 1945, Drabkin (51) described a one wavelength method in which total hemoglobin concentration was estimated by conversion to cyanmethemoglobin (49). The standard deviation of the differences between Van Slyke and spectrophotometric analyses was $\pm 2.9\%$.

b) Two Wavelength Methods for Estimating Oxygen Saturation

From equation 2.8 the optical densities of a sample at two discrete wavelengths λ_1 and λ_2 may be expressed:

$$OD_{\lambda 1} = (\epsilon_{1o}c_1 + \epsilon_{1r}c_2)d \qquad 2.11$$

$$OD_{\lambda 2} = (\epsilon_{2o}c_1 + \epsilon_{2r}c_2)d \qquad 2.12$$

By combining equations 2.11 and 2.12, an equation for oxygen saturation is obtained which is independent of the total hemoglobin concentration.

$$\%O_2 = (c_1/c)(100) = \frac{\left[\epsilon_{2r}\left[\frac{OD_{\lambda 1}}{OD_{\lambda 2}}\right] - \epsilon_{1r}\right](100)}{(\epsilon_{2r} - \epsilon_{2o})\left[\frac{OD_{\lambda 1}}{OD_{\lambda 2}}\right] - (\epsilon_{1r} - \epsilon_{1o})} \qquad 2.13$$

Nahas and associates in 1949 (170) and in 1950 (167) improved the bichromatic technique by introducing the use of the isobestic point at 5050 A. They also designed a special cuvette with a very thin sample chamber (0.01 cm) for use on undiluted samples, which could be filled anaerobically.

Referring to equation 2.13, if one of the wavelengths is isobestic for oxygenated hemoglobin (that is, $\epsilon_{2o} = \epsilon_{2r} = \epsilon_2$), the relation is simplified and results in a linear equation.

$$\%O_2 = (c_1/c)(100) = \left[\frac{-\epsilon_2\left[\frac{OD_{\lambda 1}}{OD_{\lambda 2}}\right] + \epsilon_{1r}}{(\epsilon_{1r} - \epsilon_{1o})}\right](100) \qquad 2.14$$

Nahas (168) showed that this equation could be written in the form

$$\%O_2 = (c_1/c)(100) = \left\{\frac{\left[\frac{OD_1}{OD_2}\right]_r - \left[\frac{OD_1}{OD_2}\right]_x}{\left[\frac{OD_1}{OD_2}\right]_r - \left[\frac{OD_1}{OD_2}\right]_o}\right\}(100) \qquad 2.15$$

where $(OD_1/OD_2)_o$ is the ratio of optical densities at 6050 A and 5050 A when the blood has been completely oxygenated; $(OD_1/OD_2)_r$ is the same ratio when the blood has been totally reduced by the addition of sodium dithionite; and $(OD_1/OD_2)_x$ is the ratio for the sample of unknown saturation. Since $(OD_1/OD_2)_o$ and $(OD_1/OD_2)_r$ are equivalent to $(\epsilon_1/\epsilon_2)_o$ and $(\epsilon_1/\epsilon_2)_r$, they will not vary with hemoglobin concentration but will depend only on wavelength. Calibration of the method consists in establishing these ratios for a particular spectrophotometer. Analysis for oxygen saturation requires only that readings of optical density be made on the sample at the two wavelengths and the ratio of these readings is then substituted into equation 2.15.

c) Choice of Wavelengths

The very small sample depth provided by the special cuvette designed by Nahas was necessary because of the relatively high extinction coefficient for hemoglobin at 5050 A. Jonxis and Boeve (114) and Gordy and Drabkin (74) used the isobestic point at 8050 A, where the extinction coefficient is much lower than it is at 5050 A. At 8050 A thicker cuvettes with sample depths of about 0.1 cm can be used, and Nahas (169) modified the design of his anaerobic cuvette by changing the depth from 0.01 cm to 0.1 cm.

As to the choice of the differential wavelength, Gordy

and Drabkin (74) put forth arguments in favor of 6600 A. At this wavelength methemoglobin and reduced hemoglobin show the same extinction coefficients, so that errors introduced by the presence of the pigment methemoglobin are somewhat reduced. Falholt (59) and Johnston et al (111) have chosen slightly shorter wavelengths (6200 A to 6500 A) where the differences between light absorption by oxygenated and reduced hemoglobin are greater and the absorption spectra of these pigments are relatively flat. At wavelength regions where the extinction coefficients change very rapidly the wavelength setting becomes very critical (209) and highly monochromatic light is necessary.

The wavelength 8050 A is not isobestic for all forms of hemoglobin. At this wavelength the extinction coefficient of carboxyhemoglobin is one fifth of that of oxygenated or reduced hemoglobin, and for methemoglobin it is approximately twice that of oxygenated or reduced hemoglobin. If methemoglobin or carboxyhemoglobin are present in appreciable quantities, the optical density measured at 8050 A no longer represents the total pigment concentration. In normal blood the total amount of inactive pigment present was estimated to be 1.3% by Van Slyke et al (236) and 3% by Roughton, Darling, and Root (192). The amount of methemoglobin and ferrihemoglobin was found to be less than 0.5% of the total

pigment by Van Slyke and his associates (236). However, according to Drabkin and Schmidt (51), Comroe and Walker (41), and Dempsey and Wilson (46) the amount of inactive hemoglobin is negligible. Lambertsen, Bunce, Drabkin, and Schmidt (139) and Refsum (184) showed that in the case of heavy smokers there may be significant amounts of carboxy-hemoglobin.

In cases where a considerable level of carboxyhemoglobin or methemoglobin is suspected, a method described by Gordy and Drabkin (74) for determining the percent of oxyhemoglobin in the presence of either of these pigments is useful. Since the method is of extreme complexity, it is of limited value for routine determination.

The criteria for the choice of wavelengths may be summarized: (i) the extinction coefficients should be low enough that measurements may be made on undiluted blood (assuming thin sample chambers of either 0.01 cm or 0.1 cm), (ii) the extinction coefficients at the isobestic wavelength and at the differential wavelength should be of similar order of magnitude, (iii) wavelengths should be chosen from flat regions of the absorption spectra of oxygenated and reduced hemoglobin, (iv) it is advantageous, although not essential, to choose wavelengths at which abnormal pigments show the same extinction coefficients as reduced hemoglobin.

d) Modified One Wavelength Methods

An alternative approach to overcoming interference due to the presence of other pigments has been described (60, 96, 103). These are essentially one wavelength methods and their primary object is to measure arterio-venous differences in the oxygen content of simultaneously drawn arterial and mixed venous samples. A knowledge of the A-V difference is used in the estimation of cardiac output by means of the Fick principle. A-V difference is obtained from the difference in optical density between an arterial and a mixed venous sample. In the method described by Hickam and Frayser (96) and by Huckabee (103), calibration is accomplished by correlating the optical density difference between a venous and an arterial sample with the A-V difference determined simultaneously by Van Slyke analysis. Thus A-V difference is obtained from an empirically determined regression equation. The measurement of optical density difference is made by reading the optical density of the venous sample against the arterial sample as blank. Since the optical density differences are considerably less than the absolute values of the optical densities of the individual samples, the need for extremely small sample depths is eliminated. Hickam and Frayser used a 0.05 cm cuvette, and Huckabee used a 0.3 cm cuvette. In the technique of

Feinberg and Alma (60) the calibration is based on measurements of extinction coefficients for reduced and oxygenated blood in 0.1 cm cuvettes against water blanks.

e) Evaluation of Methods for Hemolyzed Blood

(1) A-V Difference

Table 2.2 shows that the A-V difference may be determined with a high degree of accuracy using the modified one wavelength techniques. Advantages cited by the authors (60, 96, 103) on the use of one wavelength only for this determination are: (i) when using the bichromatic technique, usually one of the wavelengths is outside the optimal range of the instrument, (ii) the wavelength setting need not be changed during one series, since total hemoglobin may be determined after the series of A-V differences in optical density has been measured, (iii) methemoglobin and other inactive forms of hemoglobin will be present in both venous and arterial samples in essentially the same quantities, since both samples are withdrawn simultaneously and the effect of the inactive pigments will be eliminated.

(2) Oxygen Content

Estimation of oxygen content requires an accurate determination of total hemoglobin concentration. The bichromatic techniques rely on the isobestic reading for this determination. Nahas' comparison with Van Slyke analyses

TABLE 2.2. A-V difference, one wavelength method for hemolyzed blood

Investigator	Spectro-photometer	Wavelength (A)	Sample Depth (cm)	Hemolyzing Agent	SDD[a] (vol %)
Hickam and Frayser (96) 1949	Beckman DU	6600	0.5	Neutral saponin	±0.2
Huckabee (103) 1955	Beckman DU	6600	0.3	Freezing and thawing	±0.1
Feinberg and Alma (60) 1960	Beckman DU	6550	0.1	Saponin	±0.6

[a] Standard deviation of the differences between one wavelength method and reference methods. SDD = $\left[1/(n-1)\sum(d-\bar{d})^2\right]^{\frac{1}{2}}$.

of total hemoglobin concentration showed a mean difference of 0.09 gm/100 ml, with a standard deviation of the differences of ±0.4 gm/100 ml (169). It might be argued that the one wavelength method is superior to the bichromatic technique for determining absolute values of oxygen content, since total pigment is measured by conversion to cyanmethemoglobin. The cyanmethemoglobin method is a more accurate technique for estimating total hemoglobin. However, the one wavelength method entails the use of sample depth. Error may be introduced due to variations in sample depth when assembling the very thin cuvettes required for undiluted blood.

(3) Oxygen Saturation

Although the one wavelength method for estimating A-V difference may be used for measuring oxygen saturation, the method offers no advantage. Since the measurement depends on only one optical density reading at the chosen wavelength, the results will be subject to the same errors as the bichromatic method. In addition, determinations of absolute values of oxygen saturation by this method introduces the factors of sample depth and total hemoglobin concentration. These factors play no part in the bichromatic method since ratios of optical density are always employed, and the effect of concentration and depth are eliminated. The two wavelength

technique offers the best solution to the problem of the spectrophotometric determination of oxygen saturation. Table 2.3 shows a summary of the results obtained in the various studies comparing the two wavelength spectrophotometric method with the reference method of Van Slyke and Neill. In many cases, a high degree of accuracy was achieved. However, the results in general show a tendency for values of oxygen saturation obtained by the spectrophotometric technique to be slightly higher than those from simultaneous Van Slyke determinations (51, 74, 124, 139, 169, 184). Several authors have attempted to explain this discrepancy on the basis of inaccurate corrections for dissolved oxygen in Van Slyke determinations (59), or attributed it to the presence of inactive hemoglobin (100). However, it is improbable that these factors account entirely for this discrepancy.

f) Technical Factors

In order to reduce the error to a minimum, the refinement of measuring techniques has been dealt with in many studies.

One point of considerable importance is the efficiency of hemolyzing techniques. Several authors have found that after hemolysis there is a gradual reduction in oxygen saturation manifested by optical density changes (60, 99, 186,

TABLE 2.3. Oxygen saturation, two wavelength method for hemolyzed blood

Investigator	Year	Spectro-photometer	Wavelengths (A)	Sample Depth (cm)	Hemolyzing Agent	SDD[a] ($\%O_2$)
Nahas and Fowler (170)	1949	. .	6050, 5050	. .	Saponin	±2.2
Nahas (168)	1951	Beckman DU	6050, 5050	0.010	Saponin	±1.9
Roos and Rich (191)	1952	Beckman B	6000, 5050	0.100	Saponin pH 9.7	±1.5
Klungsøyr and Støa (124)	1954	Beckman DU	5580, 5750	0.007	Saponin	±0.4
Tsao et al (224)	1955	Beckman DU	5760, 5050	0.010	Saponin	±1.1
Jonxis and Boeve (114)	1956	Beckman	6800, 8050	0.100	Saponin	±1.3
Refsum and Sveinsson (186)	1956	Beckman DU	5760, 5600	0.007	Saponin	±1.2
				0.010	Saponin	±1.1
Refsum (184)	1957	Beckman DU	5760, 5600	0.007	Saponin	±1.0
			5760, 5060	0.007	Saponin	±1.3
			5600, 5060	0.007	Saponin	±1.3
Gordy and Drabkin (74)	1957	Beckman DU	6680, 8050	0.100	Saponin	±3.6
					Saponin	±3.4
					Saponin	±3.2
					Triton X100	±0.9

TABLE 2.3. Continued

Investigator	Year	Spectro-photometer	Wavelengths (A)	Sample Depth (cm)	Hemolyzing Agent	SDD ($\%O_2$)
Nahas (169)	1958	Beckman DU	6600, 8050	0.100	Saponin pH 7.4	$\pm$2.0 $\pm$1.7
Deibler et al (45)	1959	. .	6500, 8050	. .	Triton X100	$\pm$2.3
Holmgren and Pernow (100)	1959	Beckman B	4750, 5030	0.010	Saponin pH 7.0	$\pm$3.5 $\pm$2.1

[a] Standard deviation of the differences between spectrophotometric and Van Slyke techniques. SDD = $\left[1/(n-1)\ \sum(d - \bar{d})^2\right]^{\frac{1}{2}}$.

224). On the other hand, constant optical density values have been observed up to seven minutes (99), fifteen minutes (74), thirty minutes (59), forty minutes (96), and one hour (103).

Several authors have commented on the time required for hemolysis. Most think that hemolysis should take place in less than one minute (169, 186, 224). It has been suggested that if the mixing of saponin and blood is delayed, a protein precipitate may form at the interface of the blood and hypertonic saponin solution (224).

Saponin is the hemolyzing agent most commonly used. Some workers consider it advantageous to neutralize the acid pH of the saponin solution (96, 100, 169). Roos and Rich have varied the technique by using a highly alkaline saponin solution (pH 9.7) with the aim of shifting the oxyhemoglobin dissociation curve to the left, thus overcoming any tendency for the saturation to diminish during the analysis. This does not appear to present any advantage, since the sample must be diluted and the alkaline saponin solution must be evacuated in the Van Slyke apparatus. Triton X-100 has also been used as a hemolyzing agent (45). Its use is limited by its property of attacking lucite which is the most commonly used material for thin sample chambers. Another method of hemolysis - alternate freezing and thawing - avoids chemical

contamination (103, 209). The results of studies employing this technique do not indicate that the method is superior to the use of a chemical hemolyzing agent.

The technique of obtaining fully reduced samples of blood has been subject to some controversy. The usual method is to add sodium dithionite to blood at a concentration of approximately 10 mg/ml (59, 74, 168, 184, 224). Alternatively, Tsao (224) found it necessary to evacuate the blood sample in the Van Slyke apparatus in order to obtain a fully reduced sample and Feinberg and Alma (60) found that the results were slightly different when the evacuation method was used rather than the addition of a chemical reducing agent. According to Drabkin (51), normal blood may contain substances other than oxyhemoglobin which may combine with carbon monoxide after treatment with sodium dithionite, thus increasing the carbon monoxide combining capacity. In spite of this, Drabkin considers it a satisfactory reducing agent for calibrating the method of measuring oxygen saturation in hemolyzed blood.

Both lucite and glass cuvettes have been used, and comparison of the results does not indicate that either is superior for measuring oxygen saturation in hemolyzed blood.

Since the measurements are made on whole, hemolyzed blood, rigorous spectrophotometric technique requires that

the optical density readings made against distilled water as blank be corrected for the optical density of the plasma. This involves subtracting $\left[O.D._{plasma}(1\text{-hematocrit})\right]$ from the optical density of the whole hemolyzed blood. Except in blood with a very high lipid or bilirubin level, the optical density of plasma is negligible in comparison with that of hemolyzed blood and the added complication introduced by this correction is not justified (45).

It is difficult to estimate the relative importance of the variations in technique; however, it seems reasonable to assume that attention to detail without sacrificing efficiency and rapidity of analysis can only improve the results.

2. Nonhemolyzed Blood

While techniques for measuring oxygen saturation in hemolyzed blood were being developed and improved, methods for obtaining the same information in nonhemolyzed blood were receiving even more attention. The first methods were based on the transillumination of a layer of blood. Later, methods based on reflection of light were advanced.

The method of measurement of oxygen saturation in nonhemolyzed blood was investigated in view of its applications to (i) intact tissues, such as the pinna of the ear, (ii) exposed, unopened blood vessels, and (iii) in vitro measurements.

a) One Wavelength Transmission Methods

The first technique in which the oxygen saturation of nonhemolyzed blood was studied was that of Nicolai (175), who performed the measurement by transilluminating intact tissue. The first interdigital web of the hand was compressed with a metal ring clamp and the isolated tissue was transilluminated with light of wavelengths corresponding to the maximum absorption of hemoglobin in the visible region of the spectrum. Light transmission changes which occurred while the tissue was occluded were interpreted as a measure of the reduction time of oxyhemoglobin.

In 1935 Kramer (129) studied the absorbing properties of flowing nonhemolyzed blood in plane parallel glass cuvettes of different thicknesses. Using a Winkel-Zeiss monochromator, he studied the relationship between oxygen saturation and optical density at discrete wavelengths between 6000 A and 6800 A at sample depths varying from 0.06 to 0.24 cm. Optical density was correlated with manometric determinations of oxygen saturation. He showed that, at constant hemoglobin concentration, optical density is linearly related to oxygen saturation, as it is for hemolyzed blood (128). However, unlike hemolyzed blood, nonhemolyzed blood showed a nonlinear relationship between total hemoglobin concentration and optical density. The slope of each

line relating oxygen content to optical density varied with the hemoglobin concentration of nonhemolyzed blood, as opposed to the constancy of the slope for hemolyzed blood. These observations indicate that whole nonhemolyzed blood does not obey Beer's law. In addition, Kramer observed that the change in optical density resulting from a change from 0% to 100% oxygen saturation was much greater for nonhemolyzed blood than for hemolyzed blood of the same hemoglobin concentration.

Kramer applied the results of his studies to devise a method for measuring oxygen saturation continuously on blood diverted from opened blood vessels. A small unit which consisted of a flattened glass tube forming a sample chamber 0.1 to 0.2 cm thick, a small tungsten light source, a selenium photocell with maximum sensitivity at the red end of the spectrum, and a galvanometer, was used. No color filter was used, so that estimation of oxygen saturation was based on differences in light transmission of oxygenated and reduced hemoglobin over a broad spectral range of red and near infrared light. Calibration by manometric techniques or by Kramer's one wavelength photoelectric method for hemolyzed blood (128) was required for each hemoglobin concentration. He showed that the logarithm of the galvanometer deflection was a linear function of the oxygen content of the

blood, as estimated by the reference method.

The technique was also used on unopened vessels. The exposed vessel was placed between plane parallel plates and transilluminated by a water cooled source. Kramer claimed an extraordinary accuracy of ±1%. Both methods were used in several physiological studies involving exchange, transport, and utilization of oxygen (130, 133).

The one wavelength principle of Kramer was used by Drabkin and Schmidt in 1945 (51) for the continuous monitoring of changes in arterial saturation using a spectrophotometer. A 0.007 cm cuvette was introduced into the stream of one femoral artery in the dog. In order to determine absolute values of oxygen saturation, samples of blood were removed periodically for independent spectrophotometric analysis on hemolyzed samples.

A number of one wavelength methods for estimating the oxygen saturation of nonhemolyzed blood have been described. These methods required individual calibration for each hemoglobin concentration studied.

The method described by Sabiston and his associates (194) utilized a densitometer which was originally designed for the continuous determination of the concentration of Evans blue dye for measuring cardiac output (71). This instrument used an interference filter which provided monochromatic light.

The detector used was a photomultiplier tube. The relationship between optical density at 6300 A and oxygen saturation was shown to be linear for samples flowing through the cuvette at a constant velocity. Calibration was performed by comparing the results of Van Slyke analysis with the optical density of the blood. Statistical analysis of the results was not presented, but the authors stated that the maximum differences from Van Slyke analyses varied from 3% to 5% oxygen saturation.

In the one wavelength methods described by Handforth (84) and by Roddie, Shepperd and Whelan (189), transmittance measurements were made on stationary samples of nonhemolyzed blood. It was assumed that the relationship between optical density and oxygen saturation was linear although gelatin filters with wide transmission bands were used. The use of stationary samples and gelatin filters suggests that the accuracy of these methods would be very limited.

Hickam and Frayser in 1952 (97) presented a one wavelength method for estimating A-V differences in nonhemolyzed blood. The method is essentially the same as the method previously described for hemolyzed blood (96), that is, optical density differences between venous and arterial samples were related empirically to Van Slyke determinations of A-V differences in oxygen content. Measurements were made

on stationary samples. The authors observed that variable optical density readings were obtained for the first few seconds after blood was injected into the cuvette, due to the effect of sedimentation, but became constant and remained so after several minutes. The accuracy of the method appeared to be very good, although a separate regression line was required for hemoglobin concentrations below 5 gm/100 ml. The standard deviation of the differences between the spectrophotometric technique on nonhemolyzed blood and Van Slyke determinations of A-V differences was $^{+}$-0.4 volumes %. No results were presented on the accuracy of the method for determining oxygen saturation. Similar to the method for hemolyzed blood, measurement of total hemoglobin concentration for each sample is required.

b) Two Wavelength Transmission Methods

Concurrent with Kramer's work on nonhemolyzed blood, which began about 1935, Matthes (151) performed similar experiments with a photoelectric instrument, using red and green light transmitted through Zeiss filters to measure the oxygen saturation of nonhemolyzed blood flowing through a plane parallel glass sample chamber with a depth of 0.02 cm. He later substituted an infrared filter for the green filter because of the high optical density of blood and the relative

insensitivity of the photocells in the green region of the spectrum (153). He extended the method to measure carboxyhemoglobin in nonhemolyzed blood. This was possible because of the higher transmittance of carboxyhemoglobin in the near infrared which had been demonstrated earlier by Hartridge and Hill (92). The method was adapted for continuous measurements in opened blood vessels for estimating oxygen saturation (154) and carboxyhemoglobin (155).

The first instrument which made possible the estimation of absolute values of the oxygen saturation of nonhemolyzed blood was the bichromatic whole blood oximeter, introduced by Wood and his associates (76, 249). This technique is still employed routinely in many laboratories for clinical purposes. Light from a multiple incandescent source passes through a polyethylene tube, compressed to a lumen depth of 0.058 cm, to three selenium barrier-layer photocells. The outer cells are covered by two layers of Wratten 88A infrared gelatin filters, and the center cell is covered by a Wratten 29F red gelatin filter. The effective wavelength bands of this system extend from 7500 A to 9000 A and from 6000 A to 7500 A. Measurements are made on flowing samples. Calibration is performed empirically by relating the ratio of the optical density in the two spectral regions to oxygen saturation values obtained by Van Slyke analysis.

Although the validity of this method has been amply demonstrated in the case of hemolyzed blood, there is no theoretical justification for applying it to nonhemolyzed blood, which, as demonstrated by Kramer (129), does not obey Beer's law. The calibration curve relating the ratio of optical densities to oxygen saturation was not linear, particularly at high oxygen saturations. The authors suggested that the nonlinearity of the calibration might be due either to the failure of nonhemolyzed blood to obey Beer's law or to the use of gelatin filters which pass a wide band of wavelengths (249). States and Anderson (216) showed that wide band filter photometers yield a nonlinear relationship between concentration and optical density.

Wood compared his results with those obtained by the reference Van Slyke technique and by the spectrophotometric technique for hemolyzed blood using the Beckman spectrophotometer (251). As shown in Table 2.4, the error is of the same magnitude in both comparisons.

In 1956 Nilsson (176) presented a similar absolute reading whole blood oximeter using polyethylene tubing flattened to 0.05 cm and a Wratten 29F filter combined with two photocells of different spectral sensitivity. The resulting effective band widths were 6000 A to 7000 A and 7000 A to 10000 A, respectively. Nilsson states that the

TABLE 2.4. Oxygen saturation, two wavelength method for nonhemolyzed blood

Investigator	Year	Wavelengths (A)	Comparison	% O_2 Range	Hb Range (gm/100ml)	SDD[a] (%O_2)
Nilsson (176)	1956	6000-7000, 7000-10000	Oximeter vs Van Slyke	>90 >75 >50	. . . . . .	±2.0 ±4.4 ±7.7
Sekelj (202)	1957	6000-7500, 7500-9000	Oximeter vs Van Slyke	23-100	9.2-15.7	±1.9
		6500, 7500-9000	Oximeter vs Van Slyke	25-100	7.6-15.1	±1.8
Wood (251)	1960	6000-7500, 7500-9000	Oximeter vs Van Slyke	>90 <90	13-25.8 "	±1.9 ±2.8
			Oximeter vs hemolyzed method	>90 <90	" "	±1.7 ±3.0
Cornwall et al (42)	1963	6000-7500, 7500-9000	Oximeter vs hemolyzed method		. .	±2.2
Loewinger et al (145)	1964	6500, 8050	Oximeter vs Van Slyke	11-100	. .	±1.3

[a]Standard deviation of the differences = $\left[\frac{1}{n-1}\sum(x-\bar{x})^2\right]^{1/2}$

instrument has a linear calibration curve of optical density ratios versus Van Slyke analyses, in spite of the wide wavelength bands. However, the accuracy of the method at different levels of oxygen saturation does not support this claim. The standard deviation of the differences between oximetric and Van Slyke determinations at 90% oxygen saturation was $\pm$2%, at 75% it was $\pm$4.4%, and at 50% it was $\pm$7.7%.

In 1957 Sekelj (202) described a whole blood oximeter for obtaining absolute values of oxygen saturation. It was observed that measurements must be made on samples flowing above a limiting value, in order to obtain a high degree of repeatability. A plane parallel sample chamber was designed for flowing blood. Its sample depth was 0.07 cm. An incandescent light source diffused by a ground glass plate and selenium barrier-layer photocells covered with a Wratten 29 filter and three layers of Wratten 87 filters were used for the red and infrared regions, respectively. The resulting calibration curve was nonlinear, especially at high oxygen saturations. When an interference filter with peak transmission at 6500 A and half band width of 130 A was used in place of the Wratten 29 filter, a linear calibration curve was obtained between the ratio of optical densities and the results of Van Slyke analysis. The accuracy of the method was improved and calibration was simplified, since only a

few comparisons with the manometric technique were necessary in order to construct the calibration line. Results obtained with both systems were compared with Van Slyke analyses and are shown in Table 2.4.

Kay and Coxon (117) estimated oxygen saturation in nonhemolyzed blood using a glass cuvette inserted into the light path of a commercial ear oximeter, based on the design of Stott (219). Wide band filters were used and measurements were made on stationary samples. Accuracy was found to be ±8% of oxygen saturation.

Broch et al, in 1962 (23), presented a whole blood oximeter for measuring oxygen saturation. Gelatin filters were used. The method differed from the previously described techniques, which relate the ratio of optical densities to oxygen saturation obtained by manometric techniques. In this method the infrared light transmission of the blood was set at a predetermined value, and the sensitivity of the red circuit was adjusted accordingly. Estimation of oxygen saturation was then based on the difference between the light intensities transmitted by the blood in the two spectral regions. No theory was presented, and there appears to be no justification for the method. Comparison with spectrophotometric analyses on hemolyzed blood is presented graphically without statistical analysis. The accuracy appears

to be approximately $\pm$3%.

Cornwall, Marshall, and Boyes (42) described a method using wide band gelatin filters and cadmium sulphide cells. The method is based on a different treatment of the optical densities of nonhemolyzed blood in the red and infrared spectral regions. The theoretical discussion presented is based on Hulbert's theory (106), a form of radiative transfer theory which holds only for special boundary conditions.

Very recently, Loewinger, Gordon, Weinreb, and Gross (145) described an ingenious technique which appears to be theoretically sound and gives accurate results. The samples are centrifuged in microhematocrit tubes, and optical densities are read at 6500 A and at 8050 A on a Hilger Uvispec spectrophotometer. Since the cells are packed, the sample behaves essentially as a solution of hemoglobin of the same concentration as that present within the red blood cells. The results apparently justify this statement. The data is treated according to the method used for hemolyzed blood, that is, using Beer's law, which implies a unique linear relationship between the optical density ratios and oxygen saturation. Calibration is performed empirically by relating the optical density ratios to oxygen saturation values obtained by Van Slyke analysis. A comparison of results by this method and Van Slyke analysis is shown in Table 2.4.

In spite of the high degree of accuracy obtained by this technique, its usefulness is limited by the difficulty of collection and preparation of the sample and the prolonged time interval between sampling and measurement.

c) One Wavelength Reflection Methods

The development of oximetric techniques for measuring oxygen saturation has not been limited to transmission methods only. In 1949, Brinkman and Zijlstra (22) described a reflection oximeter, using light of about 7000 A. The blood was diluted with an equal volume of a hypertonic solution (2% NaCl, 0.3% Na salicylate, and 0.05% NaCN). The method was based on the assumption that the relationship between the amount of light reflected from a blood sample and the hemoglobin oxygen saturation was logarithmic. It was necessary to construct a calibration for each hemoglobin concentration, by measuring the reflection of an oxygenated sample and of a sample reduced by the addition of an equal volume of reducing solution (1% $Na_2S_2O_4$, 2% $Na_2B_4O_7$, and 0.3% Na salicylate).

A similar one wavelength system was developed by Refsum and Hisdal in 1958 (185). A Wratten 29 filter was used. These authors showed that the calibration line was different when the reflection value for completely reduced blood was obtained by extrapolation from points of higher saturation

than when sodium dithionite was used. In addition, it was assumed that different calibration lines for various hemoglobin concentrations were parallel. Once a family of calibration lines was constructed, the value of oxygen saturation could be read from the line corresponding to the actual value of the hemoglobin concentration. The accuracy of this method compared with a reference method showed a standard deviation of the differences of $\pm$1.4% oxygen saturation.

In 1953, Rodrigo (190) investigated the reflection method described by Brinkman and Zijlstra. His analysis was based on the light scattering theory of Schuster (199). This, like Hulbert's theory, is a particular case of radiative transfer. Rodrigo found that the relationship between the reflection of an infinitely thick, non-transmitting layer of blood and oxygen saturation was linear. He predicted this linearity from Schuster's theory by making simplifying assumptions. Rodrigo constructed a one wavelength instrument using an interference filter at 6500 A. The method required dilution and reduction solutions. He used the relation

$$R_\infty = 1/2p \qquad 2.16$$

where $p = (a/\beta s) + 1$, a is the absorption coefficient, s is the scattering coefficient, and β is the backward scatterred fraction of the total scattered light. R_∞ is the

reflection of an infinitely thick layer. When Rodrigo plotted the reciprocal of reflection against oxygen saturation, the relationship was indeed linear. Although the differences for blood of different hemoglobin concentrations were not large, he found it necessary to construct a calibration curve for each blood sample, in order to obtain adequate accuracy.

d) Two Wavelength Reflection Methods

Polanyi (181) applied the same principle used by Rodrigo to the construction of a bichromatic reflection oximeter. This was designed to be an absolute reading instrument not requiring individual calibration for each blood sample. Measurements were made using interference filters with peak transmissions at 6600 A and at 8050 A and cadmium sulphide photoconductors. The ratios of reflections at the two wavelengths are related to oxygen saturation values determined spectrophotometrically on hemolyzed blood. A single calibrating line is obtained and it is apparently independent of hemoglobin concentration. Polanyi et al (242) compared this technique to the spectrophotometric technique for hemolyzed blood and found that the standard deviation of the differences between the two methods was $\pm$1.4% oxygen saturation. They also compared the spectrophotometric technique for hemolyzed blood and the Van Slyke method. The

standard deviation of the differences was ±1.7%. These authors concluded that there was no significant difference in the standard deviation of the differences between Van Slyke, spectrophotometric, and reflection oximeter determinations of oxygen saturation.

The principle of the method described by Polanyi and his colleagues was applied by Enson et al (58) to the construction of an intravascular and intracardiac reflection oximeter for measuring oxygen saturation and for estimating dye concentration in blood. Light was focused on the end of a bundle of glass fibers contained within a Cournand arterial needle or within one lumen of a standard double lumen cardiac catheter. Light was transmitted through interference filters, with peak transmissions at 8050 A and 6600 A, alternately forty times per second. The filtered light was conducted to the blood, and the diffusely reflected light conducted back to a photomultiplier through a second group of fibers. The ratio of reflected intensities at the two wavelengths was again linear with oxygen saturation. The standard deviation of the differences between reflection oximeter readings and Van Slyke values was ±1.9% saturation.

In all reflection oximetry techniques a sample depth in excess of 0.3 cm is used, since it was observed empirically that measurements of oxygen saturation were much more

accurate if the layer of blood was thick enough to be opaque.

The results obtained with whole blood oximeters have shown that errors in oxygen saturation determinations may be considerable when the hemoglobin concentration is about 8 gm/100 ml or less (202). Hickam and Frayser (97) found that a separate calibration was required at low oxygen capacities. Enson and his colleagues found that the standard calibration of the intracardiac reflection oximeter was not accurate for blood samples with hematocrits less than 30%, and recommended that individual calibration curves be constructed for low hemoglobins. Similarly, Refsum and Hisdal (185) found that the calibration lines showed considerably more variation if the hemoglobin concentration was less than 12 gm/100 ml. These findings indicate that neither the theory advanced by Rodrigo (190) and Polanyi (181), nor that employed by Brinkman and Zijlstra (22) and Refsum and Sveinsson (185) is entirely adequate.

D. Light Transmittance, Scattering and Reflectance by Biological Materials

1. Transmittance

a) Oxygen Saturation and Hemoglobin Concentration

The study of the light transmittance of red blood cells begins essentially with Kramer's work in 1935 (129). The two main problems considered in his studies were: (i) the

variation of optical density with particle concentration and sample depth as parameters, (ii) the variation of optical density with changes in the extinction coefficient of the pigment, mediated by changing oxygen saturation at constant particle concentration and sample depth. Kramer's results showed that the relationships in the first case were non-linear, while the relationship between optical density and oxygen saturation was linear.

Sample depth was varied from 0.06 cm to 0.24 cm, concentration was increased up to 14.2 gm/100 ml, and wavelength was varied from 6000 A to 6800 A. Conventional spectrophotometric techniques were used. Extinction coefficients for nonhemolyzed blood were much higher than those for the same concentration of hemolyzed blood.

Kramer found that extinction coefficients for nonhemolyzed blood, calculated from Beer's law (ϵ_{mM}^{cm}) decreased as hemoglobin concentration increased. By varying sample depth, it was found that concentration and depth were not interchangeable as they are for solutions which obey Beer's law. In other words, equivalent variations in concentration and depth which did not change the number of red blood cells in the light path gave different values of optical density.

The relationship between optical density and oxygen content can be represented by a family of straight lines

with each line representing a different hemoglobin concentration. Beer's law predicts that these lines will be parallel for solutions. Kramer found that the lines for hemolyzed blood were indeed parallel. However, the lines for nonhemolyzed blood showed decreasing slopes with increasing hemoglobin concentration.

In 1939 Drabkin and Singer (52) studied the absorption and scattering of light by nonhemolyzed washed dog erythrocytes and suspensions of milk and cream fat particles dispersed in water and in hemoglobin solutions. Measurements were made at discrete wavelengths between 5000 A and 6300 A. The maximum and minimum extinction coefficients for oxyhemoglobin were at 5780 A (ϵ = 15.13) and at 6300 A (ϵ = 0.45), respectively. In the relationship between optical density and particle concentration their results were similar to Kramer's. The extinction coefficients of both red blood cell and fat particle suspensions decreased as particle concentration increased. Unlike Kramer, they found that concentration and depth were interchangeable. However, the experimental evidence to support this finding is limited to three observations only and the accuracy of these studies is not as high as those of Kramer.

Drabkin and Singer developed an empirical equation for determining the extinction coefficient of the absorbing

pigment from the total extinction (optical density) of the suspension. They found that the relationship between the total extinction and the pigment extinction for fat particles suspended in hemoglobin solutions could be expressed as

$$E_t = E_p + E_s \qquad 2.17$$

where E_t is the total extinction or optical density, $\log (I_o/I)$, E_p is the extinction due to the pigment hemoglobin, and E_s is the extinction due to scattering only. The empirical relationship was restated for red blood cells:

$$E_t = f_1 E_p + E_s \qquad 2.18$$

where $f_1 = \left[a(Nd)^n\right] / \left[1 + a(Nd)^n\right]$, $\log E_s = b + m\log(Nd)$, and a, b, m, and n are empirical constants. At particle concentrations greater than $3.6 \times 10^9/cm^3$ (which was equivalent to a hemoglobin concentration of 8.7 gm/100 ml) f_1 was approximately 1.0, and equation 2.18 reduced to equation 2.17.

E_s and f_1, the coefficient of E_p, were both empirical functions of N, the particle concentration. Drabkin and Singer pointed out that the use of conventional spectrophotometric techniques permitted the collection of only a very small fraction of the scattered light, and concluded that it was not possible to relate their findings to any theory of light scattering.

In 1951, Kramer, Elam, Saxton, and Elam (131) published a continuation of the investigation of the light scattering and absorbing properties of nonhemolyzed blood which Kramer had started in 1935 (129). In their study, they extended the wavelength range into the infrared. The object of the study was to measure quantitatively the transmittance of whole blood and to express the results as deviations from Beer's law. Their hypothesis was that light scattering lengthens the optical path, resulting in an increase in the absorption of light by the hemoglobin within the red blood cell, and that this would increase the difference between the extinction coefficients of reduced and oxygenated hemoglobin when these pigments are contained within the cell.

Absorption spectra from 6000 A to 11000 A were recorded on blood flowing under gravity, using conventional spectrophotometric techniques. They confirmed their previous results, that the relationship between oxygen content and optical density was linear, but the slope of the lines varied with hemoglobin concentration. Extinction coefficients for nonhemolyzed blood exceeded those of hemolyzed blood by factors of seven to twenty. The increase was greater when the corresponding extinction coefficient for hemolyzed blood was low. This can be attributed to the flattening effect obtained with conventional spectrophoto-

meters. The differences between the extinction coefficients for reduced and oxygenated blood were greatly increased, and these differences were found to be unique functions of hemoglobin concentration and sample depth.

Extinction coefficients were found to be inverse functions of both cell concentration and sample depth, and conconetration and depth were not interchangeable.

Kramer predicted that since extinction coefficients decreased as concentration increased, a densely packed mass of red cells would appear to have properties similar to those of a highly concentrated hemoglobin solution.

Kramer's work is the most thorough investigation into the light transmitting properties of nonhemolyzed blood which has appeared in the literature. But, it has two limitations. First, conventional spectrophotometric techniques rather than instrumentation designed to study light scattering were used. Second, the wavelength range was limited with respect to variation in the extinction coefficient of hemoglobin. Kramer's work was restricted to the red and near infrared regions of the spectrum. The maximum extinction coefficient for oxygenated hemoglobin in this range is 1.05 (at 6000 A). Only Drabkin and Singer studied oxyhemoglobin at highly absorbing wavelengths (between 5000 A and 6000 A).

b) Flow Effect

Many studies on the light transmittance of nonhemolyzed blood have shown that the optical density of flowing blood is different from that of stationary blood (97, 129, 180, 194, 202) and that optical density varies with flow rate. Kramer found that optical density decreased with increasing flow rate and became asymptotic at high rates of flow (129).

The flow effect has been the subject of several investigations but no definite conclusions have been reached by the authors concerned. Two main possibilities have been considered as explanations for this phenomenon. One is an orientation of the disc shaped red blood cells during flow. The other is streaming or axial accumulation of the red cells.

The problem was studied in capillary tubes by Taylor (221) and by Bayliss (13); it was studied in plane parallel cuvettes by Wever (244). Both Taylor and Bayliss measured the transmittance of the tube near the wall and at the center and found that more light was transmitted near the wall. This was considered to be evidence that axial accumulation takes place but did not provide any information concerning the orientation of the particles.

Bayliss and Wever both studied the problem of the orientation of the cells by adding lecithin to the blood, thus causing the cells to become spherical. In a plane

parallel sample chamber Wever found that optical density still changed with flow rate and concluded that axial accumulation was the pertinent factor. It is interesting to note that while the optical density of dog blood decreased with increasing flow, that of ox blood increased. Bayliss found that in human blood the flow effect was not significantly different whether the cells were discs or spheres, while the effect was present in dog blood only when the red cells were discs. Bayliss reached no definite conclusions concerning the cause of the flow effect.

c) Size and Shape of Red Blood Cells

It has been observed (142, 159) that alterations in red cell shape and size induced by osmotic pressure variations in the suspending media result in changes in the optical density of red cell suspensions. Sinclair and his colleagues (212) found that light transmission was reduced when cells were suspended in hypertonic media. Zijlstra (22) found that more light was reflected by red blood cells in hypertonic solutions. These phenomena are thought to be due to increased curvature of the cell surface, due to shrinkage.

Sinclair et al (212) studied the light transmission of canine blood recorded continuously from the femoral artery, and found that four breaths of 50% CO_2, after breathing 100% oxygen, resulted in a considerable increase in the light

transmission of the blood. Salmon, Stish, and Visscher (196) showed a similar increase in transmission with increasing carbon dioxide content. They demonstrated that an increase in carbon dioxide tension resulted in an increase in cell size. Similar observations had been made by Nasse in 1878 (171) and by Hamburger in 1892 (83). Meldahl and Ørskov (159) and Lefevre and Lefevre (142) found that light transmission was increased when red cell volume had increased, as shown by an increase in hematocrit. The evidence indicates that light transmission varies directly with cell size; an increase in cell size results in an increase in light transmission.

It may be concluded that the optical density of nonhemolyzed blood depends on a number of variables: the measuring system; sample depth; hemoglobin concentration; hematocrit; cell size and shape; the refractive index of the medium in which the cells are suspended.

d) Absorption Spectra of Red Blood Cell Suspensions

The question of the identity of hemoglobin within the red blood cell and in solution after lysis of the cell has been the subject of several studies. Observations of the absorption spectra of nonhemolyzed red blood cells by conventional spectrophotometric techniques had shown the Soret

band to be absent (3). The first explanation of this anomaly was the postulated existence of a stromatic hemoglobin compound within the red blood cell (2). In 1941, Keilin and Hartree (119) imitated a suspension of red blood cells by suspending droplets of concentrated oxyhemoglobin solution in oil. The mixture formed a suspension of very fine droplets of hemoglobin solution varying from 7 to 14 microns in diameter. Spectroscopic examination of the suspension showed that while the strength of the alpha and beta bands was at least eighty percent of that of the original solution, the Soret band had completely disappeared. On the other hand, a suspension of oil droplets dispersed in a dilute hemoglobin solution showed absorption bands of the same intensity as the corresponding bands in a pure solution of hemoglobin. They concluded that the failure to observe the Soret band was an optical phenomenon, but offered no explanation. Jope (115) showed that while a uniform suspension of red blood cells showed no Soret band, a very strong Soret band appeared if the red cells were allowed to settle under gravity. This phenomenon could now be interpreted in terms of the conclusions of Kramer (131) and of Loewinger (145), that a highly concentrated suspension assumes the optical characteristics of a solution.

Keilin and Hartree studied the absorption spectra of

red cell suspensions and other scattering materials using an entirely different approach. In 1939, they suspended colloidal heart muscle preparations in a medium with a refractive index high enough to match that of the cells (118). Similarly, Barer (11, 12) and his colleagues suspended intact red cells in bovine serum albumin. By matching the refractive index of the suspending medium to that of the cell, light scattering was greatly reduced. Barer referred to these suspensions as "clarified" cell suspensions. The results showed that a suspension of red blood cells in a 35% w/v protein solution was actually less cloudy than a lysed suspension containing the same amount of hemoglobin; the results also showed the alpha, beta, and Soret bands to be present.

2. Scattering

Latimer (140), working with scattering suspensions of chlorella, demonstrated the phenomenon of selective light scattering - that is, scattering on the long wavelength side of an absorption band due to the anomalous dispersion of the refractive index about the absorption band. Selective scattering can cause an apparent shift in the absorption maximum. The shift varies with the angle at which light is collected. It can be eliminated, to a great extent, by using the diffusing plate technique which will be

described in Chapter III.

Latimer suspended algal cells in media of different refractive indices. Optical density was measured first at selected angles, and then with diffusing plates attached to the sample and blank cells. The differences in optical density were very much reduced when diffusing plates were used, but were not completely eliminated.

Studies on scattering suspensions by Shibata et al (206, 207) and Latimer (140) have demonstrated that the diffusing plate method has two main advantages. First, the general level of optical density is reduced. Second, the detector receives a more representative sample of the light emerging from the scattering medium. The result of the second factor is that measurements of optical density are much less dependent on the geometry of the measuring system when diffused light rather than collimated light is used.

In 1961, MacRae, McClure, and Latimer (149) studied the single scattering properties of a single partial layer of orientated red blood cells. They derived an equation, similar to one which had been used by Lothian and Lewis (148) in their study of very dilute suspensions of red blood cells. The equation was developed in terms of large particle theory and allowed them to predict their results quantitatively.

3. Reflectance

In 1956 Kramer, Graf, and Overbeck (132) studied the reflection of light from nonhemolyzed blood in cuvettes and in intact tissues. They used a convergent lens, Wratten filters, and photocells separated from the sample by 2 cm. Sample depth ranged from 0.13 cm to 1.3 cm and hemoglobin concentration was varied up to 13.7 gm/100 ml. Measurements were made on fully oxygenated and fully reduced blood over a range of wavelengths from 5000 A to 10000 A. As sample depth was increased, reflection increased and became asymptotic. As concentration was increased, at constant sample depth, reflection increased, reached a maximum, and then decreased, showing a parabolic relationship to sample depth. Reflection scans of reduced and oxygenated blood were complementary to the corresponding absorption scans. In other words, regions of high transmittance also showed high reflectance.

Berzon and Schubert (16) repeated Kramer's experiments and demonstrated that reflectance values are highly dependent on the geometry of the measuring system.

With their intracardiac reflection oximeter, Enson and his colleagues (58) measured the reflectance of a layer of blood greater than 0.3 cm, at various hemoglobin concentrations. They showed a parabolic relationship between reflection and hematocrit which was similar to that shown by Kramer et al.

III. LIGHT SCATTERING

The failure of nonhemolyzed blood to obey Beer's law has been repeatedly demonstrated, and the cause has been attributed to the light scattering properties of red blood cells.

When a light ray encounters a particle whose refractive index differs from that of the surrounding medium, it is deviated from its rectilinear path. The intensity and angular distribution of the scattered light depend upon the size, shape, and orientation of the particle, its refractive index relative to that of the continuous phase, and the wavelength of the incident light. If the refractive index of the particle relative to that of the medium is complex, the particle will absorb part of the light.

A. Single Scattering

If, in a light scattering system, the particles are separated by distances sufficiently large to insure that each particle and the waves scattered from it are independent, and if there are no interference effects between scattered waves, and if the intensity scattered by N particles is N times the intensity scattered by one particle, then it is a single scattering system. An excellent survey of single scattering is given by Van de Hulst's book Light Scattering

by Small Particles.

A single scattering suspension obeys Beer's law of light transmission:

$$I = I_o e^{-C_{ext} N d} \qquad 3.1$$

N is the number of particles per milliliter, C_{ext} is the effective scattering surface area or the scattering cross section of a particle, and d is the depth of the sample.

Tables of light scattering coefficients have been published in the literature. The quantity usually listed is the ratio of the scattering surface area, or the scattering cross section of the particle to its geometrical cross section. This ratio is referred to variously as the efficiency factor, Q_{sca} (232), the total scattering coefficient, K (147), the scattering area ratio, K (162), or the scattering area coefficient, S (211).

Q_{sca} depends on several parameters: the ratio of the diameter of the particle, D, to the wavelength of the incident radiation in the suspending medium; the refractive index of the particle relative to that of the suspending medium; the shape of the particle and its orientation; the solid angles subtended by the beams of the incident and the measured radiation. Q_{sca} is usually expressed as a function of $x = \pi D/\lambda$. From Q_{sca} the intensity scattered at any

angle from the direction of incidence can be calculated.

In 1871, Rayleigh (183) derived complete analytic solutions for scattering by spherical and nonspherical particles much smaller than the wavelength of light.

For spherical particles of sizes comparable with the wavelength of light, a series solution of the Maxwell equations, describing the interaction of the particles with electromagnetic radiation, has been derived. This solution is generally referred to as the Mie theory (163). It has been pointed out (146) that although Mie published his theory in 1908, the formulas had been previously published by other authors as early as 1890.

Particles whose dimensions are large with respect to the wavelength of the incident radiation can be considered in terms of classical diffraction theory and geometrical scattering by external reflection and refraction (98). Such particles show a strong tendency to scatter light in the forward direction.

The red blood cell is a biconcave disc with a mean diameter of 8 microns. Its thickness at the center is about 1 micron and at the outer edge its thickness is about 2 microns. The index of refraction, as determined by MacRae, McClure, and Latimer (149) is 1.401. Relative to water ($m = 1.33$), its refractive index is 1.053. Due to their dimensions, red blood cells are strongly forward scattering,

and may be treated in terms of geometrical optics and classical diffraction theory.

B. Multiple Scattering

A system exhibits multiple scattering if each particle in the system is exposed to light scattered by other particles. Under these circumstances, the particles are excited not only by incident light but also by waves originating from other particles.

In a system in which the particles receive light which has been scattered by other particles there is no simple proportionality between the intensity of light scattered by the system and the number of particles present. This observation constitutes one of the tests proposed by Van de Hulst (232) for the existence of multiple scattering. The second test is a measure of the optical depth τ, where $I = I_o e^{-\tau}$. If τ is more than 0.1 but less than 0.3, then a correction for double scattering must be made. If τ is greater than 0.3, a multiple scattering theory is required.

In general, problems of multiple scattering fall into two categories: (i) those involving incoherent scattering only, and (ii) those in which coherent as well as incoherent effects must be considered. When the particles are separated by sufficient distances that the phase relations between the waves scattered by the particles are random,

the intensities of the waves may be added and the sum referred to as the "incoherent scattered intensity". If the particles are sufficiently close to one another, there will be phase coherence between the scattered waves. The interference between these waves must be considered in the computation of the scattered radiation. This scattered radiation is called the "coherent scattered intensity."

Several methods for treating scattering problems have been developed. The procedure chosen and the approximations involved are determined primarily by the relation between the wavelength and the average distance between particles. If the wavelength is very small compared to interparticle distance, coherence effects can be neglected, and a particle scattering theory can be used to treat the incoherent scattering. Another treatment for incoherent scattering consists in calculating scattering in successive orders, taking into account attenuation for each order, but neglecting interference. When particle separation and wavelength become comparable, interference must be considered and a wave treatment is necessary.

Van de Hulst (232) estimated that the particles must be separated by 1.5 diameters to insure a lack of coherence phenomena. Churchill, Clark, and Sliepcevich (40) studied the effect of particle separation by measuring the transmis-

sion of dense dispersions of spherical particles 1.2 and 0.8 microns in diameter, at various concentrations. They found that interference effects became noticeable when the distance between the centers of adjacent particles was 1.7 diameters.

1. Incoherent Scattering

a) Radiative Transfer Approach

The problem of multiple, incoherent scattering has received a great deal of attention, particularly in the study of the transmission of stellar radiation or the propagation of light through turbid media, such as fogs and stellar atmospheres in which the center-to-center distance between particles is about 100 diameters (233).

The relatively simple radiative transfer approach to the problem of incoherent, multiple scattering is based on the Boltzmann integro-differential equation for transport processes - the classical theory for the multiple scattering of particles by a random distribution of scatterers. The application of this equation to light is an approximation in which the light rays are considered as the trajectories of particles, which are then treated in terms of classical particle mechanics. In other words, it is a "ray" treatment of a "wave" problem.

Although less complex than a wave treatment, the

radiative transfer approach to the multiple scattering of light rays still presents enormous mathematical difficulties. The integro-differential equations must be solved by iterative procedures on electronic computers.

The essence of the integro-differential equation of transport is:

[the net rate of change of the intensity in the light path] = - [the rate of decrease in intensity due to loss by absorption and by primary scattering] + [the rate of increase in intensity by multiple scattering]

The equation of radiative transfer has been integrated only for the highly restricted conditions that the material is continuous, and that the single scattering is of the simplest possible form; it must be isotropic for particle scattering, or dipole for electromagnetic scattering.

The first exact solution was given by Chandrasekar in 1950 (35) and applies only to nonabsorbing scatterers.

A first approximation, referred to as either the Schuster theory (199) or the Kubelka-Munk equations (137), has been applied to a wide variety of problems. These include (i) the diffuse transmittance of opal glass (37), (ii) the diffuse reflectance of paper (116, 217), paint pigments (198), and human skin (24). This theory also forms the theoretical basis used by Rodrigo (190) and by Polanyi

(181) for their reflection oximeters, and by Cornwall et al (42) for transmission oximetry.

The Schuster theory considers diffuse radiation incident on a plane-parallel slab of a homogeneous, continuous medium, in which scattering particles of various sizes and shapes are dispersed. Kottler (126) has pointed out that as the particles become more closely packed, differences in their size and shape become less important. Hodkinson (98) showed that the single scattering by an assembly of irregular particles within a range of sizes larger than the wavelength is similar to single scattering by spheres, although the Mie theory of scattering for spherical particles cannot be applied to a single irregular particle. Schuster (199) enunciated his theory describing the escape of radiation from the self-luminous foggy atmosphere of a star. However, the theory assumes that the scattered radiation travels in only two directions: half is directed forward and half backward. This assumption is true only for Rayleigh scatterers, but not for large particles. The theory is characterized by only two constants, one for scattering and one for absorption.

Similar two constant models have been developed by Gurevich (78), Amy (5, 197), and Wurmser (253).

In 1927 Silberstein (210) generalized the Schuster theory for the case of collimated incidence, pointing out that the transmitted light consists of two parts - the

specular light which is the residue of the unscattered beam, and the diffuse light. Silberstein also removed the restriction that the forward and backward scattering coefficients are equal.

Ryde (193), in 1931, introduced separate forward and backward scattering coefficients for diffuse light, B and F, and for collimated light, B' and F'.

Duntley (53) suggested that the absorption coefficient for diffuse light was not necessarily the same as for collimated light and extended the theory to include six constants, four for scattering and two for absorption. Hulbert's theory (106) was developed along lines similar to those of Duntley.

Using the radiative transfer approach, Chu and Churchill (39) derived a six flux model. The six flux components are the forward and backward scattered power per unit area in three orthogonal directions, or, in other words, a forward component, a backward component, and four sidewise components.

All the theories mentioned above can be reduced to the Schuster theory by reducing the number of constants to two - a scattering coefficient and an absorption coefficient.

In many applications of the radiative transfer approach to multiple scattering, the observation has been made that the coefficients for scattering and absorption are constant only for certain ranges of particle concentration and sample

depth. Churchill and his associates (40) showed that when the interparticle distance is too small coherence effects become noticeable as a change in the value of the coefficients, and concluded that the theory is no longer applicable to the system when this particle concentration is reached. Kottler (125), in a study of opal glasses, found that the scattering coefficients showed a sharp rise as the thickness of very thin plates was increased, and he attributed this behaviour to the fact that much of the light was transmitted specularly in very thin samples. At larger depths, the coefficients showed a slow rise. This could not be explained, and was an indication of the inadequacy of the Schuster equations. The failure of the Schuster, or Kubelka-Munk equations, to yield constant coefficients has been observed in several studies (17, 53, 72, 85).

b) Successive Scattering

In 1940, Hartel (89) developed a theory for the multiple scattering of light by spherical particles. The angular distributions of scattered light for each successive order of scattering are determined. The theory has been applied to polystyrene latex particles by Woodward (252) for concentrations up to 0.005 gm/gm of particles 3 microns in diameter. Smart et al (213), using an improved technique, validated the theory for concentrations up to 0.01 gm/gm. The theory

is based on Mie's single scattering theory for spherical particles only. The theory has not been tested in the range of concentrations analogous to those found in blood, 0.2 to 0.7 vol/vol.

2. Coherent and Incoherent Scattering

The multiple scattering of waves has received considerable theoretical treatment (27, 225). Much of the experimental work has been done in the X-ray and microwave regions of the electromagnetic spectrum. The optical region has received less attention.

The multiple scattering of waves has been divided into two catogories: scattering by fixed configurations and periodic arrays, such as diffraction gratings; scattering by random statistical distributions, such as gases.

The second category, random distributions, is of particular interest since nonhemolyzed blood represents such a configuration. Twersky has developed a general formalism for such media (226-230). Although the theory was developed for use in the microwave region, the conditions imposed - that the particles are large compared to the wavelength of the incident light and have a relative index of refraction near 1.0 - permit its use under the appropriate circumstances in the optical region. Twersky obtains the multiple scattered amplitude in terms of the single scattered value and

of the fractional volume occupied by the scatterers. It is assumed that each particle is excited by the primary wave plus the resultant of the initially unknown total scattered fields of the other particles. Similar general procedures are given in more detail by Foldy (61) and by Lax (141).

The model used is that of a plane parallel slab, normal to the direction of incidence, of depth d in the z-direction, and of infinite dimensions in the x-y plane. There are N randomly located scatterers per unit volume. The scatterers in the slab are large compared to the wavelength, and their index of refraction relative to that of the suspending medium is close to 1.0.

Since the problem is one of a random distribution, averages must be taken over a statistical ensemble of scatterers. The quantities which are to be obtained are the average value of the wave function, $\langle u \rangle$, the square of its absolute magnitude, $\left|\langle u \rangle\right|^2$, and the average of the square of the wave function, $\langle |u|^2 \rangle$. Angular brackets denote an average over a statistical ensemble. The square of the absolute magnitude of the average value of the wave function, $\left|\langle u \rangle\right|^2$, describes the coherent aspect of scattering. It has been shown (61) that the average value of the wave function satisfies the wave equation in a continuous medium in which no scatterers are present, and in which the velocity of

propagation is different from the velocity in the original medium in the absence of scatterers. The average of the square of the wave function is, in general, different from the square of the average value, and this difference represents the incoherent scattering, V:

$$V = \left\langle |u|^2 \right\rangle - \left| \langle u \rangle \right|^2 \qquad 3.2$$

C. Techniques for Measuring Light Scattering

1. Measurement at Specified Angles

The study of the single scattering properties of particles calls for an instrument which will measure the angular distribution of the scattered light. Conventional single scattering instruments such as the commercial photometer based on the design of Brice, Halwer, and Speiser (20) measure the laterally scattered light and the light transmitted in the forward direction (turbidity). The position of the detector may be varied to measure scattering at discrete angles up to $\pm 135^{\circ}$ from the incident direction. The ideal system employs a collimated light beam, a lens-pinhole receiver with the pinhole placed precisely at the focal point of the lens, and a phototube perfectly aligned with the light source. It is important that the detector subtend a very small angle at the sample particularly in measurements of turbidity, since collection of any scattered light will

result in an underestimation of Q_{sca}, the efficiency factor or total scattering coefficient.

2. Integration of the Transmitted and Scattered Light

The object of measuring the integrated light is usually the determination of the absorption spectrum of a light scattering, pigmented material. A fundamental question which has been the subject of many investigations is whether the absorption coefficient of a pigment within a biological cell is identical to that of the extracted pigment in solution. In order to settle this question, the absorption spectrum of the suspension must be measured in such a way that the effects of light scattering are completely eliminated.

It has been well established that the absorption spectra of scattering suspensions of pigmented particles measured in a conventional spectrophotometer are shifted towards higher values than those of the same pigment in solution. The spectrum is also "flattened" - that is, the optical densities at an absorption maximum and at an absorption minimum are greatly increased but their ratio is reduced in comparison with a true solution (121, 140, 207).

These distortions of the absorption spectra of light scattering materials are due to the loss of scattered light. If the detector is far off in the forward direction and is small enough to include only a negligible amount of the

scattered wave, the extinction coefficient will have its maximum value. If, however, the detector is close enough to include all the scattered light, the total extinction will be reduced. Ideally, the detector should be placed immediately adjacent to the sample chamber in order to collect all the forward scattered light. This is practically impossible to achieve. Other methods have been devised to overcome this difficulty.

One of two methods is generally used. In one of these techniques, diffusing plates are placed immediately in front of the sample or directly behind it to reduce the optical density levels of the light scattering sample. This technique is actually an approximation of the second and more theoretically sound method, the use of an integrating sphere. Although both methods succeed in shifting the absorption spectrum to lower optical density levels, neither method measures up to the requirement of providing a "true" absorption spectrum. The simplicity of the diffusing plate technique has led to its widespread use as an alternative to the more complicated integrating sphere technique. Both methods have been employed in the present study.

These two methods have been applied to biological materials frequently during the last ten years. However, the same principles have been used for measuring the optical

density of photographic plates for about seventy-five years. In 1887, Abney (1) placed an opal glass diffusing plate in contact with an exposed photographic plate and found that the optical density was greatly reduced. In 1891, Hurter and Driffield (107) pointed out that the optical density of light scattering photographic plates depends to a considerable extent upon the geometrical arrangement of the measuring system as well as upon the interreflections between the diffusing plate and the test sample. Detailed investigations of Callier (34), in 1909, led to the development of opal glass densitometers and to the use of integrating sphere photometers for measurements on light scattering photographic plates.

In this review, the term optical density has been used with no restriction on the way in which the sample is illuminated or on the way in which the transmitted light is measured. The quantities measured with the diffusing plate or integrating sphere techniques can be interpreted more easily if optical density is defined according to the standardization used in photographic theory. Optical density may be defined in one of the following ways, depending on the way in which it is measured (158):

1) specular density

2) diffuse density: i) single diffuse density
ii) double diffuse density

These three types of optical density are illustrated in Fig. 3.1 and are defined as follows:

Specular density: the radiant flux is incident normally on the sample and only the normal component of the transmitted flux is measured. Ideally, the light source and the detector are perfectly collimated so that α and θ are both zero, and the measurement is analogous to the measurement of the turbidity of a single scattering suspension (Fig. 3.1a).

Single diffuse density: the radiant flux is incident normally on the sample and all of the transmitted and scattered flux is measured (Fig. 3.1b) or, in accordance with the optical reversibility principle, the incident radiant flux is perfectly diffuse and only the specularly transmitted component is measured (Fig. 3.1c).

Double diffuse density: the radiant flux incident on the sample is completely diffuse and all the transmitted flux is measured (Fig. 3.1d).

a) Diffusing Plate Technique

In 1954, Shibata, Benson, and Calvin (207) suggested the use of diffusing plates for measuring absorption spectra of light scattering biological materials, and the method has been used by other authors (4, 140) to study unicellular organisms, red blood cells, and suspensions of pigmented particles such as carotenes and chloroplasts.

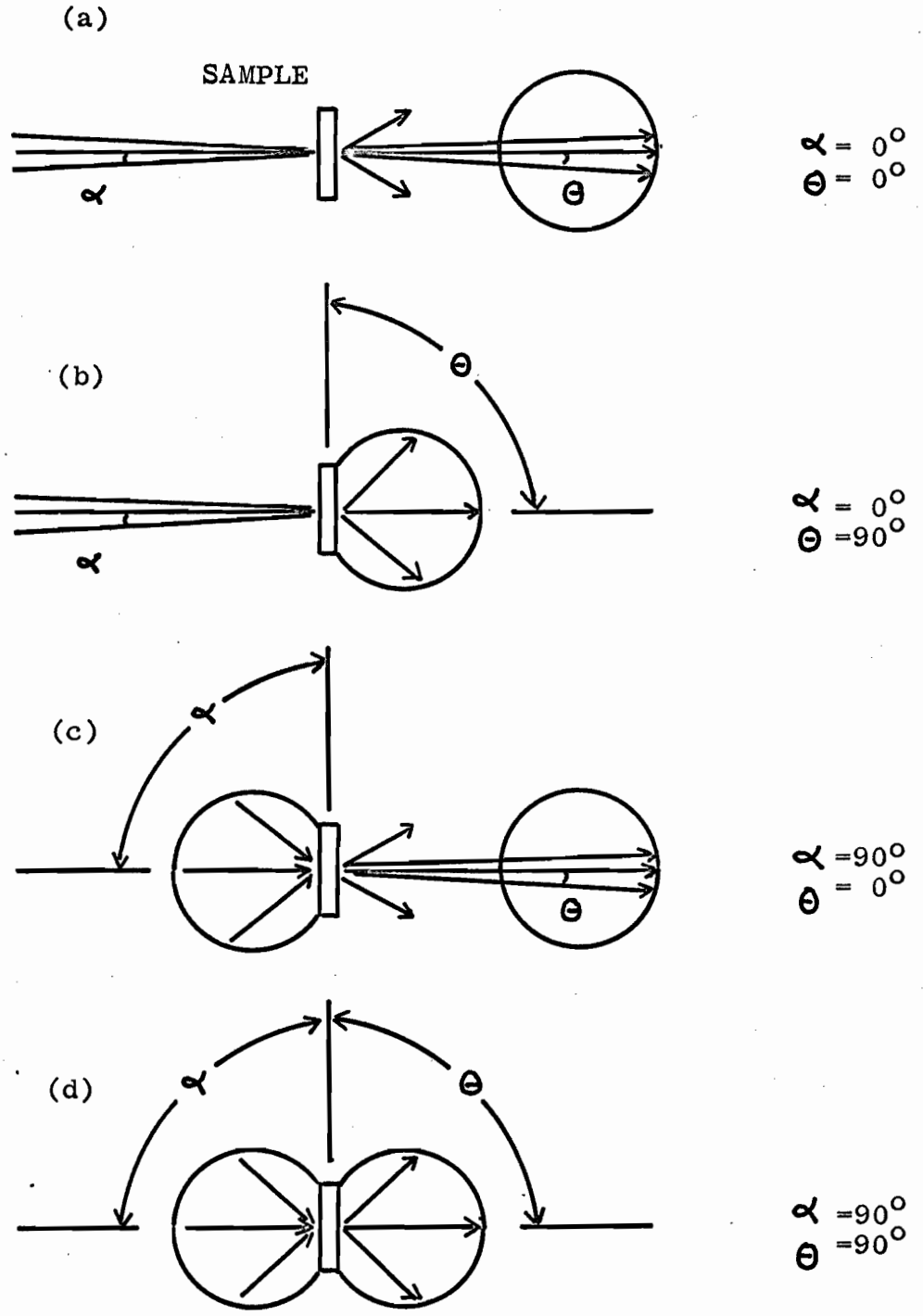

Fig. 3.1. Optical density of scattering material.
α = solid cone angle of illumination
Θ = solid cone angle of collection
(a) Specular density
(b) Single diffuse density
(c) Single diffuse density
(d) Double diffuse density

Opal glass or ground glass plates are placed on the detector side of both sample chamber and blank cell. It is assumed that the quantity of light from the diffusing plate must be proportional to the light intensity emerging from the cuvette. The theory as outlined by Shibata follows (206).

Let I_p = parallel or specular transmitted light

I_d = diffuse transmitted light

I_t = total transmitted light = $I_p + I_d$

I_a = absorbed light

I_r = reflected light

I_o = total incident light = $I_t + I_a + I_r$

In an ordinary spectrophotometer, the specular transmitted light and some of the scattered light will be intercepted by the detector, depending on the geometry of the system and particularly on the distance between the sample and detector, as shown in Fig. 3.2a. Shibata expresses the situation in the following way:

$$\text{Optical Density} = \log \frac{I_o}{I_p + fI_d} \qquad 3.3$$

where f is a constant between zero and one. In ordinary spectrophotometers f is quite small, resulting in high levels of optical density.

When diffusing plates are used,

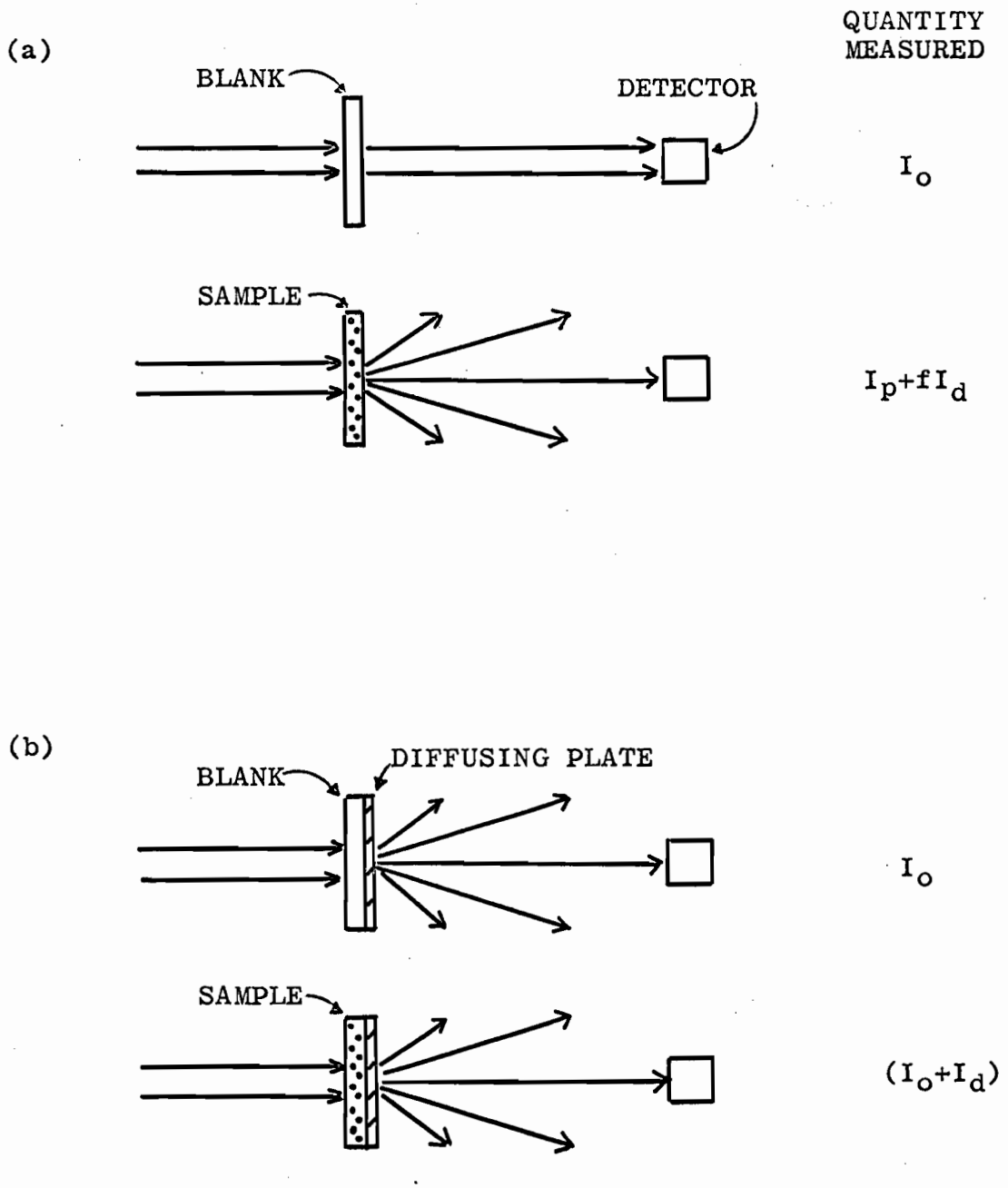

Fig. 3.2(a) Conventional spectrophotometric technique.
3.2(b) Diffusing plate technique.

$$\text{Optical Density} = \log \frac{\alpha I_o}{\alpha(I_p + I_d)} = \log \frac{I_o}{I_p + I_d} \qquad 3.4$$

and f is equal to one. This is equivalent to a measurement of single diffuse density. Equivalent results should be obtained if the diffusing plates are placed on the light source side of the cuvettes (206, 207).

According to this theory the only fractions of light not received by the detector are the absorbed and reflected fractions, and optical density should correspond to that obtained in an integrating sphere. This type of measurement still does not give a "true" absorption spectrum, since the back scattered component is not measured.

At this point we may point out our objection to the theoretical validity of the opal glass method. The assumption is made that the same fraction, α , of the incident and transmitted light is collected by the detector. However, the incident light is measured as the light transmitted by the opal glass when it is illuminated by collimated light. The transmittance of the sample is measured as the light transmitted by the opal glass when it is illuminated by diffuse light. It has been shown (53, 106, 126, 137, 193) that scattering coefficients, and consequently transmittance, will differ, depending on whether the incident light is collimated or diffuse. Therefore, the assmuption that α is

the same for both incident light and for light transmitted through the sample is not strictly true. It may be concluded that the method cannot provide absolute values of log (I_o/I_t) and it is not equivalent to an integrating sphere. However, it appears to be a very good approximation.

b) Integrating Sphere

The theory of the integrating sphere was first enunciated in 1893 by Sumpner (220). If a source of light is placed inside a hollow sphere which is coated internally with a perfectly diffusing material, the luminance of any part of the surface due to light reflected from the remainder of the sphere is the same and is proportional to the total flux. The flux received per unit area by one part of the surface of a sphere from a given area of any other part is the same and is independent of the relative positions of the two parts of the sphere. Only reflected light reaches the detector, and this reflected light is the same at any point of the sphere wall.

The integrating sphere may be used to measure diffuse transmittance (transmission and scattering in forward directions) or diffuse reflectance (scattering in backward directions) as illustrated in Fig. 3.3.

To measure diffuse transmittance, the sample chamber is located at the entrance aperture of the sphere (Fig. 3.3a).

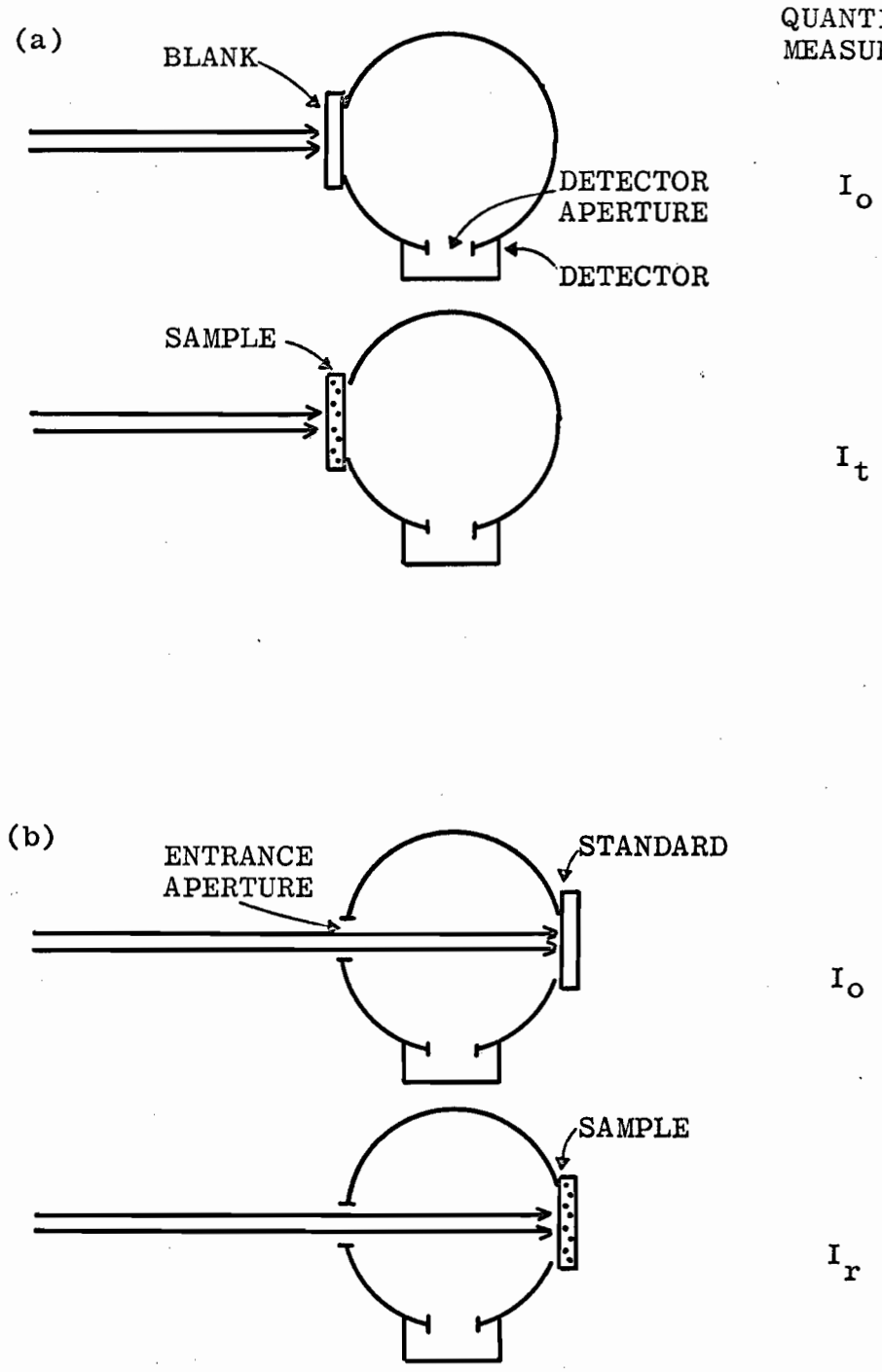

Fig. 3.3(a) Integrating sphere technique for measuring diffuse transmittance.

Fig. 3.3(b) Integrating sphere technique for measuring diffuse reflectance.

The ratio of the luminance of a portion of the sphere wall with and without the sample in place gives the transmission factor of the medium. Similarly, for diffuse reflectance, the sample is placed so that it forms a part of the sphere wall (Fig. 3.3b). The reflectance is obtained from the ratio of the luminance of the sphere wall, with the sample in place, to its luminance when the sample area is replaced with a standard of the same material coating the inside of the sphere.

Different values are obtained for both transmittance and reflectance depending on whether the incident light is collimated or diffuse. If reflectance with collimated incidence is being measured, the sphere must be designed so that specular reflection will either exit via the entrance aperture, or be caught in a light trap.

The precaution must be taken that none of the incident light reaches the detector before it has suffered multiple reflections within the sphere. For this purpose a screen is placed in the direct path between the entrance aperture and the detector.

The elementary theory of the integrating sphere has been presented by Walsh (241). A detailed discussion of the general theory for reflectance was given by Jacquez et al (110).

Although the theory of the integrating sphere is fairly simple, practical application presents difficulties which are unavoidable and limit its usefulness. It is impossible to build an integrating sphere which completely fulfills the conditions of the theory. The accuracy which may be obtained is limited by the presence of the sample, the entrance and exit apertures, and the screen, which interfere with the internal reflections and act as light sinks. In addition, it is impossible to obtain a perfectly diffusely reflecting surface on the inside of the sphere. Even a freshly prepared coat of magnesium oxide has a reflectance of only 0.98 in the visible region. Magnesium surfaces are very fragile, do not show long term stability, and are difficult to reproduce with identical reflectance properties (25). Barium sulphate may be substituted for magnesium oxide. It is easier to prepare and has a reflectance almost as high as that of magnesium oxide, 0.96 (25).

For maximum sphere efficiency, the sphere should be as small as possible. On the other hand, it should be sufficiently large that the entrance and sample apertures and detector port occupy as small a fraction of the total area as possible. A compromise must be made between a large sphere to minimize error and a small sphere to maximize efficiency.

Two procedures for measuring diffuse transmittance or reflectance are possible - the substitution method and the comparison or simultaneous method. In the substitution method, a measurement is made with and without the sample at the sample aperture. In order to use the comparison method, there must be two sample ports and two entrance ports placed symmetrically in relation to the photocell aperture; one is for the standard or blank, and one is for the sample. Both remain in place during the measurements. Measurements are made first with the incident beam on the sample and then on the standard. Both procedures should yield the same result, but the comparison method is generally found to be more accurate (86, 110).

IV. MEASUREMENT OF THE OXYGEN SATURATION OF WHOLE NONHEMOLYZED BLOOD*

A. Introduction

In 1935 Kramer (129) demonstrated that the relationship between oxygen saturation and optical density, at a given hemoglobin concentration, was linear. With respect to total hemoglobin concentration, however, Kramer showed that the light transmitted by nonhemolyzed blood did not obey Beer's law. A method for estimating the oxygen saturation of nonhemolyzed blood was described. Individual calibration was required for each hemoglobin concentration. Similar one wavelength methods were described by Drabkin and Schmidt (51), Sabiston et al (194), Handforth (84), Roddie, Shepperd, and Whelan (189), and Hickam and Frayser (97).

The first absolute method for measuring oxygen saturation in nonhemolyzed blood was the two wavelength technique of Wood and his associates (249). The method uses the principle on which the bichromatic technique for hemolyzed blood is based. The ratio of the optical density of a blood sample at two wavelengths is related to the oxygen saturation obtained from another type of measurement, such as Van Slyke analysis. The method is theoretically sound for hemolyzed blood which obeys

*Published in part. Anderson, N.M. and P. Sekelj: J. Lab. Clin. Med. 65: 153, 1965.

Beer's law. Unfortunately, nonhemolyzed blood deviates from Beer's law; consequently, there is no theoretical justification for using this technique. The method may be considered absolute since it is not necessary to calibrate for each hemoglobin concentration. But an initial empirical calibration against reference techniques is required. In Wood's bichromatic oximeter, the use of gelatin filters with wide pass bands results in a nonlinear calibration. The curvature is particularly high for oxygen saturations over 90%. Sekelj (202) used an interference filter rather than a Wratten 29 filter in his cuvette oximeter and obtained a linear calibration curve.

At normal hemoglobin concentrations the method is clinically adequate but lacks scientific precision. The standard deviation of the differences between oximetric oxygen saturation determinations and Van Slyke analyses is about $\pm$2%. Observations made over eight years in this laboratory have shown that errors in oxygen saturation determinations may be considerable when the hemoglobin concentration is about 8 gm/100 ml or less. Both transmission and reflection methods are unreliable at low hemoglobin concentrations. Enson and his associates (58), using an intravascular reflection oximeter, found that individual calibration curves were required for hematocrits below 30%.

One of the first objects of these studies was to investigate the possibility of devising an independent method for

determining the oxygen saturation of whole nonhemolyzed blood - a method which would not require standardization against reference methods and which would possess uniform accuracy over the whole range of hemoglobin concentrations.

B. Instrumentation

The measuring system is shown in Fig. 4.1. The housing is of stainless steel.

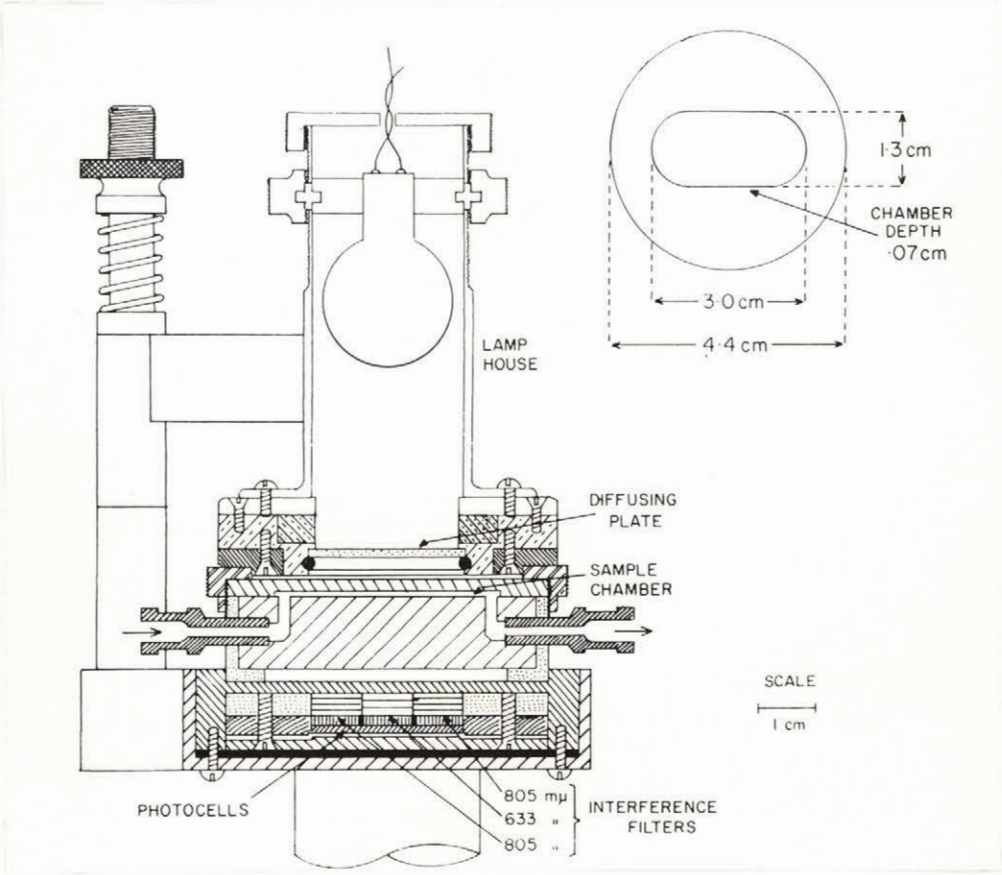

Fig. 4.1. Cross section of cuvette assembly. Inset shows the dimensions of the sample chamber.

Reprinted from
THE JOURNAL OF LABORATORY AND CLINICAL MEDICINE
St. Louis

Vol. 65, No. 1, Pages 153-166, January, 1965

1. Light Source. The light source consists of a 6 volt, 0.5 ampere flashlight bulb with a ground glass diffusing plate at the base of the lamp house. The diameter of the diffusing plate is 1.63 cm.

2. Sample Cuvette. The sample cuvette consists of two contacting lucite plates. The sample chamber is milled out of the upper plate. Before assembling the cuvette, a thin layer of silicone grease is applied between the two contacting surfaces.

The cuvette is designed so that measurements can be made on flowing samples. In order to minimize streaming effects, the sample cuvette is designed so that the sample enters and leaves the chamber through pinholes which cause turbulence to occur.

The dimensions of the sample chamber are 3.0 by 1.3 cm. The area occupied by the sample chamber is larger than the area of the detector. In order to prevent light from reaching the detector without passing through the sample, a thin metal plate with a central rectangular aperture was placed on the upper surface of the lucite cuvette. The plate, painted with nonreflecting black paint, prevents light from passing around the sample chamber to the detector.

Sample depth may be varied by changing the upper plate of the cuvette. An estimate of sample depth was made with a

micrometer; a more precise value was established according to the method of Drabkin and Austin (50) using a solution of Coomassie blue dye.

3. Photocells and Filters. The detector is located 2.27 cm below the sample chamber and consists of three selenium barrier layer photocells (Electrocell, Type N) covered with interference filters (Schott-Jena).

The area occupied by the three photocells is 1.86 cm by 1.0 cm. The area surrounding the photocells and filters is coated with nonreflecting black paint. The two outer photocells have interference filters with maximum transmission at 8050 A. The interference filter covering the central cell has its maximum transmission at 6330 A.

Since the wavelength at which an interference filter transmits maximally depends on the angle at which light is incident on the filter (79), we considered the possibility that the transmission of the filters might be altered by the use of diffuse incident light. The interference filters were scanned in the Beckman DU spectrophotometer (Fig. 4.2). With diffuse light the maximum transmission was shifted 40 A towards shorter wavelengths and the half intensity band width was broadened from 140 A to 170 A. These differences are negligible for oximetric purposes.

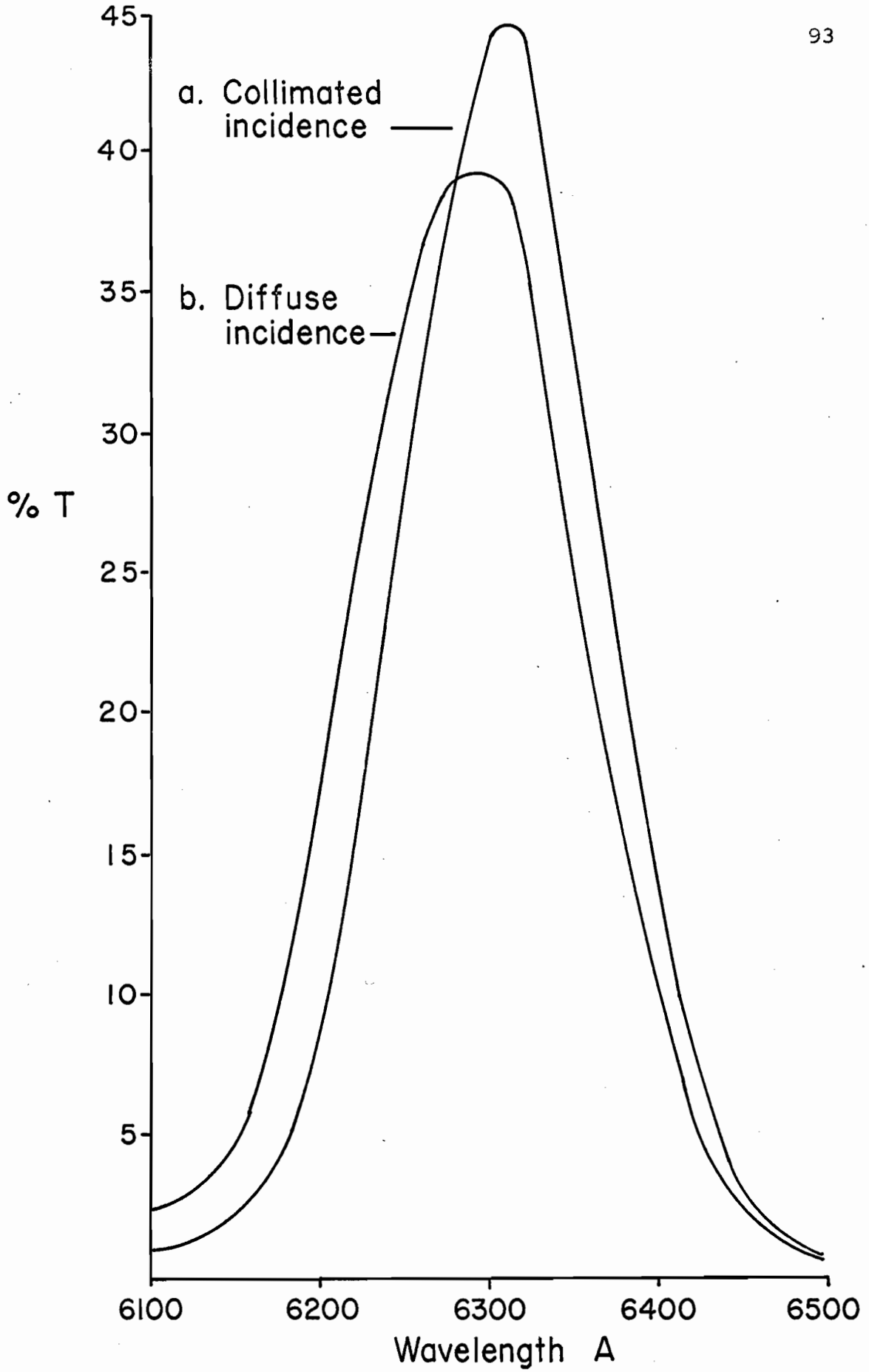

Fig. 4.2. Scans of red interference filter: (a) collimated incidence, (b) diffuse incidence.

C. Material and Methods

Citrated human blood from the blood bank was used. Fifty milliliter aliquots of blood were rotated in a 1,000 ml tonometer for 20 minutes. At 7 minute intervals, the equilibrating gas (5% CO_2 in compressed air or 5% CO_2 in N_2, bubbled through water) was allowed to flow through the tonometer for 15 seconds. Oxygen saturation and capacity were determined by Van Slyke analysis; the two samples were mixed in varying proportions to produce samples of intermediate saturation.

Measurements on nonhemolyzed blood were made at a flow rate of 3.8 ml/minute using a constant speed withdrawal pump (Harvard Apparatus Co. Inc.).

Hemolyzed samples were prepared by adding 10 mg/ml saponin in a 50% solution. Measurements were made on stationary hemolyzed samples.

D. Results

With this instrument it was possible to reaffirm the validity of Beer's law for hemolyzed blood. Fig. 4.3 shows that the relationship between the oxygen content of hemolyzed blood and optical density at various hemoglobin concentrations and at two sample depths was linear. The line joining the points of 100% saturation shows that the relationship between oxygen capacity, or total hemoglobin concentration, was also linear.

Fig. 4.3 (a).
Legend accompanies Fig. 4.3 (b).

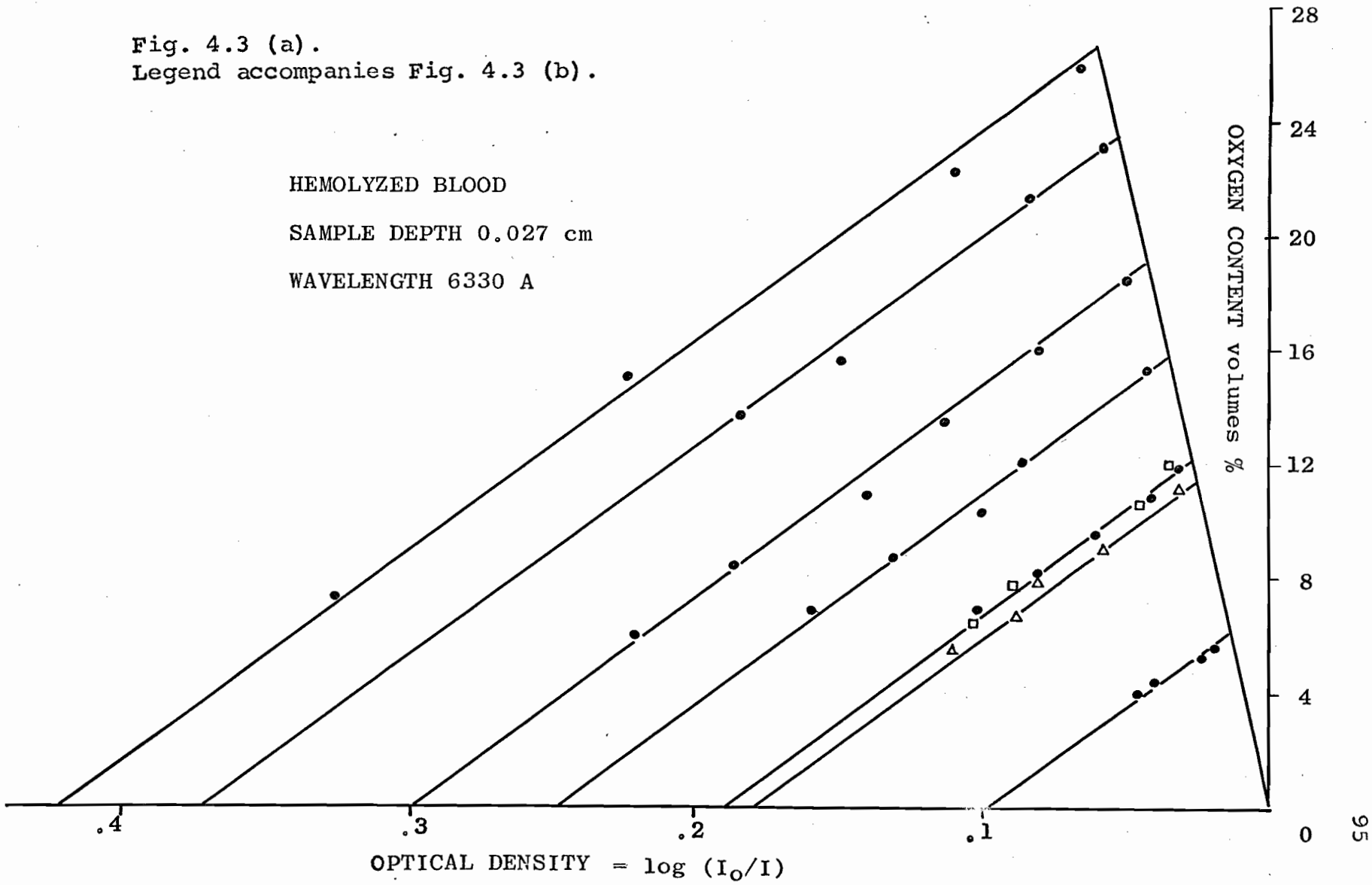

Fig. 4.3 (b).

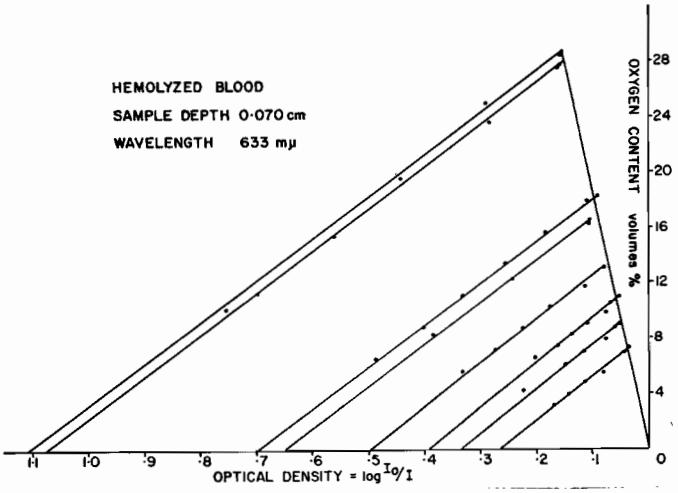

Fig. 4.3. Hemolyzed blood: oxygen content is plotted against optical density at 6330 A. The line joining points of 100% oxygen saturation shows the linear relationship between oxygen capacity and optical density.

(a) Sample depth 0.027 cm.

(b) Sample depth 0.071 cm. (Reprinted from J. Lab. Clin. Med. 65: 153, 1965).

Extinction coefficients were calculated according to Beer's law. Table 4.1 shows the values obtained for the extinction coefficients of hemolyzed blood at 6330 A and 8050 A in the present study compared with those obtained by Gordy and Drabkin (74) using (1) the Beckman DU spectrophotometer and (2) using a Bausch and Lomb Spectronic 20 diffraction grating spectrophotometer. The results obtained with the cuvette oximeter show very close agreement with those obtained by Gordy and Drabkin using the Beckman DU spectrophotometer. The extinction coefficients they measured with the Bausch and Lomb diffraction grating spectrophotometer do not agree very well with either their own results from the Beckman DU spectrophotometer or with our cuvette oximeter values.

Our next step was to see whether the observations of Kramer et al (129, 131) using conventional spectrophotometric techniques on whole nonhemolyzed blood could be reproduced with our measuring system. Results were obtained at two sample depths (0.027 cm and 0.071 cm) and are shown in Fig. 4.4. As in the case of hemolyzed blood, oxygen content was linearly related to optical density at a given hemoglobin concentration. This observation is in agreement with that of Kramer. However, there is one major difference between the present results and those of Kramer. The straight lines relating oxygen content

TABLE 4.1. Extinction coefficients for hemolyzed blood

Instrument	Extinction Coefficients		
	6330 A		8050 A
	HbO_2	Hb reduced	HbO_2 and Hb reduced
Beckman DU Spectrophotometer[a] (quartz prism)			
Mean	0.175	1.060	0.196
S.D.[b]	0.011	0.040	0.010
S.E.[c]	±.004	±.014	±.004
Bausch & Lomb Spectronic 20[a] (diffraction grating)			
Mean	0.263	1.240	0.254
Whole Blood Oximeter			
0.027 cm sample depth			
Mean	0.180	1.263	0.174
S.D.	0.012	0.034	0.007
S.E.	±.004	±.012	±.002
0.071 cm sample depth			
Mean	0.172	1.195	0.175
S.D.	0.017	0.040	0.004
S.E.	±.006	±.014	±.001

TABLE 4.1. Continued

[a]See Gordy and Drabkin (74), p. 293, p. 296.

[b]Standard deviation = $\left[1/(n-1)\ \sum(x-\bar{x})^2\right]^{\frac{1}{2}}$.

[c]Standard error of the mean = $S.D./n^{\frac{1}{2}}$.

Fig. 4.4 (a).
Legend accompanies Fig. 4.4 (c).

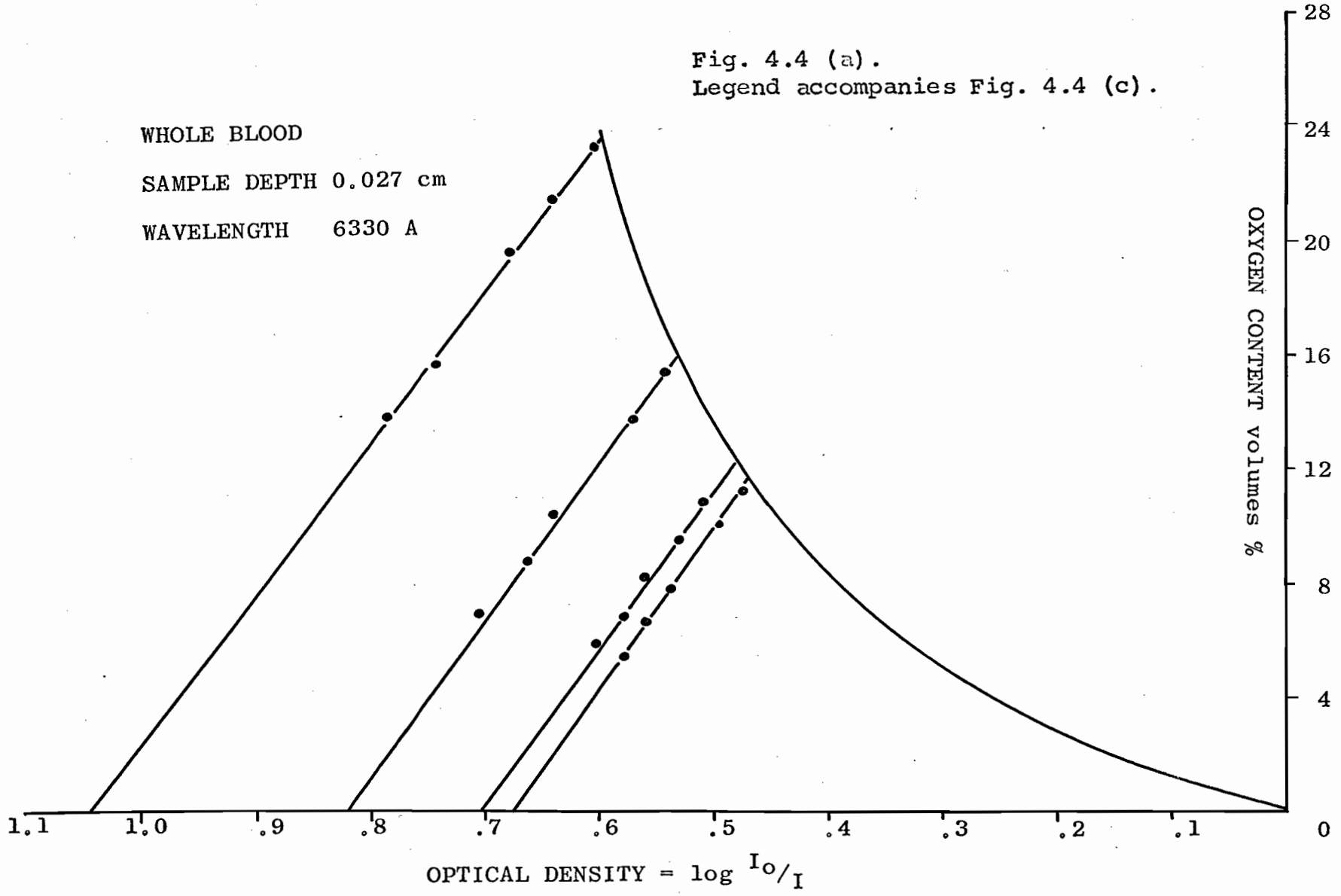

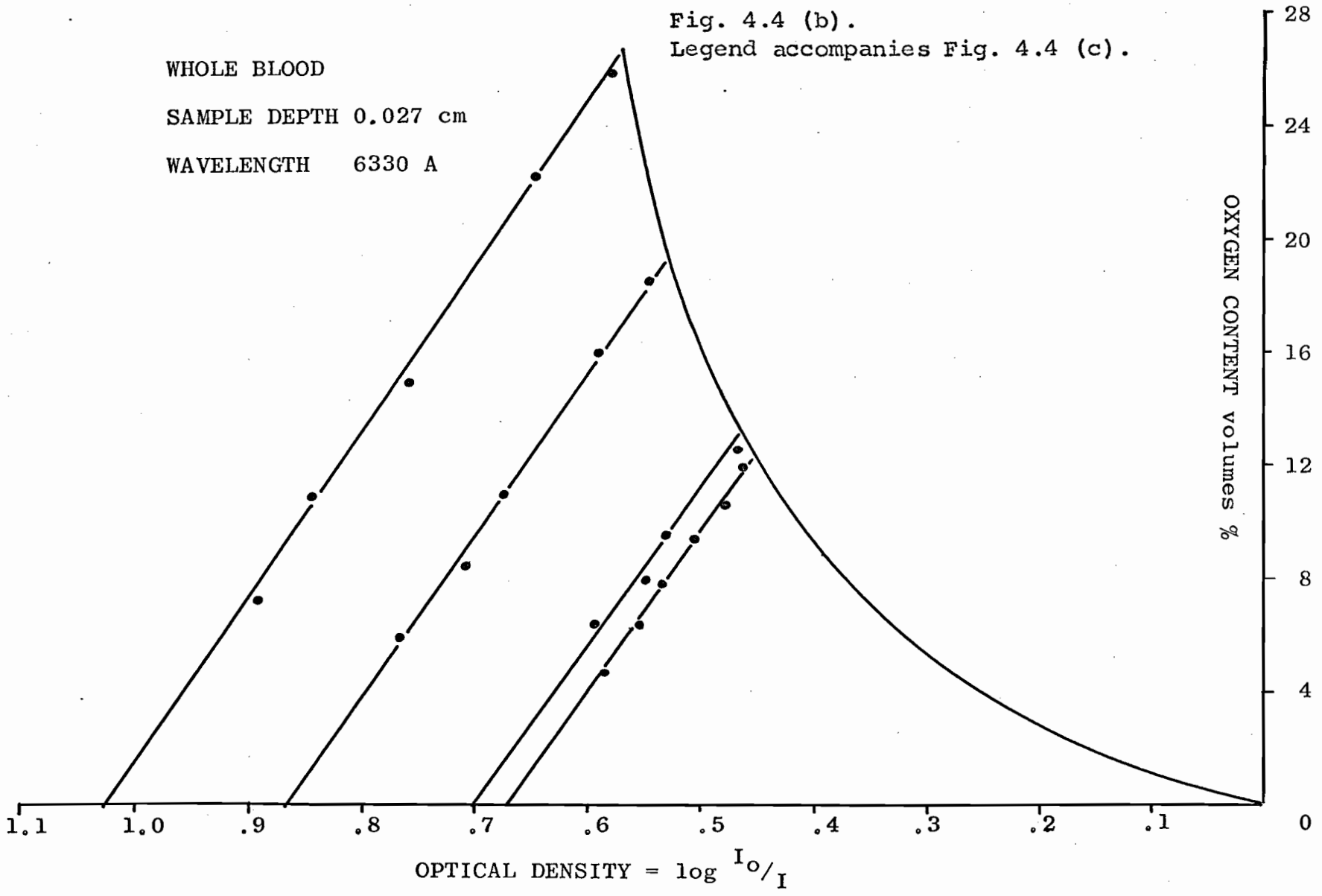

Fig. 4.4 (b).
Legend accompanies Fig. 4.4 (c).

Fig. 4.4 (c).

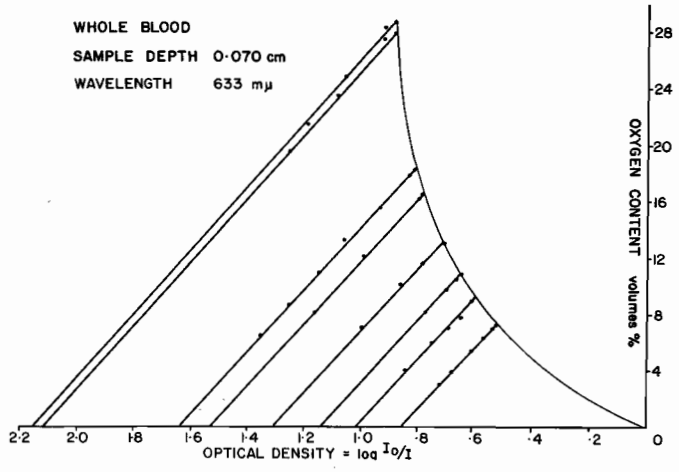

Fig. 4.4. Whole nonhemolyzed blood: oxygen content is plotted against optical density at 6330 A. The lines relating oxygen content to optical density are linear. The line which relates oxygen capacity to optical density in each graph is not linear.

(a) Sample depth 0.027 cm, Series A.
(b) Sample depth 0.027 cm, Series B.
(c) Sample depth 0.071 cm. (Reprinted from J. Lab. Clin. Med. 65: 153, 1965).

to optical density were parallel rather than divergent as Kramer and his colleagues found using a sample depth of 0.13 cm and a wavelength of 6530 A. They found that the difference between extinction coefficients for oxygenated and reduced blood at 5 volumes % capacity was 1.00 and at 20 volumes % capacity it was 1.70. Similarly, Hickam and Frayser (97) showed an increase in the difference between extinction coefficients with increasing hemoglobin concentration but of small magnitude. At a wavelength of 6600 A, these workers found a difference of 1.02 for a group of blood samples whose oxygen capacity ranged from 3.3 to 7.1 volumes %, and 1.15 for a group with a capacity range of 16.6 to 25.1 volumes %, at a sample depth of 0.163 cm. Kramer performed the same experiment at a wavelength of 10230 A. The lines were again divergent. It should be noted that the sample depths used in our cuvette oximeter were considerable smaller than those used in the studies of Kramer et al, and of Hickam and Frayser; also the diffusing plate technique was used rather than the conventional spectrophotometric techniques of the other workers. We concluded that the difference between our results and those of the other groups must be due to the differences in the geometrical and optical systems of the instruments.

The linear relationship between oxygen content and

optical density shows that Beer's law is partially valid for nonhemolyzed blood. The optical densities due to the individual pigments, oxyhemoglobin and reduced hemoglobin, are additive even when present in the form of a suspension as long as the hemoglobin concentration and sample depth are maintained constant.

The relationship between oxygen capacity or total hemoglobin concentration was nonlinear. This is demonstrated in Fig. 4.4 by the line joining the points of 100% saturation at each hemoglobin concentration.

The nonlinear relationship between oxygen capacity or total hemoglobin concentration and optical density is essentially the same as that obtained by Drabkin and Singer (52), Kramer (131), and Hickam and Frayser (97).

Two different sets of results were obtained at the 0.027 cm sample depth, due to a slight change in the geometry of the measuring system. The importance of the geometrical arrangement of the measuring system was discussed in Chapter III.

The first set of results was obtained with the lamp of the cuvette oximeter situated at the top of the chimney of the lamp house (see Fig. 4.1). The lamp was moved closer to the diffusing plate before the next set of experiments was performed. Two different curves of optical density versus

hemoglobin concentration were obtained (Fig. 4.4, a and b). At a given hemoglobin concentration, optical density was greater in the first set of experiments (Series A) than in the second set (Series B). On the other hand, the results obtained on hemolyzed samples showed no difference between Series A and Series B. We concluded that the differences in the results obtained on nonhemolyzed blood were the result of an optical phenomenon and provided a subject for further investigation (Chapter V). When experiments were performed at 0.071 cm sample depth, care was taken to insure that the geometry of the measuring system was in no way altered. As Fig. 4.4c shows, a unique relationship between optical density and oxygen capacity was obtained.

Extinction coefficients were calculated for oxygenated and for reduced nonhemolyzed blood, using the relationship of Beer's law:

$$\log (I_o/I) = \text{Optical Density} = \epsilon cd \qquad 4.1$$

ϵ is expressed in terms of 1 cm depth and 1 mM/liter concentration. We found that the extinction coefficients for nonhemolyzed blood decreased as hemoglobin concentration increased. By curve fitting, using Newton's method of successive approximations, the following expression relating extinction coefficients and hemoglobin concentration at a

constant depth was obtained:

$$\epsilon_{rbc} = 1/(ac + b) \qquad 4.2$$

ϵ_{rbc} signifies the extinction coefficient for nonhemolyzed blood. Hemoglobin concentration in mM/liter is represented by c; a and b are constants depending on the geometrical and optical characteristics of the measuring system. Fig. 4.5 shows extinction coefficients for oxygenated and reduced blood at 6330 A and for blood at the isobestic wavelength, 8050 A, plotted against hemoglobin concentration in mM/liter. The curves were calculated from equation 4.2. Comparison between calculated and measured values of extinction coefficients is presented in Table 4.2. At a sample depth of 0.027 cm the standard deviation of the differences between experimentally obtained extinction coefficients and those calculated from equation 4.2 were: at 6330 A, oxygenated blood $\pm$0.018 (0.7% of the mean value) and reduced blood $\pm$0.017 (0.4% of the mean value); at 8050 A, $\pm$0.018 (1.1% of the mean value). At a sample depth of 0.071 cm, these values were: at 6330 A, oxygenated blood $\pm$0.028 (1.6% of the mean value) and reduced blood $\pm$0.049 (1.6% of the mean value); at 8050 A, $\pm$0.014 (1.3% of the mean value).

Next, we attempted to derive unique equations which would express the oxygen saturation of whole blood (a) in a one wavelength system using two readings of optical density -

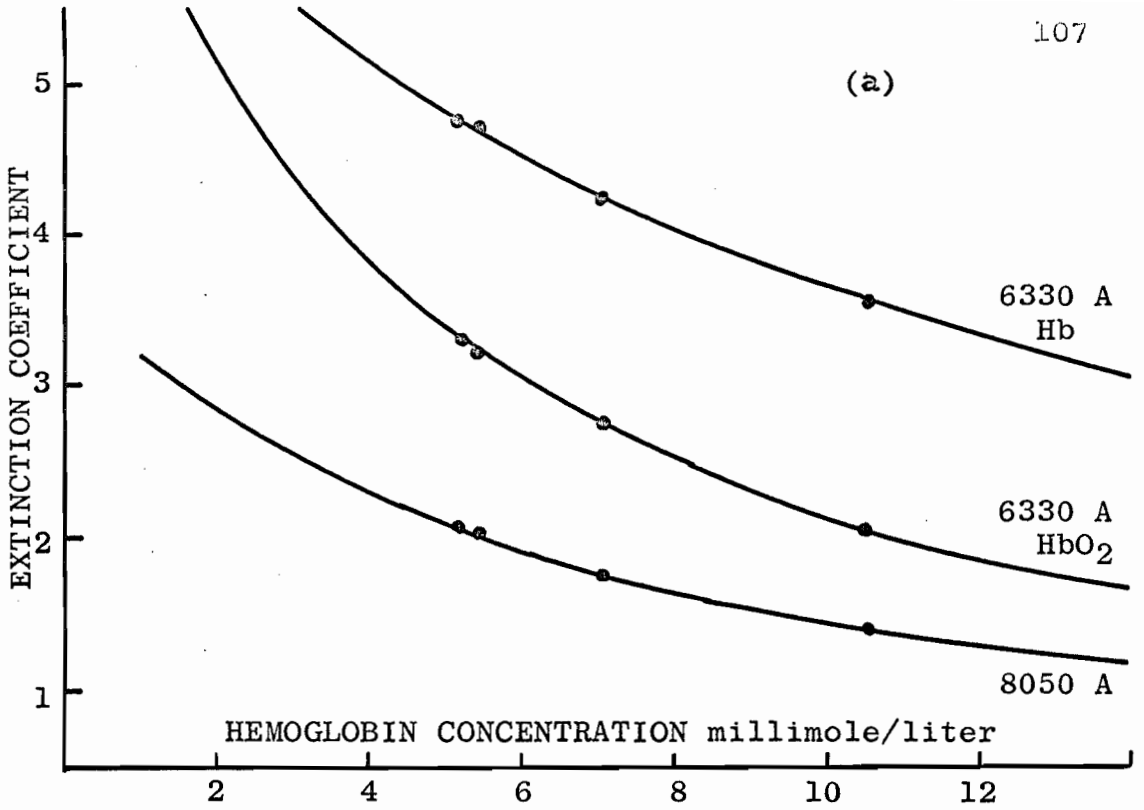

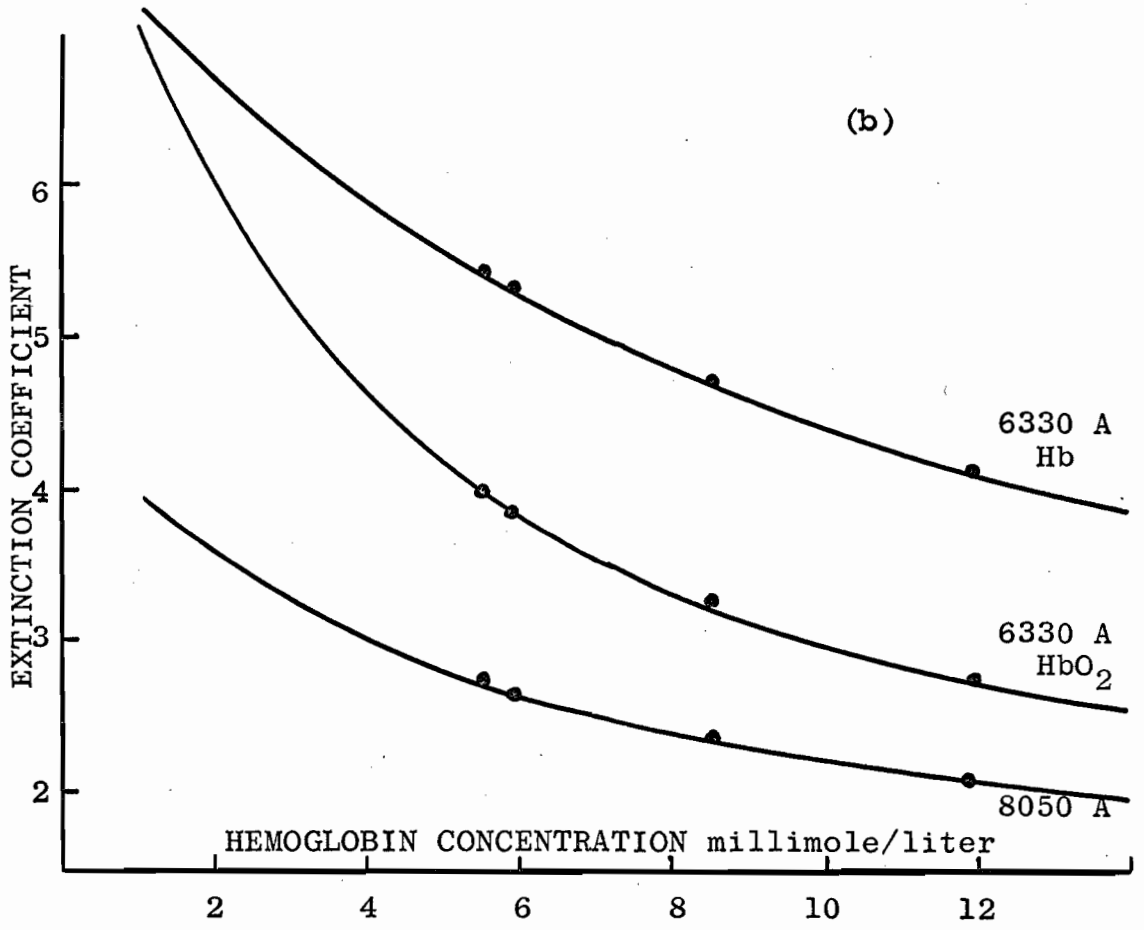

Fig. 4.5. Legend accompanies Fig. 4.5 (c).

Fig. 4.5 (c).

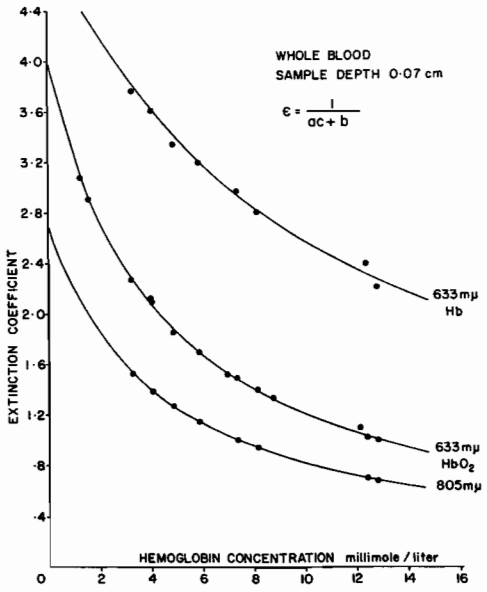

Fig. 4.5. Variation of extinction coefficients of whole nonhemolyzed blood with hemoglobin concentration for oxygenated and reduced blood at 6330 A and at 8050 A.
(a) Sample depth 0.027 cm, Series A.
(b) Sample depth 0.027 cm, Series B.
(c) Sample depth 0.071 cm. (Reprinted from J. Lab. Clin. Med. 65: 153, 1965).

TABLE 4.2. Comparison of extinction coefficients for nonhemolyzed blood obtained by experiment with those obtained by calculation from equation 4.2

Sample Depth (cm)	Hemoglobin Concentration (mM/l)	Extinction Coefficients					
		6330 A				8050 A	
		HbO_2		Hb reduced		HbO_2 and Hb reduced	
		Exp.	Eq. 4.2	Exp.	Eq. 4.2	Exp.	Eq. 4.2
0.027	5.2	3.294	3.304	4.760	4.764	2.063	2.064
	5.4	3.225	3.212	4.725	4.682	2.043	2.019
	5.5	3.004	2.988	4.438	4.417	1.742	1.726
	5.9	2.873	2.872	4.353	4.316	1.659	1.671
	7.1	2.754	2.730	4.238	4.248	1.752	1.777
	8.5	2.280	2.232	3.707	3.700	1.380	1.352
	10.6	2.058	2.066	3.545	3.540	1.415	1.414
	11.9	1.739	1.735	3.134	3.125	1.068	1.085
	S.D.D.[a]	±0.018		±0.017		±0.018	
	% of Mean[b]	0.7%		0.4%		1.1%	
0.071	1.2	3.117	3.109	. .	. .	. .	. .
	1.6	3.024	2.946	. .	. .	. .	. .
	3.3	2.280	2.284	3.765	3.814	1.530	1.539
	4.0	2.027	2.077	. .	. .	. .	. .
	4.0	2.100	2.074	3.610	3.617	1.400	1.399
	4.9	1.856	1.876	3.338	3.413	1.270	1.266
	5.9	1.696	1.697	3.197	3.214	1.152	1.147

TABLE 4.2. Continued

Sample Depth (cm)	Hemoglobin Concentration (mM/l)	Extinction Coefficients					
		6330 A				8050 A	
		HbO_2		Hb reduced		HbO_2 and Hb reduced	
		Exp.	Eq. 4.2	Exp.	Eq. 4.2	Exp.	Eq. 4.2
0.071	7.0	1.535	1.536	. .	. .	. .	. .
	7.4	1.494	1.482	2.980	2.952	1.006	1.002
	8.2	1.406	1.386	2.792	2.826	0.940	0.938
	8.8	1.328	1.320	. .	. .	. .	. .
	12.2	1.090	1.053	. .	. .	. .	. .
	12.4	1.030	1.036	2.395	2.310	0.697	0.702
	12.8	1.006	1.011	2.321	2.271	0.685	0.686
	S.D.D.	±0.028		±0.049		±0.014	
	% of Mean	1.6%		1.6%		1.3%	

[a]Standard deviation of the differences between experimental and calculated values
S.D.D. = $\left[1/(n-1) \sum(d - \bar{d})^2\right]^{\frac{1}{2}}$.

[b]Standard deviation of the differences expressed as a percent of the mean extinction coefficient value.

one of the sample at collection and one of the same sample fully oxygenated, and (b) in a two wavelength system where optical density is measured at a wavelength where the extinction coefficients of oxygenated and reduced hemoglobin are different, and at an isobestic wavelength.

Two equations were derived: one equation is based on measurements at 6330 A only, and the other is based on readings at two wavelengths, 6330 A and 8050 A. The first equation was derived from equation 2.10 by substituting equation 4.2 into it:

$$\%O_2 = \frac{c_1}{c}(100)$$

$$= \frac{\left\{OD_x\left[OD_{100\%}(a_2b_1 - b_2a_1) + b_2d\right] - b_1d\ OD_{100\%}\right\}(100)}{OD_{100\%}\left[OD_{100\%}(a_2b_1 - b_2a_1) + (b_2 - b_1)d\right]} \qquad 4.3$$

where OD_x is the optical density of the sample on collection, and $OD_{100\%}$ is that of the sample after oxygenation. The symbols a_1, b_1 and a_2, b_2 represent the constants of equation 4.2 for oxygenated and reduced whole blood, respectively. The second equation was obtained by substituting equation 4.2 into equation 2.14:

$$\%O_2 = \frac{c_1}{c}(100)$$

$$= \frac{\left[OD_{805}(a_1b_3 - a_3b_1) + b_1d\right]\left[OD_{633}OD_{805}(a_2b_3 - b_2a_3) + (b_2OD_{633} - b_3OD_{805})d\right](100)}{OD_{805}\, b_3d \left\{OD_{805}\left[a_3(b_1 - b_2) + b_3(a_2 - a_1)\right] + (b_2 - b_1)d\right\}} \quad 4.4$$

OD_{633} and OD_{805} represent optical density at 6330 A and at 8050 A, respectively. The final equations with the appropriate constants substituted into them are shown in Table 4.3. The symbols a_3 and b_3 represent the constants of equation 4.2 at 8050 A.

The equations can be expressed graphically as shown in Fig. 4.6. The lower part of the graph shows a family of straight lines in which percent oxygen saturation is plotted against optical density at 6330 A. Each line represents a specific hemoglobin concentration. The hemoglobin concentration is obtained from one of the two upper graphs, depending on whether the one wavelength or two wavelength system is being used.

Oxygen saturation measurements were compared with those obtained by single Van Slyke analyses. The comparison is shown in Fig. 4.7 and Table 4.4. At a sample depth of 0.027 cm, forty samples were analyzed; the samples ranged in hemoglobin concentration from 8.6 to 19.9 gm/100 ml, and

TABLE 4.3. Equations for calculating oxygen saturation using one wavelength (equation 4.3) and two wavelengths (equation 4.4)

Sample Depth (cm)	Equation Number	Equation
0.027[a]	4.3	$\%O_2 = \frac{OD_x(-2.996OD_{100\%} + 3.836) - 3.507OD_{100\%}\ (100)}{-2.996(OD_{100\%})^2 + 0.329OD_{100\%}}$
	4.4	$\%O_2 = \frac{(0.380OD_{805} + 0.351)(-0.216OD_{633}OD_{805} + 0.384OD_{633} - 0.740OD_{805})\ (100)}{-0.441(OD_{805})^2 + 0.024\ OD_{805}}$
0.027[b]	4.3	$\%O_2 = \frac{OD_x(-3.650OD_{100\%} + 4.000) - 3.480OD_{100\%}\ (100)}{-3.650(OD_{100\%})^2 + 0.521OD_{100\%}}$
	4.4	$\%O_2 = \frac{(0.004OD_{805} + 0.003)(-0.364OD_{633}OD_{805} + 0.400OD_{633} - 0.781OD_{805})\ (100)}{-0.593(OD_{805})^2 + 0.041OD_{805}}$

TABLE 4.3. Continued

Sample Depth (cm)	Equation Number	Equation
0.071	4.3	$\%O_2 = \frac{OD_x(-0.693OD_{100\%} + 1.417) - 1.758OD_{100\%}\ (100)}{-0.693(OD_{100\%})^2 - 0.342OD_{100\%}}$
	4.4	$\%O_2 = \frac{(0.040OD_{805} + 1.758)(-1.004OD_{633}OD_{805} + 1.416OD_{633} - 2.630OD_{805})\ (100)}{-2.748(OD_{805})^2 - 0.899OD_{805}}$

[a]Equations for Series A.
[b]Equations for Series B.

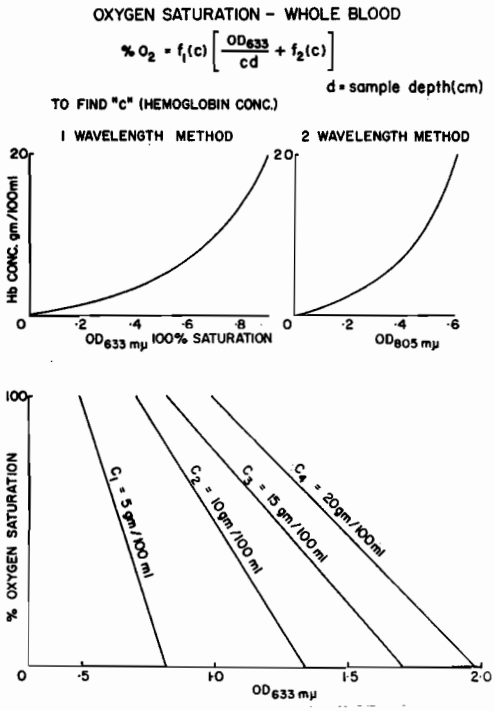

Fig. 4.6. Graphic illustration of equations 4.3 and 4.4 for oxygen saturation in whole nonhemolyzed blood. The upper graphs relate hemoglobin concentration to optical density at 6330 A and 8050 A. The lower graph relates oxygen saturation to optical density at 6330 A. (Reprinted from J. Lab. Clin. Med. 65: 153, 1965).

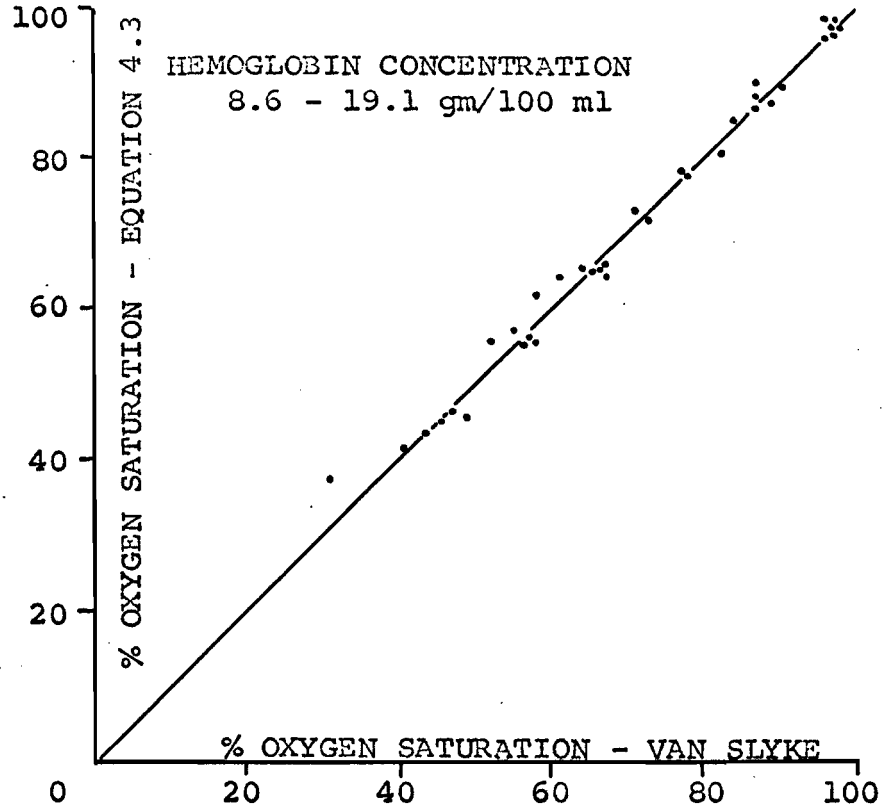

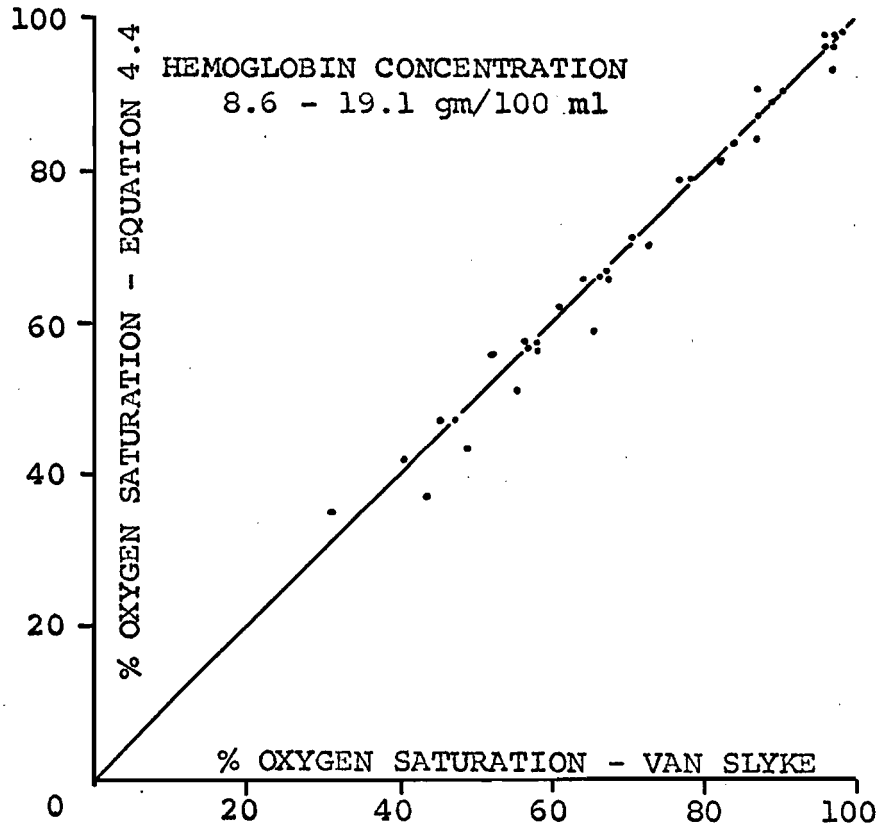

Fig. 4.7. Oxygen saturation obtained from the one wavelength method, equation 4.3, (a), and from the two wavelength method, equation 4.4, (d), versus oxygen saturation obtained by Van Slyke analysis, at a sample depth of 0.027 cm.

(a) One wavelength method: the standard deviation of the differences is ±2.08%.

(b) Two wavelength method: the standard deviation of the differences is ±2.61%.

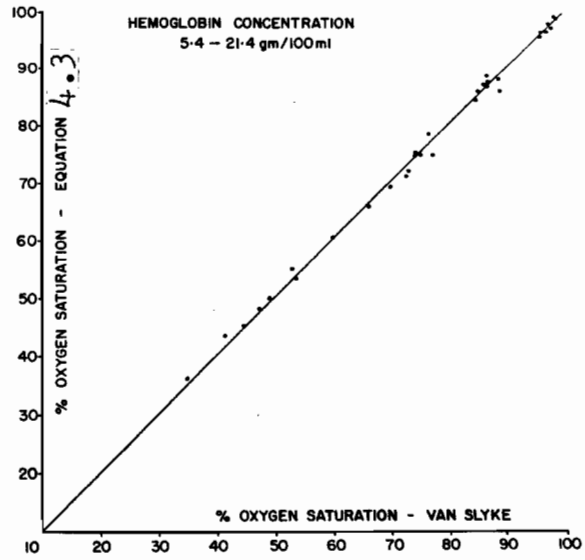

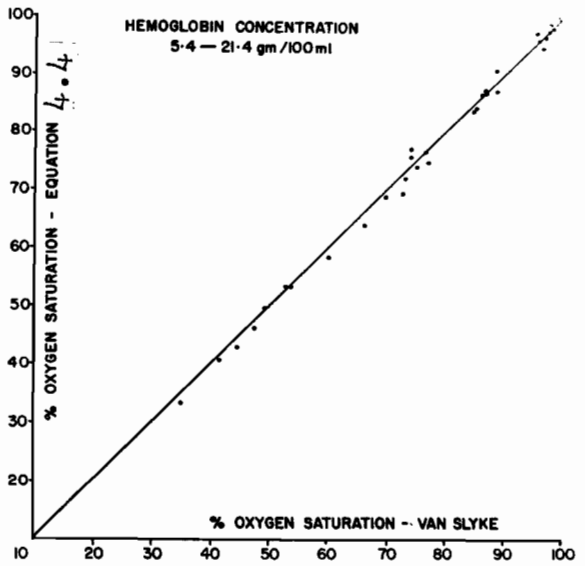

Fig. 4.7. Continued. Oxygen saturation obtained from the one wavelength method, equation 4.3, (c), and from the two wavelength method, equation 4.4, (d), versus oxygen saturation obtained by Van Slyke analysis, at a sample depth of 0.071 cm.

(c) One wavelength method: the standard deviation of the differences is $\pm$1.07%.

(d) Two wavelength method: the standard deviation of the differences is $\pm$1.37%.

(Figures 4.7c and 4.7d were reprinted from J. Lab. Clin. Med. 65: 153, 1965).

TABLE 4.4. Comparison of oxygen saturation values obtained by Van Slyke analysis with those obtained by calculation from equations 4.3 and 4.4

Sample Depth (cm)	Hemoglobin Concentration gm/100ml	mM/l	Oxygen Saturation Van Slyke	Eq. 4.3	Eq. 4.4
0.027	8.6	5.2	96.20	96.10	96.20
			86.96	86.39	87.18
			67.27	65.57	66.53
			57.25	55.76	56.81
			47.15	46.26	47.39
	9.1	5.4	88.81	87.08	88.73
			78.19	77.38	78.68
			67.49	64.01	65.48
			56.54	56.05	57.61
			45.55	45.00	46.72
	9.2	5.5	97.32	97.49	97.78
			86.86	90.24	90.54
			76.88	78.08	78.42
			63.91	65.08	65.51
			52.23	55.42	55.88
			40.55	41.39	41.92
	9.8	5.7	95.90	98.59	97.37
			73.13	71.57	69.87
			61.03	63.96	62.14
			49.01	45.36	43.21
	11.8	7.1	96.90	96.83	93.05
			86.84	88.18	83.90
			65.44	64.79	59.13
			55.32	57.07	50.96
			43.61	43.54	36.64
	14.2	8.5	97.01	97.17	96.11
			83.92	85.03	83.72
			70.74	72.78	71.22
			57.90	61.48	59.69
			31.23	37.45	35.16
	17.6	10.6	98.00	97.50	98.12
			90.55	89.50	90.23
			82.58	80.35	81.21
			66.40	65.16	66.22
			58.26	55.16	56.36
	19.9	11.9	97.00	98.57	96.69
			83.52	83.84	81.27

TABLE 4.4. Continued

Sample Depth (cm)	Hemoglobin Concentration gm/100ml	mM/l	Oxygen Saturation Van Slyke	Eq. 4.3	Eq. 4.4
0.027			56.25	58.74	54.97
			41.42	40.89	36.27
			27.35	29.62	24.46
	Mean		69.46	69.76	68.74
	S.D.D.[a] ($\%O_2$)			±2.08	±2.61
0.071	5.5	3.3	96.17	96.22	96.05
			86.46	87.29	87.10
			75.51	75.05	74.82
			53.00	55.17	54.89
			41.60	43.07	42.76
	6.7	4.0	97.01	96.49	94.95
			87.17	88.79	87.08
			77.10	78.81	76.98
			66.37	66.14	63.92
			44.69	45.59	42.90
	8.2	4.9	95.92	95.58	97.36
			89.11	88.82	91.05
			74.59	74.78	77.44
	9.8	5.9	100.00	99.91	100.04
			89.23	87.09	87.51
			77.54	74.93	75.09
			53.79	53.34	53.52
	12.4	7.4	97.88	97.22	96.83
			73.66	72.24	71.62
			49.30	50.25	49.43
	13.7	8.2	97.50	97.79	96.72
			84.50	85.84	84.46
			70.00	71.36	69.62
			60.20	60.59	58.57
			47.50	48.50	46.17
			34.90	35.99	33.34
	20.8	12.4	99.00	98.38	98.27
			84.90	84.25	84.06
			70.20	69.37	69.09
	21.5	12.8	98.78	98.67	99.37

TABLE 4.4. Continued

Sample Depth (cm)	Hemoglobin Concentration gm/100ml mM/l	Oxygen Saturation		
		Van Slyke	Eq. 4.3	Eq. 4.4
0.071		86.96	86.74	87.66
		74.64	75.25	76.38
	Mean	76.10	76.23	75.78
	S.D.D. ($\%O_2$)		±1.09	±1.37

[a]Standard deviation of the differences between experimental and calculated values = $\left[1/(n-1) \sum(d - \bar{d})^2\right]^{\frac{1}{2}}$.

in saturation from 27.4% to 98%. The standard deviations of the differences between oxygen saturation values obtained using the whole blood equations and those obtained by single Van Slyke analyses were: one wavelength equation ±2.08%; two wavelength equation ±2.61%. At a sample depth of 0.071 cm, thirty-two samples were analyzed; the samples ranged in hemoglobin concentration from 5.4 to 21.4 gm/100 ml, and in saturation from 34.9% to 100%. At this sample depth, the standard deviations of the differences were: one wavelength equation ±1.09%; two wavelength equation ±1.37%. The results obtained at 0.071 cm sample depth show a much higher degree of accuracy than those at 0.027 cm. The error was higher at 0.027 cm sample depth for two reasons. First, there was more variability in

sample depth as a result of reassembling the sample cuvette for each experiment. Second, the absolute error in optical density units was approximately the same at both sample depths, but at the smaller sample depth, the error represented a larger fraction of the total optical density.

To avoid the time consuming calculations, a nomogram (144) was constructed for the two wavelength equation for a sample depth of 0.071cm. It is shown in Fig. 4.8.

In order to construct the nomogram, the equation was rearranged as follows:

$$\%O_2 = f_1\ (OD_{805}) - f_2\ (OD_{633})\ f_3\ (OD_{805}) \qquad 4.5$$

Two linear scales were drawn 20 units apart, one representing percent oxygen saturation and the other representing optical density at 6330 A. Both these scales were arbitrarily set to 20 units. The Cartesian coordinates of the curve for optical density at 8050 A were then obtained according to the following equations, using zero percent on the percent oxygen saturation scale as the origin:

$$X = \frac{400\ f_3\ (OD_{805})}{20\ f_3\ (OD_{805}) + 10} \qquad 4.6$$

$$Y = \frac{200\ f_1\ (OD_{805})}{20\ f_3\ (OD_{805}) + 10} \qquad 4.7$$

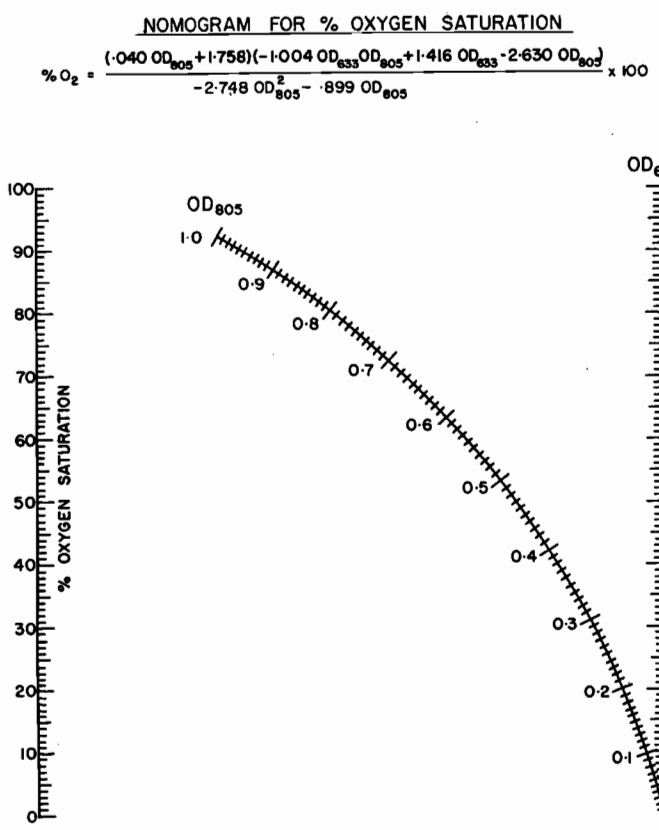

Fig. 4.8. Nomogram for percent oxygen saturation from equation 4.4, for two wavelengths. A line joining optical density at 6330 A on the scale at the right and optical density at 8050 A on the curved scale in the middle crosses the scale at the left to give percent oxygen saturation. (Reprinted from J. Lab. Clin. Med. 65: 153, 1965).

In order to compare our newly developed method with the previous technique of relating OD_R/OD_{IR} to percent oxygen saturation determined by a reference method, we have used the optical density values obtained in the present study to calculate oxygen saturation according to both techniques. Previously, the error encountered in the range of hemoglobin concentrations from 9 to 21 gm/100 ml was of the order of $\pm 2\%$, but it was greatly increased at low hemo-

globin concentrations. This is demonstrated in Fig. 4.9. The closed circles refer to the previously used technique. The crosses show the mean absolute error in percent using the method described in this chapter. It can be seen that the degree of accuracy achieved by the present method is considerably greater than that obtained with previous whole blood oximetric techniques, especially at low hemoglobin concentrations.

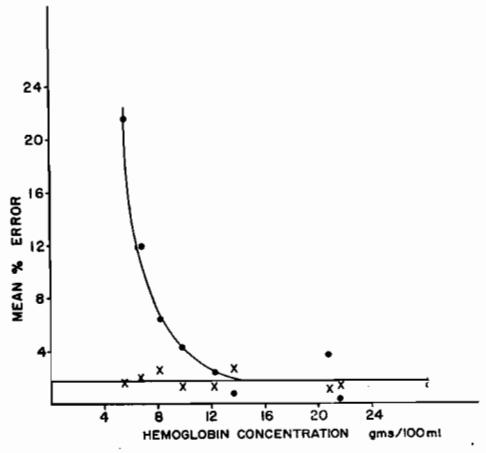

Fig. 4.9. Mean percent error versus hemoglobin concentration. Closed circles refer to the previously used method of standardization, and show greatly diminishing accuracy with decreasing hemoglobin concentration. The crosses refer to the method described in this study, showing that the error is fairly uniform over the entire range of hemoglobin concentrations studied. (Reprinted from J. Lab. Clin. Med. 65: 153, 1965).

E. Conclusions

The observations of Kramer et al (129, 131) on the light transmittance of nonhemolyzed whole blood have been verified with one major difference - the linear relationship between optical density and oxygen saturation consisted of a family of parallel lines in the present study, rather than divergent lines as obtained by Kramer and by Hickam and Frayser (97). We have concluded that the cause of this discrepancy is the loss of a large fraction of the scattered light in the conventional spectrophotometric techniques employed by these authors. In the present study, the use of the diffusing plate technique permitted a large quantity of the forward scattered light to be collected.

The nonlinear relationship between total hemoglobin concentration and optical density was similar to that obtained by Kramer, by Drabkin and Singer (52), and by Hickam and Frayser. This nonlinearity shows that the former whole blood oximetric techniques in which the data were treated according to the method for hemolyzed blood were theoretically unjustified and failed to provide sufficiently accurate results. By recognizing that this relationship deviates from Beer's law, and expressing it mathematically, we obtained a new method for estimating oxygen saturation.

An initial standardization of the system is required

which is analogous to that required by the spectrophotometric technique for hemolyzed blood, such as that of Nahas (168) using the Beckman DU spectrophotometer. All that is required by the present method is the establishing of three curves of extinction coefficients versus hemoglobin concentration, one for oxygenated whole blood at a wavelength in the red region of the spectrum, one for reduced blood at the same wavelength, and one for whole blood at an isobestic wavelength. The latter curve may be obtained at the same time as the other curves since readings are made simultaneously at both wavelengths on a double beam galvanometer.

Although the equation for the oxygen saturation of nonhemolyzed blood at two wavelengths contains several constants, its simple form permitted the construction of a nomogram to avoid tedious calculations.

This method of estimating the oxygen saturation of whole nonhemolyzed blood has several advantages: (a) it is independent of hemoglobin concentration, (b) it shows a high degree of accuracy over the entire range of oxygen saturations tested (27% to 100%), (c) it shows an accuracy which is the same over the whole range of hemoglobin concentrations tested (5.5 to 21.5 gm/100 ml), and (d) it does not require comparison with standard methods of determining oxygen saturation.

V. FACTORS INFLUENCING THE "APPARENT" OPTICAL DENSITY OF SCATTERING SUSPENSIONS

A. Introduction

Instruments for measuring light scattering fall into two main categories. One type measures the light scattered at discrete angles and requires that both light source and detector be highly collimated. Such measurements are meaningful only for single scattering suspensions. The second type of instrument is the integrating sphere spectrophotometer; this instrument integrates the light transmitted and scattered by either single or multiple scattering suspensions.

Conventional spectrophotometers do not fall into either category since the detector is not collimated, nor does it collect all the light scattered into the forward hemisphere. In a conventional spectrophotometer, a maximum value of optical density is obtained if the incident illumination is collimated and the detector is placed sufficiently far away from the sample that very little, if any, of the scattered light is collected. Keilin and Hartree (121) showed that as the detector is moved closer to the sample so that more scattered light is collected, the optical density diminishes. Thus, the optical density of a scattering suspension depends to a great extent upon the geometrical arrangement of the measuring system. For this reason, the term optical density

is often preceeded by the adjective "apparent" when the term is used with reference to a scattering suspension.

The inadequacy of conventional spectrophotometers for studying scattering suspensions has frequently been commented upon. Drabkin and Singer (52) considered that it was impossible to relate their results to a light scattering theory because such a large fraction of the scattered light was not measured by their spectrophotometer. It is well known that unless all the light scattered by a scattering suspension of a pigmented material is collected, its absorption spectrum is flattened and shifted towards higher optical density values.

An approximation of the integrating sphere technique may be obtained using a conventional spectrophotometer if diffusing plates are placed on the light source side or the detector side of both the blank and the sample chambers. Shibata et al (206, 207) showed that the diffusing plate technique resulted in an increase in the proportion of scattered light received by the detector; in their studies of algae and red blood cell suspensions, the optical density levels of the absorption spectra were greatly reduced and the definition was markedly increased. Shibata's theory for the diffusing plate technique was outlined in Chapter III, Section C2a. In Chapter IV, Section D, we noted that studies made at a sample depth of 0.027 cm resulted in different values of optical density for nonhemolyzed blood when the

lamp was moved closer to the diffusing plate; however, in the same series of experiments, the results for hemolyzed blood were independent of the measuring system. This finding emphasizes the point that the diffusing plate technique is only an approximation of the theoretically sound integrating sphere method.

The geometry of the measuring system not only affects the results numerically but may alter the relationships between optical density and the various parameters of the scattering suspension. We noted, in the previous chapter, that the relationship between the optical density of nonhemolyzed blood and oxygen saturation obtained using conventional spectrophotometric techniques differed from that obtained when the diffusing plate technique was used. In the former case, the relationship consisted of a family of divergent lines, while in the latter case, the lines were parallel.

We proposed to make a detailed investigation of the dependence of the apparent optical density of nonhemolyzed blood and of scattering suspensions on the geometry of the measuring system when both conventional spectrophotometric and diffusing plate techniques are employed.

The effect of flow on the optical density has been the subject of considerable controversy, as we pointed out earlier (Chapter II, Section D1b). Studies have been per-

formed on blood flowing through tubes (13, 221) and through plane parallel sample chambers (244). Conflicting results have been obtained in these studies; some of the results suggest that optical density increases as flow rate increases while others suggest the opposite. Two main causes for the flow effect have been suggested - axial accumulation and particle orientation. In the present study we measured the changes in optical density produced by varying flow rate.

In this chapter we also studied the effect of the formation of rouleaux on the optical density of nonhemolyzed blood.

B. Material and Methods

In order to eliminate the possibility that the observed changes in optical density might be due to differences in the light transmitting properties of the interference filters under various experimental conditions, two sets of experiments were carried out (a) on nonscattering solutions, hemolyzed blood or aqueous solutions of Coomassie blue dye, and (b) on scattering materials, nonhemolyzed blood and scattering emulsions of n-butyl benzoate (Eastman Kodak) in water.

All blood samples were fully oxygenated by rotating 50 ml aliquots in a 1,000 ml tonometer for 20 minutes. A

slow stream of 5% CO_2 in oxygen was first bubbled through water and then passed continuously through the tonometer. Hemoglobin concentration was determined by the cyanmethemoglobin method (49).

The butyl ester of benzoic acid, n-butyl benzoate, is a colorless oil. Light absorbing as well as nonabsorbing emulsions were prepared. Emulsions of n-butyl benzoate in water were prepared using Tween 20 (Atlas Chemical Industries Canada, Ltd.) as an emulsifying agent. The mixture was ultrasonicated in 100 ml aliquots for 10 minutes. The resulting particles were spherical with diameters ranging from 1 to 4 microns. In order to make a light absorbing emulsion, Sudan blue stain was added to the n-butyl benzoate at a concentration of 25 mg/l and the emulsions were then prepared as described above. Sudan blue is completely insoluble in water and, consequently, it is entirely restricted to the emulsified particles. Sudan blue was scanned in the Beckman DU spectrophotometer (Fig. 5.1). Since it shows two absorption peaks, one at 6000 A and one at 6400 A, it is a suitable pigment for study in the cuvette oximeter where the maximum transmission of the red filtered photocell is 6330 A.

Preliminary experiments were performed using the measuring system described in Chapter IV for the estimation of

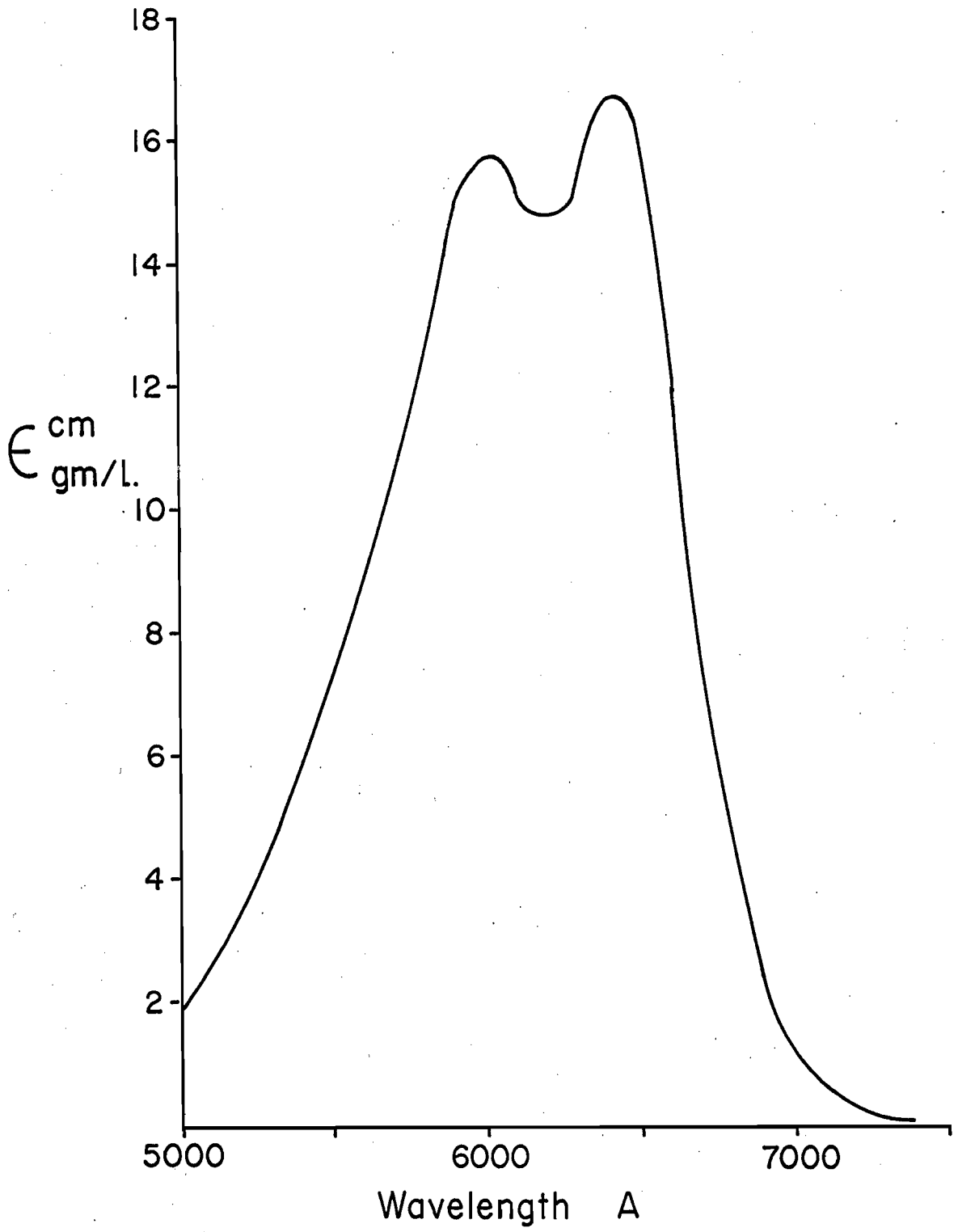

Fig. 5.1. Scan of Sudan blue stain. The extinction coefficient is expressed in terms of 1 cm path length and 1 gm/l concentration.

oxygen saturation in nonhemolyzed blood.

For the final experiments, a new light source was designed to provide a constant and uniform source of illumination. The light source is shown in Fig. 5.2. It can provide either collimated or diffuse illumination. Light from a 6 volt, 10 watt lamp is rendered parallel for collimated illumination. For diffuse illumination, ground glass plates, separated by 0.75 cm are placed at the base of the lamp house. The optical density of nonhemolyzed blood was found to be smaller if three, rather than one, or two, diffusing plates were used.

Sample depth and flow rate were held constant at 0.025 cm and 3.8 ml/minute, respectively, for the experiments in Sections 1,2, and 3. A small sample depth was chosen for most of the experiments of this chapter since previous experiments had shown that variations in optical density due to variations in the geometry of the measuring system were more pronounced as sample depth was decreased.

C. Experimental Results

1. Instrumental Variations

To ascertain that the measured values of optical density were independent of the geometry of the system and of light intensity levels, the experiments shown in Outlines 1a and 1b were performed. An additional aim of these experiments was

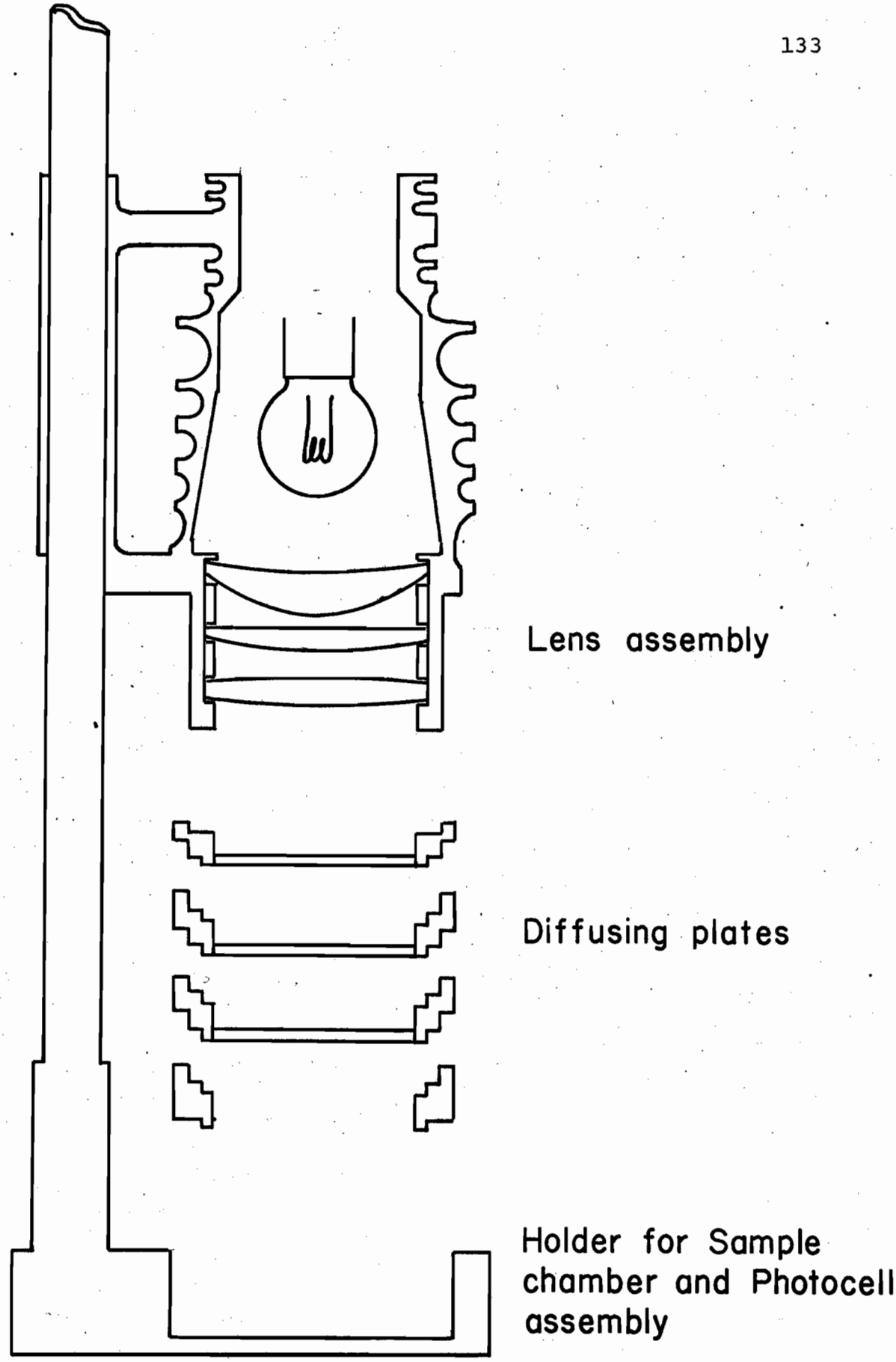

Fig. 5.2. Light source for cuvette oximeter. Diffusing plates may be removed for collimated incidence.

OUTLINE I. INSTRUMENTAL VARIATIONS

Variable	Ia. ILLUMINANCE	
Experiments	PRELIMINARY	FINAL
Material	DYE SOLUTIONS BLOOD, NONHEMOLYZED	
Incident Illumination	DIFFUSE	DIFFUSE COLLIMATED
Results	Table 5.1a	

Variable	Ib. PHOTOCURRENT	
Experiments	PRELIMINARY	FINAL
Material	DYE SOLUTIONS BLOOD, NONHEMOLYZED	
Incident Illumination	DIFFUSE	DIFFUSE COLLIMATED
Results	Table 5.1b	

to make certain that the photocell response was linear with light intensity over a wide range.

Ia. Illuminance. Lamp voltage was varied in order to change the illuminance at the detector. The illuminance (lumen/ft^2) was measured using a photographic light meter. There were no significant differences in apparent optical density although illuminance was varied over wide ranges, from 9 to 180 lumen/ft^2 for diffuse incidence, and from 95 to 310 lumen/ft^2 for collimated incidence ($0.1 < p < 0.2$), as shown in Table 5.1a.

Ib. Photocurrent. As a further check to establish that the response of the instrument was independent of the experimental variations, the photocurrent for the incident light was set at two different values, on successive measurements, by reducing the photocurrent to one half of its initial value for the second reading. The results of Table 5.1b show that, again, no significant differences were observed ($0.8 < p < 0.9$).

2. Geometrical Variations

IIa. Distance between the light source and the diffusing plate. Only preliminary experiments were performed to investigate the effect of the distance between the lamp and the diffusing plate on optical density since the improved light source for the final experiments has a colli-

TABLE 5.1a. Instrumental variations: illuminance

Material	Incident Illumination	6330 A				8050 A			
		4.0 Volts		5.2 Volts		4.0 Volts		5.2 Volts	
		Illum.[a]	O.D.	Illum.	O.D.	Illum.	O.D.	Illum.	O.D.
Preliminary Experiments									
Dye Solution, 197 mg/l	Diffuse	9	0.116	34	0.122				
		16	0.126	59	0.126				
		50	0.121	180	0.116				
Blood[b]									
9.2 gm/100 ml	Diffuse	50	0.213	155	0.208	50	0.174	155	0.168
9.4 "		10	0.394	32	0.388	10	0.260	32	0.268
9.4 "		16	0.438[c]	59	0.449	16	0.278	59	0.268
11.7 "		10	0.482	36	0.494	10	0.309	36	0.291
11.7 "		50	0.227	180	0.212	50	0.191	180	0.187
Final Experiments									
Dye Solution, 197 mg/l	Diffuse	22	0.116	77	0.111				
	Collimated	95	0.117	310	0.115				
Blood[b], 11.4 gm/100 ml	Diffuse	22	0.446	77	0.452	22	0.304	77	0.300
	Collimated	95	0.592	310	0.585	95	0.386	310	0.381

[a] Illuminance was measured in lumen/ft.^{2}

[b] Nonhemolyzed blood.

[c] Different values of optical density at the same hemoglobin concentration were obtained by varying the geometry of the system as described in Section C2, IIa.

TABLE 5.1b. Instrumental variations: Photocurrent

Material	Incident Illumination	Optical Density			
		6330 A		8050 A	
		Photocurrent		Photocurrent	
		x	2x	x	2x
Preliminary Experiments					
Dye Solution 197 mg/l	Diffuse	0.126	0.126		
		0.120	0.125		
		0.119	0.118		
Blood, Nonhemolyzed 9.4 gm/100 ml	Diffuse	0.439	0.448	0.272	0.274
		0.389	0.392	0.269	0.259
11.7 "		0.487	0.488	0.303	0.298
		0.229	0.219	0.191	0.189
Final Experiments					
Blood, Nonhemolyzed 11.4 gm/100 ml	Diffuse	0.588	0.589	0.385	0.382
	Collimated	0.444	0.454	0.301	0.304

OUTLINE II. GEOMETRICAL VARIATIONS

Variable	IIa. DISTANCE BETWEEN LAMP AND DIFFUSING PLATE
Experiments	PRELIMINARY
Material	BLOOD, HEMOLYZED BLOOD, NONHEMOLYZED
Incident Illumination	DIFFUSE
Results	Table 5.2a Fig. 5.3

Variable	IIb. DISTANCE BETWEEN LIGHT SOURCE AND SAMPLE CHAMBER	
Experiments	PRELIMINARY	FINAL
Material	DYE SOLUTIONS	BLOOD, NONHEMOLYZED
Incident Illumination	DIFFUSE	DIFFUSE COLLIMATED
Distance	0.6 to 2.0 cm	0.5 to 4.9 cm
Results	Table 5.2b	

Variable	IIc. DISTANCE BETWEEN SAMPLE CHAMBER AND DETECTOR	
Experiments	PRELIMINARY	FINAL
Material	DYE SOLUTIONS	BLOOD, NONHEMOLYZED
Incident Illumination	DIFFUSE	DIFFUSE COLLIMATED
Distance	2.3 to 5.5 cm	
Results	Table 5.2c	

mated beam of light while the light in the original lamp house is uncollimated. Measurements were made on hemolyzed and nonhemolyzed blood. Fig. 5.3 shows the optical density of both these materials plotted against the distance of the lamp from the diffusing plate. While there was no change in optical density with hemolyzed blood, with nonhemolyzed blood there were increases of 77.7% and 55.5% in optical density at 6330 A and 8050 A, respectively, when the lamp was moved from 0.8 cm to 8.1 cm from the diffusing plate at the base of the lamp house. This experiment demonstrates that the diffusing plate technique does not provide an absolute method of measuring optical density since the results depend on the way in which the diffusing plate is illuminated and on the diffusing properties of the diffusing plate.

IIb. Distance between the light source and the sample. To see whether the distance between the diffusing plate and the sample chamber affected the apparent optical density of the samples, this distance was varied by inserting metal tubes between the base of the lamp house and the sample chamber. The metal tubes were coated inside with nonreflecting black paint.

Preliminary experiments were carried out using a solution of Coomassie blue dye as the test substance and final

TABLE 5.2a. Geometrical variations: Distance between the light source and the diffusing plate

Material	Incident Illumination	Distance (cm)	Optical Density	
			6330 A	8050 A
Preliminary Experiments				
Blood, Hemolyzed 11.5 gm/100ml	Diffuse	0.8	0.036	0.030
		1.5	0.039	0.030
		2.7	0.039	0.030
		4.0	0.037	0.029
		5.7	0.037	0.029
		6.8	0.035	0.031
		7.5	0.036	0.027
		8.2	0.039	0.030
Blood, Nonhemolyzed 11.5 gm/100ml	Diffuse	0.8	0.323	0.202
		1.2	0.361	0.222
		2.0	0.393	0.240
		3.3	0.454	0.261
		4.8	0.506	0.282
		5.8	0.520	0.296
		6.5	0.546	0.294
		7.0	0.555	0.301
		7.6	0.567	0.306
		8.1	0.574	0.314

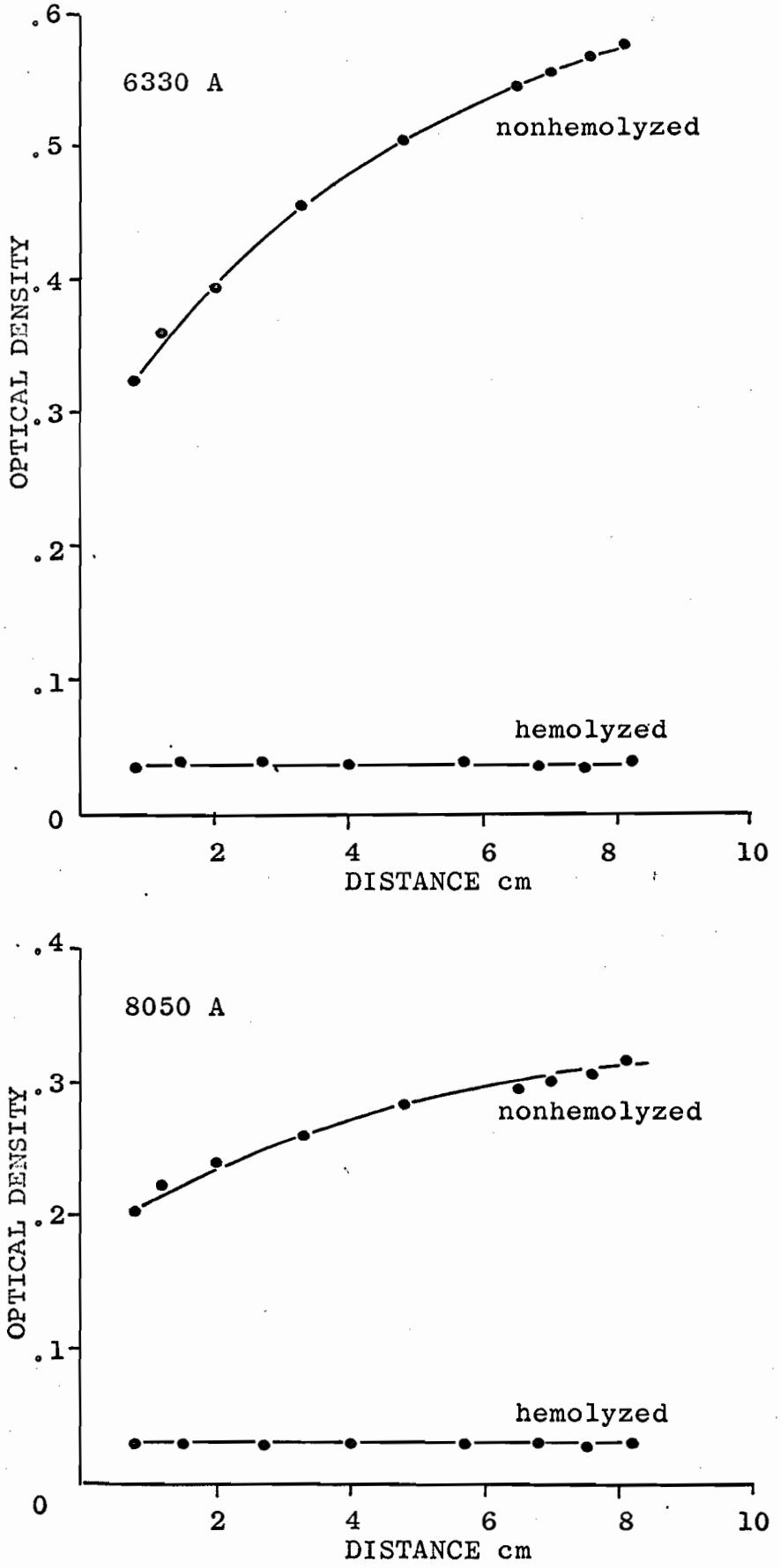

Fig. 5.3. Optical density is plotted against d, the distance of the uncollimated light source from the diffusing plate. Sample depth is 0.025 cm, hemoglobin concentration is 11.5 gm per 100 ml, and flow rate is 3.82 ml per minute.

experiments were performed on whole nonhemolyzed blood. The results are shown in Table 5.2b. No differences in optical density were observed when a solution of Coomassie blue dye was the test substance. However, the results obtained on nonhemolyzed blood showed that optical density increased systematically as the diffusing plate was moved away from the sample; a total increase of 6% to 8.5% of the initial optical density value for a ten-fold change in distance was obtained. This is not surprising since it may be expected that the light becomes less diffuse as a unit of effective surface area is moved away from the source. This experiment again demonstrates that the diffusing plate technique does not provide absolute optical density values.

With collimated incidence, optical density showed a slight systematic decrease in optical density as the collimated light source was moved away from the sample. The changes were -1% and -3.3% of the initial value at 6330 A and 8050 A, respectively. A strictly parallel beam of light maintains the same intensity at any distance from the source, but perfectly collimated light is difficult to obtain. The present source showed slight divergence, and decreasing optical density is to be expected under these circumstances.

TABLE 5.2b. Geometrical variations: Distance between the light source and the sample

Material	Incident Illumination	Distance (cm)	Optical Density	
			6330 A	8050 A
Preliminary Experiments				
Dye Solution 197 mg/l	Diffuse	0.6	0.118	
		2.0	0.118	
Final Experiments				
Blood, Nonhemolyzed 11.4 gm/100ml	Diffuse	0.5	0.488	0.324
		2.7	0.504	0.328
		3.7	0.515	0.333
		4.9	0.529	0.333
	% change from initial value:		+8.5	+6.0
	Collimated	0.5	0.621	0.405
		2.7	0.620	0.392
		3.7	0.616	0.390
		4.9	0.614	0.392
	% change from initial value:		-1.0	-3.3

IIc. Distance between the sample and the detector. Keilin and Hartree showed that the apparent optical density of red cell suspensions varied with the distance between the sample and the detector when conventional spectrophotometric techniques were used (121). However, according to Shibata's theory for the diffusing plate technique (described in Chapter III), this distance should have no effect on optical density when a diffusing plate is used.

The normal distance in our system between the sample and detector is 2.27 cm. This distance was doubled using the same spacers as in Section IIb. Preliminary experiments on solutions of Coomassie blue dye showed no differences in optical density. Final experiments with nonhemolyzed blood showed that even with diffuse illumination, the apparent optical density increased 32% at 6330 A, and 60% at 8050 A when the distance between the sample chamber and the detector was doubled. With collimated incidence the increases were much larger - increases of 75% and 123% at 6330 A and 8050 A, respectively. Even with diffuse illumination, the distance between sample and detector is very important in determining the optical density value, although the differences are much smaller than those obtained with collimated light.

TABLE 5.2c. Geometrical variations: Distance between the sample and the detector

Material	Incident Illumination	Distance (cm)	Optical Density	
			6330 A	8050 A
Preliminary Experiments				
Dye Solution 197 mg/l	Diffuse	2.3	0.118	
		5.5	0.117	
Final Experiments				
Blood, Nonhemolyzed 11.4 gm/100ml	Diffuse	2.3	0.488	0.324
		5.5	0.642	0.517
	% change from initial value:		+31.7	+59.6
	Collimated	2.3	0.621	0.404
		5.5	1.088	0.900
	% change from initial value		+75.2	+122.8

3. Edge Effects

Edge effects always present a problem in the study of light scattering materials. For edge effects to be negligible, the sample must be of infinite extent in the plane perpendicular to the direction of incidence (200, 213). This is definitely not the case in the cuvette oximeter since the sample area is smaller than that of the light source and slightly larger than the detector area. In order to gain a qualitative idea of the importance of the edge effects in determining the optical density of a scattering suspension, the following experiments were undertaken.

We mentioned in Chapter IV that a thin metal black disc with a central rectangular aperture was used in order to prevent light from reaching the detector without passing through the sample. Additional discs were constructed with apertures of 0.2 cm, 0.6 cm, and 1.0 cm. The length of each aperture was maintained constant at 2.4 cm.

IIIa. Variation of the sample area and the detector area. In the first series of experiments, the aperture of the sample was varied from 0.6 to 1.0 cm while the detector aperture was fixed first at 1.0 cm and then at 0.2 cm.

Preliminary experiments on a solution of Coomassie blue dye showed that the optical density did not vary under the various experimental conditions imposed, as shown in Table 5.3a.

The results for the final experiments, performed on

OUTLINE III. EDGE EFFECTS

Variable	IIIa. SAMPLE AREA AND DETECTOR AREA	
Experiments	PRELIMINARY	FINAL
Material	DYE SOLUTIONS	BLOOD, NONHEMOLYZED EMULSIONS
Incident Illumination	DIFFUSE	DIFFUSE COLLIMATED
Results	Table 5.3a	

Variable	IIIb. RELATIVE ALIGNMENT OF SAMPLE AND DETECTOR	
Experiments	PRELIMINARY	FINAL
Material	DYE SOLUTIONS	BLOOD, NONHEMOLYZED EMULSIONS
Incident Illumination	DIFFUSE	DIFFUSE COLLIMATED
Results	Table 5.3b	

nonhemolyzed blood and on nonabsorbing emulsions, were qualitatively the same for both collimated and diffuse incidence although the differences were much larger when the incident light was collimated.

When the detector aperture was 1.0 cm, the optical density of both nonhemolyzed blood and the emulsion was the same whether the sample aperture was 0.6 cm or 1.0 cm. Thus, when the detector area was larger than or equal to the sample area, further reduction in sample area had no effect.

However, when the width of the detector aperture was only 0.2 cm, the optical density was much smaller than it was when the detector aperture was 1 cm, particularly when the sample area was as large as possible. Upon reducing the detector aperture from 1.0 to 0.2 cm, the optical density was reduced an average of 3.3% and 7.2% for diffuse and collimated incidence, respectively, when the sample aperture was 0.6 cm. With a sample aperture of 1.0 cm, these changes were 13.8% and 36.9%. Therefore, optical density was reduced when the detector aperture was made smaller than the sample aperture, and under this condition, the larger the sample area was, the greater was the decrease in optical density. This means that minimum optical density values can be approached by using a small detector area and a very large sample area.

TABLE 5.3a. Edge effects: Variation of the sample area and the detector area

Material	Incident Illumination	Apertures (cm)		Optical Density	
		Detector	Sample	6330 A	8050 A
Preliminary Experiments					
Dye Solution 197 mg/l	Diffuse	1.0	0.6	0.118	
			1.0	0.119	
		0.2	0.6	0.122	
			1.0	0.120	
Final Experiments					
Blood, Nonhemolyzed 8.4 gm/100ml	Diffuse	1.0	0.6	0.353	0.239
			1.0	0.350	0.231
		0.2	0.6	0.338	0.231
			1.0	0.306	0.188
	Collimated	1.0	0.6	0.447	0.282
			1.0	0.456	0.290
		0.2	0.6	0.392	0.252
			1.0	0.298	0.138
Emulsion 2.5%	Diffuse	1.0	0.6	0.625	0.470
			1.0	0.622	0.453
		0.2	0.6	0.602	0.461
			1.0	0.540	0.405

TABLE 5.3a. Continued

Material	Incident Illumination	Apertures (cm)		Optical Density	
		Detector	Sample	6330 A	8050 A
Emulsion 2.5%	Collimated	1.0	0.6	0.814	0.592
			1.0	0.810	0.594
		0.2	0.6	0.780	0.582
			1.0	0.629	0.404

IIIb. Relative alignment of the sample and the detector. When a 0.2 cm aperture is placed over the photocells, the detector may be considered as a slit relative to the sample. Since blood cells are large particles with respect to light scattering, they should not scatter uniformly in all directions and optical density may be expected to vary as the detector slit is moved relative to the sample.

The sample aperture was held constant at 1.0 cm. Optical density was measured when the 0.2 cm aperture was placed at the edge of the detector and again when the aperture was at the center of the detector. The apparent optical density measured under these circumstances was compared with the control value of optical density, obtained with the whole detector exposed.

Preliminary experiments on nonhemolyzed blood showed that the optical density of a clear, nonscattering solution did not depend on which part of the detector was exposed.

In the final experiments on blood and on a scattering emulsion, there were very large differences between values of optical density measured when the 0.2 cm detector aperture was in the optical axis and values obtained when the detector slit was off to the edge. When compared with the control values, the optical density was very much reduced by exposing only the central area of the detector, as the results of Table 5.3b show, and considerably in-

TABLE 5.3b. Edge effects: Relative alignment of the sample and the detector

Material	Incident Illumination	Detector Aperture (cm)	Position of Detector Aperture	Optical Density 6330 A	Optical Density 8050 A
			Preliminary Experiments		
Dye Solution, 197 mg/l	Diffuse	1.0		0.123	
		0.2	center	0.120	
		0.2	edge	0.122	
			Final Experiments		
Blood, Nonhemolyzed, 9.9 gm/100 ml	Diffuse	1.0		0.404	0.267
		0.2	center	0.344	0.223
		0.2	edge	0.436	0.351
	Collimated	1.0		0.532	0.352
		0.2	center	0.358	0.192
		0.2	edge	0.660	0.497
Emulsion, 2.5%	Diffuse	1.0		0.622	0.453
		0.2	center	0.540	0.405
		0.2	edge	0.616	0.526
	Collimated	1.0		0.810	0.594
		0.2	center	0.629	0.404
		0.2	edge	1.004	0.794

creased when only the edge of the detector was exposed. When the 0.2 cm aperture was placed over the central part of the detector, so that primarily forward scattered light was collected, the mean reductions in optical density were 13.8% and 33.2% for diffuse and collimated incidence, respectively, from the control value. With the aperture placed at the edge of the detector, the changes amounted to increases of 14.9% and 38% over the control value, for diffuse and collimated incidence, respectively.

Evidently, when the detector is off the axis of the system, it collects less of the light scattered in forward directions and a greater proportion of the laterally scattered light. Thus, the light scattered in the direction of incidence constitutes the greatest part of the light being scattered. These experiments show that red blood cells scatter light according to large particle optics - that is, the forward component of the scattered light is by far the largest.

4. Flow Effect and Rouleaux Formation

IVa. Flow rate. Preliminary measurements were made at two sample depths, 0.025 cm and 0.071 cm, and at two flow rates, 3.8 ml/minute and 7.6 ml/minute. Diffuse incident light was used; hemoglobin concentration was varied.

The results (Table 5.4a) showed no differences at 0.071 cm,

OUTLINE IVa. FLOW RATE

Experiments	PRELIMINARY	FINAL
Material	BLOOD, NONHEMOLYZED	BLOOD, NONHEMOLYZED EMULSIONS, NONPIGMENTED EMULSIONS, PIGMENTED
Incident Illumination	DIFFUSE	DIFFUSE
Results	Table 5.4a	

OUTLINE IVb. ROULEAUX

Experiments	FINAL
Material	BLOOD, NONHEMOLYZED
Incident Illumination	DIFFUSE COLLIMATED
Results	Table 5.4b

TABLE 5.4a. Flow rate

Material	Incident Illumination	Sample Depth (cm)	Optical Density									
			6330 A					8050 A				
			Flow Rate (ml/minute)					Flow Rate (ml/minute)				
			1.9	3.8	7.6	15.3	38.2	1.9	3.8	7.6	15.3	38.2
Preliminary Experiments												
Blood, Nonhemolyzed	Diffuse	0.025										
2.5 mM/l			.212	.201				.164	.157			
3.8			.292	.288				.229	.220			
5.4			.369	.350				.285	.271			
6.4			.400	.384				.310	.297			
8.8			.469	.441				.353	.340			
	Diffuse	0.071										
1.5			.280	.280				.192	.192			
5.1			.594	.594				.439	.442			
7.5			.701	.702				.528	.529			
10.3			.824	.826				.611	.612			
11.3			.854	.854				.629	.633			
Final Experiments												
Blood, Nonhemolyzed												
6.8 mM/l	Diffuse	0.025	.431	.411	.401	.379	.369	.264	.254	.251	.239	.234
6.8 mM/l	Collimated	0.025	.450	.440	.412	.395	.377	.247	.236	.223	.205	.199

TABLE 5.4a. Continued

Material	Incident Illumination	Sample Depth (cm)	Optical Density									
			6330 A					8050 A				
			Flow Rate (ml/minute)									
			1.9	3.8	7.6	15.3	38.2	1.9	3.8	7.6	15.3	38.2
Emulsion, 10%	Diffuse	0.025	.799	.799	.799	.799	.799	.632	.632	.632	.632	.632
Emulsion, Pigmented 2.5%	Diffuse	0.025	.632	.632	.632	.633	.632	.422	.421	.422	.423	.421

but, at 0.025 cm optical density was significantly lower at the higher flow rate ($p > 0.001$).

For the final experiments, the smaller sample depth, 0.025 cm, was chosen. Using both diffuse and collimated incidence, measurements were made at one hemoglobin concentration while flow rate was varied from 1.9 to 38.2 ml/minute. Measurements were also made on nonpigmented and pigmented emulsions using diffuse incident light. At 0.025 cm sample depth, flow rate exerts a considerable effect on the optical density of nonhemolyzed blood. The use of diffuse incident light serves to minimize this effect to some extent. On the other hand, emulsions of spherical particles showed no variation in optical density over the same wide range of flow rates. In the historical review (Chapter II) it was mentioned that there were no conclusive studies on the cause of the flow effect, although two factors were thought to be of importance; axial accumulation and particle orientation were considered to be the main causes of the flow effect. Since, in our experiments, it was the spherical emulsified particles which did not exhibit any flow effect, it would appear that orientation of the red blood cells is responsible for the changes in optical density observed when flow rate is changed. However, Wever (244) and Bayliss (13) found that the flow effect was still present

in suspensions of spherical red cells. Further investigation is necessary to see whether lecithin treated blood cells show flow dependency in our experimental system.

IVb. Rouleaux. When rouleaux formation occurs in blood, the cells suffer a redistribution in the suspending material. To see the effect on optical density of the accumulation of red blood cells to form aggregates, rouleaux formation was produced in fresh human blood by the addition of dextran. 1.5 ml of 6% dextran in normal saline was added to 15 ml of blood. Control samples were prepared by adding 1.5 ml of normal saline to blood. Rouleaux formation was confirmed by increased sedimentation rates. Microscopic examination revealed that the majority of the cells had formed rouleaux consisting of 8 to 10 cells; the range was approximaetly 4 to 20 cells. Control samples showed a few rouleaux consisting of 2 cells, but the majority of the cells were single.

Optical density showed a small but significant decrease when rouleaux were present as shown in Table 5.4b ($p > 0.001$).

D. Conclusions

We have shown that the measured transmittance or optical density of a scattering suspension is highly dependent on the conditions under which the observation is made when both conventional spectrophotometric and diffusing plate techniques are used.

TABLE 5.4b. Rouleaux

Material	Incident Illumination	Sample Depth (cm)	Optical Density			
			6330 A		8050 A	
			Control	Rouleaux	Control	Rouleaux
Final Experiments						
Blood, Nonhemolyzed						
6.1 gm/100ml	Diffuse	0.025	0.517	0.493	0.353	0.332
6.4 "			0.552	0.543	0.380	0.370
6.1 "	Collimated	0.025	0.430	0.405	0.464	0.446
6.4 "			0.722	0.709	0.501	0.491
6.1 "	Diffuse	0.071	0.969	0.954	0.718	0.708
6.4 "			0.981	0.978	0.746	0.734
6.1 "	Collimated	0.071	1.185	1.169	0.874	0.865
			$p < 0.01$		$p < 0.001$	

It is known that the diffusing plate technique results in decreased values of optical density when scattering suspensions are being studied. In the present study we have shown that the technique also greatly minimizes the effects caused by varying the geometrical parameters of the measuring system. However, the diffusing plate technique possesses several shortcomings. The optical density value is dependent upon the degree to which the light is diffused as it emerges from the diffusing plate; this is in turn determined by the diffusing properties of the plate itself and by the manner in which it is illuminated. The most important factor appears to be the distance between the sample chamber and the detector in both the diffusing plate and conventional spectrophotometric techniques. Another important consideration is the problem of edge effects. Light scattering theories are usually developed for a plane parallel slab of scattering material of infinite dimensions in the plane perpendicular to the optical axis of the measuring system. We have also found that this factor plays a very important role in determining the apparent optical density of a suspension. Variation of the position of the detector provided evidence that light scattering by blood is predominantly in the forward direction.

With both conventional spectrophotometric techniques and with the diffusing plate technique it is almost impossible

to define the quantity of scattered light being collected. In addition, the quantity which is being measured does not fall into any of the categories of optical density which were defined in Chapter III, that is - specular, single diffuse, or double diffuse density. The reason is that the detector is neither a point detector, nor is it one which subtends a solid cone angle of 180^{o}. Consequently, such systems cannot provide absolute values of transmittance or of optical density.

In the present studies an increase in flow rate from 3.8 ml/minute to 7.6 ml/minute produced no change in optical density at the larger sample depth (0.071 cm). However, at the smaller sample depth (0.025 cm), the optical density showed large reductions in optical density when flow rate was increased from 1.9 ml/minute to 38.2 ml/minute; at this sample depth the values of optical density at 3.8 ml/minute and at 7.6 ml/minute were significantly different ($p < 0.001$). The decrease in optical density with increasing flow rate was smaller when diffusing plates were used. These results indicate that the geometry of the measuring system plays an important role in the flow effect. The cause of the flow effect on optical density remains a problem to be investigated.

Rouleaux formation also caused a small decrease in

optical density. The small but significant decrease in optical density was attributed to the formation of aggregates of the pigmented particles.

In designing an instrument for the practical purpose of measuring the oxygen saturation of nonhemolyzed blood, the following points should be considered. The ideal system should provide low values of optical density at a sample depth large enough to insure repeatability and to minimize variations in optical density due to such factors as flow rate and rouleaux formation. The high optical density of nonhemolyzed blood makes a very small sample depth necessary. A compromise must be made between a very small sample depth and accuracy of measurement. A larger sample depth may be used if the diffusing plate technique is employed and the geometrical system arranged so that the maximum amount of scattered light is collected by the detector; this may be accomplished by placing the detector as near as possible to the sample and by providing a sample area much larger than the detector area. In order to keep the quantity of blood required for a determination to a minimum, a rather small flow rate is an advantage. The results have shown that a flow rate of 3.8 ml/minute is satisfactory.

VI. DEVIATIONS FROM BEER'S LAW BY NONHEMOLYZED BLOOD AND OTHER SCATTERING SUSPENSIONS

A. Introduction

Studies on the light transmitting properties of nonhemolyzed blood and red cell suspensions which have appeared in the literature were described in the historical review (Chapter II) in detail. A brief summary of these studies follows.

Extensive experiments were performed by Kramer and his colleagues (129, 131) on the relationships between the optical density of blood and oxygen saturation, total hemoglobin concentration, and sample depth (0.06 cm to 0.24 cm) at wavelengths between 6000 A and 11000 A. The studies of Drabkin and Singer (52) were concerned mainly with the relationship between optical density and total hemoglobin concentration; their measurements were made in a region of the spectrum which shows much higher light absorption, 5000 A to 6300 A, than that studied by Kramer et al.

These studies demonstrated that the relationship between optical density and oxygen saturation, at a constant hemoglobin concentration, is linear; in other words, it follows Beer's law. On the other hand, the relationship between optical density and total hemoglobin concentration

deviates from Beer's law. Verification of these findings in our laboratory was described in Chapter IV.

Kramer found that the relationship between optical density and sample depth was nonlinear. Alternatively, in their empirical equations describing the relationship between optical density and concentration, Drabkin and Singer used the product of red cell concentration times sample depth, suggesting that the optical density of nonhemolyzed blood varies linearly with sample depth. However, in their study, the majority of observations were made at a depth of 0.007 cm. Measurements at other sample depths consisted of two determinations at a depth of 1 cm and one estimation at a depth of 10 cm; these results did not prove the existence of a linear relationship between optical density and sample depth. Furthermore, Kramer demonstrated that concentration and depth are not interchangeable for nonhemolyzed blood as they are for hemolyzed blood.

Extinction coefficients for nonhemolyzed blood were calculated by Kramer et al using the relationship of Beer's law. Instead of remaining constant as they do in the case of a nonscattering solution, they decreased as hemoglobin concentration increased. Similar results were obtained by Hickam and Frayser (97). This observation led Kramer to suggest that at very high hemoglobin concentrations the

light transmitting properties of nonhemolyzed blood approach those of hemolyzed blood.

In Chapter IV we showed that the relationship between extinction coefficients for nonhemolyzed blood and total hemoglobin concentration at 6330 A and at 8050 A could be expressed with a high degree of accuracy by the empirical equation

$$\epsilon_{rbc} = \frac{1}{(ac + b)} \qquad 4.2$$

We decided to continue the investigation of the relationship between optical density and sample depth at 6330 A, employing two measuring techniques: the diffusing plate technique using the cuvette oximeter; and conventional spectrophotometric techniques using the Beckman DU spectrophotometer. We attempted to apply equation 4.2 to the results obtained on whole nonhemolyzed blood, suspensions of red cells, and scattering emulsions, at five sample depths and using both types of measuring systems.

In this chapter we will also explore the possibility of using equation 4.2 to describe the results obtained on nonhemolyzed blood by previous authors who used conventional spectrophotometric techniques - Kramer et al, Hickam and Frayser, and Drabkin and Singer. Equation 4.2 was derived from results at 6330 A and 8050 A. At both these wave-

lengths the extinction coefficient of hemoglobin is fairly low. Similarly, the wavelengths studied by Kramer (6530 A to 10230 A), and by Hickam and Frayser (6600 A) as well as one of the wavelengths studied by Drabkin and Singer (6300 A) showed very low extinction coefficients. The extinction coefficient for oxygenated hemoglobin does not exceed 0.45 at wavelengths of 6300 A or longer. Of the shorter wavelengths studied by Drabkin, that with the highest extinction coefficient was 5780 A where ϵ = 15.13. We expected that if equation 4.2 could be used to describe results obtained by other authors, it would be more likely to apply with greater accuracy at wavelengths with low extinction coefficients.

B. Material and Methods

The following materials were studied: oxygenated whole nonhemolyzed blood; oxygenated red blood cells suspended in isotonic, hypotonic, and hypertonic saline; scattering emulsions, pigmented and nonpigmented. The scattering emulsions of n-butyl benzoate in water were prepared as described in Chapter V.

Measurements were made on flowing samples using the diffusing plate technique with the cuvette oximeter, and using the Beckman DU spectrophotometer with the cuvette oximeter sample chamber inserted in the light path.

As in Chapter V, the experiments have been divided into a series of preliminary experiments and a series of final experiments. The preliminary experiments were performed using the cuvette oximeter and the first light source, which was described in Chapter IV. These experiments were carried out on whole nonhemolyzed blood only. The final experiments were performed using the cuvette oximeter with the second light source (described in Chapter V) and also using the Beckman DU spectrophotometer. Final experiments were carried out on whole nonhemolyzed blood, red blood cell suspensions, and emulsions, both nonpigmented and pigmented.

Since it was observed in Chapters IV and V that the apparent optical density of nonhemolyzed blood measured in the cuvette oximeter with the first light source depended on the distance between the lamp and the diffusing plate, the preliminary experiments were performed with the lamp positioned at one of three levels within the chimney of the lamp house.

All measurements were made at a constant flow rate of 3.8 ml/minute. Five sample depths were used: 0.012, 0.025, 0.035, 0.055, and 0.071 cm. Depth was determined according to the method of Drabkin and Austin (50) using Coomassie blue dye. The cuvette must be dissassembled and an interface of

silicone grease applied between the two contacting plates of the chamber before assembling the sample chamber prior to each experiment; this resulted in a slight uncertainty in sample depth. The mean and standard deviation for each sample depth is given in Table 6.1.

C. Results

All the materials studied showed the known deviations from Beer's law exhibited by nonhemolyzed blood; the relationship of optical density to both sample concentration and depth was nonlinear. Complete numerical results for all materials at the five sample depths and at various particle concentrations are presented in Table 6.2.

1. Optical Density and Sample Depth

The relationship between optical density and sample depth was nonlinear for all the scattering materials studied. Fig. 6.1 shows this relationship for nonhemolyzed whole blood. One hemoglobin concentration is represented for the preliminary experiments, one for the final experiment using the cuvette oximeter, and one for the final experiments using the Beckman DU spectrophotometer.

TABLE 6.1. Sample depth

	Sample Depth (cm)				
	0.0119	0.0227	0.0332	0.0540	0.0706
	0.0123	0.0250	0.0363	0.0550	0.0707
	0.0125	0.0264	0.0349	0.0543	0.0708
	0.0111	0.0265	0.0358	0.0556	0.0722
	0.0122	0.0243	0.0347	0.0559	0.0711
Mean	0.0120	0.0250	0.0350	0.0550	0.0711
S.D.[a]	±.0005	±.0016	±.0012	±.0008	±.0001

[a]Standard deviation = $\left[1(n-1) \sum(x - \bar{x})^2\right]^{\frac{1}{2}}$.

TABLE 6.2. Comparison of optical density values at 6330 A for various scattering suspensions obtained by experiment with those obtained by calculation from equation 6.1

Material	Optical Density									
	Sample Depth (cm)									
	0.012		0.025		0.035		0.055		0.071	
	Exp.	Eq. 6.1	Exp.	Eq. 6.1	Exp.	Eq. 6.1	Exp.	Eq. 6.1	Exp.	Eq. 6.1
Preliminary Experiments, Cuvette Oximeter										
	Lamp Close to the Diffusing Plate									
Blood										
0.7 mM/l	0.035	0.034	0.058	0.059	0.083	0.084	0.125	0.122	0.153	0.146
3.8	0.125	0.129	0.232	0.228	0.312	0.313	0.439	0.435	0.504	0.507
6.7	0.180	0.177	0.326	0.318	0.440	0.427	0.580	0.583	0.656	0.672
9.2	0.205	0.204	0.372	0.370	0.407	0.491	0.658	0.664	0.752	0.762
11.3	0.220	0.221	0.398	0.404	0.522	0.532	0.718	0.714	0.837	0.817
	Lamp at an Intermediate Distance from the Diffusing Plate									
Blood										
1.2 mM/l	0.063	0.071	0.121	0.128	0.156	0.162	0.229	0.234	0.276	0.270
1.6	0.080	0.086	0.150	0.154	0.196	0.193	0.286	0.278	0.334	0.320
4.0	0.174	0.172	0.310	0.298	0.389	0.376	0.513	0.515	0.580	0.595
7.0	0.249	0.234	0.414	0.398	0.513	0.502	0.668	0.667	0.761	0.771
8.8	0.273	0.262	0.440	0.440	0.552	0.555	0.719	0.728	0.834	0.842
12.2	0.290	0.298	0.483	0.495	0.619	0.624	0.815	0.805	0.943	0.932

TABLE 6.2. Continued

Material	Optical Density									
	Sample Depth (cm)									
	0.012		0.025		0.035		0.055		0.071	
	Exp.	Eq. 6.1	Exp.	Eq. 6.1	Exp.	Eq. 6.1	Exp.	Eq. 6.1	Exp.	Eq. 6.1
	Lamp Distant from the Diffusing Plate									
Blood										
1.2 mM/l	0.083	0.089	0.162	0.163	0.213	0.216	0.300	0.286	0.373	0.353
3.1	0.182	0.182	0.321	0.320	0.404	0.412	0.531	0.543	0.625	0.642
7.0	0.314	0.292	0.497	0.493	0.633	0.616	0.802	0.805	0.900	0.914
9.4	0.338	0.335	0.553	0.555	0.678	0.687	0.896	0.896	0.994	1.002
12.3	0.370	0.373	0.610	0.609	0.741	0.747	0.970	0.971	1.086	1.075
Final Experiments, Beckman DU Spectrophotometer[a]										
Blood										
1.8 mM/l	0.320	0.325	0.485	0.465	0.581	0.577	0.767	0.759	0.816	0.817
5.1	0.469	0.484	0.780	0.775	0.939	0.940	1.179	1.177	1.216	1.243
7.0	0.533	0.520	0.884	0.855	1.053	1.031	1.266	1.275	1.344	1.340
8.6	0.550	0.541	0.920	0.903	1.097	1.085	1.331	1.330	1.398	1.397
11.8	0.560	0.566	0.940	0.964	1.140	1.154	1.410	1.405	1.462	1.468
Final Experiments, Cuvette Oximeter										
Blood										
1.0 mM/l	0.052	0.068	0.106	0.123	0.156	0.169	0.236	0.243	0.293	0.292
1.0	0.059	0.068	0.118	0.123	0.162	0.170	0.249	0.244	0.301	0.292
1.4	0.093	0.092	0.170	0.164	0.234	0.224	0.341	0.320	0.407	0.382
1.7	0.090	0.110	0.189	0.197	0.253	0.268	0.365	0.378	0.446	0.449
2.5	0.141	0.148	0.254	0.262	0.345	0.352	0.482	0.489	0.578	0.577

TABLE 6.2. Continued

Material	Optical Density									
	Sample Depth (cm)									
	0.012		0.025		0.035		0.055		0.071	
	Exp.	Eq. 6.1	Exp.	Eq. 6.1	Exp.	Eq. 6.1	Exp.	Eq. 6.1	Exp.	Eq. 6.1
2.7 mM/l	0.150	0.154	0.280	0.272	0.368	0.365	0.503	0.506	0.602	0.597
3.3	0.174	0.179	0.324	0.314	0.416	0.419	0.575	0.574	0.660	0.674
4.1	0.204	0.206	0.363	0.359	0.489	0.475	0.623	0.644	0.739	0.752
4.9	0.231	0.227	0.416	0.393	0.530	0.517	0.699	0.696	0.803	0.810
6.4	0.274	0.261	0.442	0.448	0.588	0.584	0.779	0.776	0.904	0.899
7.8	0.284	0.289	0.495	0.492	0.644	0.637	0.829	0.838	0.944	0.967
8.2	0.293	0.294	0.490	0.500	0.656	0.647	0.860	0.849	0.974	0.979
8.9	0.305	0.306	0.516	0.518	0.677	0.668	0.866	0.873	0.999	1.006
9.3	0.312	0.311	0.531	0.526	0.682	0.678	0.898	0.885	1.018	1.019
10.2	0.322	0.322	0.541	0.543	0.702	0.698	0.916	0.907	1.058	1.043
11.3	0.332	0.335	0.547	0.562	0.717	0.720	0.941	0.933	1.086	1.070
RBC 0.6%NaCl										
1.8 mM/l	0.105	0.141	0.223	0.246	0.286	0.303	0.400	0.416	0.473	0.465
2.5	. .	. .	. .	. .	. .	. .	. .	. .	0.573	0.575
3.1	. .	. .	. .	. .	. .	. .	. .	. .	0.596	0.647
3.3	0.210	0.206	0.373	0.368	0.456	0.449	0.614	0.600	0.680	0.671
3.6	. .	. .	. .	. .	. .	. .	. .	. .	0.738	0.705
3.9	0.203	0.224	0.399	0.401	0.493	0.489	0.644	0.648	0.722	0.726
4.6	. .	. .	. .	. .	. .	. .	. .	. .	0.805	0.785
5.8	0.264	0.269	0.496	0.487	0.597	0.592	0.762	0.769	0.839	0.863
7.3	0.308	0.294	0.550	0.535	0.670	0.648	0.835	0.833	0.930	0.935
8.3	0.320	0.306	0.578	0.559	0.682	0.677	0.865	0.865	0.976	0.971
11.0	0.350	0.332	0.610	0.611	0.729	0.738	0.928	0.933	1.043	1.049

TABLE 6.2. Continued

Material	Optical Density, Sample Depth (cm)									
	0.012		0.025		0.035		0.055		0.071	
	Exp.	Eq. 6.1	Exp.	Eq. 6.1	Exp.	Eq. 6.1	Exp.	Eq. 6.1	Exp.	Eq. 6.1
RBC 0.9%NaCl										
1.8 mM/l	0.177	0.192	0.313	0.318	0.408	0.406	0.526	0.506	0.618	0.581
2.4	. .	. .	. .	. .	. .	. .	. .	. .	0.658	0.679
3.1	. .	. .	. .	. .	. .	. .	. .	. .	0.758	0.767
3.6	. .	. .	. .	. .	. .	. .	. .	. .	0.815	0.820
3.9	0.310	0.300	0.483	0.485	0.593	0.596	0.718	0.742	0.830	0.845
4.3	0.332	0.314	0.519	0.507	0.627	0.620	0.779	0.771	0.868	0.878
4.6	. .	. .	. .	. .	. .	. .	. .	. .	0.866	0.891
7.8	0.413	0.404	0.651	0.640	0.778	0.759	0.935	0.943	1.076	1.067
10.3	0.435	0.442	0.703	0.693	0.821	0.813	1.009	1.009	1.133	1.139
11.9	0.422	0.459	0.683	0.718	0.822	0.838	1.033	1.039	1.168	1.172
RBC 1.4%NaCl										
1.1 mM/l	0.154	0.158	0.273	0.306	0.357	0.347	0.485	0.409	0.458	0.451
1.6	0.224	0.214	0.399	0.392	0.486	0.446	0.522	0.532	0.639	0.591
2.3	0.272	0.276	0.449	0.476	0.555	0.543	0.678	0.654	0.742	0.735
2,4	0.274	0.282	0.467	0.484	0.549	0.552	0.682	0.666	0.754	0.748
3.1	. .	. .	. .	. .	. .	. .	. .	. .	0.827	0.862
3.1	. .	. .	0.550	0.549	0.644	0.628	0.764	0.764	0.854	0.866
3.3	0.327	0.345	. .	. .	. .	. .	. .	. .	. .	. .
3.9	0.387	0.381	0.576	0.601	0.668	0.688	. .	. .	. .	. .
4.0	. .	. .	. .	. .	. .	. .	0.866	0.856	0.962	0.976
4.1	0.394	0.392	0.590	0.612	0.702	0.702	0.845	0.862	. .	. .
4.7	. .	. .	0.658	0.643	0.760	0.738	0.896	0.910	1.002	1.042
5.3	0.463	0.449	0.683	0.670	0.773	0.770	. .	. .	. .	. .
5.8	0.462	0.468	0.671	0.689	0.787	0.792	0.951	0.982	. .	. .

TABLE 6.2. Continued

Material	Optical Density									
	Sample Depth (cm)									
	0.012		0.025		0.035		0.055		0.071	
	Exp.	Eq. 6.1	Exp.	Eq. 6.1	Exp.	Eq. 6.1	Exp.	Eq. 6.1	Exp.	Eq. 6.1
6.6 mM/l	. .	. .	. .	. .	. .	. .	1.041	1.026	1.171	1.186
6.6	. .	. .	. .	. .	0.861	0.825	1.040	1.027	1.186	1.187
8.1	0.560	0.542	0.780	0.754	0.881	0.869	1.078	1.088	1.258	1.263
8.8	0.573	0.558	. .	. .	. .	. .	1.138	1.110	1.312	1.292
10.2	0.581	0.588	0.805	0.792	0.942	0.914	1.171	1.150	1.308	1.343
12.8	0.520	0.630	0.834	0.824	0.967	0.952	1.235	1.204	. .	. .
14.4	0.462	0.651	0.801	0.839	0.965	0.970	1.238	1.229	1.476	1.443
Emulsion										
2.5%	0.455	0.449	0.574	0.551	0.665	0.589	0.736	0.646	0.776	0.728
5.0	0.617	0.611	0.714	0.733	0.775	0.792	0.865	0.873	0.933	0.958
10.0	0.721	0.746	0.864	0.878	0.944	0.958	1.035	1.079	1.109	1.137
15.0	0.800	0.805	0.926	0.940	1.004	1.030	1.127	1.141	1.207	1.213
20.0	0.839	0.838	0.965	0.975	1.063	1.070	1.178	1.187	1.272	1.255
30.0	0.879	0.874	1.034	1.012	1.125	1.113	1.280	1.236	1.314	1.300
Emulsion, Pigmented										
2.5% 0.62 mg/l[b]	0.446	0.454	0.632	0.601	0.736	0.667	0.869	0.778	0.966	0.910
5.0 1.25	0.667	0.660	0.846	0.859	0.969	1.000	1.206	1.228	1.394	1.435
10.0 2.50	0.851	0.852	1.114	1.098	1.380	1.333	1.778	1.728	2.079	2.016

[a]Collimated incidence. All other values were obtained with diffuse incident light.
[b]Concentration of Sudan blue in the emulsion.

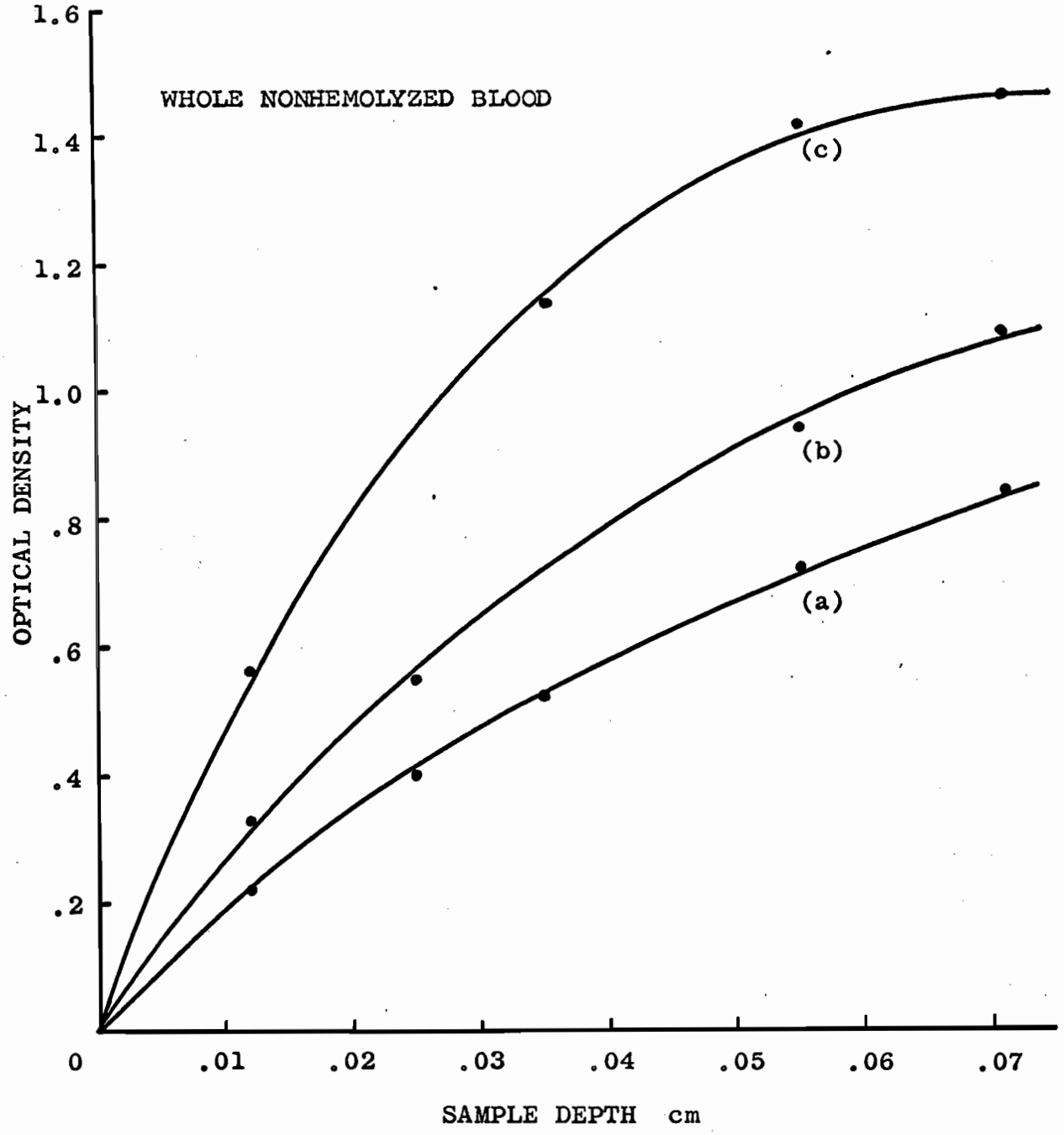

Fig. 6.1. Relationship between optical density and sample depth for nonhemolyzed whole blood at 6330 A. The lines do not represent an equation.
Curve (a): preliminary experiment with the lamp close to the diffusing plate; hemoglobin concentration 11.3 mM/l.
Curve (b): final experiment with the cuvette oximeter; hemoglobin concentration 11.3 mM/l.
Curve (c): final experiment with the Beckman DU spectrophotometer; hemoglobin concentration 11.8 mM/l.

2. Optical Density and Particle Concentration

The results demonstrating the relationship between optical density and particle concentration are depicted graphically only for the sample depth of 0.071 cm. (Fig. 6.2 and 6.3) The dots show the experimental results. The lines represent the equation for optical density obtained by substituting equation 4.2 into Beer's law:

$$\text{Optical Density} = \left[\epsilon_{rbc}\ c\ d\right] = \left[\frac{1}{(ac + b)}\ c\ d\right] \qquad 6.1$$

Optical density values calculated from equation 6.1 are presented in Table 6.2. Statistical analysis is given in Table 6.3 and shows the standard deviation of the differences between experimental and calculated optical density values.

a) Whole Nonhemolyzed Blood

Fig. 6.2 shows all the results obtained on whole nonhemolyzed blood at a sample depth of 0.071 cm. Curves (a), (b), and (c) are the results of the preliminary experiments. It may be seen that the lowest optical density values were obtained when the lamp was closest to the diffusing plate. As the lamp was moved away, the optical density values increased. Curve (d) shows the final cuvette oximeter

TABLE 6.3. Statistical analysis of the results of Table 6.2: standard deviation of the differences between experimental values and values calculated from equation 6.1

Material	Standard Deviation of the Differences (in optical density units)				
	Sample Depth (cm)				
	0.012	0.025	0.035	0.055	0.071
Preliminary Experiments, Cuvette Oximeter					
	Lamp Close to the Diffusing Plate				
Blood	±0.003[a] (1.7%)[b]	±0.006 (2.0%)	±0.008 (2.3%)	±0.005 (0.9%)	±0.015 (2.5%)
	Lamp at an Intermediate Distance from the Diffusing Plate				
Blood	±0.010 (5.4%)	±0.010 (3.3%)	±0.008 (2.1%)	±0.008 (1.5%)	±0.012 (2.0%)
	Lamp Distant from the Diffusing Plate				
Blood	±0.011 (4.2%)	±0.003 (0.6%)	±0.011 (2.0%)	±0.009 (1.3%)	±0.016 (2.0%)
Final Experiments, Beckman DU Spectrophotometer					
Blood	±0.012 (2.4%)	±0.021 (2.6%)	±0.014 (1.4%)	±0.007 (0.6%)	±0.012 (1.0%)
Final Experiments, Cuvette Oximeter					
Blood	±0.007 (3.6%)	±0.010 (2.8%)	±0.009 (1.9%)	±0.011 (1.7%)	±0.012 (1.6%)

TABLE 6.3. Continued

Material	Standard Deviation of the Differences (in optical density units)				
	Sample Depth (cm)				
	0.012	0.025	0.035	0.055	0.071
RBC 0.6%NaCl	±0.021 (8.2%)	±0.014 (3.1%)	±0.013 (2.3%)	±0.010 (1.3%)	±0.022 (2.9%)
RBC 0.9%NaCl	±0.020 (5.8%)	±0.018 (3.2%)	±0.011 (1.7%)	±0.015 (1.8%)	±0.017 (1.9%)
RBC 1.4%NaCl	±0.058 (14.3%)	±0.020 (3.4%)	±0.016 (2.3%)	±0.025 (2.7%)	±0.025 (2.6%)
Emulsion	±0.012 (1.6%)	±0.019 (2.3%)	±0.038 (4.0%)	±0.049 (4.7%)	±0.029 (2.6%)
Emulsion, Pigmented	±0.007 (1.1%)	±0.022 (2.6%)	±0.052 (5.2%)	±0.057 (4.6%)	±0.058 (4.0%)

[a]Standard deviation of the differences between experimental and calculated optical density values = $\left[1/(n-1)\ \sum(d - \bar{d})^2\right]^{\frac{1}{2}}$.

[b]Standard deviation of the differences expressed as a percent of the mean optical density value.

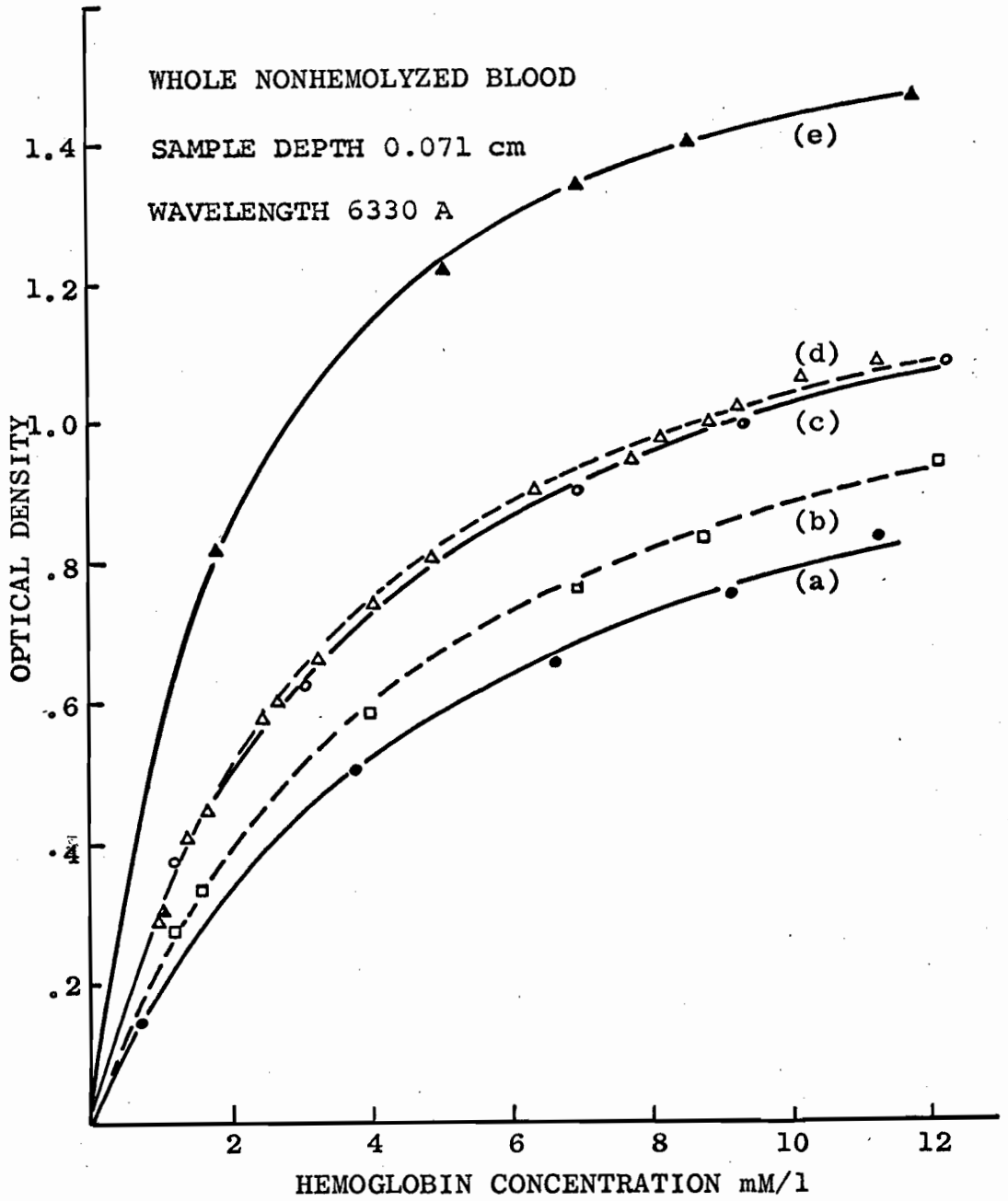

Fig. 6.2. The points represent experimental values. The solid lines were calculated from equation 6.1

Curve (a), ● : preliminary experiment with the lamp close to the diffusing plate.

Curve (b), □ : preliminary experiment with the lamp at an intermediate distance from the diffusing plate.

Curve (c), ○ : preliminary experiment with the lamp distant from the diffusing plate.

Curve (d), △ : final experiment , cuvette oximeter.

Curve (e), ▲ : final experiment, Beckman DU spectrophotometer.

results. This curve almost coincides with curve (c) of the preliminary experiments, where the lamp was distant from the diffusing plate. These results again demonstrate that optical density values measured with the diffusing plate technique are not absolute but depend on the manner in which the diffusing plate is illuminated.

The highest values for the optical density of nonhemolyzed whole blood were obtained with the Beckman DU spectrophotometer. A strict comparison between optical density values obtained with the two different techniques cannot be made; the means of providing monochromatic light and the degree of monochromacy are very different; the spectrophotometer uses a phototube as detector and the cuvette oximeter employs selenium barrier layer photocells. However, a qualitative comparison shows that, as expected from the known phenomenon of the shift to higher optical density values when conventional spectrophotometric techniques are used, optical density values are higher than those obtained with the cuvette oximeter system employing diffuse incident light.

We found that the equation

$$O.D. = \frac{1}{(ac + b)} c\, d$$

could be used with a high degree of accuracy to describe

the results obtained on whole nonhemolyzed blood in both the preliminary and final experiments. As shown in Table 6.3, the largest standard deviation of the differences between experimental and calculated values was 0.021 optical density units. Expressed as percent of the mean optical density value, this amounts to 2.6%.

b) Red Blood Cell Suspensions

In Fig. 6.3, curves (a), (b), and (c) show the relationship between optical density and the total hemoglobin concentration of red blood cells suspended in NaCl solutions. Red cells suspended in NaCl solutions of different tonicity showed considerable differences in apparent optical density. This confirms the findings of other investigators (212) who found that optical density increased when red cells were suspended in hypertonic saline and decreased when the cells were suspended in hypotonic saline. These authors attributed the results to the osmotically induced changes in cell size. Curve (d) for whole nonhemolyzed blood was plotted for comparison with the red cell suspensions. The optical density of red cells suspended in isotonic saline was greater than that of whole blood of the same hemoglobin concentration. The curve for whole blood (d) is almost coincident with that for red blood cells in 0.6% NaCl. The differences in optical

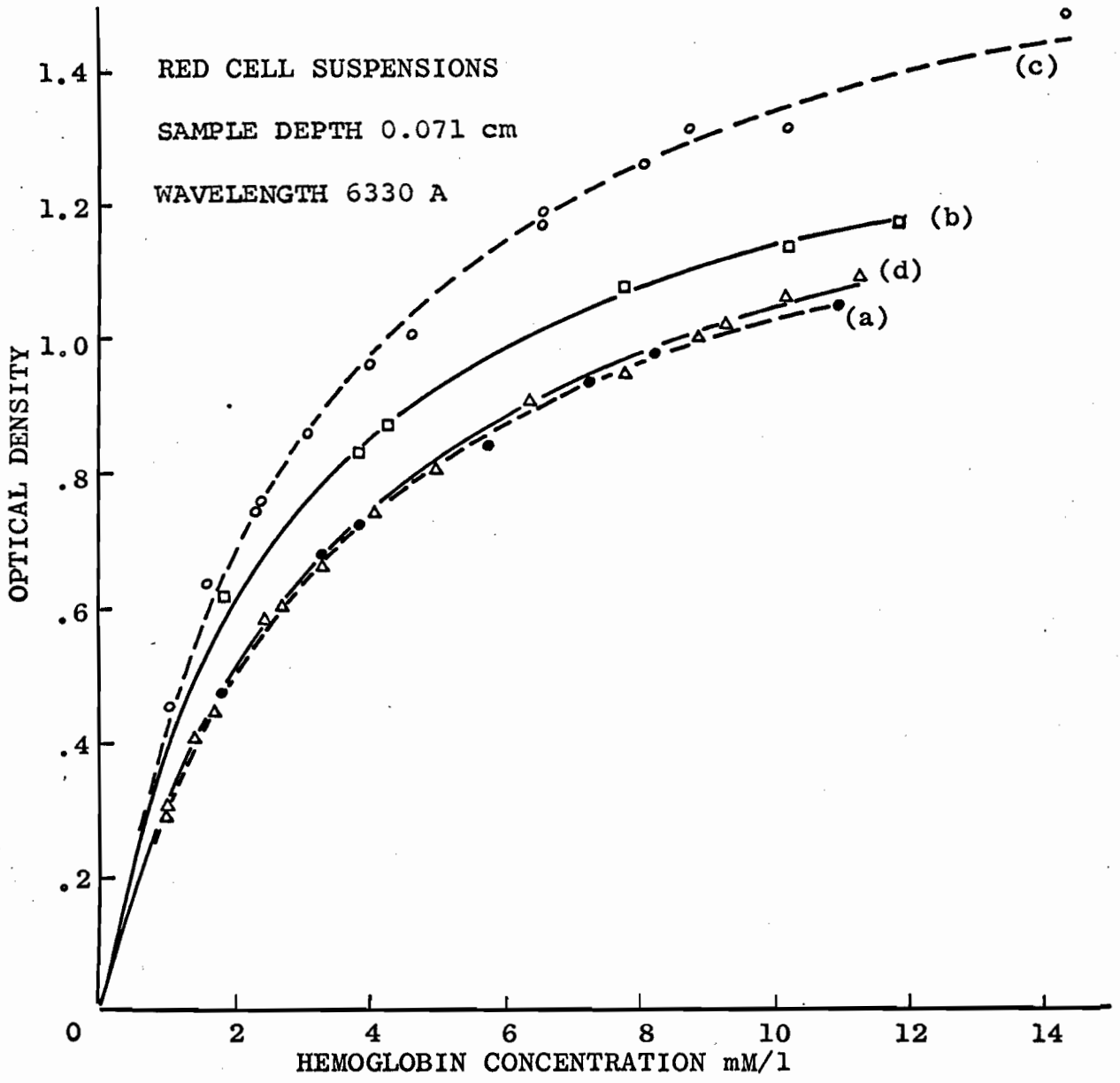

Fig. 6.3. Relationship between optical density at 6330 A and hemoglobin concentration for red blood cell suspensions. Sample depth was 0.071 cm. The lines were calculated from equation 6.1.
Curve (a), ● : red blood cells suspended in 0.6% NaCl.
Curve (b), □ : red blood cells suspended in 0.9% NaCl.
Curve (c), o : red blood cells suspended in 1.4% NaCl.
Curve (d), △ : whole nonhemolyzed blood.

density between red blood cells suspended in plasma and red cells suspended in normal saline is probably due to the difference in refractive index between plasma and 0.9% NaCl. Barer (11, 12) showed that scattering by red blood cells was eliminated by suspending the cells in a solution whose refractive index matched that of the cells. He found that a protein solution with a concentration of 35 gm/100 ml was sufficient to cause a suspension of red blood cells to take on the appearance of a solution. Since plasma contains about 7 to 7.5 gm/100 ml protein, the refractive index difference is reduced and consequently the red cells scatter less light in plasma than in isotonic saline.

The degree of accuracy achieved using equation 6.1 to describe the results was again very high for the isotonic and hypotonic suspensions. It was slightly less for the hypertonic suspensions. The maximum standard deviation of the differences between calculated and experimental values was 0.22 optical density units for the isotonic and hypotonic suspensions. This is 2.9% of the mean optical density value. The maximum standard deviation of the differences for the hypertonic suspensions was disproportionately high at the sample depth of 0.012 cm. It was 0.058 optical density units, representing 14.3% of the mean optical density value. This high deviation is largely due

to considerable differences between calculated and experimental values at the two highest hemoglobin concentrations. At the other sample depths, the error was much smaller (0.025 optical density units representing 2.7% of the mean value).

c) Emulsions

Fig. 6.4 shows the relationship between optical density and the volume concentration of emulsified droplets of n-butyl benzoate, both nonpigmented (curve a) and pigmented (curve b). Equation 6.1 was again used with a considerable degree of accuracy. The agreement between calculated and experimental values was of the same order for the nonpigmented and pigmented emulsions. The maximum standard deviation of the differences between calculated and experimental values for the nonabsorbing emulsion was 0.049 optical density units. For the absorbing emulsion, the maximum standard deviation of the differences was 0.058 optical density units, representing 4.0% of the mean optical density value.

The standard deviation of the differences between calculated and experimental values was of comparable magnitude at all five sample depths. However, since the optical density values increase as sample depth increases,

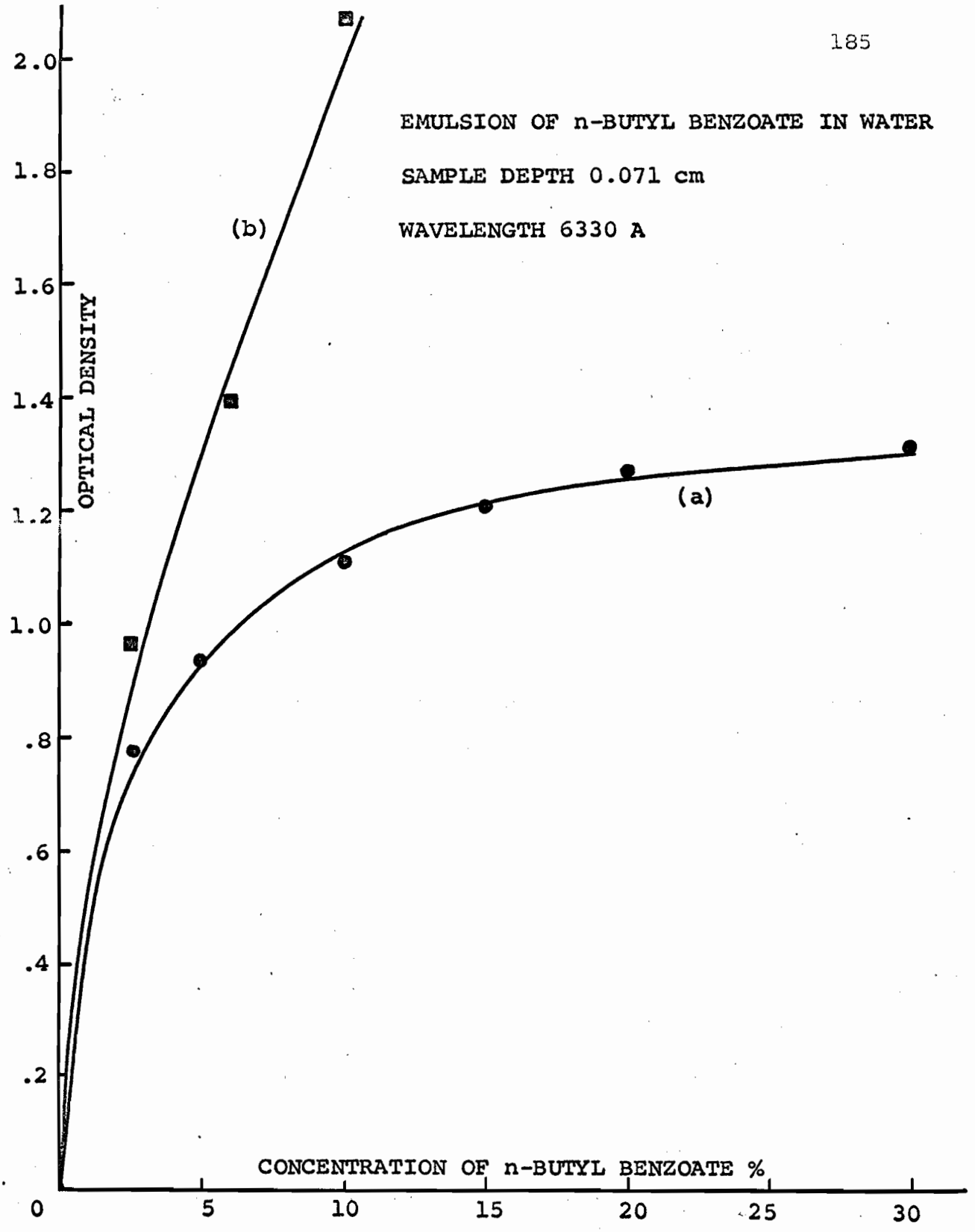

Fig. 6.4. Relationship between optical density at 6330 A and volume concentration of n-butyl benzoate emulsions. Sample depth was 0.071 cm. The solid lines were calculated from equation 6.1.
Curve (a), ● : nonpigmented emulsion.
Curve (b), ■ : pigmented emulsion.

the percentage difference between calculated and experimental observations was smaller at large sample depths.

3. Optical Density and the Product of Concentration and Depth

Kramer demonstrated that, due to the deviations from Beer's law, concentration and depth were not interchangeable for nonhemolyzed blood, and thus, when optical density was plotted against the product of concentration times sample depth, a family of nonlinear curves resulted, with one curve for each sample depth (131). Similar graphs (Figures 6.5 and 6.6) were constructed for the results of the final cuvette oximeter experiments on nonhemolyzed blood and on nonabsorbing emulsions. Families of curves resulted for both of these scattering materials.

4. Application of Equation 6.1 to Results in the Literature

Data in the literature on the relationship between optical density and total hemoglobin concentration was available from: Kramer et al (131), Figures 8a and 8b; Hickam and Frayser (97), Fig. 3; Drabkin and Singer (52), Tables I, II, and III. In order to apply equation 6.1 to data reported in the literature, these were reproduced and indicated by dots in Figures 6.7 (a) to 6.7 (h).

Equation 6.1 was used to describe all these results

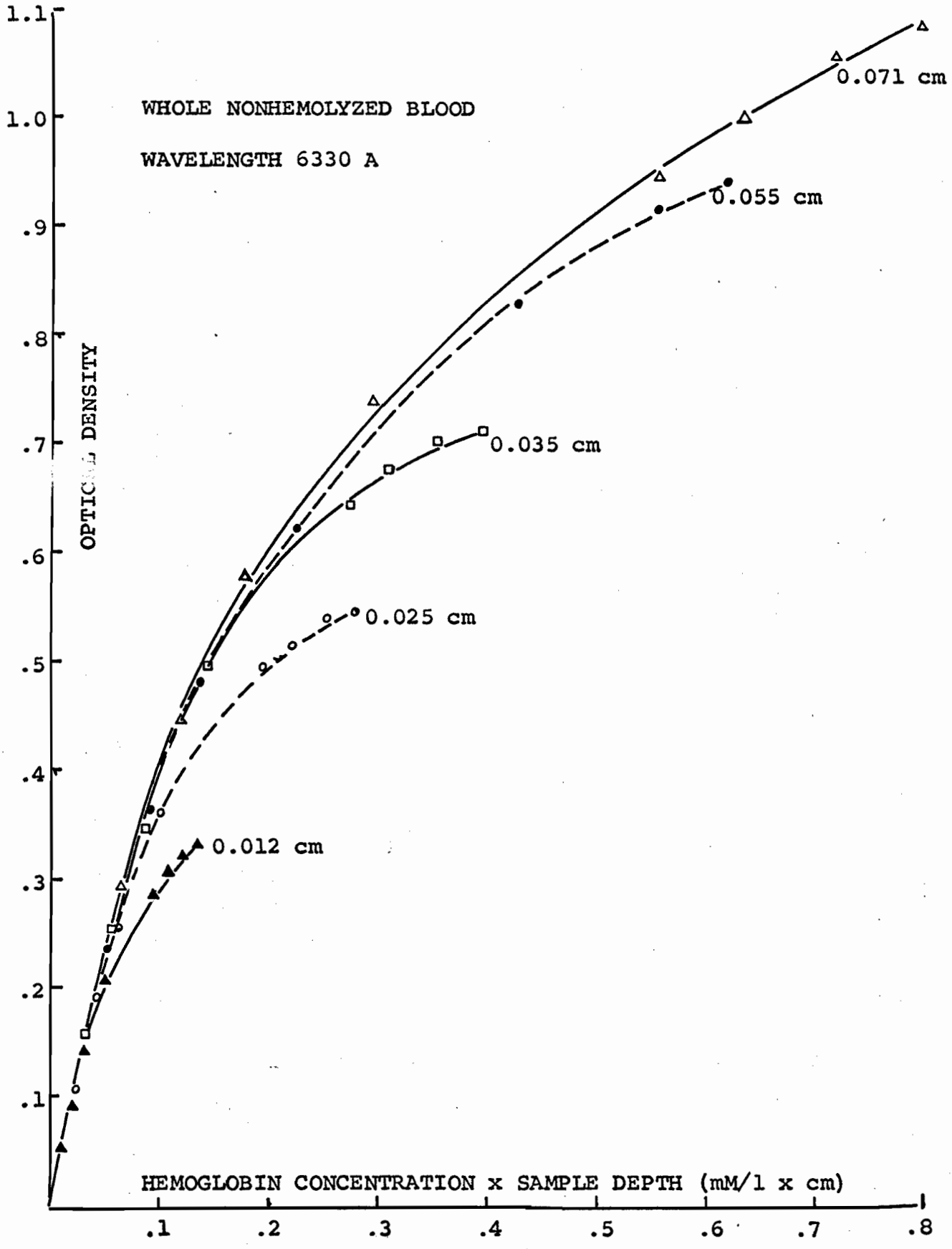

Fig. 6.5. Relationship between optical density and the product of hemoglobin concentration times sample depth for whole non-hemolyzed blood, at 6330 A. Sample depth was varied from 0.012 cm to 0.071 cm. The lines do not represent equations.

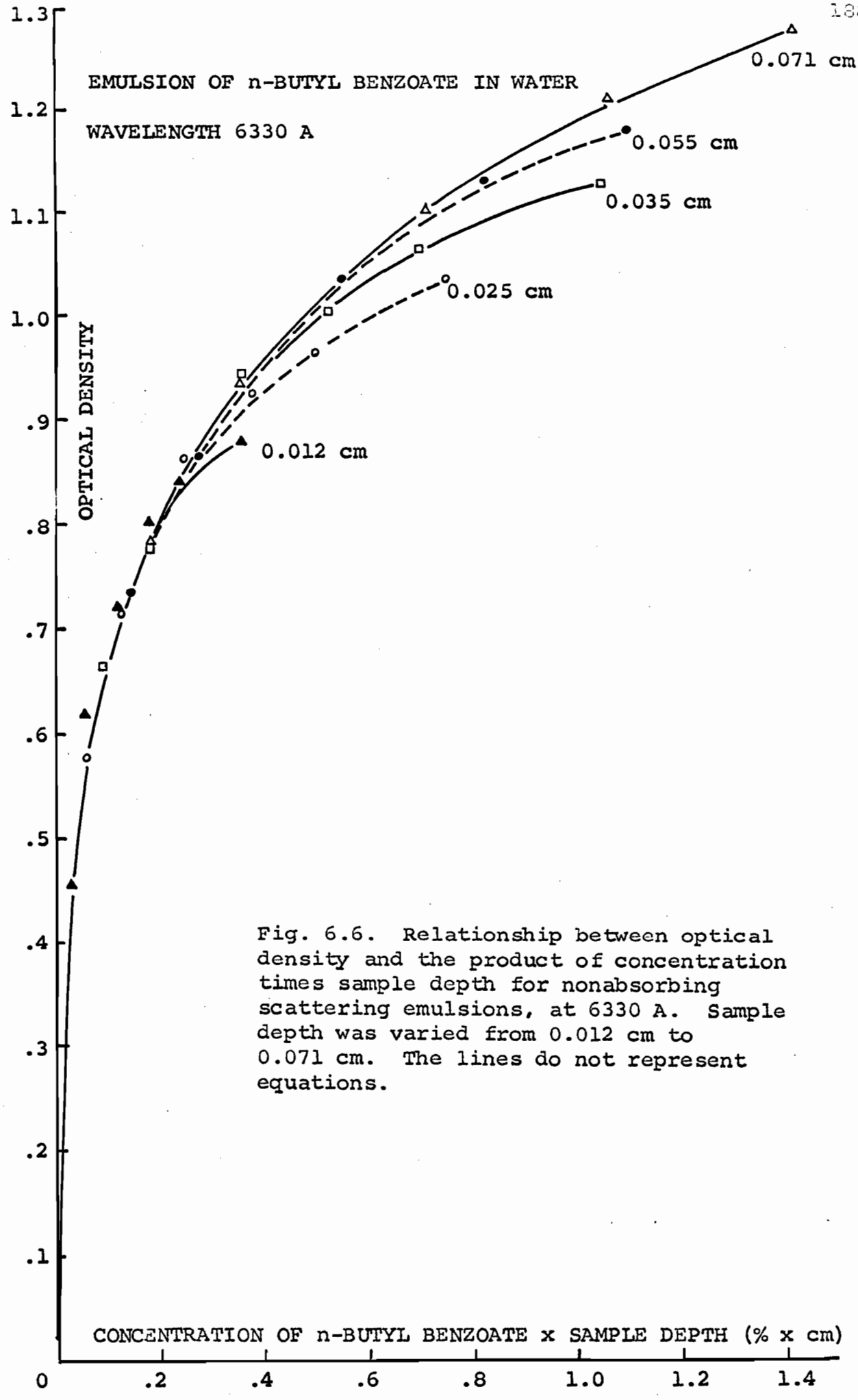

Fig. 6.6. Relationship between optical density and the product of concentration times sample depth for nonabsorbing scattering emulsions, at 6330 A. Sample depth was varied from 0.012 cm to 0.071 cm. The lines do not represent equations.

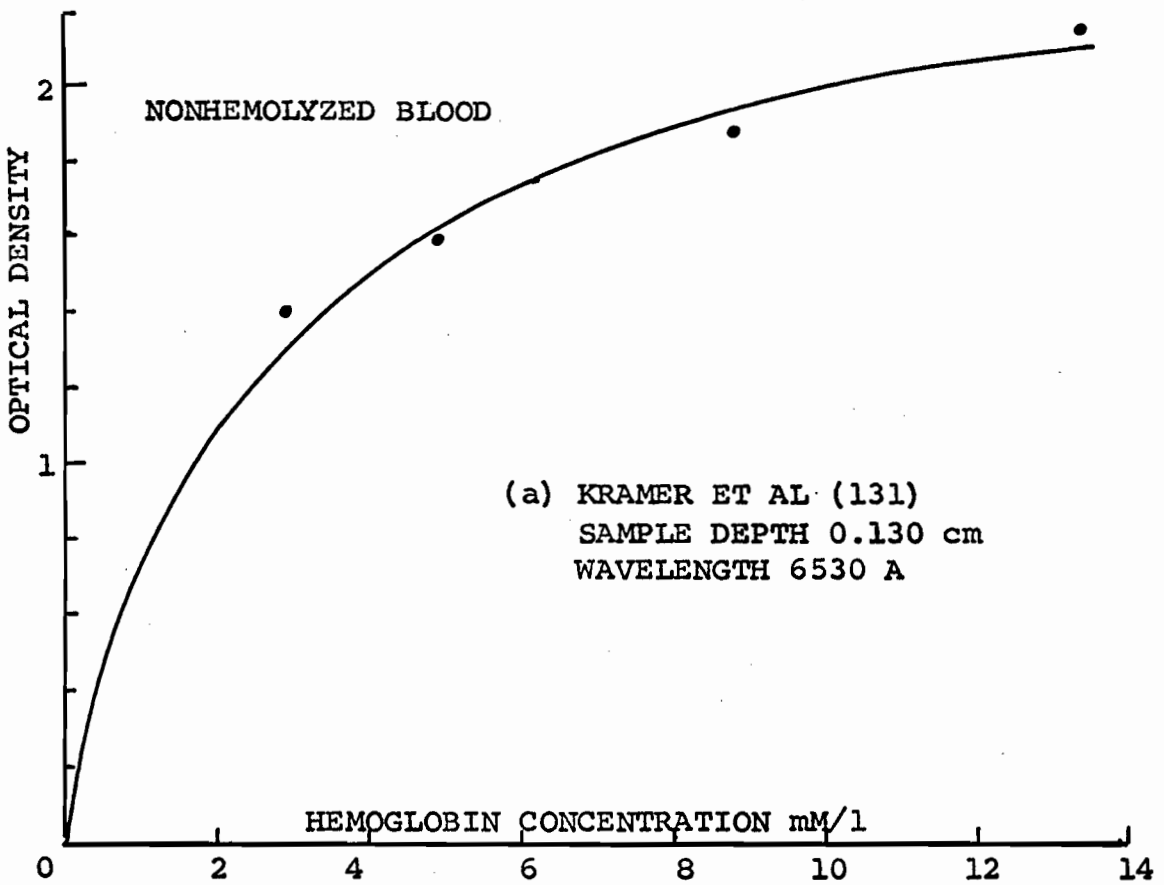

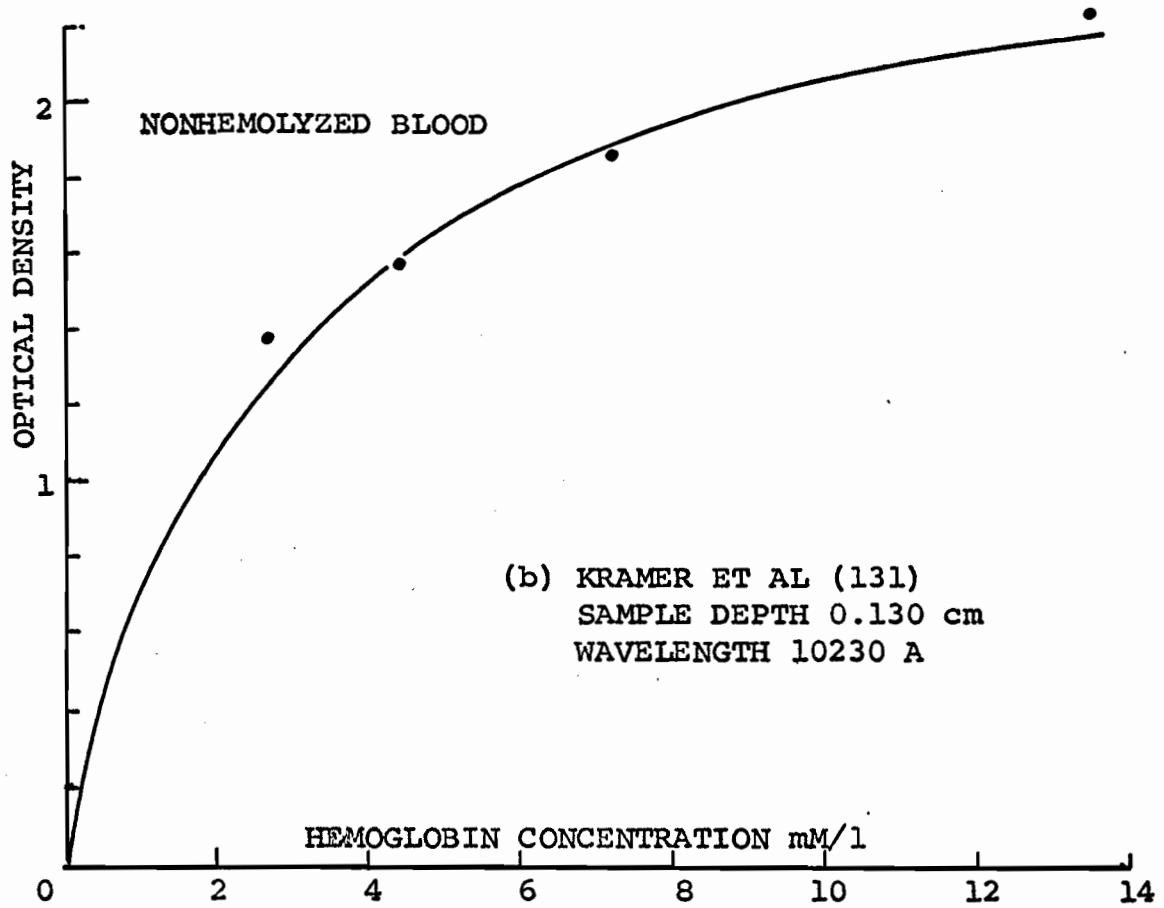

Fig. 6.7. Relationship between optical density and hemoglobin concentration for nonhemolyzed blood. The dots represent experimental data taken from the literature. The solid lines were calculated from equation 6.1.

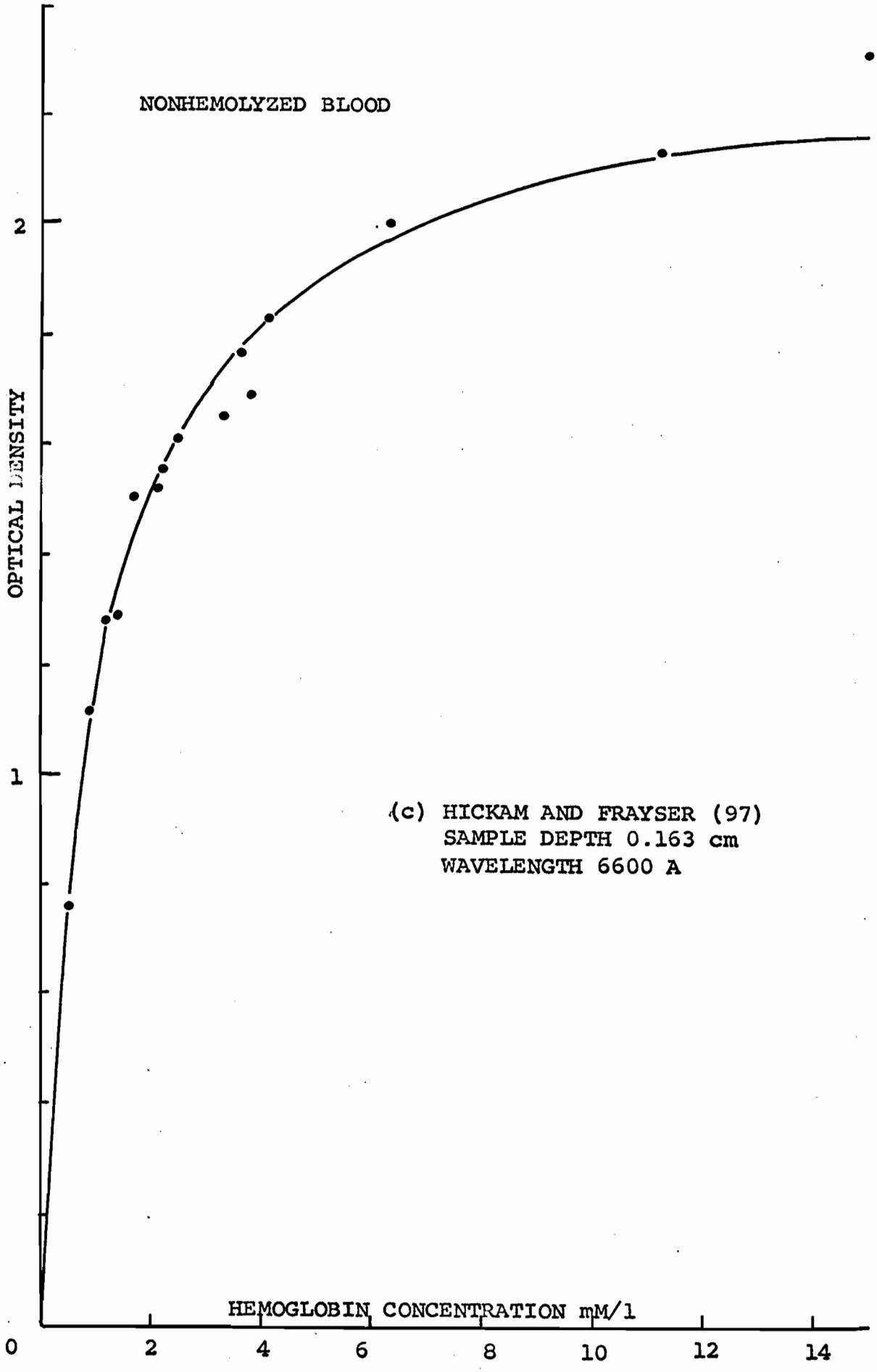

Fig. 6.7. Continued.

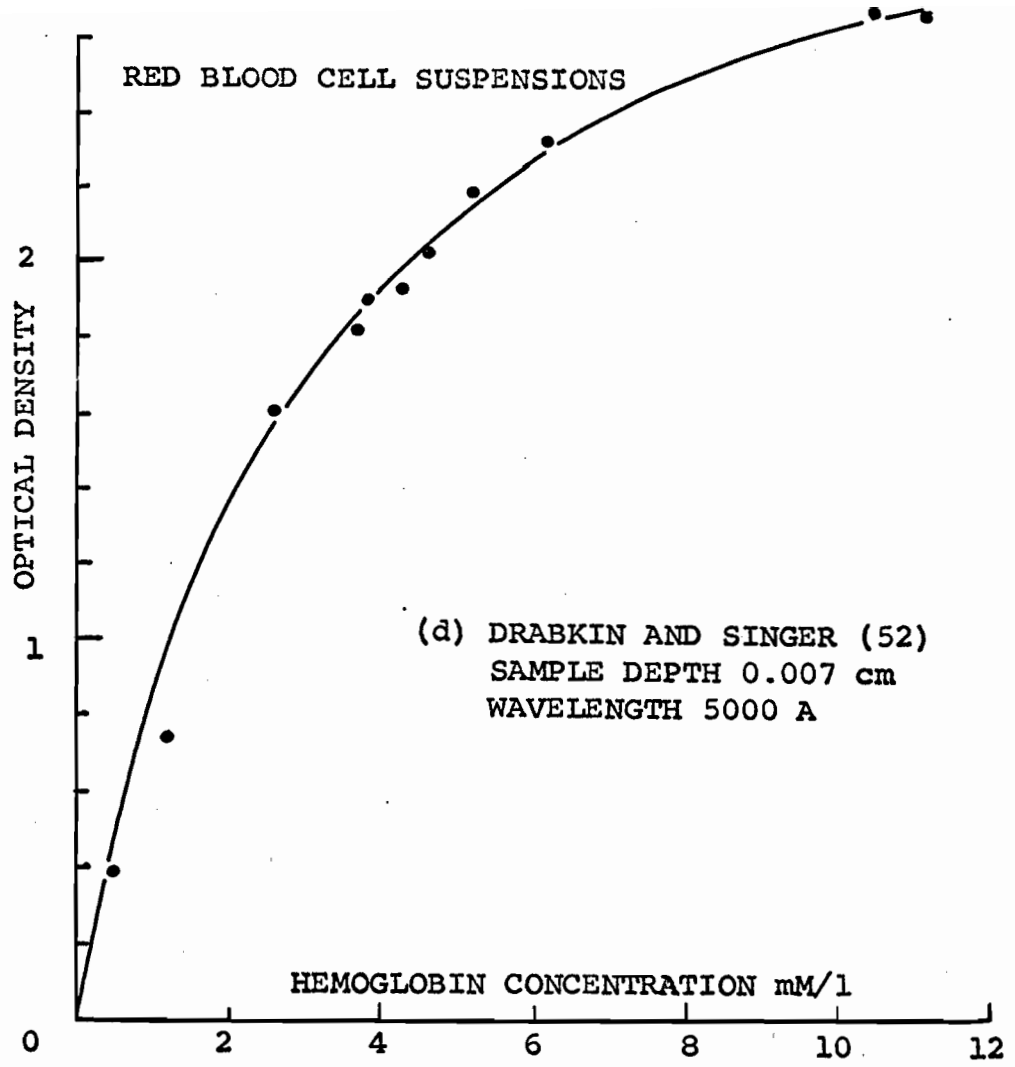

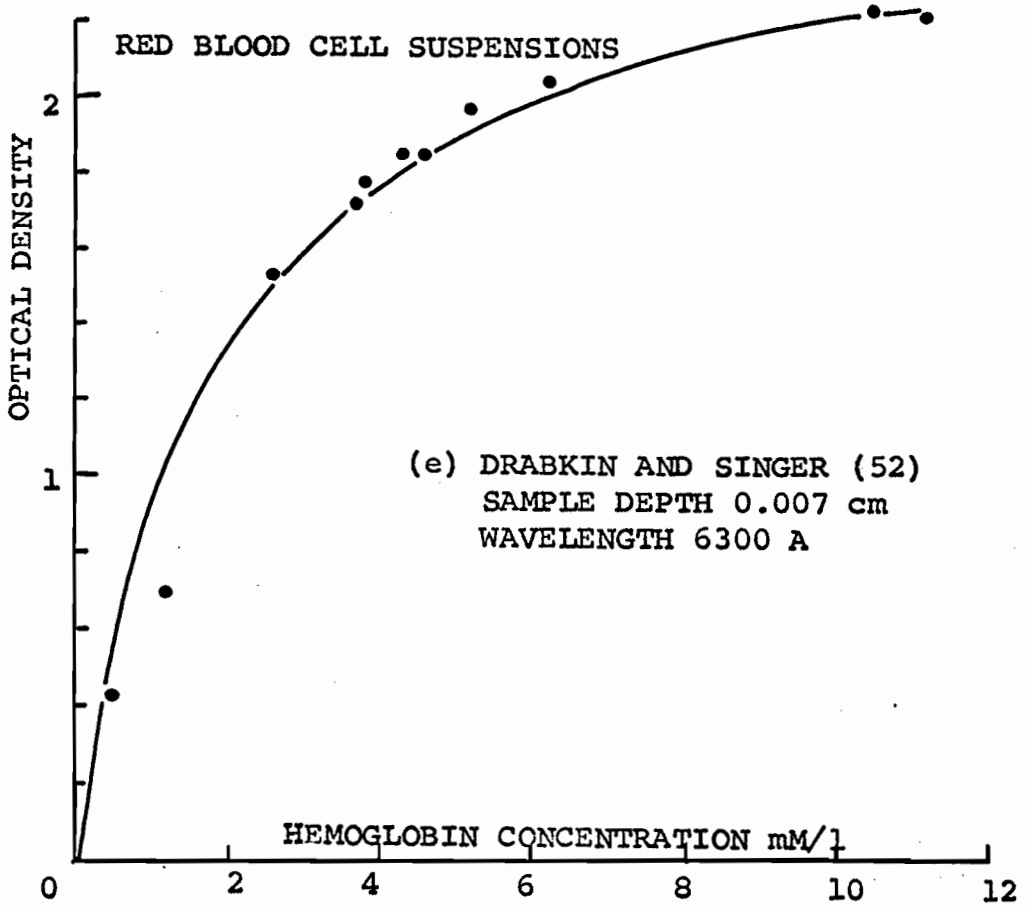

Fig. 6.7. Continued.

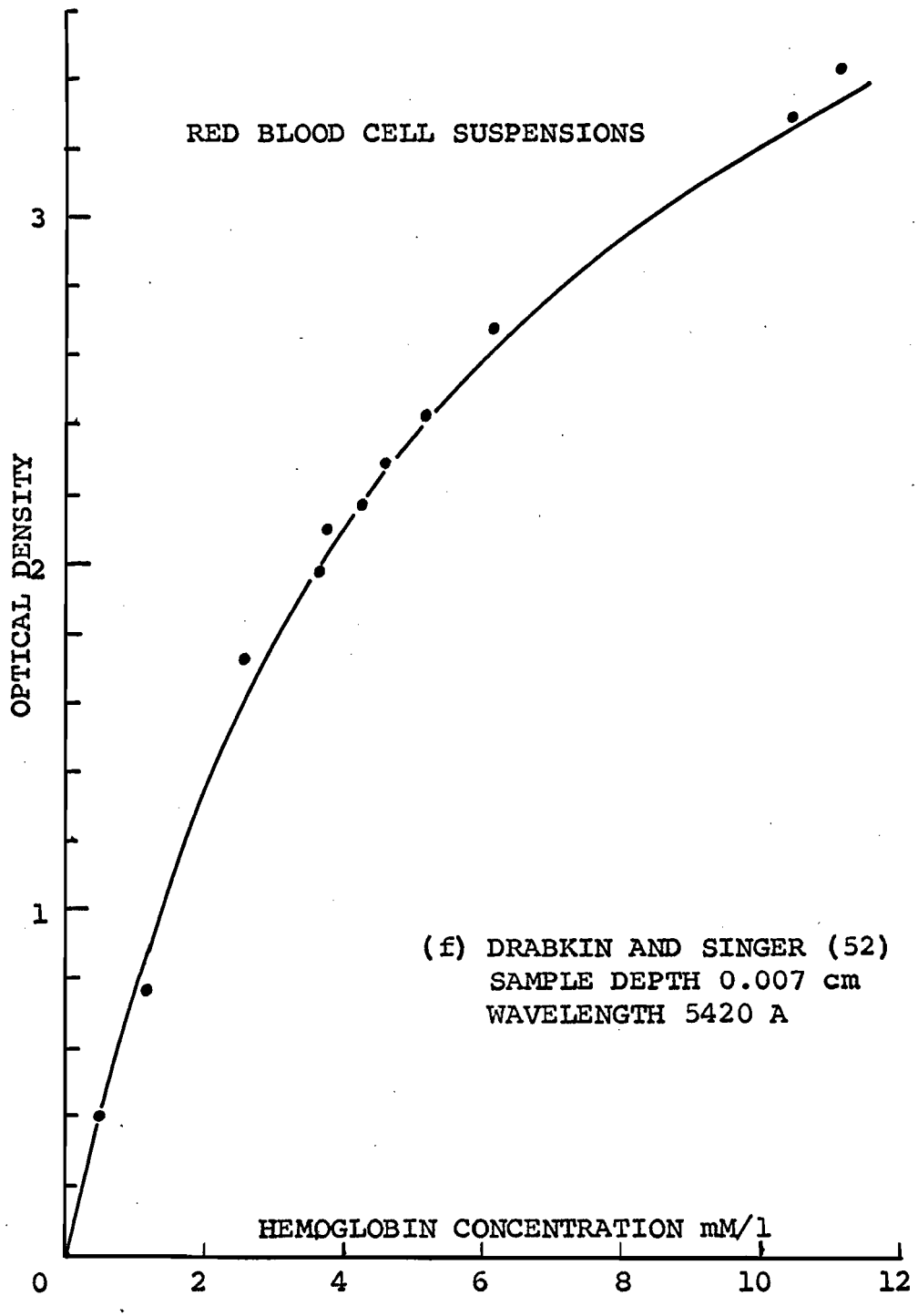

Fig. 6.7. Continued.

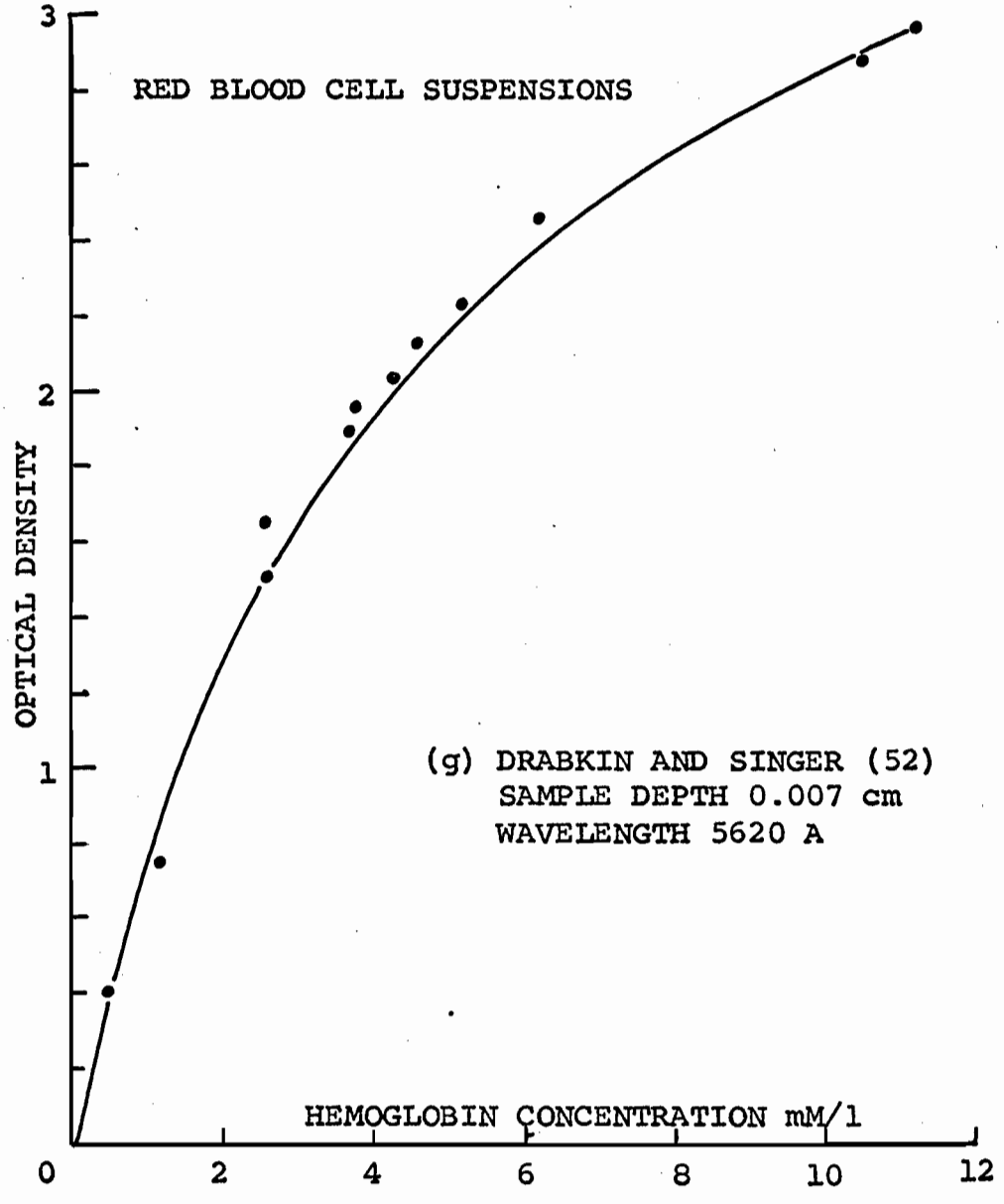

Fig. 6.7. Continued.

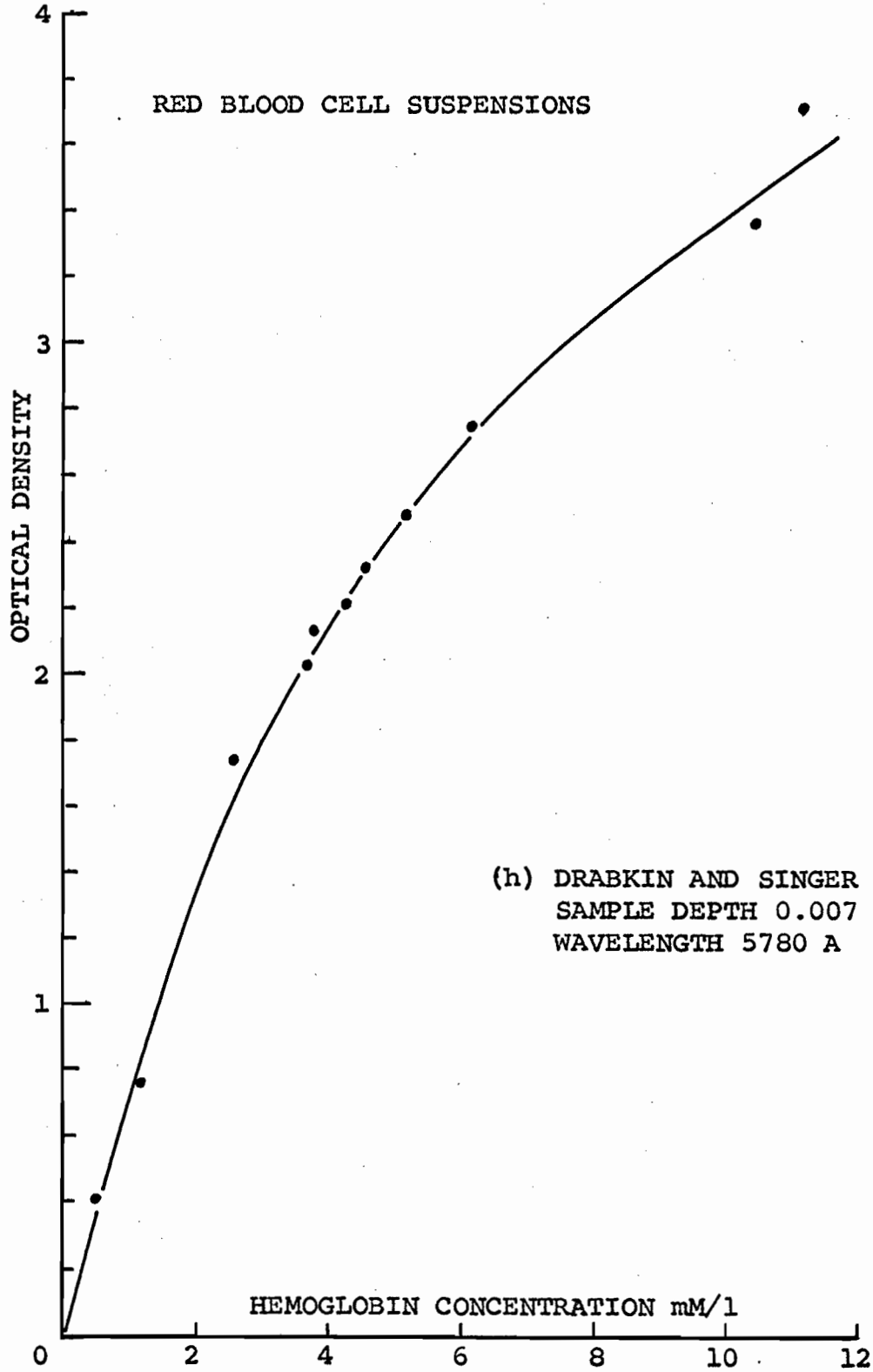

Fig. 6.7. Continued.

as shown in Fig. 6.7(a-h). The lines were calculated from this equation and the points represent the experimental values obtained by the various authors. The numerical results are given in Table 6.4. Statistical analysis (Table 6.5) shows that the standard deviation of the differences between calculated and experimental results is greater for the data obtained from the literature than for the results obtained in the present study (shown in Table 6.2). However, it may be seen from Fig. 6.7 that the differences are due, to a large extent, to the fairly high degree of scatter of experimental data about a line of best fit in the studies from which the data was taken. The evolution of the experimental and calculated curves shows quite close agreement. Table 6.5 shows that the standard deviation of the differences is fairly uniform for all the results. Except in the study of Drabkin and Singer at 6300 A, where the standard deviation of the differences is 7.1% of the mean optical density value, the value ranges from 0.062 to 0.089 representing 3.5% and 4.1% of the mean optical density values, respectively).

These results indicate that equation 6.1 is of greater general validity than we had expected. It was originally derived for results obtained using the diffusing plate technique, at sample depths of 0.027 cm and 0.071 cm, and at

TABLE 6.4. Comparison of optical density values for nonhemolyzed blood in the literature with those obtained by calculation from equation 6.1

Authors	Hb Conc. (mM/l)	Optical Density									
		Exp.	Eq. 6.1	Exp.	Eq. 6.1	Exp.	Eq. 6.1	Exp.	Eq. 6.1	Exp.	Eq. 6.1
		6530 A		10230 A							
Kramer et al[a] (131)	2.9	1.405	1.315								
	4.9	1.588	1.629								
	8.8	1.879	1.937								
	13.4	2.150	2.108								
	2.7			1.380	1.276						
	4.4			1.567	1.584						
	7.2			1.855	1.883						
	13.5			2.230	2.178						
		6600 A									
Hickam and Frayser[b] (97)	0.5	0.762	0.776								
	0.9	1.116	1.089								
	1.2	1.278	1.209								
	1.4	1.289	1.323								
	1.7	1.505	1.434								
	2.1	1.513	1.530								
	2.2	1.554	1.561								
	2.5	1.607	1.615								
	3.3	1.653	1.751								
	3.6	1.768	1.782								
	3.8	1.689	1.813								

TABLE 6.4. Continued

Authors	Hb Conc. (mM/l)	Optical Density									
		Exp.	Eq. 6.1	Exp.	Eq. 6.1	Exp.	Eq. 6.1	Exp.	Eq. 6.1	Exp.	Eq. 6.1
	4.1	1.827	1.837								
	6.3	1.998	1.979								
	11.2	2.132	2.113								
	15.0	2.313	2.161								
		5000 A		5420 A		5620 A		5780 A		6300 A	
Drabkin and Singer[c] (52)	0.5	0.392	0.507	0.398	0.424	0.405	0.416	0.408	0.418	0.432	0.573
	1.2	0.753	1.001	0.770	0.920	0.753	0.873	0.761	0.903	0.695	1.046
	2.6	1.610	1.590	1.727	1.613	1.661	1.500	1.738	1.617	1.544	1.526
	3.7	1.822	1.888	1.986	2.021	1.887	1.856	2.033	2.051	1.715	1.740
	3.8	1.900	1.898	2.099	2.037	1.957	1.869	2.134	2.068	1.785	1.748
	4.3	1.928	2.005	2.170	2.194	2.033	2.005	2.208	2.238	1.847	1.819
	4.6	2.033	2.062	2.289	2.280	2.134	2.078	2.322	2.333	1.847	1.857
	5.2	2.189	2.164	2.427	2.442	2.228	2.215	2.478	2.511	1.971	1.924
	6.2	2.324	2.293	2.679	2.654	2.457	2.392	2.748	2.747	2.041	2.004
	10.5	2.686	2.638	3.290	3.281	2.871	2.905	3.360	3.465	2.228	2.210
	11.2	2.653	2.675	3.430	3.353	2.960	2.963	3.710	3.549	2.208	2.231

[a]Sample depth = 0.130 cm
[b]Sample depth = 0.163 cm
[c]Sample depth = 0.007 cm

TABLE 6.5. Statistical analysis of the results of Table 6.4: standard deviation of the differences between experimental results in the literature and optical density values calculated from equation 6.1

Authors	Standard Deviation of the Differences (in optical density units)				
	6530 A	10230 A			
Kramer[a] et al (131)	0.070 (4.0%)	0.062 (3.5%)			
	6600 A				
Hickam and Frayser[b] (97)	0.066 (4.1%)				
	5000 A	5420 A	5620 A	5780 A	6300 A
Drabkin and Singer[c] (52)	0.086 (4.7%)	0.070 (3.3%)	0.072 (3.7%)	0.089 (4.1%)	0.118 (7.1%)

[a]Sample depth = 0.130 cm
[b]Sample depth = 0.163 cm
[c]Sample depth = 0.007 cm

wavelengths of 6330 A and 8050 A. The results presented in Table 6.2 of this chapter showed that it may be applied with a high degree of accuracy to results obtained on scattering emulsions as well as blood, using the diffusing plate cuvette oximeter and the Beckman DU spectrophotometer. We have also shown that it applies (with somewhat lower accuracy) to results obtained by other authors using conventional spectrophotometric techniques, over a much wider range of sample depths (0.007 cm to 0.163 cm), and at wavelengths from 5000 A to 10230 A where ϵ varies from 15.13 to less than 0.2.

D. Conclusions

We have verified the observation that whole nonhemolyzed blood and red blood cell suspensions do not obey Beer's law with respect to particle concentration and sample depth, and that, unlike clear, nonscattering solutions, sample depth and particle concentration may not be interchanged. The results for pigmented and nonpigmented emulsions of n-butyl benzoate in water were qualitatively the same as those for blood.

We have again demonstrated that the optical density of red blood cell suspensions and whole blood depends on the measuring technique used. The diffusing plate technique gives lower optical density values than conventional spectro-

photometric techniques as shown by comparing the cuvette oximeter results with the Beckman DU spectrophotometer results. However, it does not provide absolute optical density values.

The nonlinear relationship between optical density and the concentration of scattering material may be described with a high degree of accuracy using the empirically determined equation

$$O.D. = \frac{1}{(ac + b)} c\ d$$

This equation was derived originally to describe the relationship between total hemoglobin concentration in nonhemolyzed blood and the optical density measured using the diffusing plate technique at 6330 A and 8050 A. We found that it could be applied to suspensions of red blood cells and scattering emulsions, both absorbing and non-absorbing, as well as to nonhemolyzed whole blood. We also found that it could be used for results obtained using conventional spectrophotometric techniques in our studies on nonhemolyzed blood and may be applied to studies by Kramer et al (131), Hickam and Frayser (97), and Drabkin and Singer (52). The application of this equation to the results of Drabkin and Singer is particularly interesting since these studies included wavelengths in the highly

absorbing region of the spectrum between 5000 A and 6000 A, rather than in the red and near infrared regions in which little absorption occurs.

The successful application of the above equation to all these results indicates that, although it was derived for a specific set of parameters, it is of considerable general validity with respect to wavelength, type of suspension, and measuring system employed.

VII. APPLICATION OF MULTIPLE SCATTERING THEORY TO LIGHT TRANSMISSION BY BLOOD AND OTHER SUSPENSIONS

A. Introduction

One of our principal aims was to treat the problem of light absorption and scattering by undiluted blood in terms of a light scattering theory. The particle concentration of undiluted blood is so high that a multiple scattering theory which accounts for both coherent and incoherent scattering must be used. We attempted to apply a theory developed by Twersky (226-230) for a random distribution of particles larger than the wavelength of the incident light and with a relative refractive index close to 1.0 to the investigation of the scattering and absorbing properties of whole nonhemolyzed blood. In a recent publication, Loewinger, Gordon, Weinreb, and Gross (145) pointed out that this scattering theory might be applicable to blood.

Twersky's theory defines the amount of light transmitted and scattered into the forward half space. In Chapter V, we showed that the diffusing plate technique results in the collection of a large amount of scattered light. However, this technique does not entirely eliminate, but only reduces, the effects due to the geometry of the measuring system on optical density. Since it is almost impossible to estimate

the fraction of the scattered light being collected in such a measuring system, the diffusing plate technique does not provide absolute measurements of the forward transmitted and scattered light. In order to evaluate quantitatively the scattering and absorption of light by concentrated suspensions of red blood cells, a different measuring system is necessary - one in which the quantity of light being measured can be defined in precise terms. The closest approximation to the ideal instrument is the integrating sphere.

In Chapters IV and VI we showed that the nonlinear relationship between the optical density of nonhemolyzed blood and hemoglobin concentration may be represented by an equation of the form

$$\text{Optical Density} = \epsilon_{rbc} cd = \left[\frac{1}{(ac + b)}\, cd\right] \qquad 6.1$$

and that this equation may be applied to suspensions of red blood cells in hypotonic, isotonic, and hypertonic solutions, and also to emulsions of both absorbing and nonabsorbing spherical particles. It may be applied to results obtained using both the diffusing plate technique and conventional spectrophotometric techniques. Its successful application to data from the literature obtained using conventional spectrophotometers over a wide range of wavelengths and

sample depths indicates that it is of considerable general validity. A further aim of this chapter is an attempt to validate its applicability to the integrating sphere results on red blood cell suspensions, scattering emulsions, and suspensions of large artificial red blood cells.

B. Multiple Light Scattering Theory Applied to Concentrated Red Blood Cell Suspensions

The intensity which is transmitted into the forward half space by a random distribution of discrete scatterers is given by Twersky (230) in the following relation:

$$I/I_o = e^{-\rho\sigma d} + q(\delta)(e^{-[\rho\sigma d \oplus \rho\sigma_s d]} - e^{-\rho\sigma d}) \qquad 7.1$$

The total attenuation cross section for one scatterer, σ, is equal to $\sigma_a + \sigma_s$ (absorption + scattering); $q = \sigma_s \rho$, where ρ is the particle density or number of scatterers per unit volume; $q(\delta)$ is the fraction of the total scattering cross section of one scatterer in free space received by the detector.

For scatterers which do not absorb light, equation 7.1 reduces to

$$I/I_o = e^{-\rho\sigma_s d} + q(\delta)(1 - e^{-\rho\sigma_s d}) \qquad 7.2$$

For absorbing scatterers, equation 7.1 may be written in the form

$$I/I_o = e^{-\varphi \sigma_{ad}} \left[e^{-\varphi \sigma_{sd}} + q(\delta)(1 - e^{-\varphi \sigma_{sd}}) \right] \qquad 7.3$$

The factor outside the square brackets on the right hand side is the only term which contains σ_a, the absorption coefficient. This term corresponds to absorption by the hemoglobin within the cell. The terms in the square bracket account for the scattering by the red cells. The first term in the square brackets describes the coherent scattering and the second term, $q(\delta)(1 - e^{-\varphi \sigma_{sd}})$ corresponds to incoherent scattering.

For large scatterers with relative refractive index near 1.0, Twersky has shown (227) that the scattering attenuation coefficient is given by

$$\varphi \sigma_s = 2x^2 b(m - 1)^2 H(1 - H) \qquad 7.4$$

where $x = 2\pi r/\lambda$, b is a length factor determined by the dimensions of the particles, m is the relative index of refraction, and H is the fractional volume occupied by the scattering particles. The above expression shows that the attenuation due to scattering has a parabolic distribution with respect to particle concentration, due to the factor

$H(1-H)$. Equation 7.3 may now be written

$$I/I_o = e^{-\varsigma \sigma_a d} \left[e^{-2x^2 b (m-1)^2 H(1-H) d} + q(\delta)(1 - e^{-2x^2 b (m-1)^2 H(1-H) d}) \right] \qquad 7.5$$

For simplification in applying this theory to problems in light transmission, this equation was expressed using the base 10 rather than e. Taking logarithms on both sides, equation 7.5 may be written in terms of optical density:

$$\log I_o/I = O.D. = \varsigma \sigma_a d - \log \left[10^{-2x^2 b (m-1)^2 H(1-H) d} + q(\delta)(1 - 10^{-2x^2 b (m-1)^2 H(1-H) d}) \right] \qquad 7.6$$

It may be seen that the first term on the right, $\varsigma \sigma_a d$, is equivalent to Beer's law, where density, ς, is used instead of concentration, c. The second term on the right corresponds to scattering; it is independent of absorption since σ_a does not appear. Scattering is related to the red blood cell concentration in terms of hematocrit, or the fractional volume of the system occupied by the blood cells.

From equation 7.6 it may be seen that the relationship between concentration and absorption is exponential while the relationship between concentration and scattering is

parabolic.

In order to apply this theory to nonhemolyzed blood, conventional spectrophotometric terms have been introduced: concentration, c, in millimoles per liter was substituted for density, ρ ; ϵ was substituted for σ_a; H represents hematocrit. Thus equation 7.6 becomes

$$O.D. = \epsilon cd - \log \left[10^{-sH(1-H)d} + q(\delta)(1 - 10^{-sH(1-H)d})\right] \qquad 7.7$$

where s was substituted for $2x^2b(m-1)^2$.

At constant hemoglobin concentration and sample depth, the second term on the right hand side, corresponding to scattering is constant and equation 7.7 is that of a straight line, $O.D. = m'\epsilon + b'$, where m' = slope = (cd), and b' = y—intercept = $-\log \left[10^{-sH(1-H)d} + q(\delta)(10^{-sH(1-H)d})\right]$. In other words, with concentration and depth held constant, the extinction coefficient of the pigment within the scattering particle is the only independent variable and it is linearly related to optical density.

If the optical density of nonhemolyzed blood at a constant hemoglobin concentration and sample depth is plotted against ϵ , a straight line with a slope m' and a y—intercept, b', should result. Since $m'\epsilon = \epsilon cd$, then $m'\epsilon$ is necessarily the optical density of hemolyzed blood.

Now if the optical density of nonhemolyzed blood at a constant hemoglobin concentration is plotted against the optical density of hemolyzed blood, a straight line with a slope of 1.0 and the same y-intercept, b', as defined above should result.

C. Integrating Sphere

An integrating sphere 7 inches in diameter was built in our laboratory to be used with the Beckman DU spectrophotometer (Fig. 7.1). It was designed to measure single diffuse density. Collimated light from the spectrophotometer strikes the sample chamber at normal incidence; the sample chamber is situated in the usual sample position of the instrument. The detector is placed at 90^{o} relative to the entrance aperture. A screen between the entrance and detector apertures prevents light from reaching the detector before it has been reflected from the walls of the sphere. A photomultiplier attachment is used for wavelengths up to 6300 A.

The entrance and detector apertures are 1.0 cm and 1.35 cm in diameter, respectively. The area of the sample aperture for transmittance measurements is identical to that of the entrance aperture, 0.78 cm^2.

The sphere was prepared by first coating the inside metallic surface with flat white paint, and then spraying the surface 9 times with a 67% barium sulphate suspension

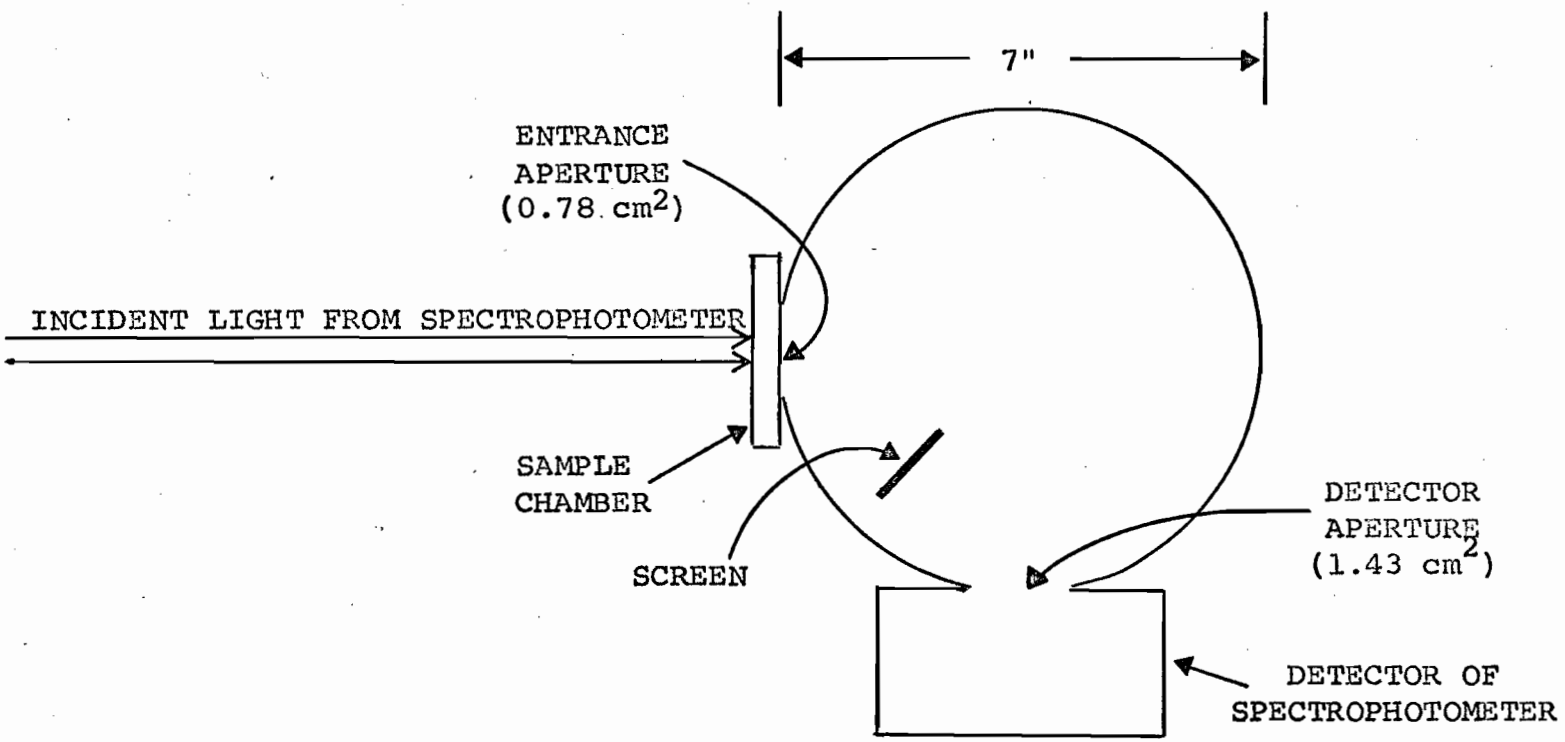

Fig. 7.1. Integrating sphere attachment for measuring transmittance, built for the Beckman DU spectrophotometer.

in water with carboxymethylcellulose as a binder.

Since the Beckman DU spectrophotometer is a single beam instrument, the substitution rather than the comparison method must be used. To measure transmittance, the instrument is standardized with distilled water in the sample chamber to read zero optical density, that is, 100% transmittance - according to the usual procedure for spectrophotometry. The sample is then drawn through the cuvette at a constant flow rate (3.8 ml/minute) and the optical density or percent transmittance reading is taken.

As in the cuvette oximeter experiments, the sample chamber must be disassembled and an interface of silicone grease applied between the two contacting plates of the cuvette before assembling the sample chamber prior to each experiment. The technique for measuring sample depth was described in Chapter VI. The means and standard deviations for the sample depths are given in Table 7.1. Five sample depths were used: 0.011, 0.025, 0.035, 0.048, and 0.071 cm.

D. Materials

The following materials were studied: fully oxygenated nonhemolyzed red blood cells suspended in isotonic saline; emulsions of n-butyl benzoate in water; semipermeable microcapsules consisting of droplets of a hemoglobin solution

TABLE 7.1. Sample depth

	Sample Depth (cm)				
	0.0112	0.0248	0.0356	0.0404	0.0707
	0.0105	0.0245	0.0351	0.0487	0.0685
	0.0110	0.0233	0.0364	0.0494	0.0709
	0.0111	0.0253	0.0355	0.0467	0.0743
	0.0112	0.0267	0.0339	0.0456	0.0721
	0.0112	0.0262	0.0334	. .	0.0701
	. .	0.0240	. .	. .	. .
	. .	0.0242	. .	. .	. .
Mean	0.0110	0.0249	0.0350	0.0480	0.0711
S.D.[a]	±.0003	±.0011	±.0011	±.0017	±.0019

[a]Standard deviation = $\left[1/(n-1)\ \sum(x - \bar{x})^2\right]^{\frac{1}{2}}$.

encapsulated in nylon membranes (36).

The red cell suspensions and emulsions were prepared as described in Chapter V.

The semipermeable microcapsules were prepared in the Physiology Department of McGill University by Dr. T. M. S. Chang. The particles have a mean diameter of 40 microns, with a standard deviation of ±20 microns. Contained within the microcapsule is a solution of hemoglobin (methemoglobin and oxyhemoglobin) at a concentration of approximately one third that present within the normal red blood cell.

Measurements were made at discrete wavelengths between 5000 A and 6300 A.

E. Results

1. Red Blood Cells

Two interesting features of Twersky's theory are first, the exponential relationship between absorption and concentration, showing that absorption obeys Beer's law, and second, the parabolic relationship between scattering and the fractional volume occupied by the scattering material.

a) Relationship between Optical Density and Wavelength

The optical density of red blood cell suspensions at various hemoglobin concentrations was measured in the integrating sphere at four wavelengths. Wavelengths at which the extinction coefficient for oxyhemoglobin covers a wide range were chosen: 5400 A (ϵ = 15.5); 5600 A (ϵ = 9.3); 5050 A (ϵ = 5.2); 6000 A (ϵ = 0.8).

Fig. 7.2 shows optical density plotted against hemoglobin concentration at the four wavelengths mentioned. The relationship between optical density and concentration was almost linear at the wavelength at which ϵ is highest. With decreasing ϵ the evolution of the curve became more and more parabolic as predicted by Twersky's theory. The results indicate that at wavelengths with high extinction coefficients, the absorption term is dominant, while at wavelengths with low extinction coefficients the scattering term predominates.

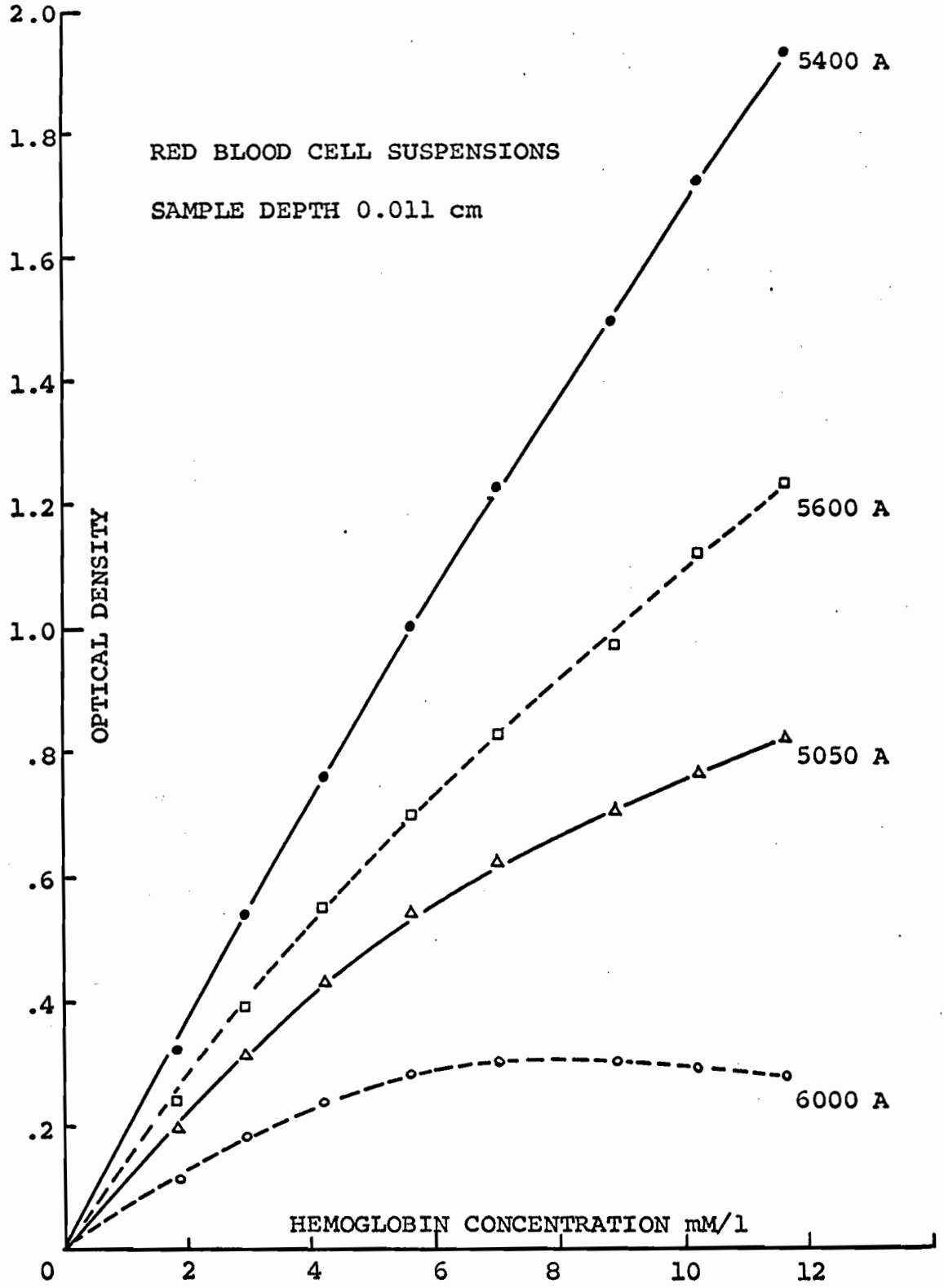

Fig. 7.2. Optical density at a sample depth of 0.011 cm is plotted against hemoglobin concentration at four wavelengths at which the extinction coefficient for oxygenated hemoglobin has a wide range of values: at 5400 A, ϵ is 15.5; at 5600 A, ϵ is 9.3; at 5050 A, ϵ is 5.2; at 6000 A, ϵ is 0.8.

b) Relationship between Optical Density and Sample Depth

Optical density was measured at five sample depths and at two wavelengths - 5050 A and 6300 A. Fig. 7.3 shows optical density plotted against sample depth at these two wavelengths. The relationship between optical density and depth for all hemoglobin concentrations tested was almost linear at 5050 A where ϵ is quite high (ϵ = 5.2), while at 6300 A, where ϵ is 26 times smaller (ϵ = 0.2), the relationship was markedly nonlinear.

c) Relationship between the Optical Density of Nonhemolyzed Blood and the Optical Density of Hemolyzed Blood

In section B of this chapter we said that if the optical density of nonhemolyzed blood at a constant hemoglobin concentration and sample depth is plotted against the extinction coefficient of hemoglobin, a straignt line with a slope $m' = cd$ and a y—intercept b' should result; or, if the optical density of nonhemolyzed blood is plotted against that of hemolyzed blood, a straight line with a slope of 1.0 and the same y—intercept, b', should result.

Optical density was varied by changing the wavelength. Three different concentrations of nonhemolyzed and hemolyzed blood, ranging from 2.5 to 6.3 mM/l (4.1 to 10.6 gm/100 ml) in hemoglobin concentration were scanned at 100 A intervals between 5000 A and 6200 A at a sample depth of 0.011 cm.

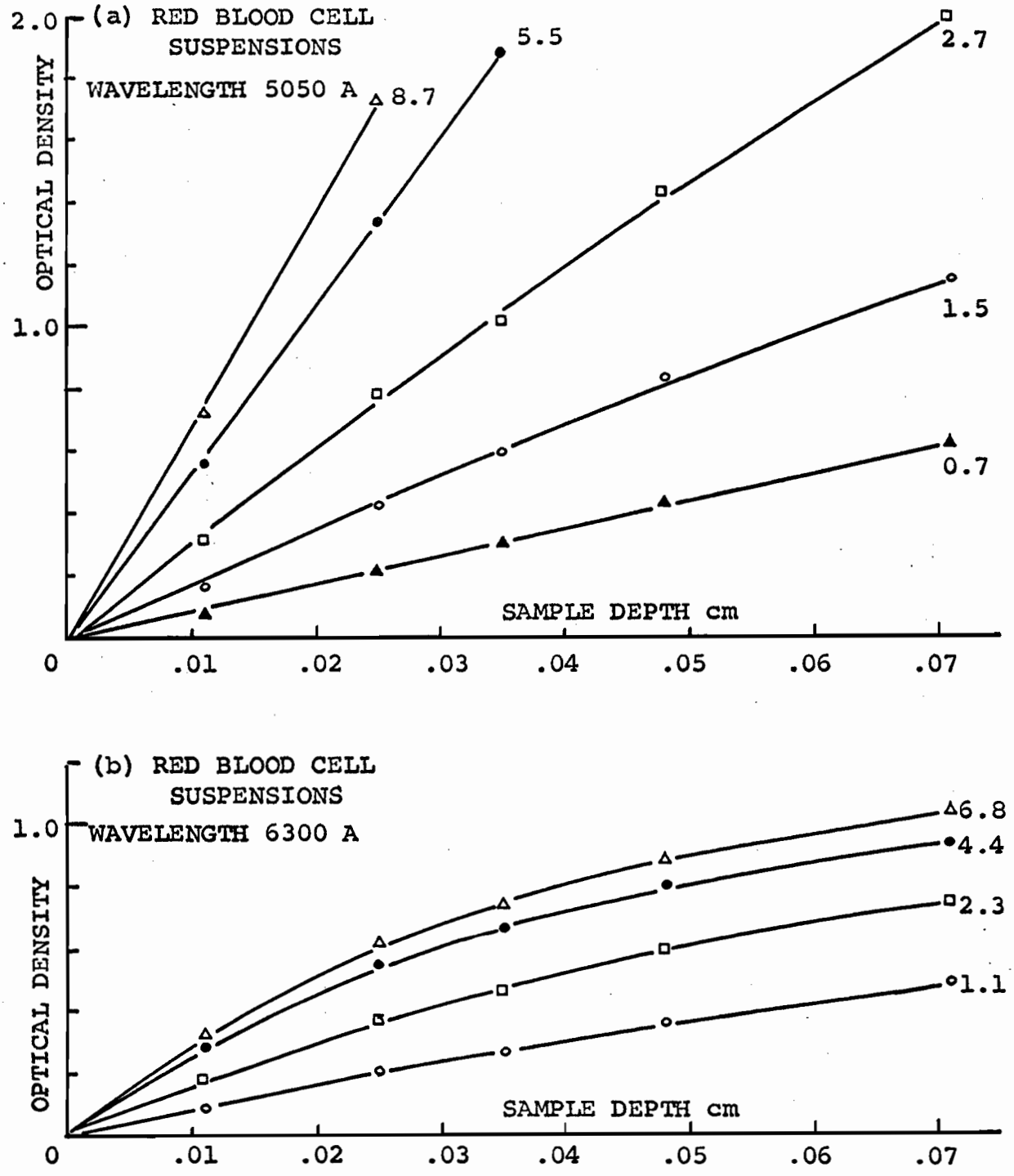

Fig. 7.3. Optical density is plotted against sample depth at two wavelengths, 5050 A (Fig. a) and 6300 A (Fig. b). At 5050 A, the extinction coefficient for oxygenated hemoglobin is 5.2; at 6300 A, it is 0.2. Each line represents a different hemoglobin concentration in mM/l, as shown by the value beside each curve.

At longer wavelengths, the sensitivity of the measuring system was diminished, making the use of wide slits necessary, resulting in less monochromatic incident light. The optical density of nonhemolyzed blood was plotted against the optical density of hemolyzed blood of the same concentration. In each case the result was a straight line with a y intercept, as shown in Fig. 7.4 for a hemoglobin concentration of 4.3 mM/l. The mean slope at the three hemoglobin concentrations studied was close to 1.0 (0.92).

To show that this linear relationship was valid at all sample depths, measurements were made at discrete wavelengths between 5050 A and 5900 A. At sample depths greater than 0.011 cm, measurements could be made only at fairly low hemoglobin concentrations due to the high extinction coefficients of hemoglobin in this region of the spectrum.

The relationship between the optical density of nonhemolyzed red blood cell suspensions and the optical density of hemolyzed blood at a constant hemoglobin concentration was linear at all sample depths. The slope at the various sample depths is shown in Table 7.2. There appears to be a slight trend towards an increase in slope with increasing sample depth. However, the mean of the slopes at all sample depths was 0.97. This was considered to be close enough to the theoretical prediction of 1.0 to be considered

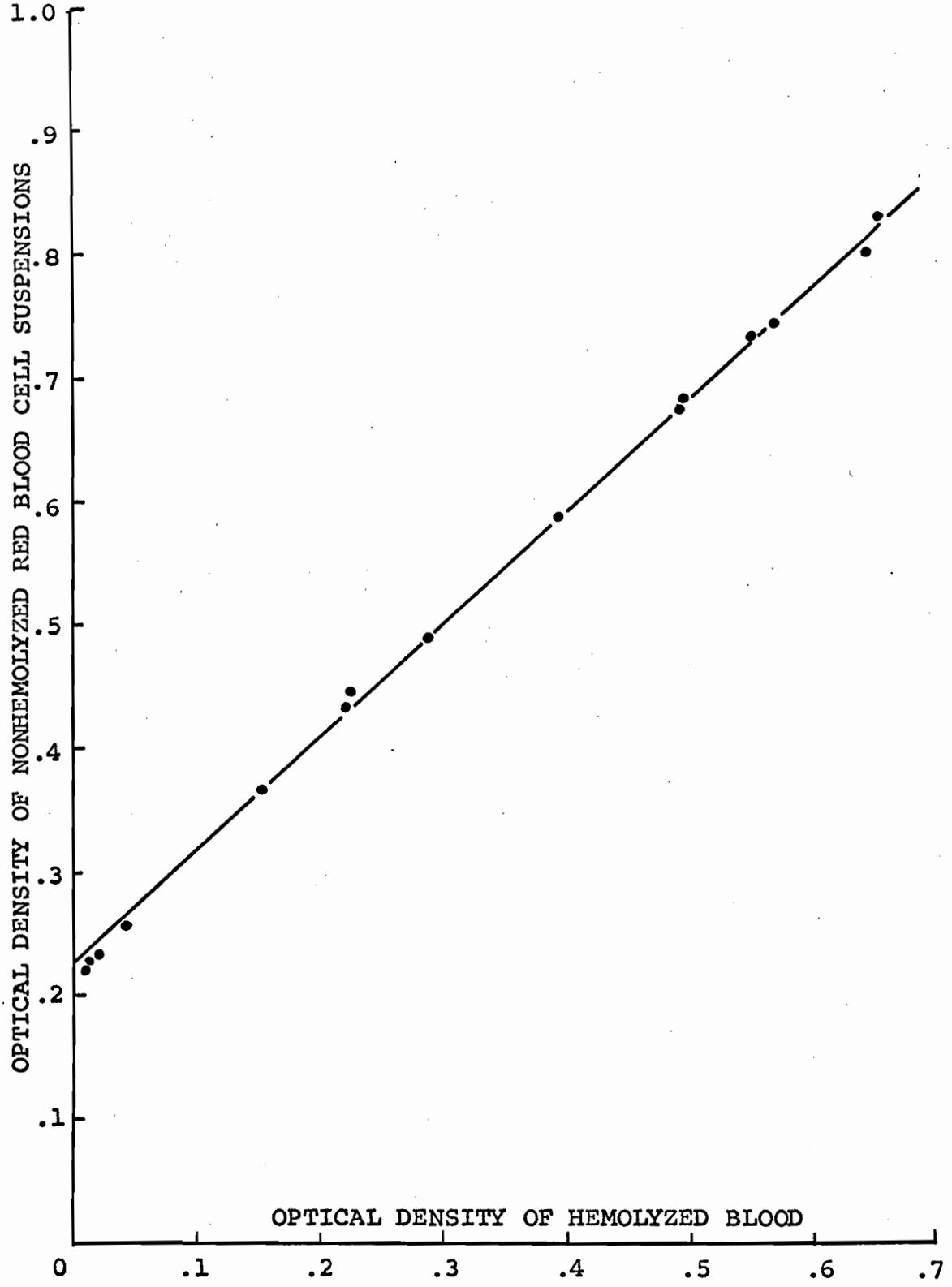

Fig. 7.4. The relationship between the optical density of nonhemolyzed blood and that of hemolyzed blood is linear at a constant hemoglobin concentration and sample depth. Each point represents a pair of measurements at one wavelength. The wavelength range was 5200 A to 6200 A, and measurements were made at 100 A intervals. Hemoglobin concentration was 4.3 mM/l and sample depth was 0.011 cm

TABLE 7.2. Constants used in the application of Twersky's theory to nonhemolyzed blood

Sample Depth (cm)	Hemoglobin Concentration Range	n[a]	Slope	s
0.011	2.5 - 11.7 mM/l 4.1 - 19.5 gm/100 ml	9	0.94	109.1
0.025	0.6 - 2.1 mM/l 0.9 - 3.5 gm/100 ml	4	0.91	
	0.6 - 5.0 mM/l 0.9 - 8.3 gm/100 ml	4		149.4
0.035	0.3 - 3.1 mM/l 0.6 - 5.3 gm/100 ml	7	0.96	150.2
0.048	0.3 - 3.1 mM/l 0.6 - 5.3 gm/100 ml	7	1.03	150.2
0.071	0.3 - 3.1 mM/l 0.6 - 5.3 gm/100 ml	7	1.00	150.2
		Mean	0.97	

[a]Number of observations.

as such in subsequent calculations.

This straight line relationship is very significant. It shows that the linear relationship of Beer's law between optical density and the extinction coefficient of hemoglobin is valid for hemoglobin even when it is contained within scattering particles.

The question of the identity of the absorbing properties of hemoglobin within the red blood cell and of free hemoglobin

had been raised by Adams, Bradley, and Macallum (3), Keilin and Hartree (119), Jope (115), and Barer (11, 12). Drabkin and Singer found it necessary to use a fairly complicated expression to relate light absorption by hemoglobin in intact red cells to the extinction coefficient of hemoglobin in solution.

Barer was able to show that if scattering was completely eliminated by suspending red blood cells in concentrated protein solutions, the suspension behaved like a hemoglobin solution (11, 12). In the present experiment, the straight line relationship of Fig. 7.4 demonstrates that light absorption by the hemoglobin molecule within the red blood cell is the same as light absorption by free hemoglobin in solution.

d) Application of Twersky's Theory

In order to express optical density in terms of Twersky's theory, it was necessary to obtain values for the constants s and $q(\delta)$ of equation 7.7. Values of s were obtained at each sample depth and are shown in Table 7.2. It may be seen that, except at 0.011 cm, the values of s are almost identical at sample depths from 0.025 cm to 0.071 cm. The mean of s at the four largest sample depths, 150.1, was used to calculate the results at these sample depths. At 0.011 cm, s was

109.1. The value of $q(\delta)$ was found to be 0.4 at all sample depths.

Optical density was calculated from equation 7.7 using these constants. Table 7.3 shows the experimental values and the calculated values. The results are presented graphically in Figures 7.5a to 7.5d. The dots represent the experimental values and the solid lines were calculated from equation 7.7.

The agreement between experimental and calculated values was very good. Statistical analysis is presented in Table 7.4. The mean of the standard deviations of the differences between experimental observations and values calculated from Twersky's theory for all four wavelengths and five sample depths was 0.015 optical density units, or 2.0% of the mean optical value. The maximum standard deviation of the differences was 0.038 optical density units, representing 5.4% of the mean value at a sample depth of 0.011 cm and a wavelength of 5600 A.

The demonstration that Twersky's theory may be applied to nonhemolyzed blood is particularly interesting since it enables us to separate the effects of absorption from the effects of scattering on the optical density of blood. Fig. 7.6 shows the results at 5050 A and at a sample depth of 0.071 cm. In this illustration, the optical density

TABLE 7.3. Comparison of optical density values for red blood cell suspensions obtained by experiment with those obtained by calculation from equations 7.7 and 6.1

λ (A)	Hb Conc. mM/l	Optical Density											
		Sample Depth (cm)											
		0.011			0.025			0.035			0.048			0.071		
		Exp.	Eq. 7.7	Eq. 6.1	Exp.	Eq. 7.7	Eq. 6.1	Exp.	Eq. 7.7	Eq. 6.1	Exp.	Eq. 7.7	Eq. 6.1	Exp.	Eq. 7.7	Eq. 6.1
5050	0.3	. .	. .	. .	. .	. .	. .	0.148	0.157	0.153	0.210	0.214	0.220	0.319	0.316	0.334
	0.6	. .	. .	. .	0.180	0.177	0.193	. .	. .	. .	. .	. .	. .	. .	. .	. .
	0.6	. .	. .	. .	. .	. .	. .	0.275	0.272	0.270	0.388	0.372	0.386	0.583	0.549	0.576
	0.6	. .	. .	. .	0.206	0.205	0.221	. .	. .	. .	. .	. .	. .	. .	. .	. .
	0.7	0.078	0.079	0.098	0.208	0.227	0.245	0.301	0.316	0.312	0.427	0.433	0.444	0.615	0.635	0.661
	0.9	. .	. .	. .	. .	. .	. .	0.404	0.398	0.393	0.557	0.543	0.557	0.820	0.798	0.820
	1.1	. .	. .	. .	0.346	0.339	0.357	. .	. .	. .	. .	. .	. .	. .	. .	. .
	1.2	. .	. .	. .	. .	. .	. .	0.538	0.527	0.518	0.731	0.718	0.729	1.063	1.061	1.051
	1.4	0.405	0.429	0.447	. .	. .	. .	. .	. .	. .	. .	. .	. .	. .	. .	. .
	1.5	0.161	0.158	0.189	0.426	0.450	0.472	0.593	0.617	0.628	0.815	0.858	0.864	1.196	1.242	1.243
	1.6	. .	. .	. .	0.502	0.499	0.509	. .	. .	. .	. .	. .	. .	. .	. .	. .
	1.8	0.192	0.199	0.232	. .	. .	. .	. .	. .	. .	. .	. .	. .	. .	. .	. .
	2.1	. .	. .	. .	. .	. .	. .	0.893	0.876	0.854	1.176	1.188	1.183	1.668	1.701	1.662
	2.1	. .	. .	. .	0.652	0.647	0.642	. .	. .	. .	. .	. .	. .	. .	. .	. .
	2.5	0.253	0.260	0.296	. .	. .	. .	. .	. .	. .	. .	. .	. .	. .	. .	. .
	2.5	. .	. .	. .	. .	. .	. .	1.041	1.031	1.002	1.364	1.390	1.376	1.932	1.971	1.907
	2.6	. .	. .	. .	0.756	0.763	0.760	. .	. .	. .	. .	. .	. .	. .	. .	. .
	2.7	0.310	0.282	0.318	0.779	0.790	0.796	1.070	1.101	1.069	1.432	1.481	1.463	2.002	2.078	2.015
	3.0	0.313	0.307	0.341	. .	. .	. .	. .	. .	. .	. .	. .	. .	. .	. .	. .
	3.2	. .	. .	. .	. .	. .	. .	1.264	1.254	1.215	1.662	1.678	1.651	. .	. .	. .
	3.8	. .	. .	. .	1.040	1.078	1.031	. .	. .	. .	. .	. .	. .	. .	. .	. .

TABLE 7.3. Continued

λ (A)	Hb Conc. mM/l	Optical Density											
		Sample Depth (cm)											
		0.011			0.025			0.035			0.048			0.071		
		Exp.	Eq. 7.7	Eq. 6.1	Exp.	Eq. 7.7	Eq. 6.1	Exp.	Eq. 7.7	Eq. 6.1	Exp.	Eq. 7.7	Eq. 6.1	Exp.	Eq. 7.7	Eq. 6.1
	4.2	0.430	0.415	0.443	. .	. .	. .	. .	. .	. .	. .	. .	. .	. .	. .	. .
	4.3	0.434	0.423	0.449	. .	. .	. .	. .	. .	. .	. .	. .	. .	. .	. .	. .
	5.0	. .	. .	. .	1.305	1.323	1.232	. .	. .	. .	. .	. .	. .	. .	. .	. .
	5.5	0.557	0.518	0.534	1.342	1.431	1.317	1.886	1.947	1.896	. .	. .	. .	. .	. .	. .
	5.6	0.543	0.528	0.540	. .	. .	. .	. .	. .	. .	. .	. .	. .	. .	. .	. .
	6.3	0.590	0.579	0.585	. .	. .	. .	. .	. .	. .	. .	. .	. .	. .	. .	. .
	7.0	0.622	0.625	0.623	. .	. .	. .	. .	. .	. .	. .	. .	. .	. .	. .	. .
	8.7	0.704	0.738	0.707	. .	. .	. .	. .	. .	. .	. .	. .	. .	. .	. .	. .
	8.9	0.697	0.736	0.713	. .	. .	. .	. .	. .	. .	. .	. .	. .	. .	. .	. .
	10.3	0.766	0.801	0.770	. .	. .	. .	. .	. .	. .	. .	. .	. .	. .	. .	. .
	11.7	0.822	0.855	0.820	. .	. .	. .	. .	. .	. .	. .	. .	. .	. .	. .	. .
5200	0.3	. .	. .	. .	. .	. .	. .	0.164	0.177	0.173	0.234	0.242	0.244	0.370	0.358	0.370
	0.6	. .	. .	. .	0.201	0.201	0.202	. .	. .	. .	. .	. .	. .	. .	. .	. .
	0.6	. .	. .	. .	. .	. .	. .	0.305	0.309	0.307	0.429	0.423	0.429	0.645	0.624	0.645
	0.9	. .	. .	. .	. .	. .	. .	0.452	0.453	0.449	0.628	0.618	0.624	0.929	0.910	0.928
	1.1	. .	. .	. .	0.387	0.385	0.386	. .	. .	. .	. .	. .	. .	. .	. .	. .
	1.2	. .	. .	. .	. .	. .	. .	0.599	0.596	0.601	0.819	0.819	0.823	1.204	1.212	1.201
	1.6	. .	. .	. .	0.567	0.569	0.568	. .	. .	. .	. .	. .	. .	. .	. .	. .
	2.1	. .	. .	. .	. .	. .	. .	1.010	1.004	1.001	1.364	1.363	1.358	. .	. .	. .
	2.1	. .	. .	. .	0.746	0.734	0.744	. .	. .	. .	. .	. .	. .	. .	. .	. .
	2.5	0.287	0.297	0.293	. .	. .	. .	. .	. .	. .	. .	. .	. .	. .	. .	. .
	2.5	. .	. .	. .	. .	. .	. .	1.171	1.185	1.183	1.594	1.600	1.594	. .	. .	. .

TABLE 7.3. Continued

λ (A)	Hb Conc. mM/l	Optical Density											
		Sample Depth (cm)											
		0.011			0.025			0.035			0.048			0.071		
		Exp.	Eq. 7.7	Eq. 6.1	Exp.	Eq. 7.7	Eq. 6.1	Exp.	Eq. 7.7	Eq. 6.1	Exp.	Eq. 7.7	Eq. 6.1	Exp.	Eq. 7.7	Eq. 6.1
	3.2	. .	. .	. .	. .	. .	. .	1.456	1.446	1.452	1.936	1.941	1.936	. .	. .	. .
	4.3	0.489	0.487	0.480	. .	. .	. .	. .	. .	. .	. .	. .	. .	. .	. .	. .
	6.3	0.672	0.674	0.672	. .	. .	. .	. .	. .	. .	. .	. .	. .	. .	. .	. .
5300	0.3	. .	. .	. .	. .	. .	. .	0.212	0.237	0.233	0.303	0.314	0.317	0.479	0.480	0.480
	0.6	. .	. .	. .	0.257	0.270	0.264	. .	. .	. .	. .	. .	. .	. .	. .	. .
	0.6	. .	. .	. .	. .	. .	. .	0.400	0.412	0.416	0.567	0.569	0.565	0.854	0.841	0.850
	0.9	. .	. .	. .	. .	. .	. .	0.598	0.611	0.603	0.827	0.835	0.830	1.240	1.230	1.243
	1.1	. .	. .	. .	0.508	0.518	0.507	. .	. .	. .	. .	. .	. .	. .	. .	. .
	1.2	. .	. .	. .	. .	. .	. .	0.800	0.813	0.802	1.102	1.110	1.108	1.658	1.632	1.652
	1.6	. .	. .	. .	0.747	0.767	0.749	. .	. .	. .	. .	. .	. .	. .	. .	. .
	2.1	. .	. .	. .	. .	. .	. .	1.360	1.371	1.350	1.896	1.867	1.888	. .	. .	. .
	2.1	. .	. .	. .	0.987	0.998	0.986	. .	. .	. .	. .	. .	. .	. .	. .	. .
	2.5	0.381	0.414	0.407	. .	. .	. .	. .	. .	. .	. .	. .	. .	. .	. .	. .
	2.5	. .	. .	. .	. .	. .	. .	1.600	1.625	1.597	2.250	2.204	2.248	. .	. .	. .
	3.2	. .	. .	. .	. .	. .	. .	1.957	1.998	1.962	. .	. .	. .	. .	. .	. .
	4.3	0.676	0.688	0.675	. .	. .	. .	. .	. .	. .	. .	. .	. .	. .	. .	. .
	6.3	0.956	0.971	0.956	. .	. .	. .	. .	. .	. .	. .	. .	. .	. .	. .	. .
5600	0.3	. .	. .	. .	. .	. .	. .	0.185	0.205	0.198	0.263	0.280	0.274	0.419	0.424	0.414
	0.6	. .	. .	. .	0.228	0.232	0.228	. .	. .	. .	. .	. .	. .	. .	. .	. .
	0.6	. .	. .	. .	. .	. .	. .	0.346	0.358	0.353	0.484	0.488	0.485	0.738	0.723	0.738
	0.9	. .	. .	. .	. .	. .	. .	0.516	0.525	0.517	0.712	0.717	0.710	1.068	1.056	1.057
	1.1	. .	. .	. .	0.442	0.446	0.440	. .	. .	. .	. .	. .	. .	. .	. .	. .

TABLE 7.3. Continued

λ (A)	Hb Conc. mM/l	Optical Density											
		Sample Depth (cm)											
		0.011			0.025			0.035			0.048			0.071		
		Exp.	Eq. 7.7	Eq. 6.1	Exp.	Eq. 7.7	Eq. 6.1	Exp.	Eq. 7.7	Eq. 6.1	Exp.	Eq. 7.7	Eq. 6.1	Exp.	Eq. 7.7	Eq. 6.1
	1.2	. .	. .	. .	. .	. .	. .	0.689	0.697	0.688	0.943	0.951	0.943	1.377	1.397	1.377
	1.6	. .	. .	. .	0.648	0.649	0.650	. .	. .	. .	. .	. .	. .	. .	. .	. .
	1.8	0.238	0.272	0.268	. .	. .	. .	. .	. .	. .	. .	. .	. .	. .	. .	. .
	2.1	. .	. .	. .	. .	. .	. .	1.176	1.171	1.165	1.582	1.592	1.587	. .	. .	. .
	2.1	. .	. .	. .	0.857	0.855	0.857	. .	. .	. .	. .	. .	. .	. .	. .	. .
	2.5	0.341	0.357	0.350	. .	. .	. .	. .	. .	. .	. .	. .	. .	. .	. .	. .
	2.5	. .	. .	. .	. .	. .	. .	1.369	1.385	1.382	1.886	1.875	1.878	. .	. .	. .
	3.0	0.391	0.423	0.410	. .	. .	. .	. .	. .	. .	. .	. .	. .	. .	. .	. .
	3.2	. .	. .	. .	. .	. .	. .	1.710	1.698	1.704	2.310	2.287	2.305	. .	. .	. .
	4.2	0.548	0.579	0.554	. .	. .	. .	. .	. .	. .	. .	. .	. .	. .	. .	. .
	4.3	0.588	0.590	0.564	. .	. .	. .	. .	. .	. .	. .	. .	. .	. .	. .	. .
	5.6	0.701	0.747	0.706	. .	. .	. .	. .	. .	. .	. .	. .	. .	. .	. .	. .
	6.3	0.824	0.825	0.778	. .	. .	. .	. .	. .	. .	. .	. .	. .	. .	. .	. .
	7.0	0.829	0.922	0.843	. .	. .	. .	. .	. .	. .	. .	. .	. .	. .	. .	. .
	8.9	0.970	1.082	1.006	. .	. .	. .	. .	. .	. .	. .	. .	. .	. .	. .	. .
	10.3	1.116	1.202	1.116	. .	. .	. .	. .	. .	. .	. .	. .	. .	. .	. .	. .
	11.7	1.229	1.310	1.217	. .	. .	. .	. .	. .	. .	. .	. .	. .	. .	. .	. .

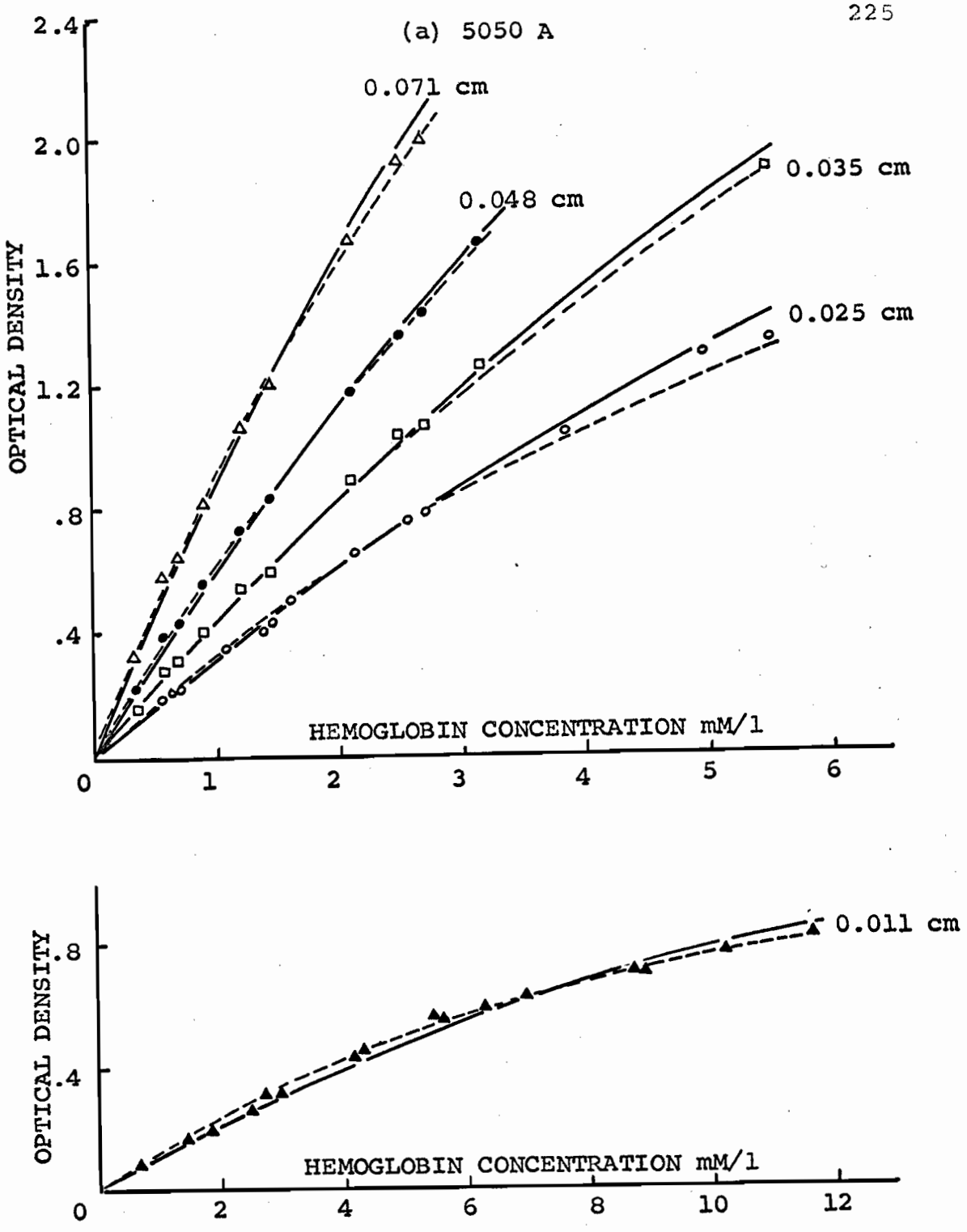

Fig. 7.5. Optical density is plotted against hemoglobin concentration. The dots represent experimental values of optical density. The solid lines represent optical density values calculated according to equation 7.7, based on Twersky's theory. The dotted lines were calculated from the empirical relationship of equation 6.1. Results are shown at five sample depths - 0.011, 0.025, 0.035, 0.048, and 0.071 cm, and at four wavelengths - 5050 A (Fig. a), 5200 A (Fig. b), 5300 A (Fig. c), and 5600 A (Fig. d).

(b) 5200 A

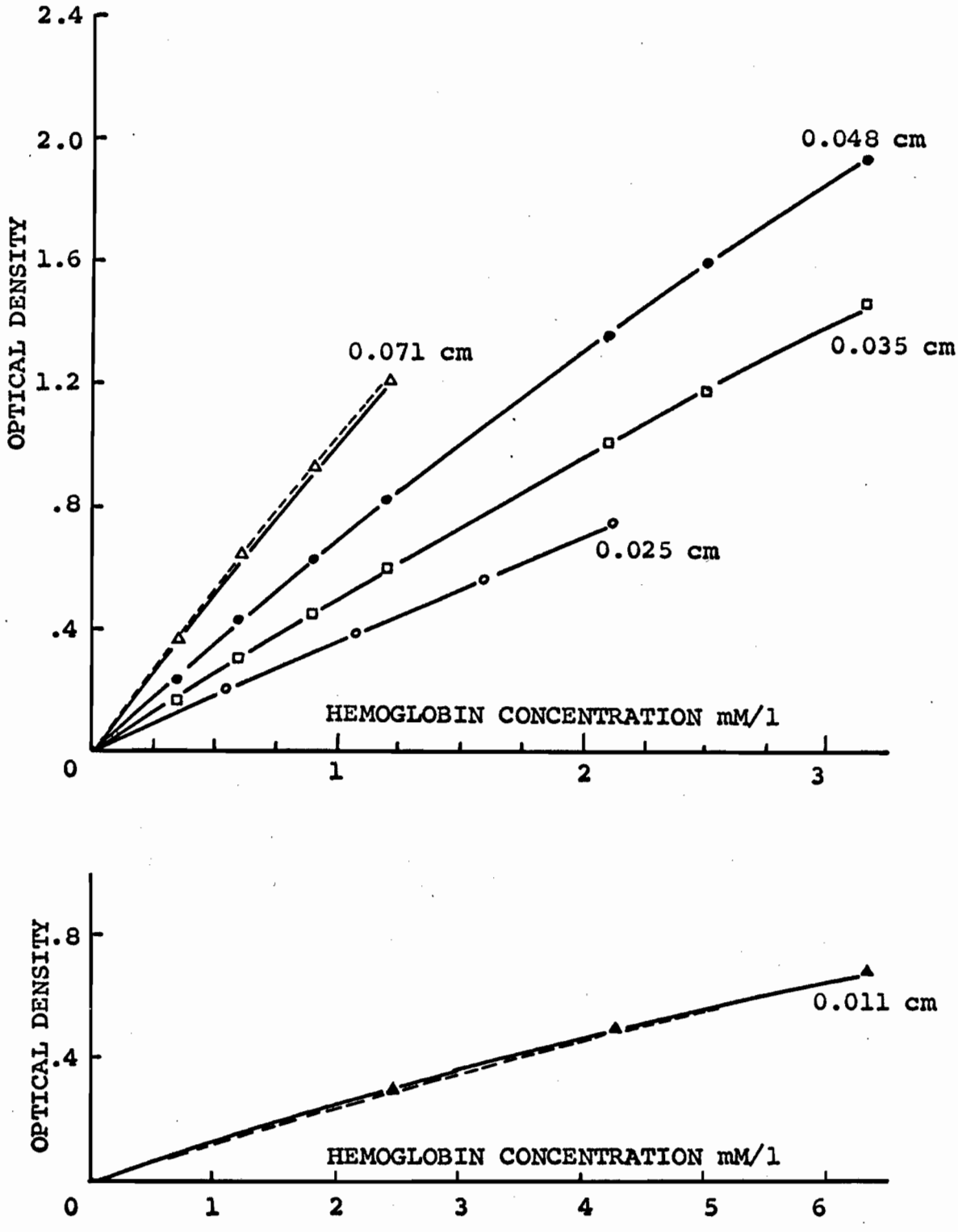

Fig. 7.5. Continued.

(c) 5300 A

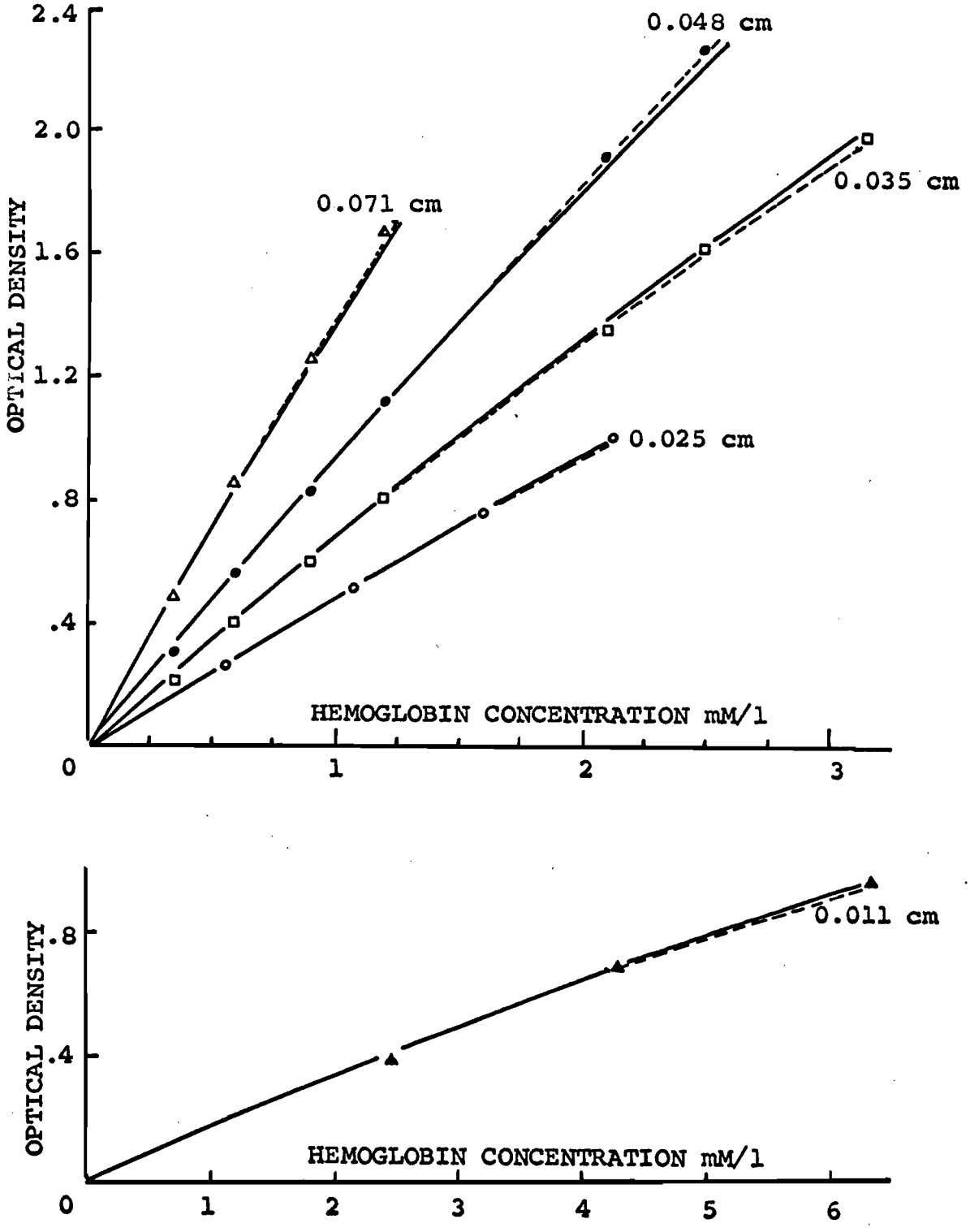

Fig. 7.5. Continued.

(d) 5600 A

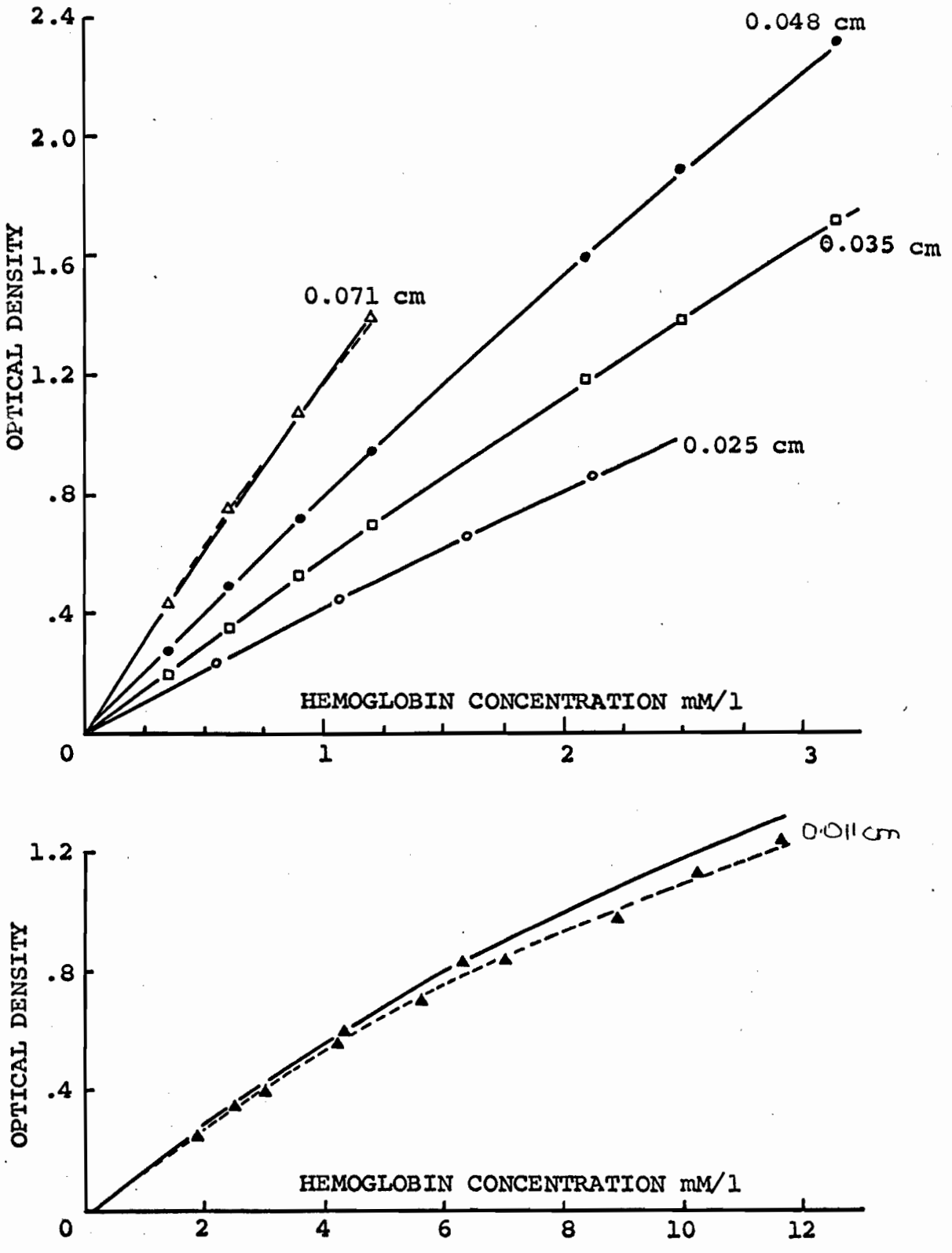

Fig. 7.5. Continued.

TABLE 7.4. Statistical analysis of the results of Table 7.3: standard deviation of the differences between experimental values and values calculated from equations 7.7 and 6.1

Wavelength (A)	Standard Deviation of the Differences (in optical density units)									
	Sample Depth (cm)									
	0.011		0.25		0.035		0.048		0.071	
	Eq.7.7	Eq.6.1	Eq.7.7	Eq.6.1	Eq.7.7	Eq.6.1	Eq.7.7	Eq.6.1	Eq.7.7	Eq.6.1
5050	±0.024[a]	±0.016[b]	±0.025	±0.030	±0.025	±0.024	±0.023	±0.004	±0.034	±0.024
	(5.1%)[c]	(3.5%)	(3.9%)	(4.2%)	(3.2%)	(3.1%)	(2.6%)	(0.5%)	(3.0%)	(2.1%)
5200	±0.006	±0.007	±0.006	±0.001	±0.009	±0.007	±0.007	±0.005	±0.008	±0.004
	(1.3%)	(1.5%)	(1.3%)	(0.3%)	(1.2%)	(1.0%)	(0.7%)	(0.5%)	(1.0%)	(0.5%)
5300	±0.011	±0.015	±0.004	±0.002	±0.010	±0.010	±0.024	±0.008	±0.011	±0.003
	(1.7%)	(2.3%)	(0.7%)	(0.3%)	(1.1%)	(1.0%)	(2.1%)	(0.7%)	(1.0%)	(0.3%)
5600	±0.038	±0.024	±0.003	±0.002	±0.011	±0.009	±0.014	±0.006	±0.016	±0.007
	(5.4%)	(3.3%)	(0.5%)	(0.3%)	(1.3%)	(1.1%)	(1.2%)	(0.5%)	(1.8%)	(0.7%)

[a]Standard deviation of the differences between experimental optical density values and those calculated from equation 7.7.

[b]Standard deviation of the differences between experimental optical density values and those calculated from equation 6.1

$$S.D.D. = \left[1/(n-1) \sum (d - \bar{d})^2\right]^{\frac{1}{2}}.$$

[c]Standard deviation of the differences expressed as a percent of the mean optical density value.

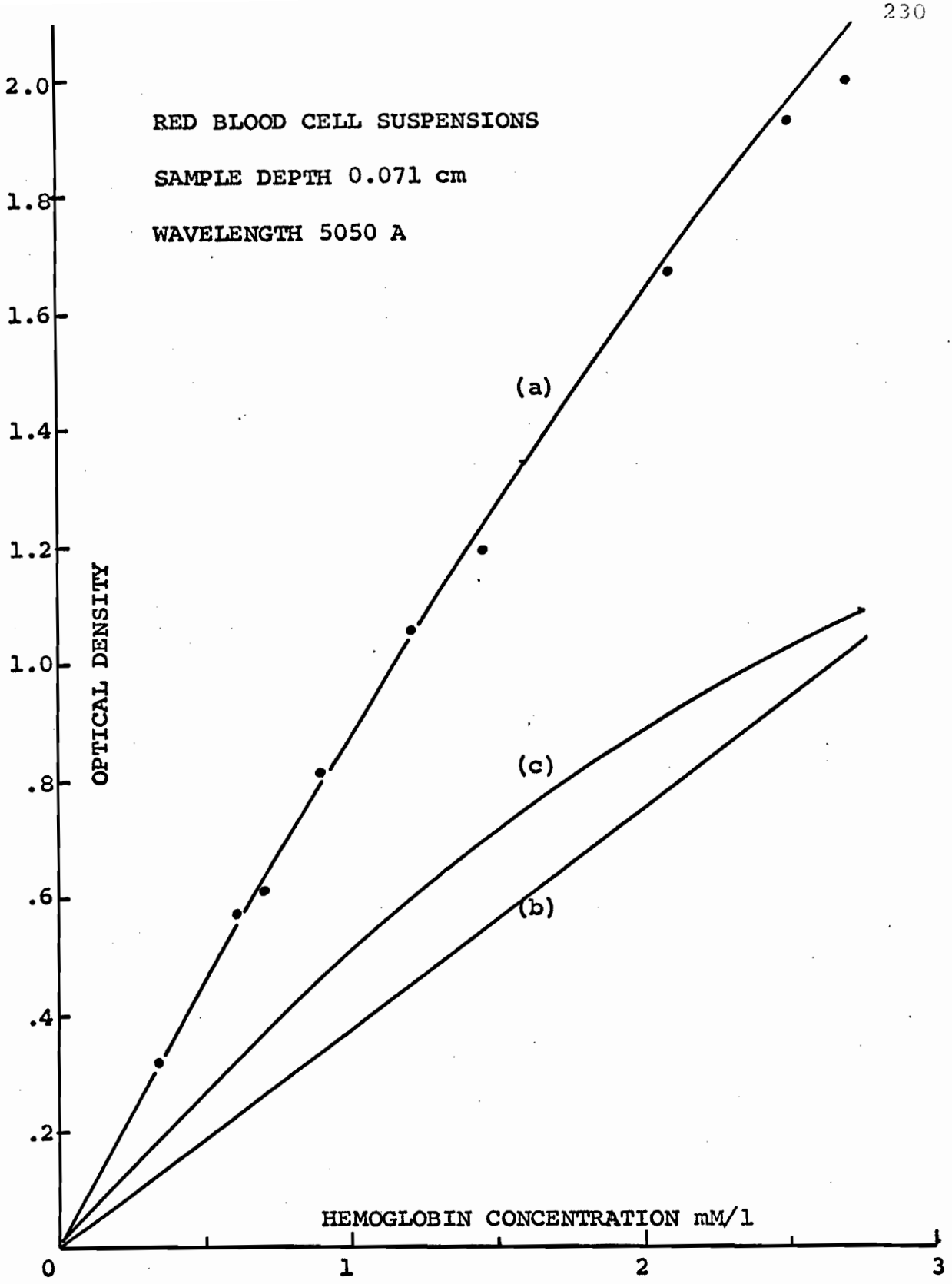

Fig. 7.6. The optical density components due to scattering (curve c) and absorption (curve b) have been plotted separately. Total optical density is represented by curve a.

components due to scattering and absorption have been plotted separately. Curve (b) shows the linear relationship between optical density and absorption. Curve (c) shows the parabolic relationship between optical density and scattering, and curve (a) is the composite curve showing the nonlinear relationship between total optical density and concentration. Curve (c), which represents the scattering component, remains the same for this sample depth when the wavelength is varied. Thus, the optical density at 5300 A, for example, is obtained by changing only curve (b), which now becomes the product of the extinction coefficient for hemoglobin at 5300 A times the sample concentration and depth, and then summing curve (c) with the new curve (b).

The results show that Twersky's theory for the multiple scattering of waves by a random distribution of arbitrary scatterers may be applied to nonhemolyzed blood using only the constants required by the theory, s and $q(\delta)$. Numerical values for the two constants were obtained empirically. As mentioned in section B, s was substituted for $2x^2b(m-1)^2$ where $x = 2\pi r/\lambda$, b is a factor determined by the dimensions of the particles, and m is the relative refractive index. $q(\delta)$ depends on the solid cone angle subtended by the detector.

In view of the technical difficulties inherent in the

integrating sphere technique, it was impossible to insure that all scattered light was collected; consequently, we did not feel justified in trying to analyze the components which contribute to s (refractive index and cell size) or the exact significance of $q(\delta)$. In Chapter III we pointed out that, theoretically, the integrating sphere collects all light scattered into either the forward or backward hemisphere; however, in practice, it is extremely difficult to obtain absolute transmittance values for the following reasons. (i) The presence of screens and apertures results in a departure from the ideal measuring system. (ii) It is known (200) that in a sample chamber consisting of plane parallel plates, there is always a loss of scattered light from the sides of the sample chamber. (iii) The incident light from the Beckman DU spectrophotometer is slightly divergent rather than parallel. (iv) A very important technical factor is the problem of surface reflections. This problem arises when the index of refraction of the medium surrounding the sample chamber or sample differs from that of the sample. Extremely complicated measuring systems have been devised to circumvent this problem (53, 247); these methods require filling the integrating sphere with a material of the same refractive index as the matrix or suspending material.

We have not included wavelength in the calculations,

although the square of the wavelength appears in the denominator of the exponent of the scattering term. Since, over the wavelength range we have studied, λ changes only by 2%, and since the relationship between the optical density of nonhemolyzed blood was linearly related to ϵ over this range (as shown in Fig. 7.4), we treated this factor as a constant in the present experiments.

The size and shape of the red blood cells affect the light scattering properties of nonhemolyzed blood. However, this problem is a refinement of the basic question of the light scattering and absorption by blood.

e) Application of Equation 6.1

Our next step was to see if equation 6.1, optical density = cd/(ac + b), could be applied to results obtained with the integrating sphere. This equation was obtained empirically from cuvette oximeter experiments described in Chapter IV; its applicability to results obtained at 6330 A on a wide variety of suspensions with various measuring systems was demonstrated in Chapter VI.

Optical density was calculated from equation 6.1 for all the results in this section. The constants a and b were redetermined for each wavelength and sample depth. The values calculated from equation 6.1 are shown by the dotted lines in Figures 7.5a to 7.5d, the same graphs in which the results

calculated using Twersky's theory were compared with the experimental values. Numerical results are presented in Table 7.3. The agreement between calculated and experimental values was slightly better for equation 6.1 than it was for equation 7.7, as shown in the statistical analysis presented in Table 7.4.

For equation 6.1, the mean of the standard deviations of the differences between experimental and calculated values was 0.009 optical density units (or 1.4% of the mean value). The maximum standard deviation of the differences was 0.030 optical density units, representing 4.2% of the mean value at a sample depth of 0.025 cm and at a wavelength of 5050 A.

A high degree of accuracy was achieved using both equations, but as we noted, it was slightly higher using equation 6.1. However, equation 6.1 is purely empirical. It provides no insight into the actual scattering and absorption of light by red blood cells. In addition, it was necessary to redetermine the constants at each sample depth and wavelength when this equation was used. Of the two constants which were required for the successful application of Twersky's thoery to nonhemolyzed blood, only one constant, s, had to be redetermined and this was necessary only at the smallest sample depth, 0.011 cm. Although the empirical relationship of

equation 6.1 does not provide insight into the scattering and absorbing phenomena occurring in the red cell suspensions, it does provide a mathematical relationship whose usefulness has been demonstrated in Chapter IV for the estimation of the oxygen saturation of nonhemolyzed whole blood. The applicability of equation 6.1 to the results obtained with the integrating sphere demonstrates that this expression may be used not only for various systems and sample depths, but also for a wide variety of wavelengths. This indicates that it should be possible for other laboratories to adopt the technique described in Chapter IV for measuring oxygen saturation, although different measuring systems may be used.

2. Semipermeable Microcapsules

The optical density of semipermeable microcapsule suspensions was measured in the integrating sphere at four wavelengths, from 5200 A to 5800 A. Since the concentration of hemoglobin within the microcapsule is only one third of that which is present in the normal red blood cell and consequently the light absorption of the microcapsules is quite low, the measurements were made at a sample depth of 0.071 cm. The fractional volume occupied by the particles was varied from 4% to 44%.

A "lysed" suspension could not be obtained since it was impossible to destroy the particle membranes completely.

Ultrasonication caused a fraction of the particles to be ruptured. After centrifuging, the clear supernatant was scanned in the Beckman DU spectrophotometer and relative values were obtained for the extinction coefficients. The scan is shown in Fig. 7.7. The pigment contained within the particles appears to be a mixture of methemoglobin and oxygenated hemoglobin.

The optical density of the microsphere suspensions was plotted against the relative extinction coefficients. The results consisted of a family of straight lines with y intercepts and with slopes equal to $33.8\,\epsilon_r cd$, where ϵ_r is the relative extinction coefficient obtained from Fig. 7.7. The factor 33.8 was necessary since the relationship between the concentration of the solution from which the relative extinction coefficients were obtained and the concentration of the solution within the particles was unknown. The constants s and $q(\delta)$ were obtained from the y-intercepts, as they were in the case of red blood cells.

A satisfactory agreement between optical density values calculated according to equation 7.7 and the experimental results was obtained as shown in Fig. 7.8 and Table 7.5. The dots represent the experimental results and the solid lines were calculated from equation 7.7. Optical density is plotted against H, the fractional volume of the suspension

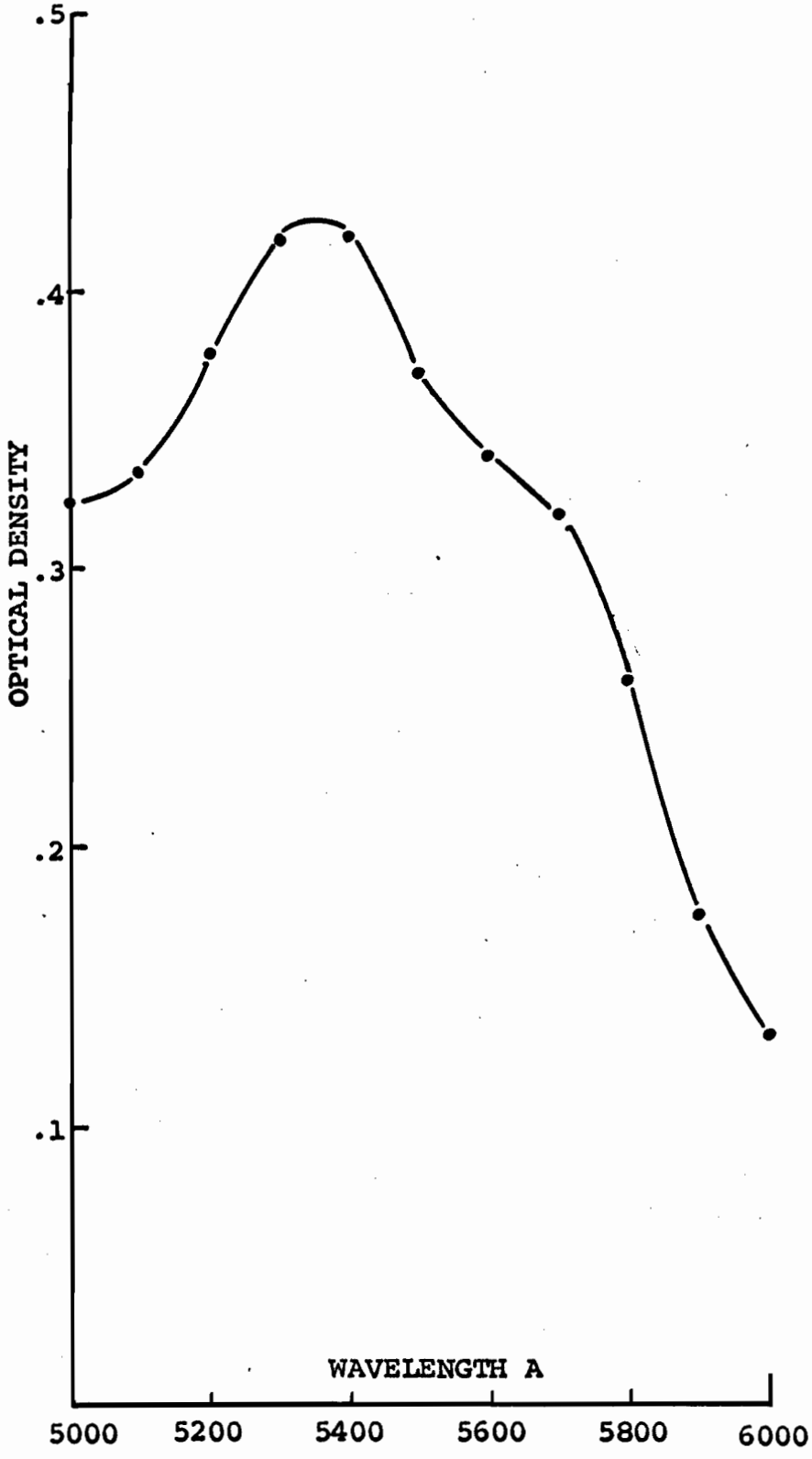

Fig. 7.7. Scan of supernatant after a suspension of semi-permeable microcapsules was ultrasonicated and centrifuged.

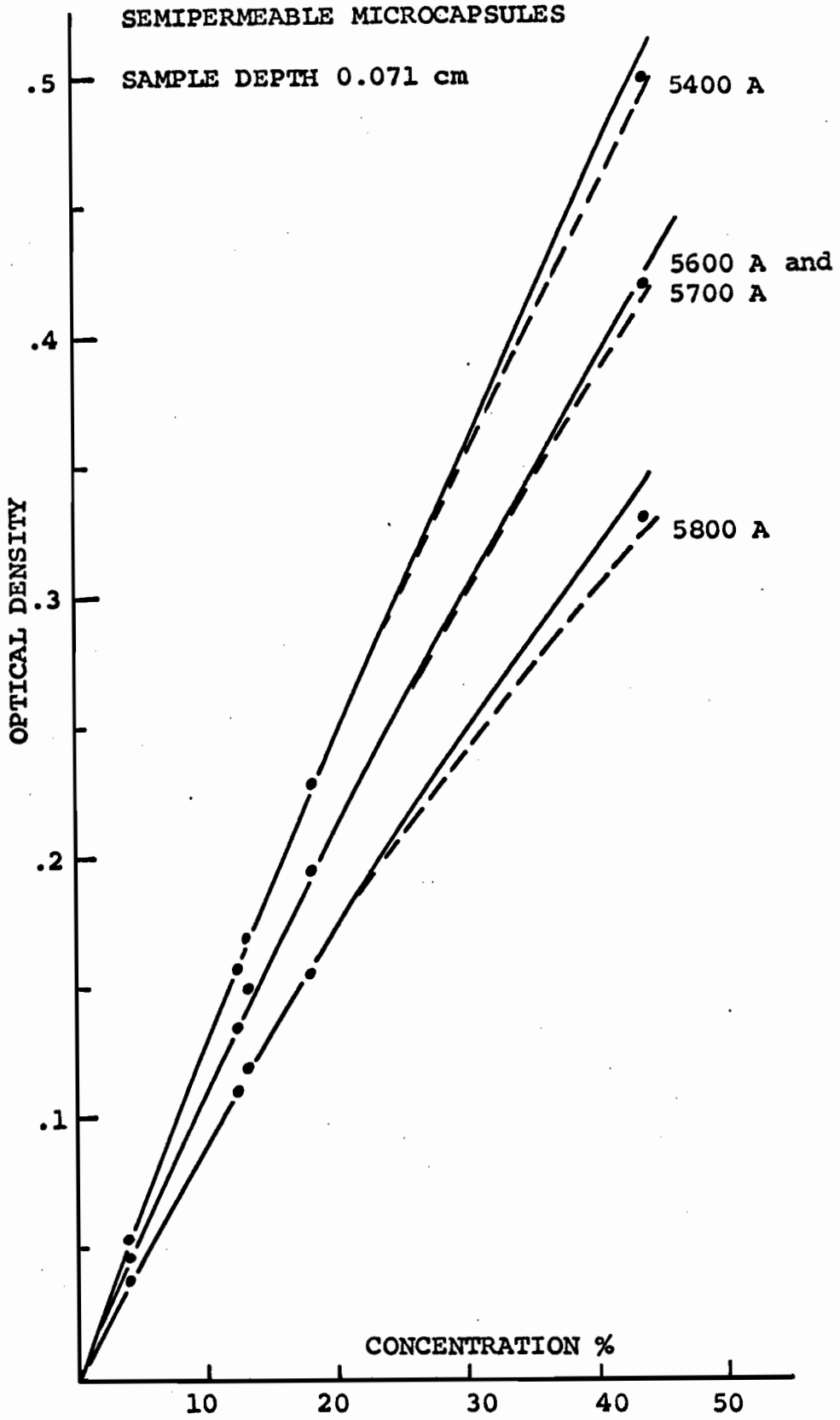

Fig. 7.8. Optical density is plotted against % concentration. The dots represent experimental values. The solid lines were calculated from equation 7.7, and the dotted lines, from equation 6.1. Results are shown at a sample depth of 0.071 cm and at four wavelengths. The results at 5200 A and at 5600 A coincided.

TABLE 7.5. Comparison of optical density values for suspensions of semipermeable microcapsules at a sample depth of 0.071 cm obtained by experiment with those obtained by calculation from equations 7.7 and 6.1

Conc. (%)	Optical Density											
	Wavelength (A)											
	5200			5400			5600			5800		
	Exp.	Eq.7.7	Eq.6.1	Exp.	Eq.7.7	Eq.6.1	Exp.	Eq.7.7	Eq.6.1	Exp.	Eq.7.7	Eq.6.1
3.9	0.046	0.043	0.045	0.053	0.050	0.052	0.046	0.043	0.045	0.038	0.035	0.037
12.5	0.134	0.134	0.138	0.158	0.158	0.160	0.136	0.134	0.138	0.110	0.110	0.111
13.2	0.150	0.141	0.145	0.170	0.166	0.168	0.150	0.141	0.145	0.120	0.116	0.117
18.2	0.194	0.192	0.195	0.223	0.227	0.227	0.196	0.192	0.195	0.154	0.157	0.157
43.9	0.420	0.429	0.418	0.500	0.513	0.494	0.420	0.429	0.418	0.330	0.345	0.326
S.D.D.[a]		±.007	±.004		±.007	±.004		±.007	±.002		±.007	±.003
% of Mean[b]		3.5	2.0		3.1	1.5		3.5	1.3		5.0	1.9

[a]Standard deviation of the differences between experimental and calculated values.
S.D.D. = $\left[1/(n-1)\ \sum(d - \bar{d})^2\right]^{\frac{1}{2}}$.

[b]Standard deviation of the differences expressed as a percent of the mean optical density value.

occupied by the particles. The maximum standard deviation of the differences was 0.007 optical density units, representing 5.0% of the mean optical density value at 5800 A.

We found that the empirical expression O.D. = cd/(ac + b) could also be applied to this material. The agreement between calculated values of optical density (shown by dotted lines in Fig. 7.8) and experimental optical density values was extremely good. The maximum standard deviation of the differences between the experimental and calculated values was 0.004 units representing 2.0% of the mean optical density value at 5050 A.

3. Emulsions

Twersky's theory has been successfully applied to two different scattering suspensions - red blood cells and semi-permeable microcapsules. However, both these suspensions are light absorbing. So we attempted a similar experiment on nonabsorbing emulsions of n-butyl benzoate in water.

Since the emulsified particles are large compared to the wavelength (1 to 4 microns in diameter), and the refractive index of n-butyl benzoate relative to water is fairly small, 1.13 (absolute refractive index = 1.50), the requirements for applying Twersky's theory are fulfilled. Since the emulsion consists of a nonabsorbing liquid dispersed in water, optical density values were calculated

using Twersky's theory for multiple scattering by nonabsorbing particles, equation 7.2, at two wavelengths, 5000 A and 6300 A. Equation 7.2 was simplified in a manner similar to that of equation 7.3 for nonhemolyzed blood cells:

$$O.D. = -\log \left[10^{-sH(1-H)d} + q(\delta)(1 - 10^{-sH(1-H)d})\right] \qquad 7.8$$

Concentration was varied from 1.5% to 20%. Optical density was measured at 5000 A, 5200 A, 5400 A, 5600 A, 5800 A, 6000 A, and 6300 A., at a sample depth of 0.011 cm. Measurements were made only at the smallest sample depth since the optical density levels were fairly high for this light scattering material.

There was very little variation in optical density over the entire range of wavelengths, although there was a slight decrease as wavelength increased (Table 7.6).

The experimental results and calculated equations (solid lines) are shown in Fig. 7.9. The accuracy of the calculated values was not very high. Statistical analysis (Table 7.7) shows that the standard deviations of the differences between experimental and calculated results were 0.042 and 0.037 optical density units at 5000 A and 6300 A, respectively, representing 5.7% and 5.4% of the mean optical density values at these two wavelengths.

Next we tested to see if equation 6.1 could be applied to

TABLE 7.6. Optical density of emulsions of n-butyl benzoate in water at a sample depth of 0.011 cm

Concentration (%)	Optical Density						
	Wavelength (A)						
	5000	5200	5400	5600	5800	6000	6300
1.5	0.280	0.272	0.263	0.259	0.253	0.249	0.242
3.0	0.497	0.487	0.477	0.468	0.456	0.450	0.443
6.0	0.731	0.719	0.710	0.705	0.691	0.692	0.683
10.0	0.877	0.862	0.862	0.853	0.846	0.844	0.843
15.0	0.956	0.944	0.938	0.934	0.926	0.920	0.917
20.0	1.020	1.008	0.996	0.994	0.987	0.983	0.981

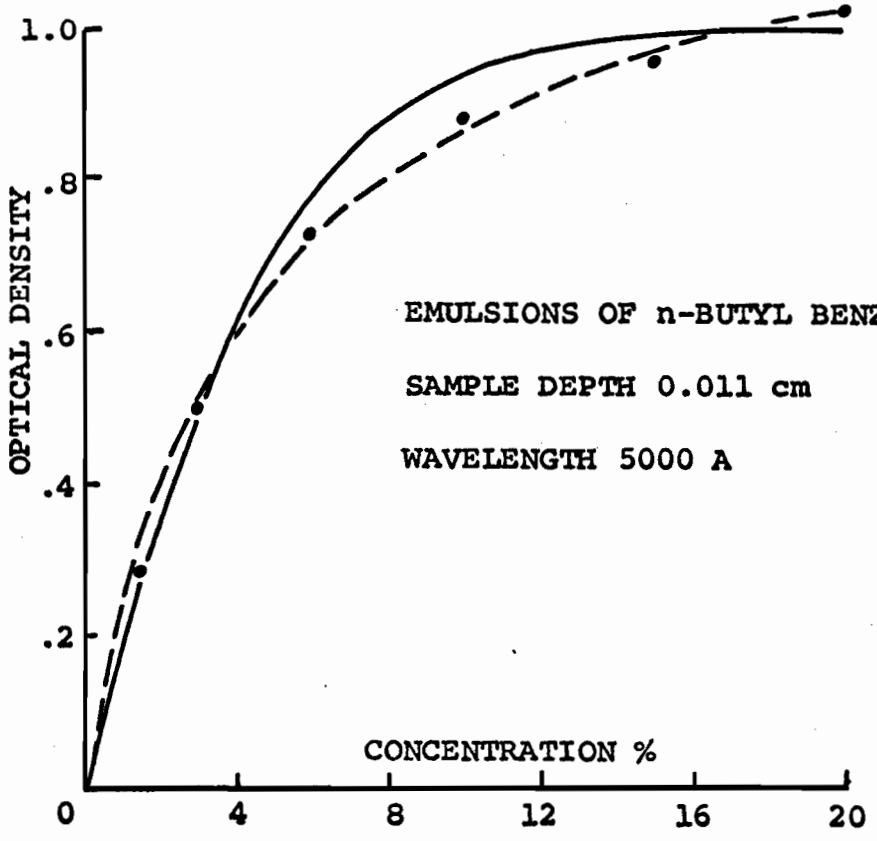

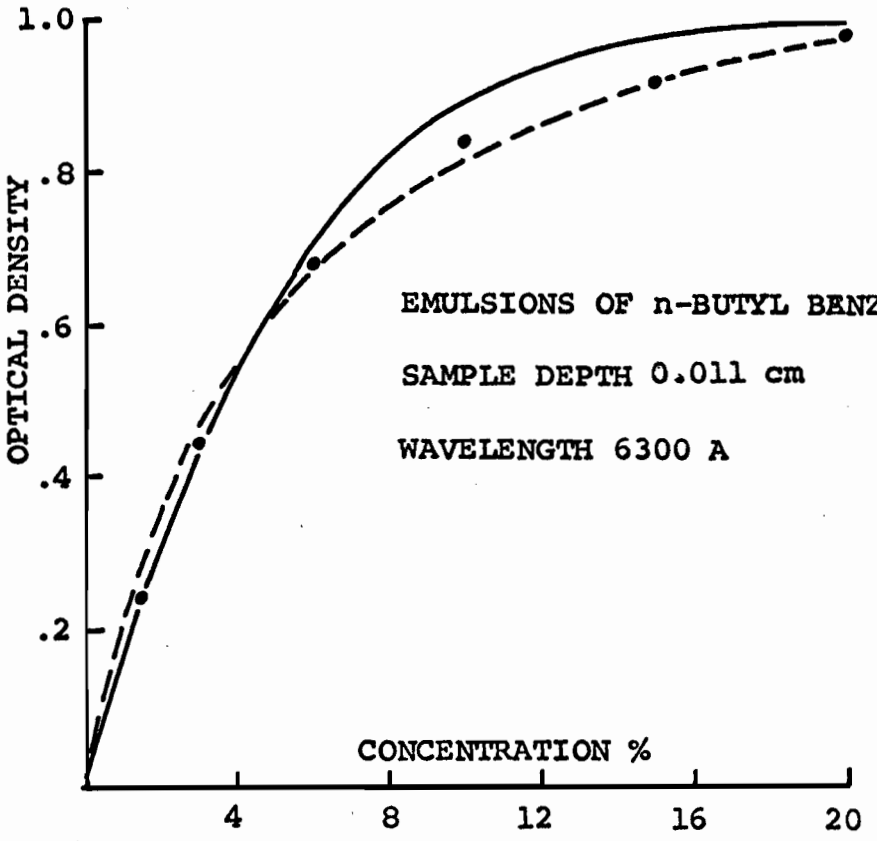

Fig. 7.9. The optical density of nonabsorbing emulsions of n-butyl benzoate is plotted against % concentration. The solid lines were calculated from equation 7.7, and the dotted lines, from equation 6.1. Results are shown at a sample depth of 0.011 cm, and at two wavelengths, 5000 A and 6300 A.

TABLE 7.7. Comparison of optical density values for emulsions of n-butyl benzoate in water at a sample depth of 0.011 cm obtained by experiment with those calculated from equations 7.7 and 6.1

Conc. (%)	Optical Density					
	Wavelength (A)					
	5000			6300		
	Exp.	Eq.7.8	Eq.6.1	Exp.	Eq.7.8	Eq.6.1
1.5	0.280	0.261	0.319	0.242	0.223	0.290
3.0	0.497	0.484	0.508	0.443	0.418	0.468
6.0	0.731	0.787	0.722	0.683	0.710	0.674
10.0	0.877	0.947	0.867	0.843	0.904	0.819
15.0	0.956	0.999	0.965	0.917	0.976	0.918
20.0	1.020	0.998	1.022	0.981	0.994	0.976
S.D.D.[a]		±.042	±.018		±.037	±.026
% of Mean[b]		5.7	2.5		5.4	3.8

[a]Standard deviation of the differences between experimental and calculated values. S.D.D. = $\left[1/(n-1)\ \sum(d - \bar{d})^2\right]^{\frac{1}{2}}$.

[b]Standard deviation of the differences expressed as a percent of the mean optical density value.

the results obtained on the nonabsorbing emulsion in the integrating sphere.

It was possible to use equation 6.1, O.D. = cd/(ac + b), to calculate optical density with a higher degree of accuracy. The calculated results are shown in Fig. 7.9 by the dotted lines. Statistical analysis (Table 7.7) shows that the standard deviations of the differences between experimental and calculated values of optical density were 0.018 and 0.026 optical density units at 5000 A and 6300 A, respectively, representing 2.5% and 3.8% of the mean value. Thus, the agreement between measured values of optical density and those calculated from equation 6.1 was considerably better than the agreement obtained when Twersky's theory was used.

F. Conclusions

The linear relationship between the optical density of nonhemolyzed blood and hemolyzed blood is a significant finding, indicating that light absorption by intracellular hemoglobin is the same as light absorption by free hemoglobin.

The results have demonstrated that the general formalism developed by Twersky for the multiple scattering of light by large particles with relative refractive index close to 1.0 may be applied to a variety of scattering suspensions. It was successfully applied to undiluted nonhemolyzed blood

and to suspensions of artificial red blood cells; it was also applied, with a smaller degree of accuracy, to nonabsorbing light scattering emulsions.

The successful use of equation 7.7 enables us to evaluate separately the contributions of absorption and scattering to the total optical density of the blood. It also demonstrates that both total hemoglobin concentration and hematocrit determine the optical density of nonhemolyzed blood; this means that the size of the red cells is an important factor and sheds light upon the observed optical density changes brought about by osmotically induced changes in cell size.

The complexity of the relationship between light transmission and light absorption by the pigment, which is the basis of whole blood oximetry, indicates why the previous oximetric technique of relating the ratio of the optical densities at two wavelengths to oxygen saturation, estimated by a reference method, gave results of limited accuracy and could be used only over a restricted range of hemoglobin concentrations. This topic will be analyzed in Chapter IX.

We also showed that the empirical expression optical density = $cd/(ac + b)$ can be used to describe the results obtained for the three scattering materials studied; the accuracy was slightly better than that obtained using

Twersky's theory. Although it does not provide any information concerning the actual absorbing and scattering processes occurring in concentrated red blood cell suspensions, this equation does provide the most practical and accurate solution to the problem of estimating oxygen saturation in nonhemolyzed whole blood.

Both equations were successfully applied to measurements made on three scattering suspensions whose mean particle diameters were 1 to 4 microns, 8 microns, and 40 microns, over a range of wavelengths encompassing a considerable change in extinction coefficients, and at five sample depths varying from 0.011 to 0.071 cm.

It is interesting to compare the form of equation 7.7, derived from Twersky's theory with the equations proposed by Drabkin and Singer to describe the optical density of suspensions of red blood cells in normal saline and of fat particles in hemoglobin solutions. These equations were quoted in Chapter II, Section D1a, and will be restated. For suspensions of fat particles in hemoglobin solutions

$$E_t = E_p + E_s \qquad 2.17$$

where E_t is the total optical density of the suspension, $E_p = \epsilon cd$, or the optical density of the hemoglobin solution alone, and E_s is the extinction due to scattering by the fat

particles. For suspensions of nonhemolyzed red blood cells,

$$E_t = f_1 E_p + E_s \qquad 2.18$$

where f_1 is a function of $(Nd)^n$, where N and d are the concentration and depth of the sample, and n is an empirical constant. For N greater than $3.6 \times 10^9/cm^3$, f_1 was approximately 1.0 and equation 2.18 reduced to 2.17.

The form of equation 2.17 is identical to that of equation 7.7 which states that the total optical density of a suspension of red blood cells is equal to the sum of the extinction due to absorption by the pigment and the extinction due to scattering by the particles. Perhaps if hemoglobin concentration and hematocrit had been used instead of N, and if a measuring system in which all the scattered light was collected had been used, it would not have been necessary to include the factor f_1 in equation 2.18 for particle concentrations less than $3.6 \times 10^9/cm^3$.

VIII. REFLECTANCE AND TRANSMITTANCE BY RED BLOOD CELL SUSPENSIONS

A. Introduction

The first measurements of the light reflected by nonhemolyzed blood were made by Brinkman and Zijlstra in 1949 (22); this was the beginning of reflection oximetry. Since this time, several techniques have been developed.

Reflection oximetry is based on the reflectance of infinitely thick layers of nonhemolyzed blood - that is, on samples which transmit no light. Brinkman and Zijlstra, Kramer et al (132), and Refsum and Hisdal (185) assumed that reflection is exponentially related to oxygen saturation (that is, to the extinction coefficient of the hemoglobin within the red cell). Another method was suggested by Rodrigo (190) who applied the Schuster theory to infinitely thick, nontransmitting layers of blood, using the relationship $R_\infty = 1/2p$ where $p = a/\beta s$; R_∞ is the reflectance of an infinitely thick layer of scattering material, a is the absorption coefficient, s is the scattering coefficient, and β is the backward scattered fraction of the total scattered light. This theory was applied by Polanyi et al (181) to the construction of a reflection oximeter. In both reflectance techniques, the accuracy and the ranges of oxygen saturation and hemoglobin concentration to which the methods may be applied are quite

limited. Enson et al (58) reported that the method is satisfactory for hematocrits between 30% and 80%, but individual calibration is required outside this range.

The aim of most reflectance studies has been the development of methods for estimating oxygen saturation on an empirical basis. Investigations into the basic reflecting properties of nonhemolyzed blood have been few. Kramer and his colleagues demonstrated three phenomena: (i) reflectance was inversely proportional to absorption - in other words, in spectral regions where transmittance was high, reflectance was also high; (ii) reflectance became asymptotic with increasing sample depth; (iii) the relationship between reflectance and hemoglobin concentration was parabolic. These measurements were made on sample depths ranging from 0.13 cm to 1.3 cm. Enson et al using an intracardiac reflection oximeter also showed that the relationship between reflectance and concentration was parabolic for infinitely thick samples.

The theoretical relationship between reflectance and the absorption of light by the hemoglobin molecule is open to question. Kramer assumed, as did Brinkman and Zijlstra, that this relationship was exponential. Rodrigo and, later, Polanyi advocated the application of the Schuster theory to light reflectance by nonhemolyzed blood. However, it was pointed out in Chapter III that the Schuster theory is a

simplified version of radiative transfer theory. Such treatments consider only the incoherent aspects of scattering; the requirement that the particle separation must be greater than that present in undiluted blood is not met.

To our knowledge, no wave treatment for the multiple scattering of light into the back half-space has been derived for the range of parameters which apply to the study of nonhemolyzed blood; these parameters include particle size, wavelength, and relative index of refraction. It does, however, seem reasonable to assume that the reflected light must follow, qualitatively, a law very similar to that followed by the forward scattered light. To investigate the validity of this assumption, results obtained from reflectance measurements were compared with those obtained at the same wavelength, sample depth, and concentration for the light transmitted by red blood cell suspensions. In order to study samples which transmitted light as well as reflected light it was necessary to use sample depths much smaller than those used in other studies.

B. Method

The seven inch sphere which was described in Chapter VII was used for transmittance measurements and an integrating sphere four inches in diameter was used for reflectance meas-

urements. The seven inch sphere was used to minimize errors caused by the presence of the sample and entrance apertures. It was found, however, that the light from the Beckman DU spectrophotometer showed considerable divergence upon reaching the sample chamber when it was in position for reflectance measurements. Although the light was still slightly divergent in the four inch sphere, this size was considered to be the best possible compromise, since errors due to apertures and screens become significant when the sphere is reduced below this size.

As in the seven inch sphere, the entrance and detector apertures of the four inch sphere are 1.0 cm and 1.35 cm in diameter, respectively. The area of the aperture in the four inch sphere for the reflectance sample is 2.33 cm^2. The sample aperture for transmittance measurements in the seven inch sphere is 0.78 cm^2.

The preparation of the inside surface of the four inch sphere was identical to that described in Chapter VII for the seven inch sphere.

The procedure for measuring the transmittance of samples in the seven inch sphere was described in Chapter VII.

In order to measure reflectance, the sample chamber is placed directly opposite the entrance aperture as shown in Fig. 8.1. The light specularly reflected from both the sample chamber and from the sample itself passes back out through

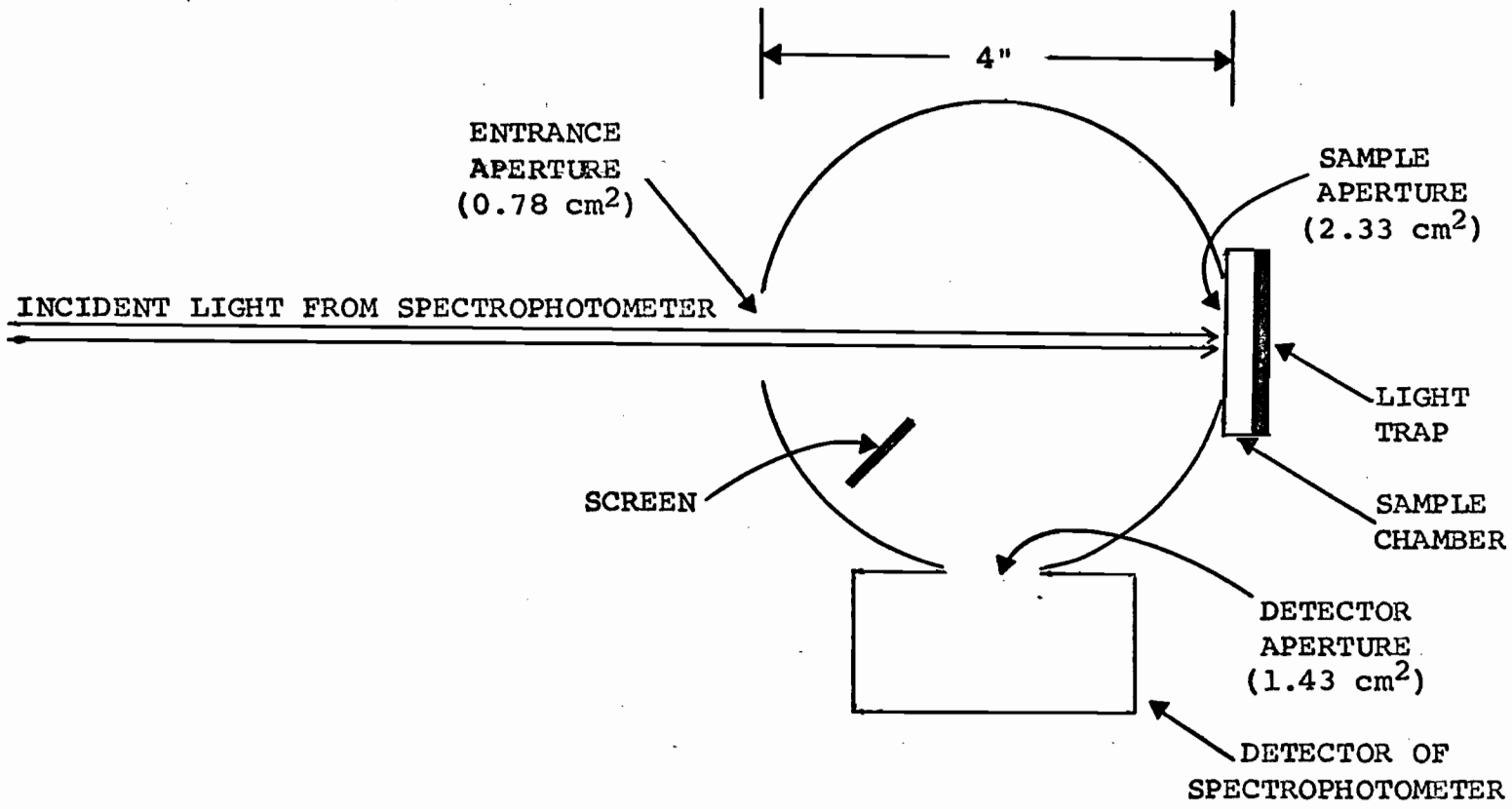

Fig. 8.1. Integrating sphere attachment for measuring reflectance, built for the Beckman DU spectrophotometer.

the entrance aperture. Thus, the instrument provides a measure of diffuse reflectance rather than total reflectance. The position of the detector is the same for both transmittance and reflectance measurements.

In order to provide a method for standardizing the integrating sphere attachment for the Beckman DU spectrophotometer, it is necessary to use a reflectance standard which can be removed from the sample chamber without disassembling the system. For this purpose, a 50% emulsion of n-butyl benzoate in water is drawn through the cuvette and the transmittance scale is set to 100%. When the sample is drawn through the cuvette, the reading is taken in percent on the transmittance scale. The values obtained are then corrected in terms of the absolute value of the reflectance of the 50% n-butyl benzoate emulsion with reference to magnesium oxide.

The reflectance of n-butyl benzoate with reference to magnesium oxide was obtained using the Beckman DK2a Spectroreflectometer (kindly lent by Domtar Research Laboratories, Senneville, Quebec). The reflectance of the 50% emulsion with reference to magnesium oxide as measured in the Beckman DK2a integrating sphere spectrophotometer was found to decrease in an approximately linear fashion over the wavelength region from 5000 A to 7000 A by about 2%. At 6300 A its reflectance

at a sample depth of 0.071 cm, was 0.51.

As described previously (Chapter IV), the sample chamber consists of two lucite plates. In order to prevent transmitted light from being reflected back into the sample and then back into the integrating sphere, a black light trap was placed behind the sample chamber. Even with the black light trap the reflectance of the sample chamber filled with saline was of the order of 1.5% with reference to magnesium oxide, measured in the Beckman DK2a spectrophotometer. This represents only a slight error.

To standardize the reflectance measurements of samples contained within the sample chamber and thus, to reduce as much as possible the effects of reflections from the surfaces of the sample chamber, the reflectance of a sample of opaque white paper showing a high degree of diffuse reflectance was measured both directly and within the sample chamber using the Beckman DK2a Spectroreflectometer. The reflectance of the paper was 0.95; its value was constant over the wavelength range from 5000 A to 7000 A. When the paper was placed in the sample chamber, its measured reflectance was 0.73. Thus, it was necessary to correct the measured reflectance values of samples contained within the sample chamber by the factor $0.95/0.73 = 1.29$. The discrepancy between the two reflectance values for the white standard is largely due to

loss of scattered light which emerges laterally from the sample chamber, since the sample chamber is separated from the sphere by the lucite sample chamber wall.

The reflectance of the 50% n-butyl benzoate emulsion was 0.51. Its corrected value was 0.51 x 1.29 = 0.66. Thus, values measured in the integrating sphere attachment built for the Beckman DU spectrophotometer were corrected by the factor 0.66 to obtain their absolute values with respect to magnesium oxide.

Measurements on concentrated suspensions of oxygenated red blood cells in isotonic saline and on emulsions of n-butyl benzoate in water were performed using the Beckman DK2a Spectroreflectometer as well as the integrating sphere built in our laboratory. Measurements were made at four sample depths: 0.025 cm, 0.035 cm, 0.048 cm, and 0.071 cm.

Since the Beckman Dk2a Spectroreflectometer is a double beam instrument, the comparison or simultaneous method is used, in contrast to the Beckman DU spectrophotometer which is a single beam instrument and requires that the less accurate substitution method be used.

C. Results

1. Red Blood Cell Suspensions

a) Beckman DK2a Recording Spectroreflectometer

Reflectance scans of red blood cell suspensions were made. We were able to confirm Kramer's observations that reflectance and absorption are inversely related. At wavelengths where the extinction coefficient is high and, consequently, the absorption is high, reflectance was decreased. Thus reflectance varies inversely with the extinction coefficient of hemoglobin; in other words, transmittance and reflectance are directly related.

Fig. 8.2 shows the relationship between the reflectance of fully oxygenated red blood cell suspensions and sample depth for two hemoglobin concentrations at 6330 A. It may be seen that reflectance increased as sample depth was increased from 0.025 cm to 0.071 cm. These results are in agreement with those obtained by Kramer et al who varied depth from 0.13 cm to 1.3 cm. Kramer found that reflectance continued to increase up to a sample depth of about 0.3 cm and became asymptotic at larger sample depths.

We have found that reflectance varies inversely with the extinction coefficient of hemoglobin. As sample depth was increased, changes in reflectance, resulting from changes in the extinction coefficient, were increased as shown in Fig. 8.3.

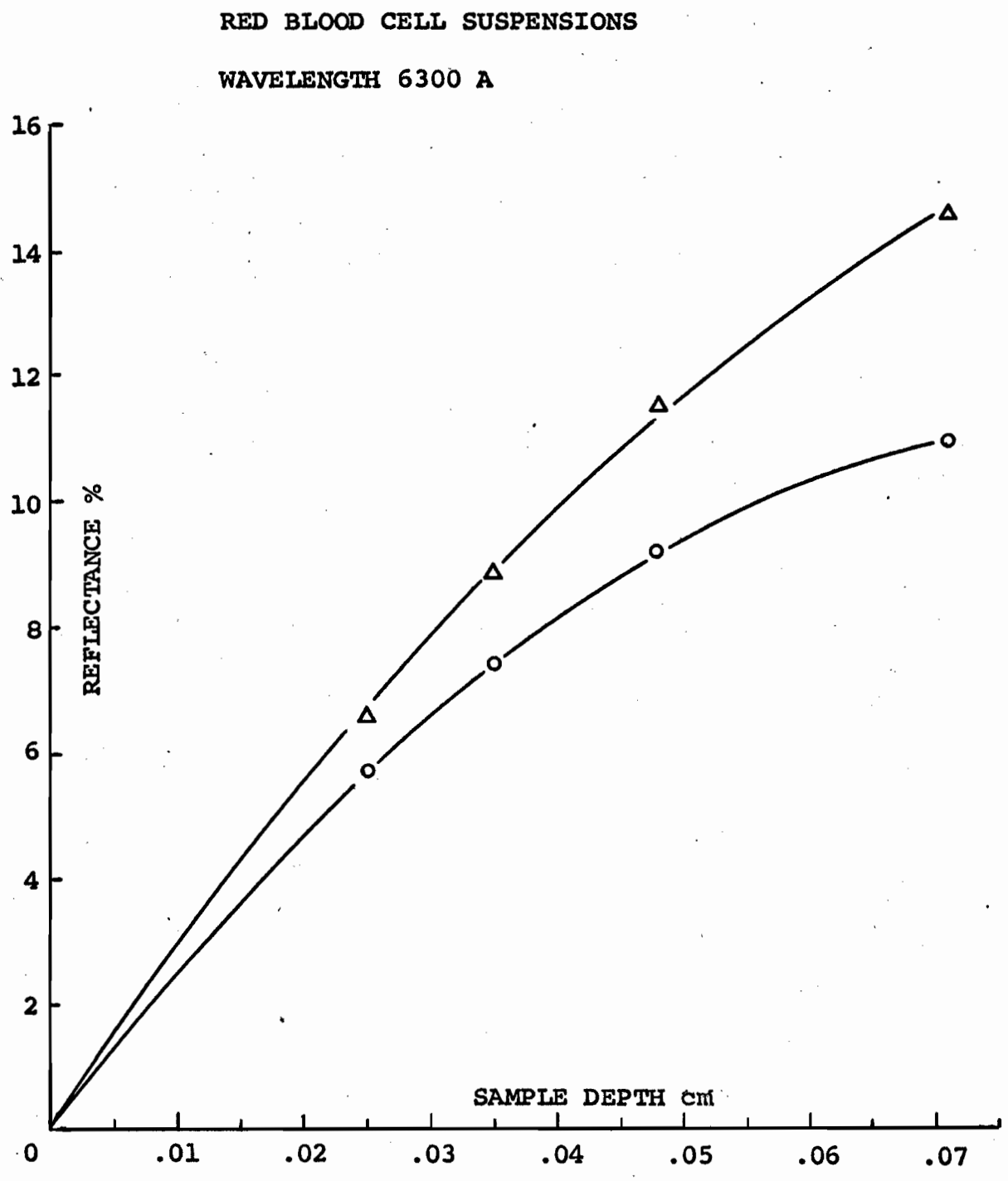

Fig. 8.2. Reflectance of two red cell suspensions with hemoglobin concentrations of 7.2 mM/l (Δ) and 10.9 mM/l (o) is plotted against sample depth at 6300 A. Data were obtained using the Beckman DK2a Spectroreflectometer.

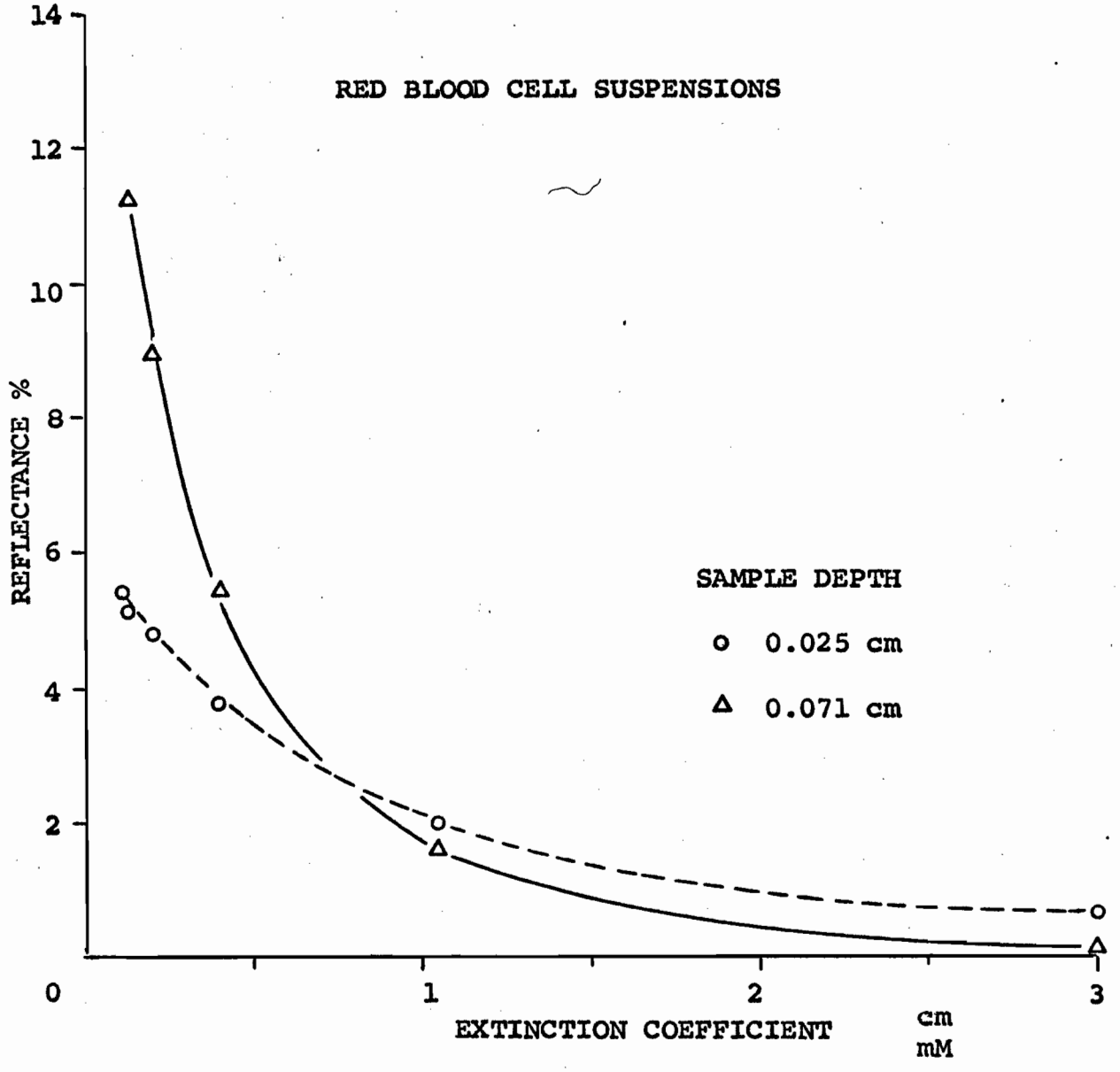

Fig. 8.3. The reflectance of a red cell suspension (hemoglobin concentration 7.2 mM/l) at two sample depths, 0.025 cm and 0.071 cm is plotted on the ordinate. On the abscissa, the extinction coefficient of oxygenated hemoglobin at various wavelengths is shown.

The depth of the sample exerted two distinct effects on reflectance. Not only were the absolute values of reflectance greater at large sample depths, but the differences in reflectance due to changes in extinction coefficients were much greater when the sample depth was large.

This observation is of great importance in the estimation of oxygen saturation by reflection techniques since it is the difference between the extinction coefficients of oxygenated and reduced hemoglobin which varies when oxygen saturation changes. Evidently, at large sample depths, the sensitivity of the measurement is increased because the total change in reflectance over the range from 0% to 100% saturation is increased. Thus, a large sample depth is advantageous in the measurement of oxygen saturation by reflection oximetry.

The relationship between reflectance and hemoglobin concentration was found to be parabolic. Results obtained using the Beckman DK2a Spectroreflectometer at 6330 A and at four sample depths are shown in Fig. 8.4. The results are similar to those reported by Kramer et al and by Enson and colleagues using an intracardiac reflection oximeter.

b) Beckman DU Spectrophotometer with Integrating Sphere Attachment

In Fig. 8.5, results obtained with the four inch integrating sphere built for the Beckman DU spectrophotometer were

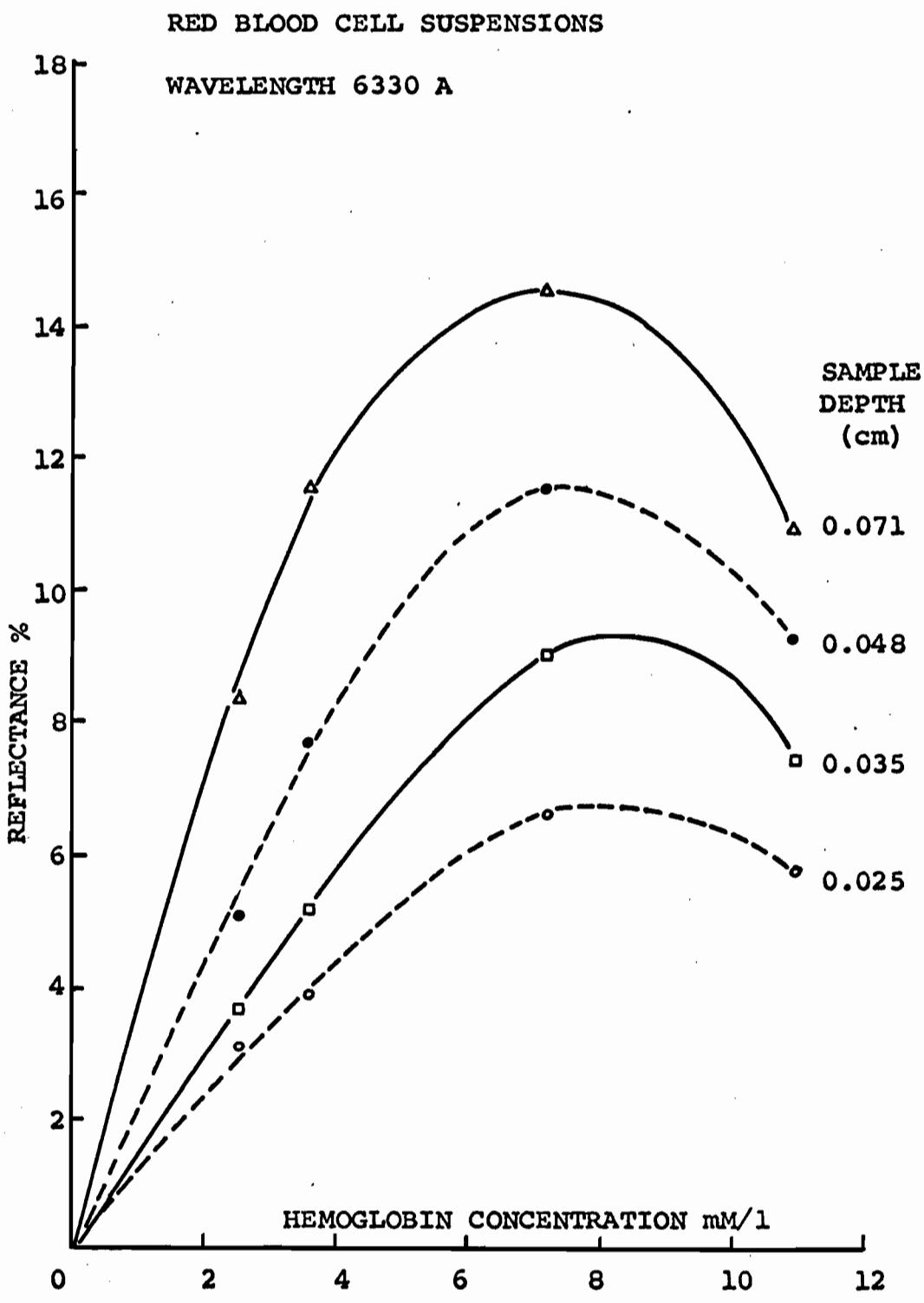

Fig. 8.4. Reflectance is plotted against hemoglobin concentration at four sample depths and at 6300 A.

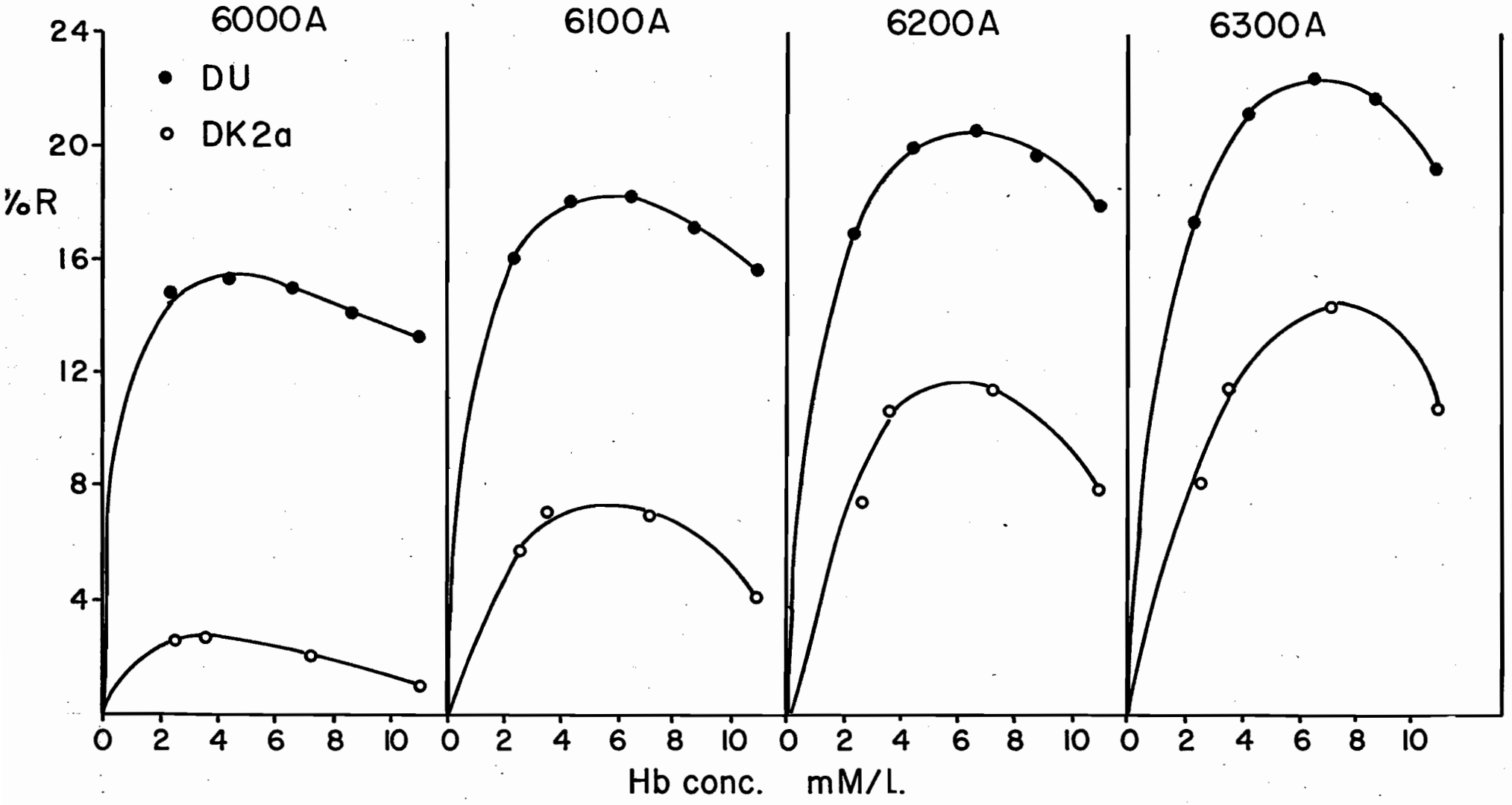

Fig. 8.5. Reflectance is plotted against hemoglobin concentration at a sample depth of 0.071 cm and at four wavelengths: 6000 A, 6100 A, 6200 A, and 6300 A. Data from both the Beckman DK2a Spectroreflectometer (open circles) and the Beckman DU spectrophotometer with the integrating sphere attachment built in our laboratory (closed circles) are shown.

compared with those obtained using the Beckman DK2a Spectro-reflectometer at a sample depth of 0.071 cm. Hemoglobin concentration was varied and measurements were made at 6000 A, 6100 A, 6200 A, and 6300 A. The extinction coefficient for oxygenated hemoglobin is highest at 6000 A and decreases progressively as the wavelength is increased to 6300 A. The values obtained in the two instruments were different; however, the evolution of the curves was identical. There was a shift of the maximum towards higher hemoglobin concentrations when there was a decrease in the extinction coefficient of hemoglobin.

The numerical differences in the results may have been due to a large extent to differences in surface reflections. Another cause of the discrepancy is that the alignment of the sample chamber perpendicular to the direction of incidence was not as precise in the integrating sphere attachment of the Beckman DU spectrophotometer as it was in the DK2a Spectro-reflectometer. It was mentioned previously that the light in the DU spectrophotometer was slightly divergent. As a result of these factors, some of the specular reflections from the sample chamber wall would not pass back out through the entrance aperture, but would strike the inside diffusely reflecting surface of the integrating sphere, adding to the apparent reflectance of the sample itself. It is also

possible that, although the measurements were made at the same nominal wavelengths, the wavelength calibration of both instruments may not have been identical; in addition, the use of different slit widths in the two instruments may have contributed to the discrepancy.

To investigate the relationship between reflectance and transmittance quantitatively, consecutive reflectance and transmittance measurements were made on samples at a sample depth of 0.071 cm. Measurements were made at 6000 A, 6100 A, 6200 A, and 6300 A, on fully oxygenated samples. When percent reflectance was plotted against percent transmittance at different wavelengths, a linear relationship was found to exist for each hemoglobin concentration. Fig. 8.6 shows this relationship for different hemoglobin concentrations. For each line, hemoglobin concentration and sample depth were maintained constant. Each point represents the transmittance and reflectance of a sample at a given wavelength. Thus, the extinction coefficient of hemoglobin was the independent variable. The relationship between reflectance and transmittance was linear; since transmittance bears an exponential relationship to ϵ, it follows that reflectance must also bear the same relationship to ϵ.

The linear relationship between reflectance and transmittance may be expressed by

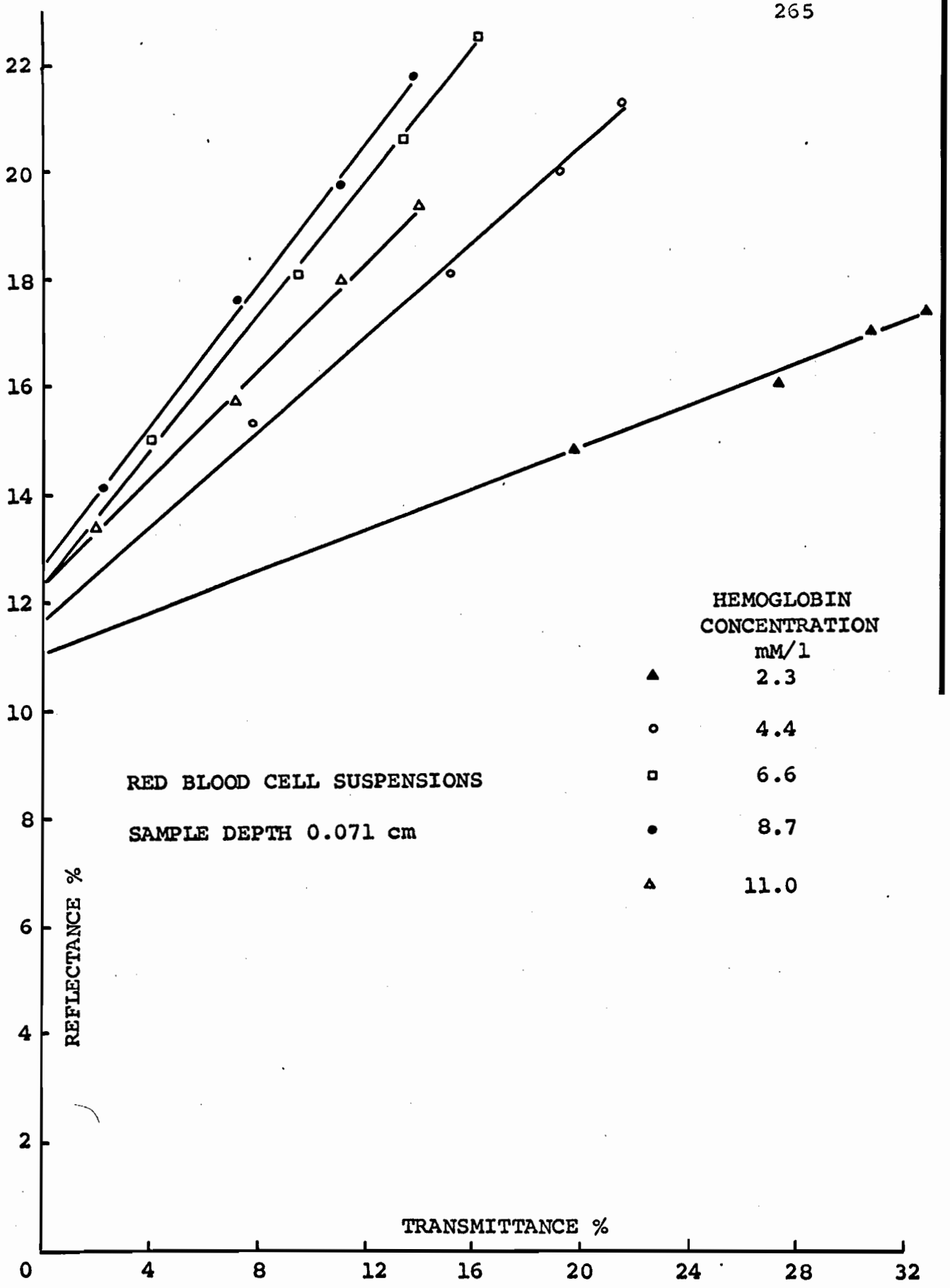

Fig. 8.6. Reflectance (%) is plotted against transmittance (%), at four wavelengths: 6000 A, 6100 A, 6200 A, and 6300A. Each line represents one hemoglobin concentration; each of the four points on a single line corresponds to one of the wavelengths specified above. Sample depth was 0.071 cm.

$$R = c_1 T + c_2 \qquad 8.1$$

where c_1 and c_2 are constants for blood of a given hemoglobin concentration and sample depth. In Chapter VII we showed that transmittance may be expressed in the form of equation 7.7:

$$T = I/I_o = 10^{-\epsilon cd}\left[10^{-sH(1-H)d} + q(\delta)(1 - 10^{-sH(1-H)d})\right]$$

Substituting equation 7.7 into equation 8.1,

$$R = c_1 T + c_2 = c_1 10^{-\epsilon cd}\left[10^{-sH(1-H)d} + q(\delta)(1 - 10^{-sH(1-H)d})\right] + c_2 \qquad 8.2$$

The value of R cannot be obtained explicitly from this expression. However, if equation 8.1 is rewritten

$$R - c_2 = c_1 T$$

then $\log (R - c_2) = \log T + \log c_1$

$$= -\epsilon cd + \log\left[10^{-sH(1-H)d} + q(\delta)(1 - 10^{-sH(1-H)d})\right] + \log c_1 \qquad 8.3$$

from which ϵ may be obtained. The constant c_2 was obtained as the y-intercept of Fig. 8.6 and subtracted from R. Fig. 8.7 shows $\log (R - c_2)$ plotted against optical density obtained from the transmittance measurements, and demonstrates that the relationship was linear when concentration and depth were

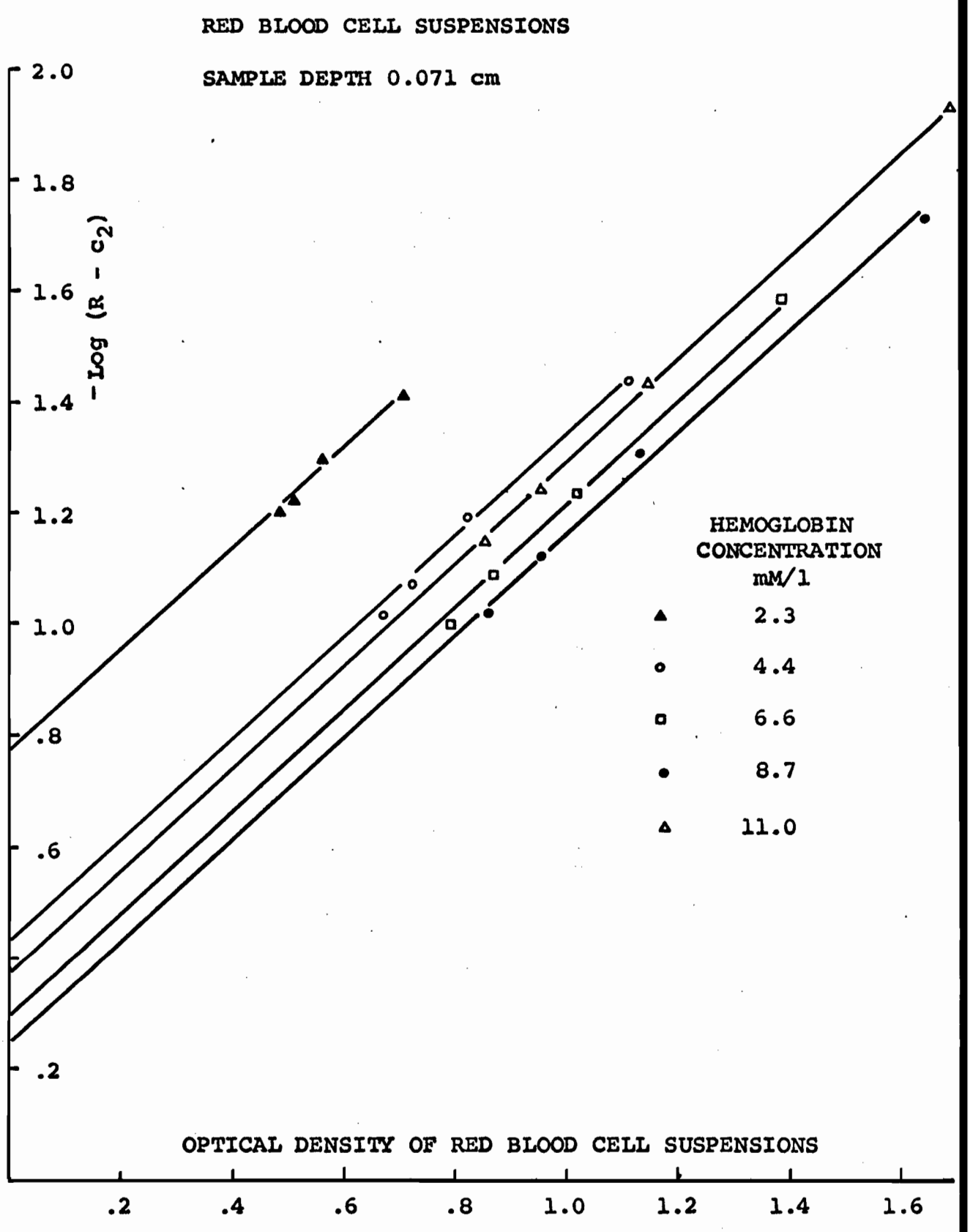

Fig. 8.7. $-\text{Log}\ (R - c_2)$ is plotted against the optical density of the red cell suspensions, obtained from transmittance measurements. c_2 was obtained from the y intercepts of Fig. 8.6. As in Fig. 8.6, each line represents one hemoglobin concentration; each of the four points on a single line corresponds to one of the following wavelengths: 6000 A, 6100 A, 6200 A, and 6300 A.

held constant and ϵ was varied by changing the wavelength.

This graph may be compared with Fig. 7.4, in which the optical density of nonhemolyzed blood, or -log T, was plotted against the optical density of hemolyzed blood, or ϵcd; the relationship between -log T and ϵ was linear. In Fig. 8.7 we now see that log $(R - c_2)$ is linearly related to -log T and hence it is linearly related to ϵ. This result supports Kramer's suggestion that reflectance must be exponentially related to the extinction coefficient of hemoglobin. In the present experiments, ϵ was varied by changing the wavelength; this is analogous to changing ϵ by varying oxygen saturation.

Equation 8.3 shows that, at constant hemoglobin concentration and sample depth, ϵ is the only variable, and the slope of the lines relating log $(R - c_2)$ and optical density should be constant. Fig. 8.7 shows that the lines for various hemoglobin concentrations were parallel.

The significance of the constants c_1 and c_2 is not explained in this analysis, but it is probable that they are due to surface reflections and the incomplete collection of the back scattered light.

It should be noted that the lines in Fig. 8.7 are not in order of hemoglobin concentration (each line represents a different hemoglobin concentration) due to the parabolic relationship between scattering and hemoglobin concentration.

2. Emulsions

Using the Beckman DK2a Spectroreflectometer, the reflectance of emulsions of n-butyl benzoate was scanned over the wavelength range from 5000 A to 7000 A at four sample depths. Concentration was varied from 1.5% to 50%. The reflectance decreased slightly (about 2%) over this wavelength range. Fig. 8.8 shows the results obtained at 5000 A. Percent reflectance is plotted against the percent of the total volume occupied by the emulsified particles at the four sample depths studied. Also shown in this graph are results obtained at 5000 A using the four inch sphere built for the Beckman DU spectrophotometer at a sample depth of 0.071 cm; the agreement between these results and those obtained using the Spectroreflectometer is very close. The relationship between reflectance and concentration is similar to that obtained with red blood cell suspensions; it appears to be parabolic, although measurements were not made on samples with concentrations in the interval between 20% and 50% where the results indicate the maximum reflectance takes place.

D. Conclusions

The present study of the reflectance of nonhemolyzed red blood cells appears to be the first investigation made using an integrating sphere; it also appears to be the first

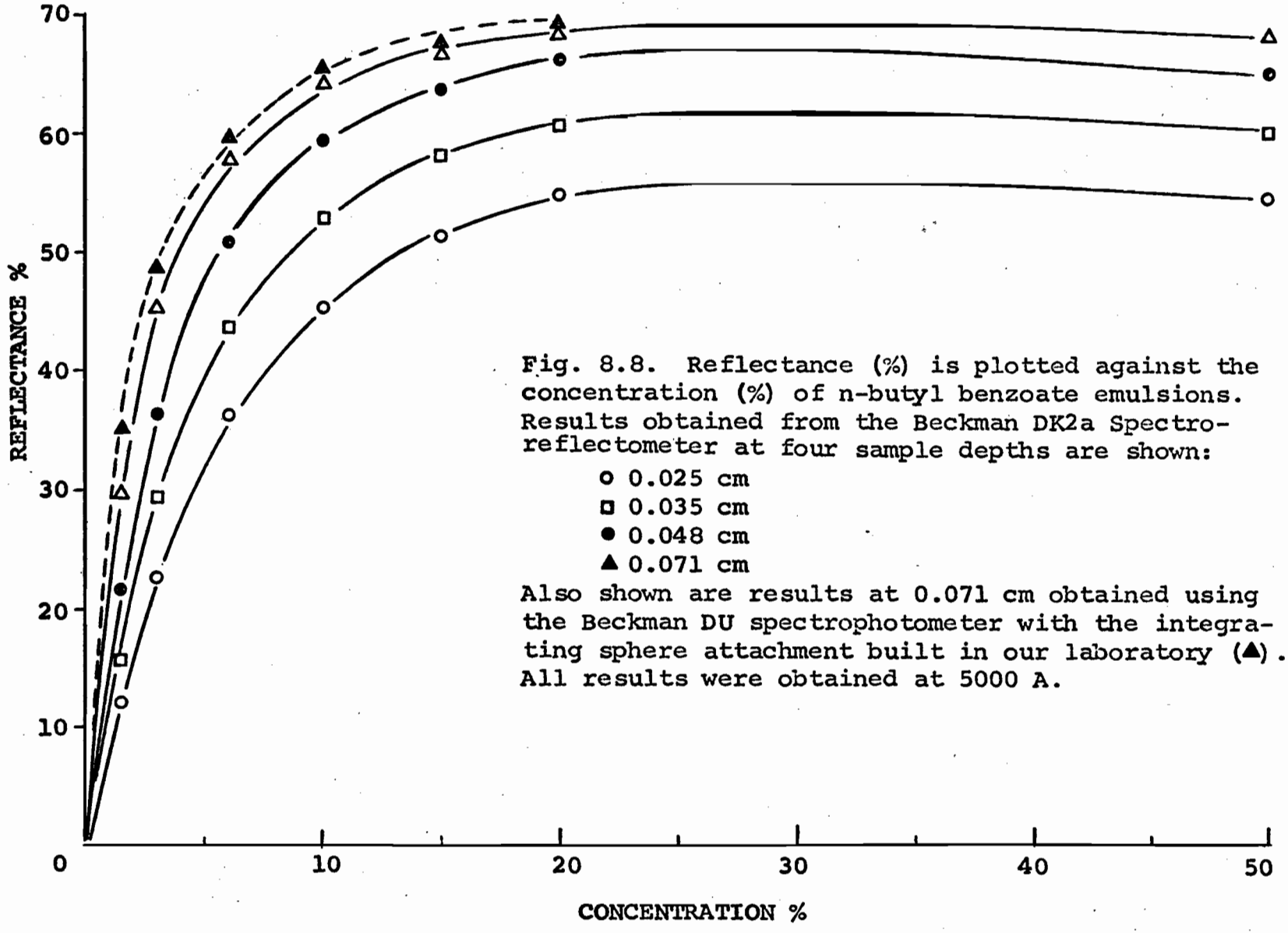

Fig. 8.8. Reflectance (%) is plotted against the concentration (%) of n-butyl benzoate emulsions. Results obtained from the Beckman DK2a Spectro-reflectometer at four sample depths are shown:

- ○ 0.025 cm
- □ 0.035 cm
- ● 0.048 cm
- ▲ 0.071 cm

Also shown are results at 0.071 cm obtained using the Beckman DU spectrophotometer with the integrating sphere attachment built in our laboratory (▲). All results were obtained at 5000 A.

study in which both the transmittance and the reflectance of the same sample were measured.

The results of reflectance measurements of very thin samples of nonhemolyzed blood were in qualitative agreement with those obtained by Kramer et al (132) at larger sample depths.

When the percent reflectance of concentrated red blood cell suspensions was plotted against percent transmittance, a linear relationship was found to exist for each hemoglobin concentration. Consequently, reflectance and transmittance are linearly related. To our knowledge, this observation has not previously been made.

Examination of the data in terms of Twersky's theory provides new insight into the problems of reflection oximetry. The results show that the relationship between reflectance and the extinction coefficient (or in the case of oximetry, oxygen saturation) must be exponential.

The results show that the empirically developed reflection oximetry techniques make advantageous use of several reflectance phenomena. A large sample depth (greater than 0.3 cm) is always used. Reflectance studies have shown that a large sample depth provides two advantages: the difference in reflectance corresponding to changes in the extinction coefficient (or oxygen saturation) is increased and the

sensitivity of the measurement is increased as a consequence; Kramer's results showed that reflectance is asymptotic with sample depth above 0.3 cm, so that, as long as this minimum depth is maintained, the actual sample depth is of no consequence.

The procedure used in reflection oximetry, suggested by Rodrigo (190), relates the reciprocal of reflectance to oxygen saturation. This technique has been used also by Polanyi et al (181) and by Enson and colleagues (58) and appears to give sufficiently accurate results within a limited range of hemoglobin concentrations and oxygen saturations. However, for practical oximetry, the use of 1/R rather than log R does not affect the results to a great extent.

IX. APPLICATION OF MULTIPLE SCATTERING THEORY TO THE ESTIMATION OF OXYGEN SATURATION IN WHOLE NONHEMOLYZED BLOOD

A. Introduction

In Chapter VII we showed that Twersky's wave treatment for multiple scattering may be used to describe the light transmission of nonhemolyzed blood and other scattering suspensions into the forward hemisphere. It should be possible, therefore, to obtain an expression for the oxygen saturation of nonhemolyzed blood on a purely theoretical basis using this theory.

In the present chapter we derive expressions for the oxygen saturation of nonhemolyzed whole blood using Twersky's theory and try to apply them to the results of Chapter IV, which were obtained with the cuvette oximeter. In Chapter V we demonstrated that, unlike the integrating sphere which measures the total light scattered and transmitted into the forward hemisphere, the cuvette oximeter measures a quantity of light which is not precisely defined. Consequently, the condition specified by Twersky's theory - the collection of all light scattered into the forward half space - is not fulfilled. However, the diffusing plate technique does provide a good approximation of this quantity. Consideration of this fact, together with the finding in Chapter IV that

the relationship between optical density and changes in the extinction coefficient of the hemoglobin pigment (caused by changing oxygen saturation) at a constant hemoglobin concentration was linear, and that this relationship consisted of a family of parallel lines for various hemoglobin concentrations, suggested to us that it might be possible to apply Twersky's theory to the oximeter results.

B. Theoretical Considerations

According to equation 7.7

$$T = I/I_o = 10^{-\epsilon cd}\left[10^{-sH(1-H)d} + q(\delta)(1 - 10^{-sH(1-H)d})\right]$$

$$\text{and } O.D. = \epsilon cd - \log\left[10^{sH(1-H)d} + q(\delta)(1 - 10^{-sH(1-H)d})\right]$$

Consider first a two wavelength system. At a wavelength in the red region of the spectrum (λ_1),

$$T_1 = 10^{-\left[\epsilon_{1o}c_1+\epsilon_{1r}(c-c_1)\right]d}\left[10^{-sH(1-H)d} + q(\delta)(1 - 10^{-sH(1-H)d})\right] \qquad 9.1$$

At λ_2, an isobestic wavelength,

$$T_2 = 10^{-\epsilon_2 cd}\left[10^{-sH(1-H)d} + q(\delta)(1 - 10^{-sH(1-H)d})\right] \qquad 9.2$$

The term in the square brackets represents the scattering term; it is the same at both wavelengths, since the only variables are concentration and sample depth. Therefore, if

the ratio of the transmittances at the two wavelengths is taken, the scattering terms will cancel.

The usual procedure employed in conventional whole blood oximetric techniques is to take the ratio of optical densities rather than transmittances. This ratio is then related empirically to oxygen saturation determined by a reference method. The ratio of optical densites at the two wavelengths is given by

$$\frac{OD_1}{OD_2} = \frac{\left[\epsilon_{1o}c_1 + \epsilon_{1r}(c-c_1)\right]d - \log\left[10^{-sH(1-H)d} + q(\delta)(1 - 10^{-sH(1-H)d})\right]}{\epsilon_{2}cd - \log\left[10^{-sH(1-H)d} + q(\delta)(1 - 10^{-sH(1-H)d})\right]} \qquad 9.3$$

This expression is not only extremely complex, but it cannot be used to calculate oxygen because it is impossible to separate c_1/c, or oxygen saturation.

A simpler expression results if the ratio of transmittances at two wavelengths, rather than optical densities, is taken:

$$\frac{T_1}{T_2} = \frac{10^{-\left[\epsilon_{1o}c_1 + \epsilon_{1r}(c - c_1)\right]d}}{10^{-\epsilon_2 cd}} \qquad 9.4$$

and

$$\log\left[\frac{T_1}{T_2}\right] = \epsilon_2 cd - \left[\epsilon_{1o}c_1 + \epsilon_{1r}(c - c_1)\right]d = \log T_1 - \log T_2 \qquad 9.5$$

which may be written

$$OD_2 - OD_1 = \left[c(\epsilon_2 - \epsilon_{1r}) + c_1(\epsilon_{1r} - \epsilon_{1o})\right]d \qquad 9.6$$

Dividing through by cd gives

$$\frac{OD_2 - OD_1}{cd} - (\epsilon_2 - \epsilon_{1r}) = \frac{c_1}{c}(\epsilon_{1r} - \epsilon_{1o})$$

from which oxygen saturation may be obtained:

$$\%O_2 = \frac{c_1}{c}(100) = \left[\frac{OD_2 - OD_1}{cd(\epsilon_{1r} - \epsilon_{1o})} - \frac{\epsilon_2 - \epsilon_{1r}}{\epsilon_{1r} - \epsilon_{1o}}\right](100) \qquad 9.7$$

Equation 9.7 shows that at a constant sample depth, it is necessary to know the hemoglobin concentration of the blood sample. Consequently, this approach based on Twersky's theory is of limited practical value for calculating the oxygen saturation of nonhemolyzed blood.

A one wavelength system, in which a measurement of the transmittance of a fully saturated sample at the red wavelength is substituted for the isobestic measurement, suffers from the same disadvantage - the hemoglobin concentration must be known.

The one wavelength system may be represented as follows:

$$T_x = 10^{-\left[\epsilon_o c_1 + \epsilon_r(c-c_1)\right]d}\left[10^{-sH(1-H)d} + q(\delta)(1 - 10^{-sH(1-H)d})\right]$$

where T_x is the transmittance of a sample of unknown saturation.

$$T_{100\%} = 10^{-\epsilon_o cd}\left[10^{-sH(1-H)d} + q(\delta)(1 - 10^{-sH(1-H)d})\right]$$

where $T_{100\%}$ represents the transmittance of a fully saturated sample. Then,

$$\frac{T_x}{T_{100\%}} = \frac{10^{-[\epsilon_o c_1 + \epsilon_r(c - c_1)d]}}{10^{-\epsilon_o cd}} \qquad 9.8$$

$$OD_{100\%} - OD_x = \epsilon_o cd - [\epsilon_o c_1 + \epsilon_r(c - c_1)]d \qquad 9.9$$

$$\frac{OD_{100\%} - OD_x}{cd} = -(\epsilon_r - \epsilon_o) + \frac{c_1}{c}(\epsilon_r - \epsilon_o)$$

and $$\%O_2 = \frac{c_1}{c}(100) = \left[\frac{OD_{100\%} - OD_x}{cd(\epsilon_r - \epsilon_o)} + 1\right](100) \qquad 9.10$$

Equation 9.10 shows that a knowledge of the total hemoglobin concentration is again required.

Equations 9.7 and 9.10 are impractical and do not provide a useful means of determining oxygen saturation. However, a successful application of this theory to the results of Chapter IV would provide further evidence that Twersky's

theory does describe the light scattering properties of undiluted nonhemolyzed blood. It must be remembered that these results were obtained using the cuvette oximeter, rather than an integrating sphere, and the transmittance measurements obtained with this system represent an undefined fraction of the forward scattered light.

C. Results

We considered the changes in oxygen saturation as changes in the extinction coefficient of hemoglobin. When Twersky's theory was applied to the results obtained using the cuvette oximeter, it was found that a constant factor, n, was required in the exponent of the term corresponding to absorption. It is interesting to note that if the results of Chapter IV had not been a series of parallel lines, but divergent as Kramer et al and Hickam and Frayser had found, n would not be constant, for the same sample depth. However, in our experiments, n was found to be constant at each of the two sample depths used. At 0.027 cm sample depth, n was 1.37 and at 0.071 cm, n was 1.44.

An attempt to calculate oxygen saturation using the two wavelength equation derived from Twersky's theory did not prove to be successful. This may suggest that the theory can be used to describe only results obtained with the integrating sphere. However, when the one wavelength equation for oxygen

saturation was used, the results were very satisfactory.

After substitution of the appropriate constants into equation 9.10, the expression for oxygen saturation at a sample depth of 0.027 cm was

$$\%O_2 = \left[\frac{OD_{100\%} - OD_x}{0.04062c} + 1\right] (100)$$

where c is hemoglobin concentration in mM/l.

At a sample depth of 0.071 cm, the equation was

$$\%O_2 = \left[\frac{OD_{100\%} - OD_x}{0.1036c} + 1\right] (100)$$

The results obtained by calculation from equation 9.10 and the optical density data of Chapter IV were compared with Van Slyke analyses (Table 9.1). Satisfactory agreement between experimental values and those calculated from the one wavelength equation based on Twersky's theory was obtained. The standard deviation of the differences between experimental and calculated values was $\pm$1.97% oxygen saturation at a sample depth of 0.027 cm. At a sample depth of 0.071 cm, the standard deviation of the differences was $\pm$1.64%. These results demonstrate that although the use of Twersky's theory for estimating oxygen saturation is not practical, it may be

TABLE 9.1. Comparison of oxygen saturation values obtained by Van Slyke analysis with those obtained by calculation from equation 9.10 based on Twersky's theory

Sample Depth (cm)	Hemoglobin Concentration gm/100ml	mM/l	Oxygen Saturation	
			Van Slyke	Eq. 9.10
0.027	8.6	5.2	96.20	96.20
			86.96	86.73
			67.27	66.42
			57.25	56.85
			47.15	47.58
	9.1	5.4	88.81	86.99
			78.19	77.24
			67.49	63.78
			56.54	55.75
			45.55	44.64
	9.2	5.5	97.32	97.50
			86.86	90.39
			76.88	78.46
			63.91	65.73
			52.23	56.25
			40.55	42.49
	9.8	5.9	95.90	98.57
			73.13	72.18
			61.03	64.76
			49.01	46.59
	11.8	7.1	96.90	96.65
			86.84	87.55
			65.44	62.93
			55.32	54.81
			43.61	40.58
	14.2	8.5	97.01	96.94
			83.92	84.04
			70.74	71.03
			57.90	59.03
			31.23	33.50
	17.6	10.6	98.00	97.53
			90.55	89.66
			82.58	80.67
			66.40	65.73
			58.26	55.90
	19.9	11.9	97.00	97.13
			83.52	83.21

TABLE 9.1. Continued

Sample Depth (cm)	Hemoglobin Concentration gm/100ml	mM/l	Oxygen Saturation Van Slyke	Oxygen Saturation Eq. 9.10
0.027			56.25	59.48
			41.42	42.61
			27.35	31.95
	Mean		69.46	69.65
	S.D.D.[a] ($\%O_2$)			±1.97
0.071	5.5	3.3	96.17	96.19
			86.46	86.94
			75.51	74.27
			53.00	53.67
			41.60	41.15
	6.7	4.0	97.01	96.33
			87.17	88.10
			77.10	77.41
			66.37	63.84
			44.69	41.83
	8.2	4.9	95.92	95.61
			89.11	88.73
			74.59	74.46
	9.8	5.9	100.00	100.00
			89.23	86.83
			77.54	74.35
			53.79	52.18
	12.4	7.4	97.88	97.27
			73.66	72.01
			49.30	49.76
	13.7	8.2	97.50	97.87
			84.50	85.84
			70.00	71.27
			60.20	60.44
			47.50	48.25
			34.90	35.66
	20.8	12.4	99.00	98.68
			84.90	86.37
			70.20	73.41
	21.5	12.8	98.78	98.96
			86.96	88.95
			74.64	79.31
	Mean		76.10	76.12
	S.D.D.			±1.64

[a] S.D.D. = $\left[1/(n-1)\ \sum(d - \bar{d})^2\right]^{\frac{1}{2}}$.

applied to measurements made at 6330 A, using our cuvette oximeter.

In the application of the one wavelength equation for oxygen saturation - equation 9.10 - to the cuvette oximeter results, only the absorption term of Twersky's theory was involved; the scattering term cancelled. An attempt was made to see if the scattering term of equation 7.7 could be used to describe the cuvette oximeter results. The endeavor was fairly satisfactory as shown in Fig. 9.1 and Table 9.2, although deviations occurred at high hemoglobin concentrations. The standard deviations of the differences between experimental and calculated values of optical density were 0.059 and 0.049 optical density units for oxygenated and reduced nonhemolyzed blood, respectively, at a sample depth of 0.071 cm.

D. Discussion

We have shown that Twersky's theory may be applied to the cuvette oximeter results and may be used to calculate the oxygen saturation of nonhemolyzed blood in a one wavelength system at 6330 A. Our unsuccessful attempts in a two wavelength system were likely due to the inadequacy of the measuring system. An examination of the geometrical arrangement of the photocells in the cuvette oximeter shows that different fractions of scattered light are collected by

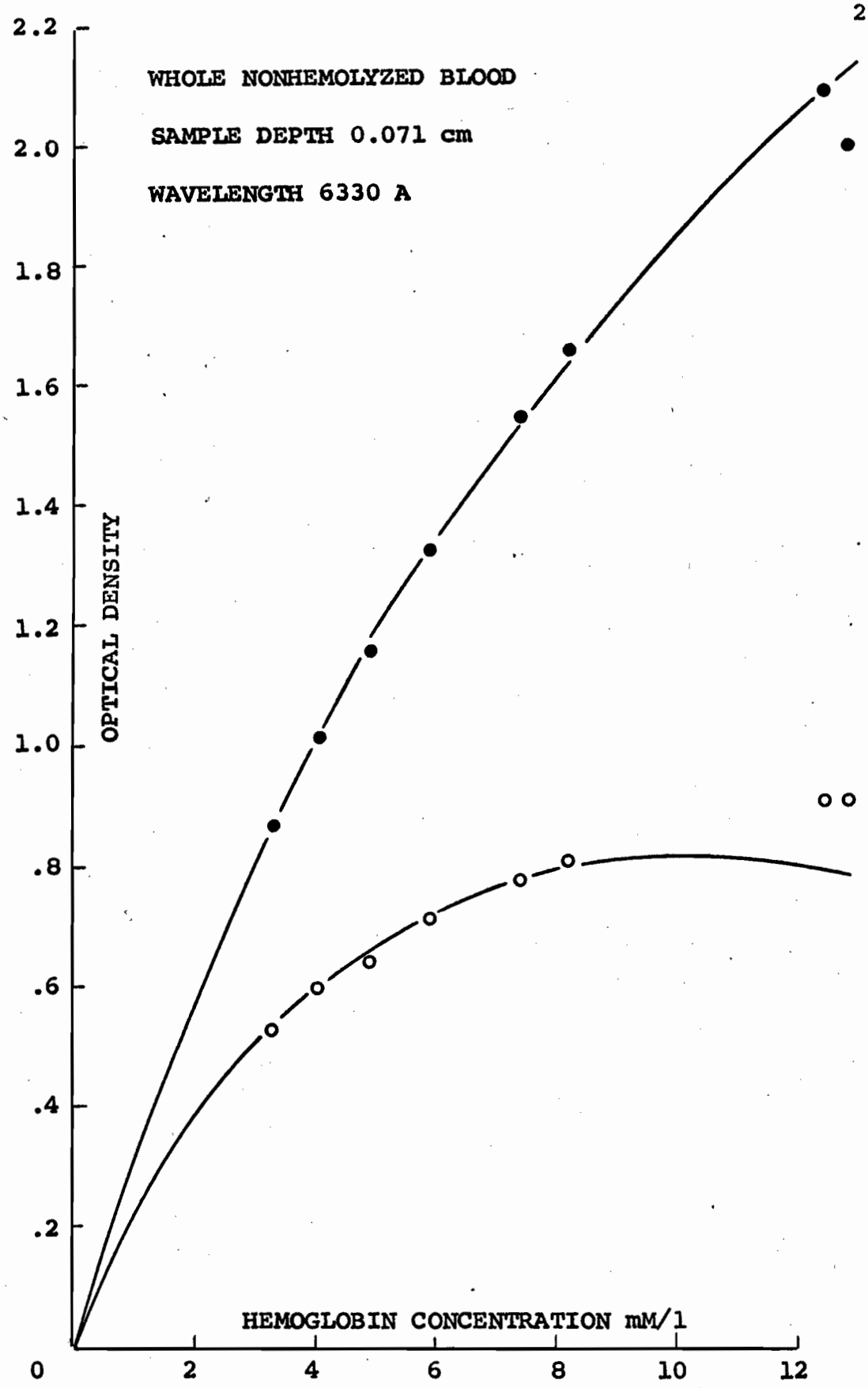

Fig. 9.1. The optical density of nonhemolyzed blood is plotted against hemoglobin concentration. The open and closed circles represent experimental values for oxygenated and reduced blood, respectively, obtained using the cuvette oximeter; the solid lines were calculated from equation 7.7, based on Twersky's theory.

TABLE 9.2. Comparison of optical density values at 6330 A for nonhemolyzed blood measured with the cuvette oximeter with those obtained by calculation from equation 7.7

Concentration (mM/l)	Optical Density			
	Oxygenated Blood		Reduced Blood	
	Exp.	Eq. 7.7	Exp.	Eq. 7.7
3.3	0.524	0.532	0.865	0.871
4.0	0.596	0.594	1.023	1.012
4.9	0.642	0.668	1.156	1.178
5.9	0.703	0.713	1.326	1.324
7.4	0.775	0.772	1.545	1.537
8.2	0.810	0.796	1.660	1.645
12.4	0.909	0.783	2.096	2.072
12.8	0.907	0.793	1.996	2.123
S.D.D.[a]	±0.059		±0.049	
% of Mean[b]	8.0		3.3	

[a]Standard deviation of the differences between experimental and calculated values. S.D.D. = $\left[1/(n-1)\ \sum(d - \bar{d})^2\right]^{1/2}$.

[b]Standard deviation of the differences expressed as a percent of the mean optical density value.

the red sensitive and by the infrared sensitive photocell. Twersky's theory was derived to describe all the light transmitted and scattered in forward directions. An exact measurement of this quantity is possible only with an integrating sphere. In the cuvette oximeter, the photocell collecting the light at 6330 A is situated in the center of the detector area and it is in the optical axis of the cuvette, with respect to the light source and sample chamber. On the other hand, the 8050 A cells are located on either side of the red cell and are not in the optical axis of the system. It appears highly probable that, while the red filtered photocell receives light scattered with little deviation from the optical axis of the system, the infrared filtered photocells receive a higher proportion of the laterally scattered light and a smaller proportion of the light transmitted along the optical axis of the system. Thus, the red and infrared cells do not receive the same fractions of the scattered light and the scattering terms do not cancel when the ratio of transmittances is taken.

E. Conclusions

Our attempt to apply Twersky's theory to the estimation of oxygen saturation in nonhemolyzed blood was successful for a one wavelength system. If the lines relating oxygen

content to optical density had been divergent, rather than parallel, it would have been impossible to apply this theory to the estimation of oxygen saturation in nonhemolyzed blood. A fairly high degree of accuracy was achieved over the whole range of oxygen saturations and hemoglobin concentrations.

Attempts to apply the two wavelength equation were not successful. The oxygen saturation equations are based on the premise that if the ratio of the two transmittance readings is taken, the scattering terms cancel. We tentatively ascribed the failure of the two wavelength equation to the geometrical arrangement of the photocells in the cuvette oximeter. The red and infrared filtered photocells receive different fractions of the scattered light. Thus, the scattering terms of equation 7.7 do not cancel.

Although theoretical equations for oxygen saturation can be derived, they are impractical since they require that the hemoglobin concentration of the sample be known.

X. THE TRANSMISSION OF RED AND INFRARED LIGHT THROUGH THE HUMAN EAR*

A. Introduction

Photometric principles have been applied not only to in vitro measurements of the oxygen saturation of blood, but also to in vivo measurements in the intact man.

Matthes described the first ear oximeter in 1935 (152). Using gelatin filters, he transmitted red and green light through the lobe of the ear. The principle of the method was identical to that of the spectrophotometric technique for hemolyzed blood; the red filtered detector was sensitive to both oxygen saturation and total hemoglobin concentration, while the green filtered detector was sensitive only to total hemoglobin concentration.

Other bichromatic devices for measuring oxygen saturation in vivo were developed in 1940 by Squire (215) and by Hartman and McClure (90) for the interdigital web of the hand, and in 1942 by Goldie (73) and by Millikan (165) for the pinna of the ear. All these instruments employed gelatin filters. Some of the early workers chose blue or green wavelengths for the measurement at an isobestic wavelength. Matthes changed from green to infrared light because he found that blood

*Published in part. Anderson, N.M., Sekelj, P., and M. McGregor: IRE Trans. Bio-Med. Electronics BME-8: 134, 1961.

transmitted more light in this spectral region. Squire also used infrared light. In 1949, Wood and Geraci (250) and Elam et al (57) pointed out that ear tissue does not transmit light of wavelengths less than 6000 A. Blue and green Wratten filters transmit light also in the infrared region of the spectrum. Although they were presumably unaware of it, the early workers all used the infrared region of the spectrum. Transmission oximeters currently in use all employ red and infrared light. The pinna of the ear has proved to be the most suitable site for the measurement of oxygen saturation in the intact man.

Although ear oximetry may be considered generally as an application of the bichromatic spectrophotometric technique for measuring oxygen saturation, the calibration procedures employed have not all adhered to the basic principles underlying the spectrophotometric technique. In the closest approximation to the spectrophotometric principle, the ear is considered as a sample cuvette in which the ear tissue comprises the sample chamber walls, and the blood within the vessels of the ear constitutes the sample. Spectrophotometric techniques have been followed by obtaining (i) a blank optical density reading on the ear when all the blood has been expelled (the so-called "bloodless ear") and (ii) a sample optical density reading on the flushed ear. The dif-

ference between the two measurements represents the optical density due to the blood in the ear. This technique was employed by Squire for the web of the hand and by Goldie and by Wood and Geraci for the ear. The ratio of the optical densities obtained in this manner in the red and infrared spectral regions is then related to oxygen saturation determined by a reference method.

In the devices of Squire, of Goldie, and of Millikan who provided the first practical oximeter, it was necessary to preset the instrument to 98% or 100% saturation while the subject was breathing air or 100% oxygen. Wood and Geraci were able to obtain calibration curves for individual ear-pieces which made it possible to obtain absolute values for oxygen saturation without calibrating for each subject. Wood et al (249) reported that the standard deviation of the differences from the mean calibration line was 2.9% saturation in the range from 13% to 100% oxygen saturation.

In Millikan's technique and the "single scale" technique of Wood et al (249) the difference between the transmittance of the ear in the red and infrared bands was related to oxygen saturation. This technique has no basis in spectrophotometric practice and shows less accuracy than the technique described above.

The application of spectrophotometric principles to the

ear neglects the requisite conditions, namely, that the sample consist of clear, nonscattering, homogenous material, contained within clear, plane parallel plates, and be illuminated by monochromatic light. Unfortunately, the ear is nonhomogeneous with respect to both sample cuvette and blood sample. The light transmitted through the ear is attenuated not only by absorption and scattering by the blood but also by the ear tissue. Thus, the technique in which the bloodless ear is considered as a blank cuvette is merely an approximation based on the assumption of the applicability of Beer's law to dense scattering ear tissue and nonhemolyzed blood. This assumption is invalid. However, a great deal of experimental evidence has shown that the method provides adequate oxygen saturation estimations for clinical purposes.

A further objection to this technique may be raised. It is doubtful that all the blood may be expelled from the transilluminated tissue by compression (177). In 1951 Sekelj suggested, as an alternative to the measurement of the light transmission of the "bloodless ear," that the ratio of the red and infrared transmittances of the ear tissue alone was a constant in anatomically normal ears.

The pinna of the ear may be considered as a series of turbid layers. The light transmitted through the ear will be attenuated depending on the amount and distribution of

the pigments and the turbidity of the tissue due chiefly to nonabsorbing cellular constituents.

In the spectral region with which we are concerned, 6000 A to 9000 A, studies on the spectral reflectance of skin have been performed by Jacquez et al (108). These studies are not particularly useful for the present investigation since they were carried out on perfused tissue.

Data in the literature on the transmittance of bloodless skin at wavelengths between 6000 A and 9000 A are rather sketchy. In 1964, Buckley and Grumm (24) showed that the light transmitted by skin samples removed during surgical procedures and washed in isotonic saline increased fairly uniformly as the wavelength was increased from 4000 A to 7000 A. The work of Bachem and Reed (8), in 1931, showed that the transmittance of epidermis plus corium reached a maximum between 8000 A and 9000 A and then began to decrease.

The most important pigment in the skin is melanin. The light transmittance of melanin was studied by Edwards, Finkelstein and Duntley (55), in 1951, between 2500 A and 6000 A. The transmittance showed a fairly uniform rise as wavelength was increased within this spectral region. Electron microscope studies by Mason et al (150) in 1947 showed melanin granules to be spheroid and about 3000 A in diameter.

There is also some light absorption in the skin by the

pigment carotene. This pigment shows an absorption maximum at 4820 A (54). Carotenoids, which are in abundance in subcutaneous fat and also present in the dermis (24) show very little absorption at wavelengths greater than 6000 A.

Elam et al obtained transmission spectra of "bloodless" pinnas of normal white subjects by compressing the ear with a transparent plexiglass cylinder covered by a translucent rubber diaphragm which allowed compression of the ear to an arbitrary pressure of 200 mm Hg (57). The transmittance at 8000 A was approximately 12% lower than it was at 6500 A. This finding is at variance with the data on the transmittance of skin and of melanin, both of which indicated that transmittance was slightly higher at 8000 A than it was at 6500 A. However, the study on the bloodless ear included the presence of subcutaneous fat, cartilage, blood vessel walls, and to some extent, residual blood which was not expelled upon compression of the ear.

In our laboratory we have found that induced anoxia sufficient to reduce the ratio of red to infrared transmitted light in the blood-filled ear by 14% will cause a reduction of this ratio in the compressed ear of approximately 1.5%, a result which can only be explained by the presence of some reduced hemoglobin in the light path. This suggests that the assumption of a constant ratio in the bloodless ear would

probably introduce less error than making the actual measurements in cyanosed subjects.

To verify experimentally that this assumption was permissible, a systematic study of ears differing widely in thickness and in pigmentation was undertaken in this laboratory.

B. Theoretical Considerations

Due to the density of the cellular constituents in the ear tissue, multiple light scattering must occur. In Chapter VII we demonstrated that Twersky's theory for the multiple scattering of waves may be applied to both absorbing suspensions (red blood cell suspensions) and nonabsorbing suspensions (emulsions of n-butyl benzoate in water). Making two simplifying assumptions, that the distribution of scattering material in the bloodless ear is fairly homogeneous throughout the tissue being transilluminated, and that the absorbing pigments are also homogeneously distributed, we attempted to apply Twersky's theory to the light transmittance of the bloodless ear.

Due to the geometrical arrangement of the earpiece, the light received by the detector is a good approximation of the light transmitted and scattered into the forward hemisphere since the detector is in contact with the sample - the ear. Also, with the ear in the earpiece, the sample may be

considered "infinitely extended" in the plane perpendicular to the optical axis of the system. Thus, apart from the lack of monochromatic light, due to the use of gelatin filters, the measuring conditions required by Twersky's theory may be considered as adequately fulfilled. The arrangement of the red and infrared filtered photocells is symmetrical with respect to the light source and sample, so that equal fractions of scattered light should be measured in both red and infrared spectral bands.

We expressed the light transmittance of the bloodless ear in a manner similar to that used in Chapter VII for non-hemolyzed blood. In the red spectral band,

$$R = \frac{I}{I_o} = 10^{-\epsilon_r cd}\left[10^{-sH(1-H)d} + q(\delta)(1 - 10^{-sH(1-H)d})\right] \qquad 10.1$$

where ϵ_r is the extinction coefficient of the absorbing material in the ear tissue (chiefly melanin) distributed throughout the cell constituents, c is the concentration of the absorbing material, d is the thickness of the ear, and H is the fractional volume occupied by the scattering cellular constituents; s and $q(\delta)$ were defined in Chapter VII, Section B.

Similarly, in the infrared band,

$$IR = \frac{I}{I_o} = 10^{-\epsilon_{ir}cd}\left[10^{-sH(1-H)d} + q(\delta)(1 - 10^{-sH(1-H)d})\right] \qquad 10.2$$

where ϵ_{ir} is the extinction coefficient of the absorbing material in the infrared band.

The ratio of the transmittances in these two spectral regions is

$$\frac{R}{IR} = \frac{10^{-\epsilon_r cd}}{10^{-\epsilon_{ir}cd}} = 10^{(\epsilon_{ir} - \epsilon_r)cd} \qquad 10.3$$

If $\epsilon_{ir} = \epsilon_r$, then R/IR = 1. However, if ϵ_{ir} is not equal to ϵ_r, then R/IR depends on c, the concentration of absorbing pigment in the ear, and on d, the thickness of the ear. Since absorption is almost entirely due to melanin, we will refer to ϵ as the extinction coefficient of melanin. If ϵ_{ir} is very close to ϵ_r, then R/IR will be very close to 1.0. If ϵ_{ir} is less than ϵ_r, then R/IR will be less than 1.0. Also, if ϵ_{ir} is less than ϵ_r, then as c or d is increased, R/IR becomes smaller. The magnitude of this change would depend on the difference between ϵ_{ir} and ϵ_r.

C. Material and Method

The ears of 70 volunteer subjects were studied. They ranged widely in pigmentation and thickness, from the thin nonpigmented ears of white children, to the heavily pigmented ears of Negro adults. In between these extreme groups was a group of Indian subjects of light brown pigmentation. No cases with suspected hypoxemia were studied. Subjects were seated at rest and were breathing room air.

The apparatus used consisted of one of our standard oximeters incorporating two separate galvanometers (201) with a Waters earpiece (Model XE-50A-No. 115, Waters Corp., Rochester, Minn.), which has a mechanism for compression of the ear to any desired pressure.

A standard filter consisting of a Wratten 23B filter sandwiched between layers of filter paper was placed in the light path of the earpiece while the controls of the red and infrared filtered photocells were adjusted to produce equal galvanometric deflections. It was necessary to standardize the earpiece on a filter due to the high incident intensity required to transmit a measurable quantity of light through the ear. However, the incident intensity on both the red and infrared filtered photocells was almost identical since the Wratten 29F filter transmits uniformly above 6000 A and the transmittance of filter paper at 8050 A is only slightly higher (6%) than it is at 6300 A. The

earpiece was then placed on the pinna of the ear and a pressure of 220 mm Hg was applied to render the ear bloodless when red and infrared galvanometer deflections were read.

Certain errors are inherent in the performance of such measurements as this. They include setting of the instrument, placement of the earpiece, and reading of galvanometer deflections. All these errors are included in the term "experimental error," and the extent of this may be judged by comparing the first ratio measurement made with the second ratio measurement made in the same manner. In order to obtain an index of the error inherent in the method, the earpiece was removed and the entire procedure repeated. The experimental error was then expressed as the standard deviation of the differences of the two consecutive ratios obtained in the same ear, expressed as percentages of the group mean.

D. Results

The results are shown in Table 10.1. The average ratios of the white children, the white female adults, and the white male adults were almost identical. The mean was 0.885. For Indian subjects the mean was 0.855, and for Negro subjects it was 0.843. The standard deviation of the ratios of all 40 white subjects was 2.85% of the mean ratio for these subjects. Equivalent values for Indian and Negro subjects were 3.10% and 6.93%, respectively.

TABLE 10.1.

RED/INFRARED RATIOS IN THE BLOODLESS EAR FOR WHITE, INDIAN, AND NEGRO GROUPS

Pigment Group		White			Indian		Negro	
N (Total)		Children (16)	Adults (24)		Adults (11)		Adults (19)	
Sex			Male (13)	Female (11)	Male (9)	Female (2)	Male (8)	Female (11)
Age (years)		4–16	21–60	21–41	22–40	22–24	20–51	18–40
R/IR Bloodless	mean	0.880	0.887	0.882	0.863	0.821	0.862	0.823
	range	0.808 to 0.920	0.846 to 0.918	0.852 to 0.912	0.831 to 0.893	0.818 to 0.824	0.780 to 0.914	0.736 to 0.949
Group Mean (SD)		0.885 (±0.025)			0.855 (±0.025)		0.843 (±0.057)	
SDD per cent		2.85			3.10		6.93	
Experimental error per cent (SDD)		2.39			1.81		2.05	

SDD per cent = SD of the differences from the mean as percentages of the mean value.
Experimental error per cent = SD of the individual differences between ratios derived from repeated observations as percentages of the mean ratio.

Reprinted from IRE TRANSACTIONS
ON *BIO-MEDICAL ELECTRONICS*
Volume BME-8, Number 2, April, 1961

PRINTED IN THE U.S.A.

The experimental error, as defined by the standard deviation of the differences of the paired observations in all white subjects was 2.39% of the mean ratio of all white subjects. The equivalent figures for the Indian and Negro subjects were 1.81% and 2.05%, respectively.

E. Discussion

The theoretical prediction that R/IR = 1.0 if $\epsilon_{ir} = \epsilon_r$ could not be entirely fulfilled in these experiments since the incident light on the red filtered photocell was approximately 6% lower than that incident on the infrared filtered photocell. Instead, a ratio slightly less than 1.0 would be obtained. If ϵ_{ir} is less than ϵ_r as indicated from transmission studies of melanin, the ratio R/IR would be further reduced from 1.0. The mean ratio for white subjects was 0.885, which supports the theoretical prediction of a ratio slightly less than 1.0. This ratio was very nearly constant for white subjects. It showed more variability in the groups with more pigmentation and the mean ratio showed progressive reduction with increasing degree of pigmentation. In the lightly pigmented Indian subjects, R/IR was 0.855, and in the more highly pigmented Negro subjects the ratio was further reduced, 0.843, as predicted by equation 10.3.

The results indicate that the assumption of a constant ratio for red to infrared transmission through the bloodless

ear is valid for white subjects and that the error introduced by this assumption differs insignificantly from the experimental error which would result from making the actual measurements in each subject as in the method of Wood and Geraci (250). The assumption that the same ratio appertains in lightly pigmented Indian subjects as in white subjects introduces a slightly greater error.

F. Conclusions

The assumption that the ratio of red to intrared transmittance in the bloodless ear is a constant has been experimentally justified for white subjects. The ratio showed more variability and was slightly reduced in a group of Indian subjects, who show light pigmentation, and further reduced in the more pigmented Negro subjects.

Application of Twersky's theory for the multiple scattering of waves to the light transmission of the bloodless ear indicated that the ratio of transmittances in the red and infrared spectral bands departs from a constant value if the extinction coefficients due to absorption by pigments (chiefly melanin) in the ear tissue differ in these two spectral bands. The ratio is theoretically 1.0 if the extinction coefficients are the same. However, if the extinction coefficients are not equal, the ratio will depart from 1.0, depending on the difference between the extinction

coefficients, the concentration of melanin, and the thickness of the ear. The ratio was very nearly constant for white subjects, and close to 1.0 (0.885), but showed progressive decreases with increasing pigmentation. This result is in accordance with the theory if the extinction coefficient for the absorbing pigments in the ear is less in the infrared band than it is in the red band, which transmission studies of melanin indicate.

XI. APPLICATION OF SPECTROPHOTOMETRIC TECHNIQUES TO THE ESTIMATION OF DYE CONCENTRATION IN NONHEMOLYZED WHOLE BLOOD

A. Introduction

1. Indicator Dilution Techniques

An important application of spectrophotometric techniques to nonhemolyzed blood is the continuous detection of dye concentration for the indicator dilution technique of estimating blood flow.

Indicator dilution techniques found their first physiological application in the measurement of the time for blood to circulate from the point of injection to the point of sampling (82, 94). The use of indicator dilution methods for estimating blood flow began with Stewart in 1893 (218). Stewart, using both the constant rate as well as the single injection technique, showed that cardiac output could be determined by injecting indicator into the venous circulation and sampling the arterial concentration.

The first dye dilution curves for estimating cardiac output were recorded by Gross and Mittermaier in 1926 (77). Earlier, Henriques had noted an important limitation of the single injection indicator dilution technique; this was the failure of the downslope of the indicator dilution curve to

return to the baseline due to the presence of a recirculation peak (93). Hamilton and his colleagues (123) suggested that the effect of recirculation could be overcome by replotting the dye dilution curve semilogarithmically and extrapolating the disappearance slope linearly to the baseline. Since that time the dye dilution technique for estimating cardiac output has been used extensively.

2. Indicators

A suitable indicator must meet several criteria. It must be nontoxic, water soluble, and nondiffusible. It must disappear from the blood as quickly as possible to avoid buildup of background indicator - an important consideration when repeated injections must be made. Dyes which bind to the plasma proteins (thus preventing loss to surrounding tissues) and which can be removed from the blood by the liver or the kidney have proved satisfactory. The indicator must be neither hypertonic nor hypotonic. It was pointed out in Chapter II and demonstrated in Chapter V that the optical density of red cell suspensions is significantly affected by osmotically induced changes in the size of the cells. Finally, the dye must absorb light in the spectral regions where blood and tissue show high transmittance, that is, at red and near infrared wavelengths.

The first dyes used successfully in dilution studies were the blue dyes, which show absorption in the red region of the spectrum. Methylene blue, a thyazine dye, was used to estimate circulation times first by Stewart in 1897 and later by Matthes and Schleicher in 1939 (156). Difficulty in the quantitation of methylene blue and its very rapid disappearance from the blood have restricted its use to studies of circulation times and the detection of intracardiac shunts.

Evans blue or T-1824, an azo dye, was chosen as an indicator in 1920 (44) and proved to be a suitable dye for quantitation; it has been used successfully for estimating cardiac output. Unfortunately, its strong affinity for the plasma proteins results in an extremely slow clearance rate; it may cause tissue coloration and staining.

In 1959, Coomassie blue was introduced as an indicator (222, 223). Like T-1824, it is an azo dye and it is bound to the albumin fraction of the plasma proteins. In contrast to T-1824, it does not cause skin coloration or tissue staining, and its clearance rate is rapid enough that repeated injections may be made.

Since the blue dyes show absorption in the red region of the spectrum where the extinction coefficients for oxygenated and reduced hemoglobin are different, the measurement of dye

concentration is subject to inaccuracies if the oxygen saturation is not constant throughout the entire inscription of a dye dilution curve. In 1957, the group at the Mayo Clinic (64) introduced the use of indocyanine green, a dye showing maximal absorption in plasma at 8000 A, an isobestic point for oxygenated and reduced hemoglobin. Thus changes in oxygen saturation do not interfere with the continuous recording of indocyanine green concentration in the blood. It is removed very rapidly by the liver (its half-life is 10 minutes) and it does not cause tissue discoloration. These properties make it particularly suitable for repeated injections.

3. Instruments for Quantitating Dye Concentration

An instrument for the continuous recording of T-1824 concentration in blood withdrawn directly from an artery was first described in 1950 by Friedlich, Heimbecker, and Bing (69). The densitometer employed collimated light, an interference filter with peak transmission at 6280 A, and a photomultiplier. The relationship between optical density and dye concentration was linear for concentrations of T-1824 in whole blood up to 60 mg/liter. Improved densitometers were developed by Gilford et al (71) and by Milnor and his associates (166).

In 1950, Nicholson and Wood reported the use of their bichromatic whole blood cuvette oximeter to measure T-1824

concentration. The relationship between recorder deflection and dye concentration was not linear (174). This is to be expected since wide band filters and a non-plane parallel cuvette were used, and transmitted intensity rather than optical density was recorded. The infrared sensitive photocell has been used to measure indocyanine green concentration in nonhemolyzed blood; again a nonlinear calibration curve was obtained (67).

Edwards, Isaacson, Sutterer, Bassingthwaighte, and Wood (56) presented results obtained with a Waters XC100A interference filter densitometer, which employs a photodiode tube as detector. Calibration curves of indocyanine green in whole nonhemolyzed blood plotted against optical density showed deviations from Beer's law of 6% to 8% over the range from 0 to 30 mg/liter of blood. The slope of the calibration curve decreased as background dye increased; a rather complicated method of zero suppression was developed to compensate for this decrease. The calibration curves for blood samples with hematocrits ranging from 32% to 76% were very similar, but the slope of the calibration curve was somewhat lower for hematocrits of 15% and 19%.

In 1961, McGregor, Sekelj, and Adam (157), using the whole blood cuvette oximeter described in Chapter IV, obtained a linear relationship between cuvette oximeter output and

Coomassie blue dye concentration in nonhemolyzed blood up to 100 mg/liter plasma. This instrument employs diffuse incident light, interference filters, and selenium barrier layer photocells in series with a low external resistance.

Reflection oximetry techniques have also been applied to the continuous recording of dye concentration. Enson, Briscoe, Polanyi, and Cournand (58) used their intravascular reflection oximeter to measure indocyanine green concentration. Interference filters and a photomultiplier were used. The ratio of intensities of diffusely reflected light at 9000 A and at 8050 A showed a linear relationship with indocyanine green dye below 10 mg/liter of blood, and was independent of hematocrit at the two values tested, 38.5% and 46.6%. The second wavelength, 9000 A, at which indocyanine green shows no appreciable absorption, was introduced to compensate for pulsatile flow.

4. Absorbing Properties of Dyes in Solution

Ideally, in order to quantitate dye dilution curves, the relationship between optical density and dye concentration should be linear. Apart from the properties of the measuring system, nonlinearity may result from the properties of the dye or of the blood. Strict adherence to Beer's law is obtained only under highly restricted conditions. Even with an ideal measuring system which employs monochromatic light

and responds linearly to optical density, a solution of dye may deviate from Beer's law.

The absorption spectrum of a dyestuff usually depends to some extent on the nature of the solvent. It is well known that, while most dyes obey Beer's law in dilute aqueous solutions, many show deviations as concentration is increased (204). This is particularly evident in the case of the thyazine dyes, of which methylene blue is a good example. As concentration is increased, an absorption band on the shorter wavelength side of the principal band becomes stronger while the principal band becomes weaker (Fig. 11.1). This is thought to be due mainly to a reversible polymerization of the dye molecules, with the principal band at 6550 A due to absorption by monomers, and the beta band arising at 6150 A due to absorption by dimers; the phenomenon is somewhat more complicated due to the presence of higher polymers (161). The same phenomenon occurs when the temperature is reduced (204). On the other hand, the azo dyes, such as T-1824 and Coomassie blue, show no very noticeable spectral anomalies in aqueous solution (204).

Studies of the absorption spectra of dyes in plasma have shown that another kind of anomaly occurs in this medium, even in dyes which obey Beer's law in aqueous solution. Compared with aqueous solutions, the absorption peak

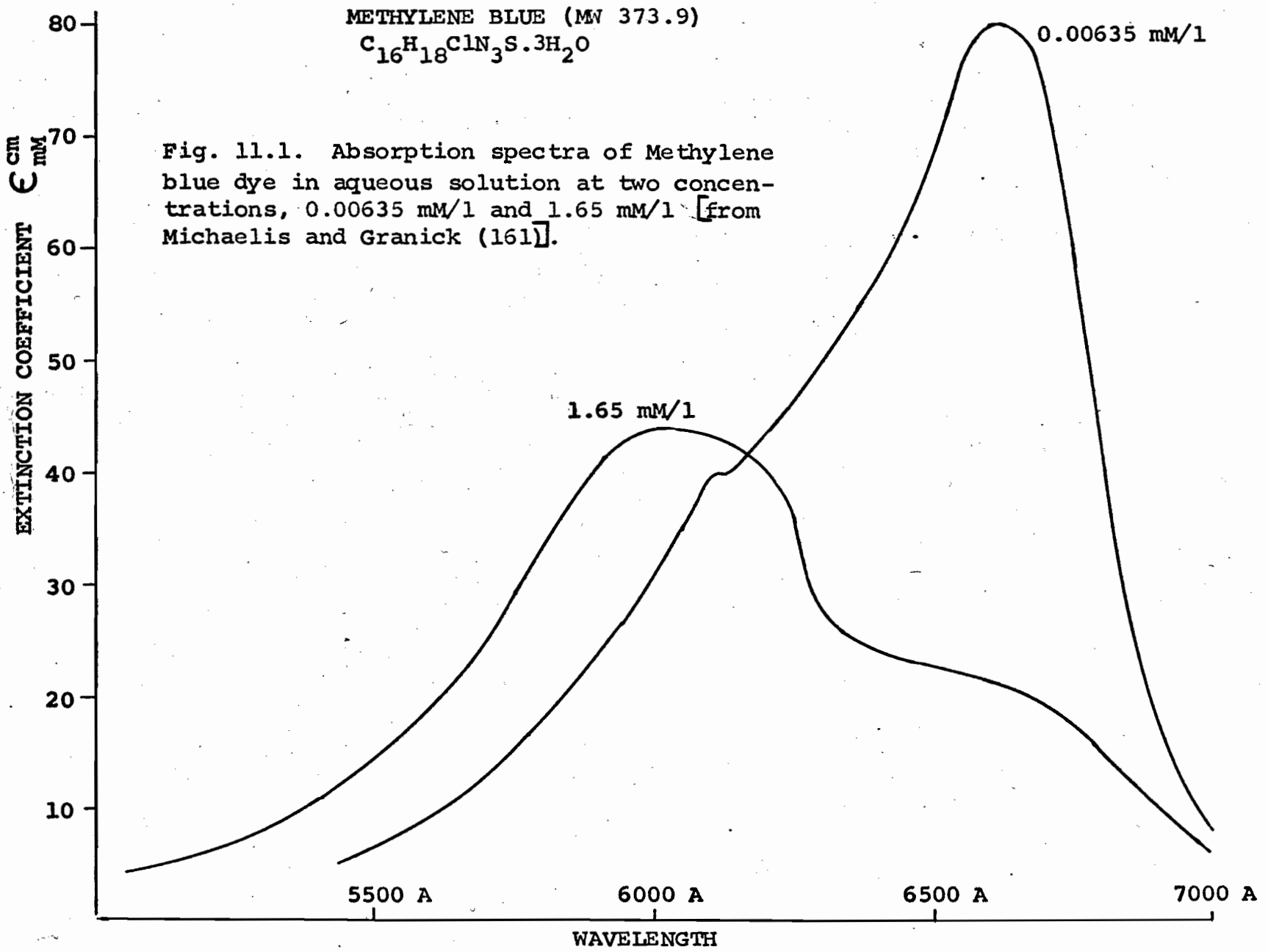

Fig. 11.1. Absorption spectra of Methylene blue dye in aqueous solution at two concentrations, 0.00635 mM/1 and 1.65 mM/1 [from Michaelis and Granick (161)].

is reduced in plasma and is shifted about 250 A towards longer wavelengths (65, 66, 75). This behaviour is due to the binding of the dye particles to the plasma proteins, particularly the albumin fraction; this results in discrete aggregates of dye rather than in a homogeneous solution. Rawson (182) performed quantitative studies on the conversion of free dye to protein and found that each mole of albumin can bind a maximum of 8 to 14 moles of T-1824.

Gregersen and Gibson (75) found that solutions of dye in NaCl also showed reduced absorption; however, the addition of NaCl to plasma produced no further depression of optical density beyond that due to the plasma alone. Changes in pH from 7.0 to 7.7 had no effect on the absorption of T-1824. Fox and Wood (66) demonstrated that indocyanine green showed no differences in absorption when pH was varied from 6 to 9.

The absorption spectra of methylene blue, T-1824, and Coomassie blue are shown in Figures 11.1, 11.2, and 11.3.

5. Absorbing Properties of Dyes in Scattering Media

The spectral anomalies discussed so far have been observed when the dye was dissolved in a nonscattering medium. In the estimation of cardiac output by dye dilution techniques, the measurement of dye concentration is further complicated by the phenomenon of multiple light scattering, caused by the presence of red cells in the blood.

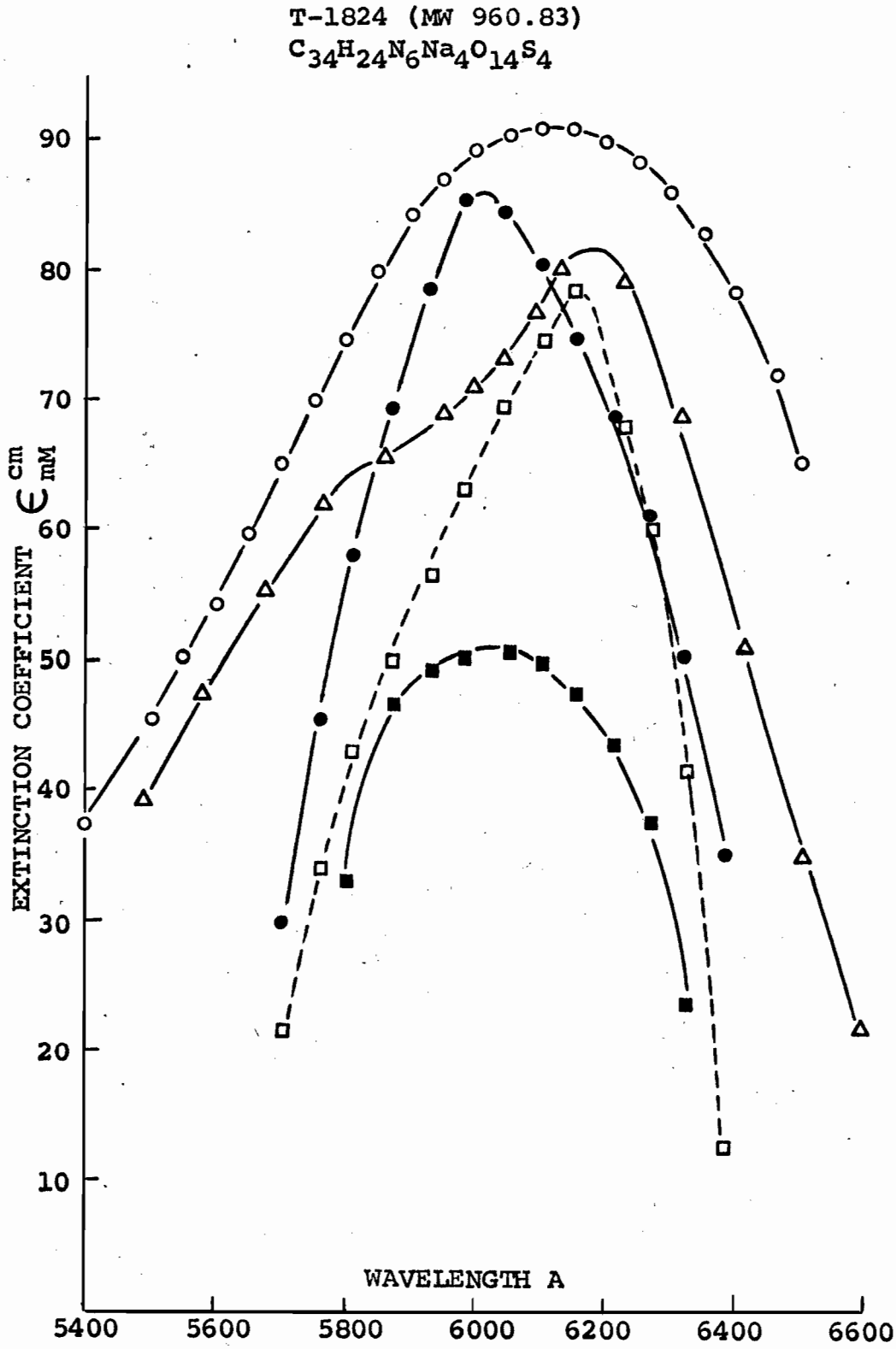

Fig. 11.2. Absorption spectra of T-1824 in phosphate buffer (● , pH 7.3), 0.9% NaCl (o), plasma (Δ), albumin (■ , 0.8 gm/100 ml), albumin (□ , 68.9 gm/100 ml), [from Rawson (182)].

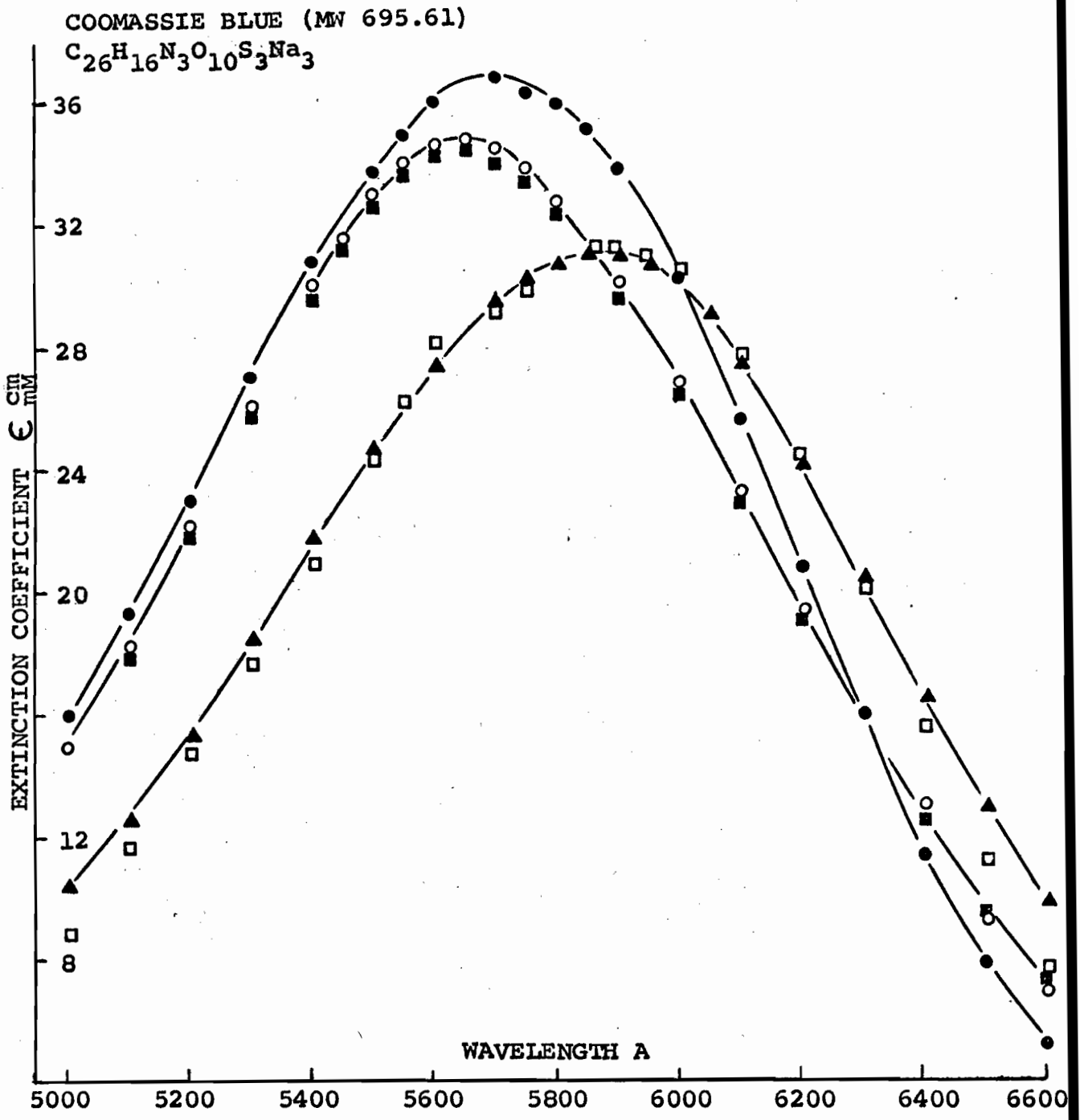

Fig. 11.3. Absorption spectra of solutions of Coomassie blue dye in water (●), 0.9% NaCl (○), plasma (▲), 9.0% NaCl (■), and hemolyzed blood (□). Data were obtained using the Beckman DU spectrophotometer.

The theory underlying the transmittance of nonhemolyzed blood containing dye has received little attention in the literature. We are faced with the problem of a mixture of two pigments - hemoglobin and dye; the hemoglobin is situated within the dispersed, scattering phase, and the dye pigment is present in the continuous phase.

Somewhat simpler systems - that is, ones in which the dispersed scattering phase shows no absorption - have been studied. In 1939, Drabkin and Singer (52) measured the optical density of a mixture consisting of scattering, nonabsorbing particles suspended in an absorbing solution. The scattering material was composed of milk or cream fat particles and was suspended in a very dilute solution of hemoglobin (about 0.06 gm/100 ml). This is essentially the antithesis of nonhemolyzed blood, where the pigment is inside the particles, and the suspending medium (plasma) is nonabsorbing. These authors measured the optical density of the scattering particles and of the dilute hemoglobin solutions separately, from 5000 A to 6300 A, and found that the sum of the optical densities was equal to the measured optical density of the mixture of fat particles and hemoglobin solution.

In contrast to this finding, Keilin and Hartree (120) found that absorption bands of solutions of hemoglobin

derivatives and of didymium salts in water and in aqueous glycerol were intensified when measured in the presence of scattering media such as kieselguhr, and at liguid air temperatures where the solvent became a white crystalline mass and was, therefore, highly turbid and light scattering. They suggested that the effective optical depth through the absorbing, continuous medium was increased due to multiple reflections, resulting in an increase in the light absorbed by the pigment.

In 1962, Butler and Norris (30) pursued this idea. The nonabsorbing scattering materials used were calcium carbonate with particles of approximately 10 microns, aluminum oxide powders with particle sizes of one micron and less, and polystyrene latexes with particle sizes of 0.09 to 1.17 microns. Absorbing pigments were solutions of reduced cytochrome c, rose bengale, and the sodium salt of copper chlorophyllin. They reaffirmed the observations of Keilin and Hartree, that absorption was intensified when scattering particles were added to solutions of pigments.

The quantitation of dye concentration in nonhemolyzed blood raises two questions. The first is whether a dye which obeys Beer's law in clear solution continues to exhibit a linear relationship between optical density and dye concentration in the presence of nonhemolyzed red blood cells. The

empirical studies described in Section A.2 of this chapter showed that the relationship between concentration and optical density is linear at least at relatively low concentrations of T-1824, Coomassie blue, and indocyanine green dye in whole nonhemolyzed blood, provided monochromatic light is used. Second, assuming that the relationship between optical density and dye is linear, does the extinction coefficient of the dye in the presence of red blood cells differ from the extinction coefficient in clear solution? In view of the experiments of Keilin and Hartree and of Butler and Norris, in which absorption was increased when scattering particles were added to pigment solutions, it is possible that red blood cells produce a similar effect on the extinction coefficient of dye. The results of Edwards et al (56) showed higher extinction coefficients for indocyanine green when the hematocrit was over 30% than when the hematocrit was less than 20%.

We decided to investigate the validity of Beer's law for Coomassie blue dye in the presence of scattering particles in two ways. First, we attempted to establish that the relationship between optical density and concentration is linear, using the cuvette oximeter and the integrating sphere. Second, using the integrating sphere, we investigated the dependence of the extinction coefficient of Coomassie blue on hematocrit.

B. Material and Methods

Preliminary experiments were carried out using the cuvette oximeter with the first light source, as described in Chapter IV. To investigate the validity of Beer's law for aqueous solutions of various dyes, measurements were made on clear solutions of methylene blue, T-1824, and Coomassie blue in 0.9% NaCl. Measurements were also made on Coomassie blue in plasma, in hemolyzed blood, and in nonhemolyzed blood. All blood samples were fully oxygenated before the dye was added.

To demonstrate the necessity of using monochromatic light in order to obtain a linear relationship between optical density and dye concentration, a wide band Wratten 29 gelatin filter was substituted for the interference filter, and measurements were made on both aqueous solutions of dye and dye in nonhemolyzed blood.

Final experiments were performed using the cuvette oximeter with the improved light source which was described in Chapter V. Measurements were made on Coomassie blue dye in nonhemolyzed blood using both diffuse and collimated incidence.

Measurements were made at a sample depth of 0.071 cm. The instrument was standardized to read zero optical density on blood containing no dye. Optical density readings corre-

spond to changes due to the presence of dye only.

Further experiments were carried out using the Beckman DU spectrophotometer with the integrating sphere attachment. Measurements were made on Coomassie blue dye in nonhemolyzed blood and in the aqueous phase of emulsions of n-butyl benzoate. Measurements were made at a sample depth of 0.025 cm. The instrument was standardized to read zero optical density on distilled water. The optical density changes due to dye were obtained by subtracting the optical density of the blood, before the dye was added, from the optical density of the blood containing dye.

C. Results

1. Preliminary Experiments

Using diffuse incident light and an interference filter with maximum transmittance at 6330 A, the optical densities of methylene blue, T-1824, and Coomassie blue in 0.9% NaCl were measured at various dye concentrations. Fig. 11.4 shows optical density plotted against dye concentration for each of the three dyes. It may be seen that Coomassie blue and T-1824 both obey Beer's law (with extinction coefficients of 18.2 and 22.2, respectively) as expected, since these are azo dyes; the thiazine dye, methylene blue, shows deviation from linearity. The relationship between optical density

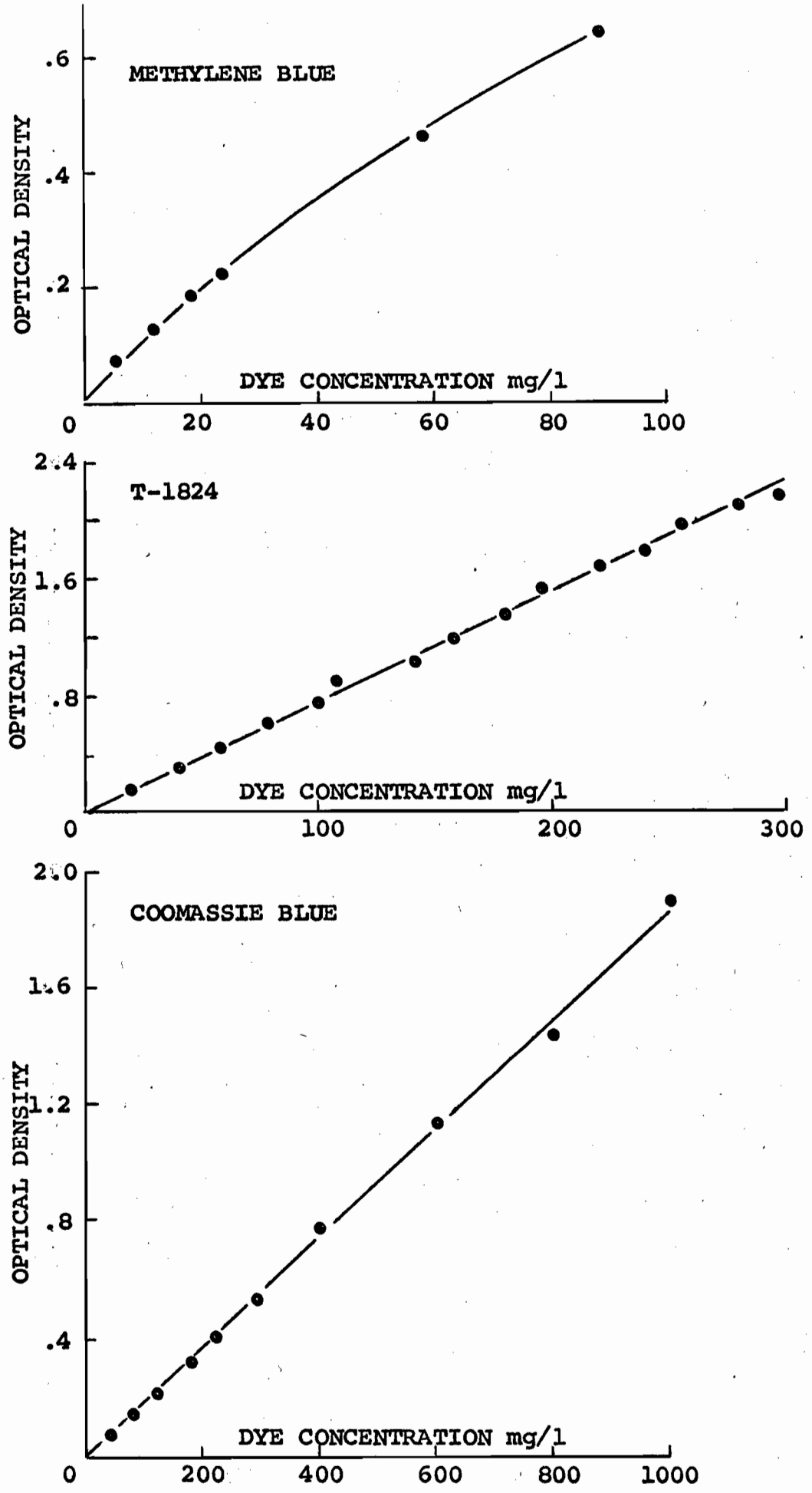

Fig. 11.4. Preliminary experiments. Relationship between optical density and dye concentration for solutions of methylene blue, T-1824, and Coomassie blue in 0.9% NaCl.

and Coomassie blue concentration was linear up to 1000 mg/liter in 0.9% NaCl.

Fig. 11.5 shows the relationship between the optical density due to dye and the concentration of Coomassie blue dye in plasma, in hemolyzed whole blood, in 0.9% NaCl, and in the two nonhemolyzed whole blood samples with the maximum and minimum hematocrits studied. The extinction coefficient of the dye is the slope of this line divided by the sample depth $\left[\epsilon = (OD/c)(1/d)\right]$. The extinction coefficients of Coomassie blue in these media are shown in Table 11.1. It may be seen that ϵ in plasma (18.71) and in hemolyzed blood (17.99) is approximately the same as it is in isotonic saline (18.17). However, it is considerably increased in nonhemolyzed blood where it may also be noted that there is a trend towards increasing ϵ with increasing hematocrit. In the hematocrit range from 27.5% to 49%, ϵ varied from 23.7 to 34.5. In 14 samples, the correlation coefficient for ϵ and hematocrit was 0.57.

A wide band gelatin filter was substituted for the monochromatic interference filter. Results obtained on isotonic saline solutions and nonhemolyzed blood containing Coomassie blue dye are shown in Fig. 11.6. The relationship between dye concentration and optical density was nonlinear in both saline and in nonhemolyzed blood; this result is not surprising

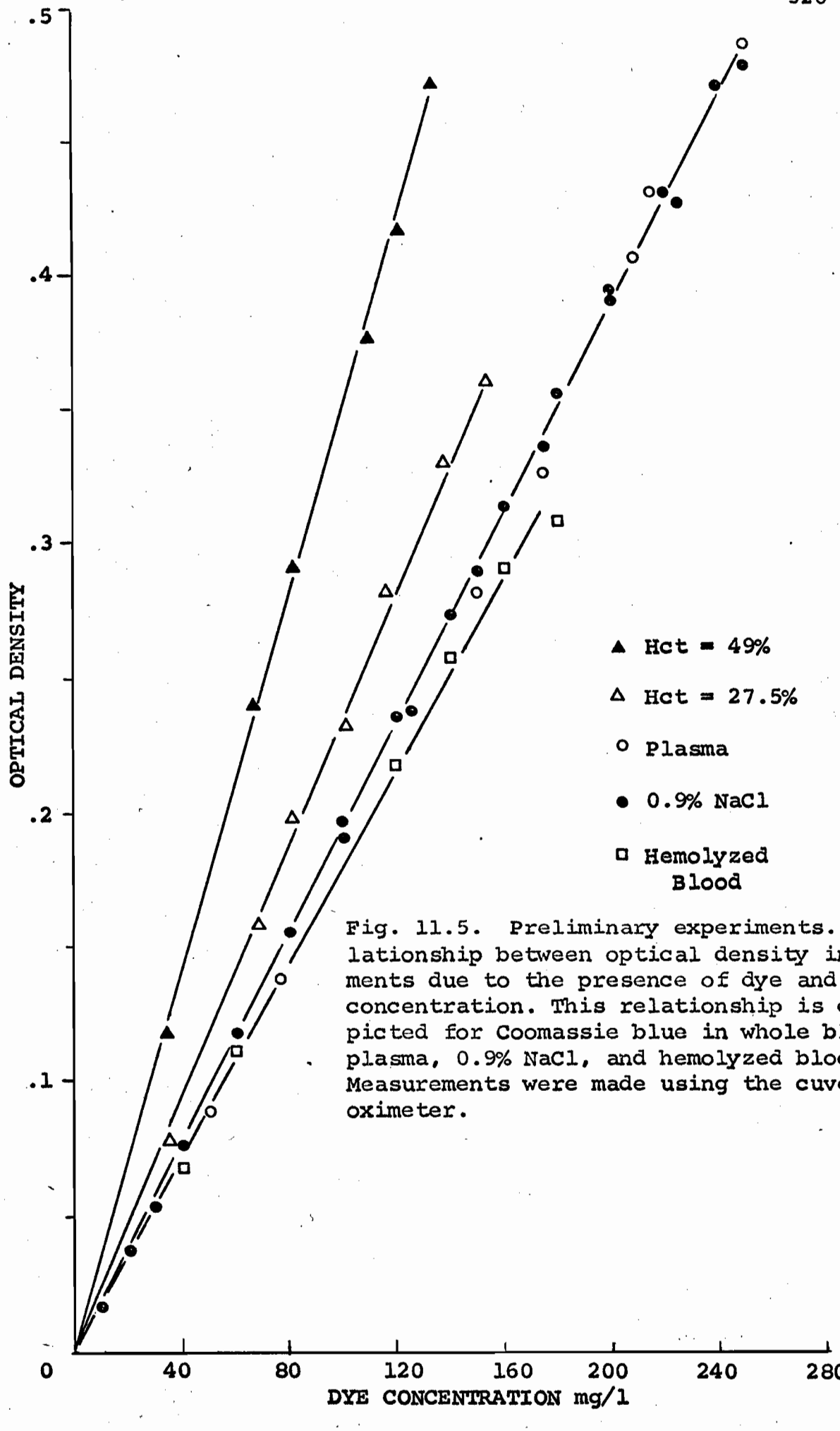

Fig. 11.5. Preliminary experiments. Relationship between optical density increments due to the presence of dye and dye concentration. This relationship is depicted for Coomassie blue in whole blood, plasma, 0.9% NaCl, and hemolyzed blood. Measurements were made using the cuvette oximeter.

TABLE 11.1. Extinction coefficients for Coomassie blue dye

Incident Illumination	Hematocrit or Concentration (%)	Extinction Coefficient					
		Suspending Material					
		Nonhemolyzed Blood	Hemolyzed Blood	Plasma	0.9% NaCl	H_2O	Emulsion
Preliminary Experiments, Cuvette Oximeter							
Diffuse			18.0	18.7	18.2		
	49.0	34.5					
	49.0	31.6					
	47.0	34.8					
	45.7	33.4					
	45.7	30.2					
	44.6	33.6					
	44.0	31.6					
	41.6	33.6					
	39.1	28.0					
	37.5	31.6					
	37.5	30.5					
	33.6	31.6					
	33.0	33.6					
	27.5	23.7					
		r = 0.57					
Final Experiments, Cuvette Oximeter							
Diffuse					17.5		
	46.1	33.3					
	27.8	31.5					

TABLE 11.1. Continued

Incident Illumination	Hematocrit or Concentration (%)	Extinction Coefficient: Suspending Material: Nonhemolyzed Blood	Hemolyzed Blood	Plasma	0.9% NaCl	H_2O	Emulsion
	27.1	31.3					
	14.8	31.5					
		r = 0.64					
Collimated	46.1	31.3					
	27.1	28.9					
Final Experiments, Integrating Sphere							
					14.8	15.5	
	60.9	23.1					
	35.0	21.5					
	32.5	23.1					
	27.1	21.5					
		r = 0.44					
	53.4[a]	29.1					
	44.3	28.6					
	38.6	28.0					
	28.4	27.2					
	21.3	26.7					
	12.6	26.2					
		r = 0.86					

TABLE 11.1. Continued

Incident Illumination	Hematocrit or Concentration (%)	Extinction Coefficient					
		Suspending Material					
		Nonhemolyzed Blood	Hemolyzed Blood	Plasma	0.9% NaCl	H_2O	Emulsion
	3.0						22.0
	2.4						20.7
	1.8						19.2
	1.5						18.7
	1.2						18.2
	0.6						16.7
							r = 0.83

[a]This series of experiments was carried out using blood from one donor only.

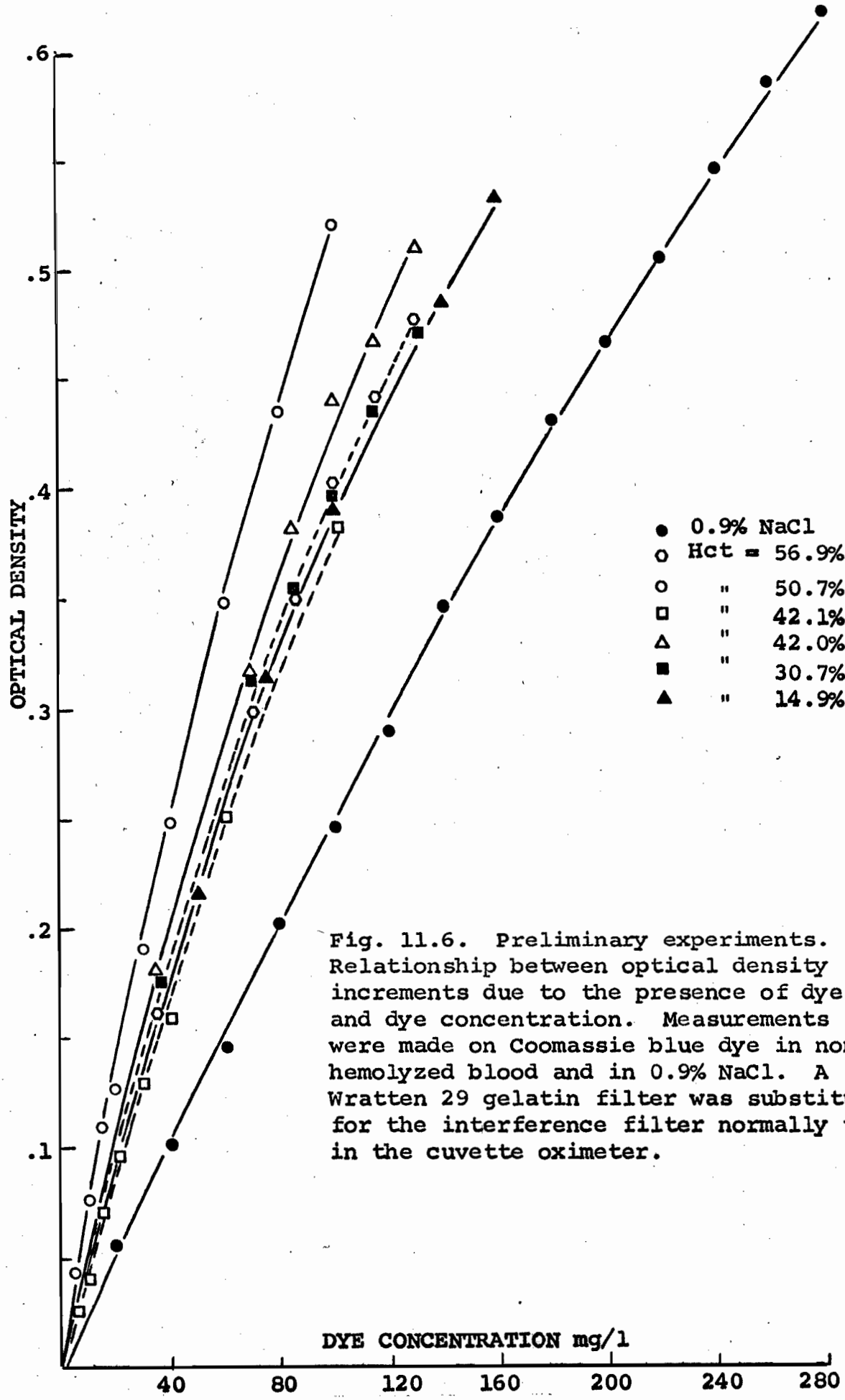

Fig. 11.6. Preliminary experiments. Relationship between optical density increments due to the presence of dye and dye concentration. Measurements were made on Coomassie blue dye in non-hemolyzed blood and in 0.9% NaCl. A Wratten 29 gelatin filter was substituted for the interference filter normally used in the cuvette oximeter.

since Beer's law is valid only if monochromatic light is used. The trend towards increasing ϵ with increasing hematocrit was not observed.

2. Final Experiments

Measurements were made first with diffuse incidence and then with collimated incident light. The results (Fig. 11.7) show that the relationship between dye concentration and optical density was linear with both types of incidence. However, it is interesting to observe that the extinction coefficients for Coomassie blue were slightly lower when collimated incidence, rather than diffuse incidence was used (Table 11.1). There was a trend towards increased ϵ with increasing hematocrit ($r = 0.64$).

3. Integrating Sphere Experiments

The experiments performed on the integrating sphere at a sample depth of 0.025 cm showed that the relationship between optical density and dye concentration remained linear at least up to 285 mg/liter Coomassie blue in nonhemolyzed blood as shown in Fig. 11.8. Extinction coefficients are shown in Table 11.1 along with the extinction coefficient for Coomassie in isotonic saline at 6330 A. In blood, ϵ varied only from 21.50 to 23.08 ($r = 0.44$). The lack of a high degree of correlation between ϵ and hematocrit in our studies and

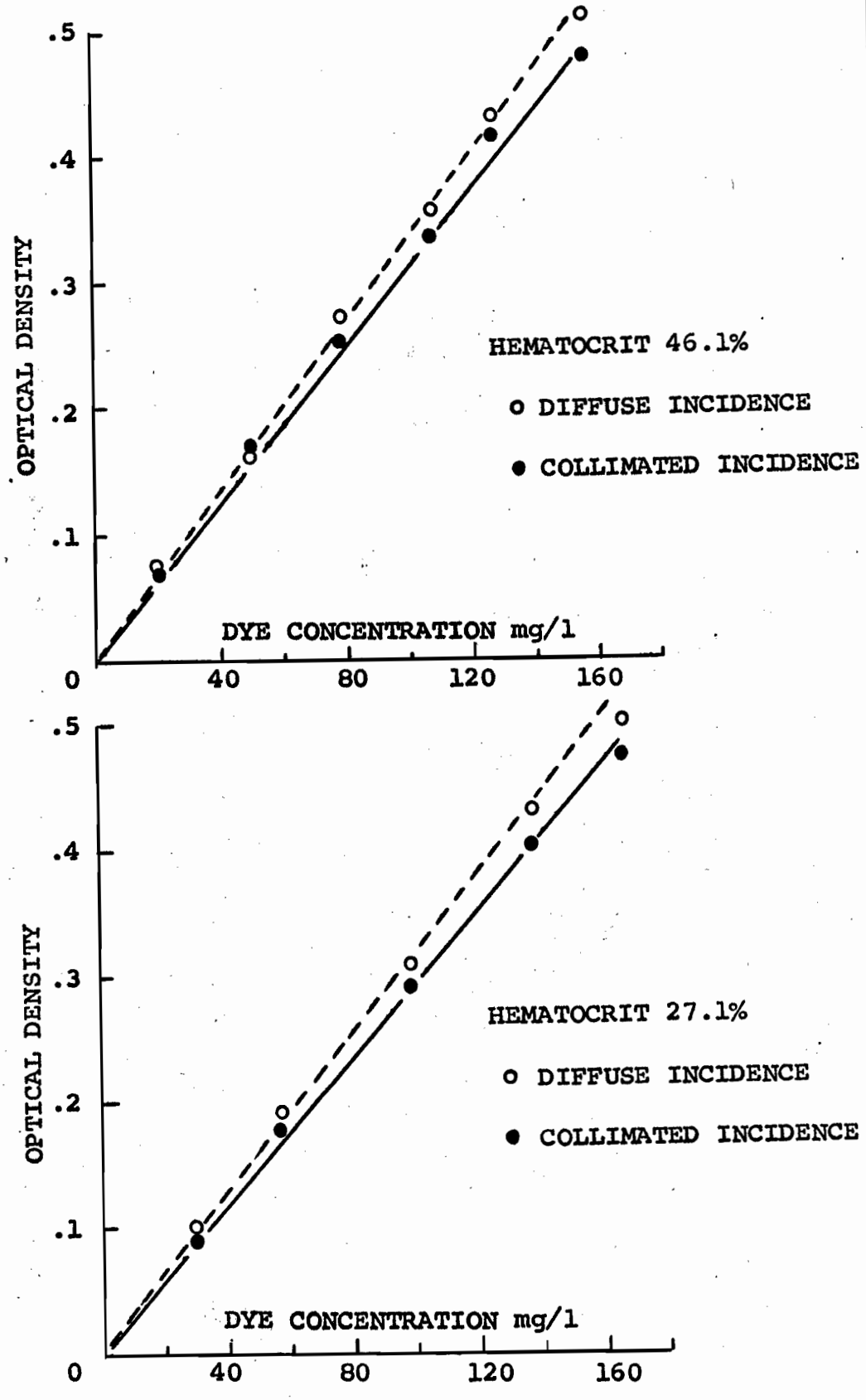

Fig. 11.7. Final experiments. Relationship between optical density increments due to Coomassie blue dye and dye concentration in nonhemolyzed blood, at two hematocrits. Measurements were made using diffuse incidence and collimated incidence.

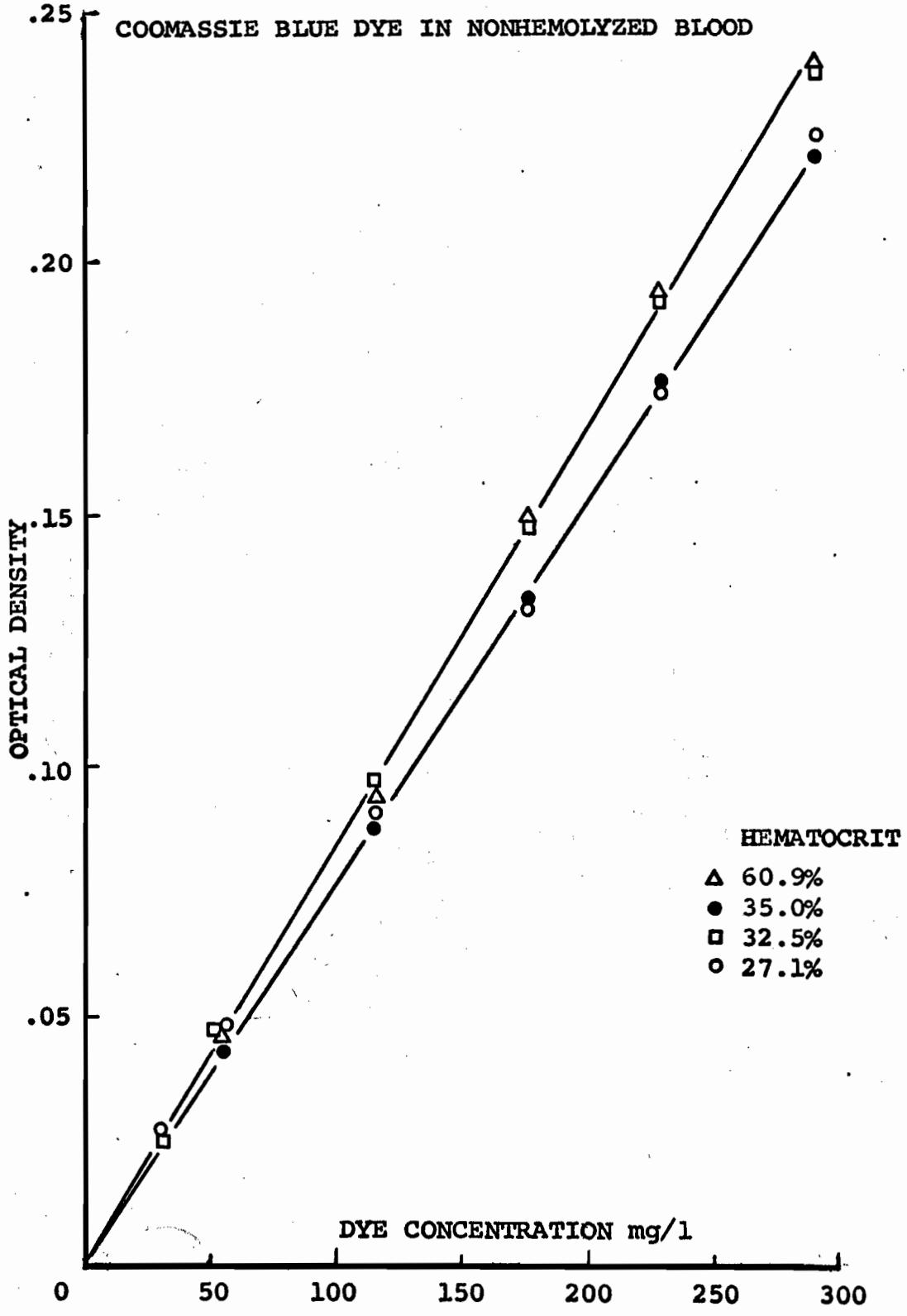

Fig. 11.8. Integrating Sphere: relationship between optical density increments due to Coomassie blue dye and dye concentration in nonhemolyzed blood, at four hematocrits.

those of Edwards et al (56) suggested that experimental error and small differences in blood samples from different donors may disguise this phenomenon.

To investigate more fully the relationship between ϵ and hematocrit, further experiments were performed. The extinction coefficient of Coomassie blue dye in blood samples of various hematocrits, prepared from whole blood from one donor only, were measured. The results of this series of experiments are shown in Fig. 11.9, where ϵ is plotted against hematocrit. The correlation coefficient between ϵ and hematocrit was 0.83.

A similar experiment was performed on Coomassie blue in emulsions of n-butyl benzoate. The dye remains in the continuous aqueous phase and the emulsified droplets constitute the nonabsorbing scattering phase. Again, ϵ increased with increasing concentration of scattering particles (Fig. 11.10, $r = 0.86$). In this case, the magnitude of the increase was much greater. In distilled water, ϵ was 15.5; in a 3% emulsion of n-butyl benzoate, ϵ increased to 22. For comparison, the results of Figures 11.9 and 11.10 were plotted on the same graph (Fig. 11.11). The common abscissa is the percent of the total volume occupied by the scattering particles, which, in the case of blood, is the hematocrit. ϵ increased much more rapidly when the concentration of the emulsified droplets was increased than when the concentration of red cells

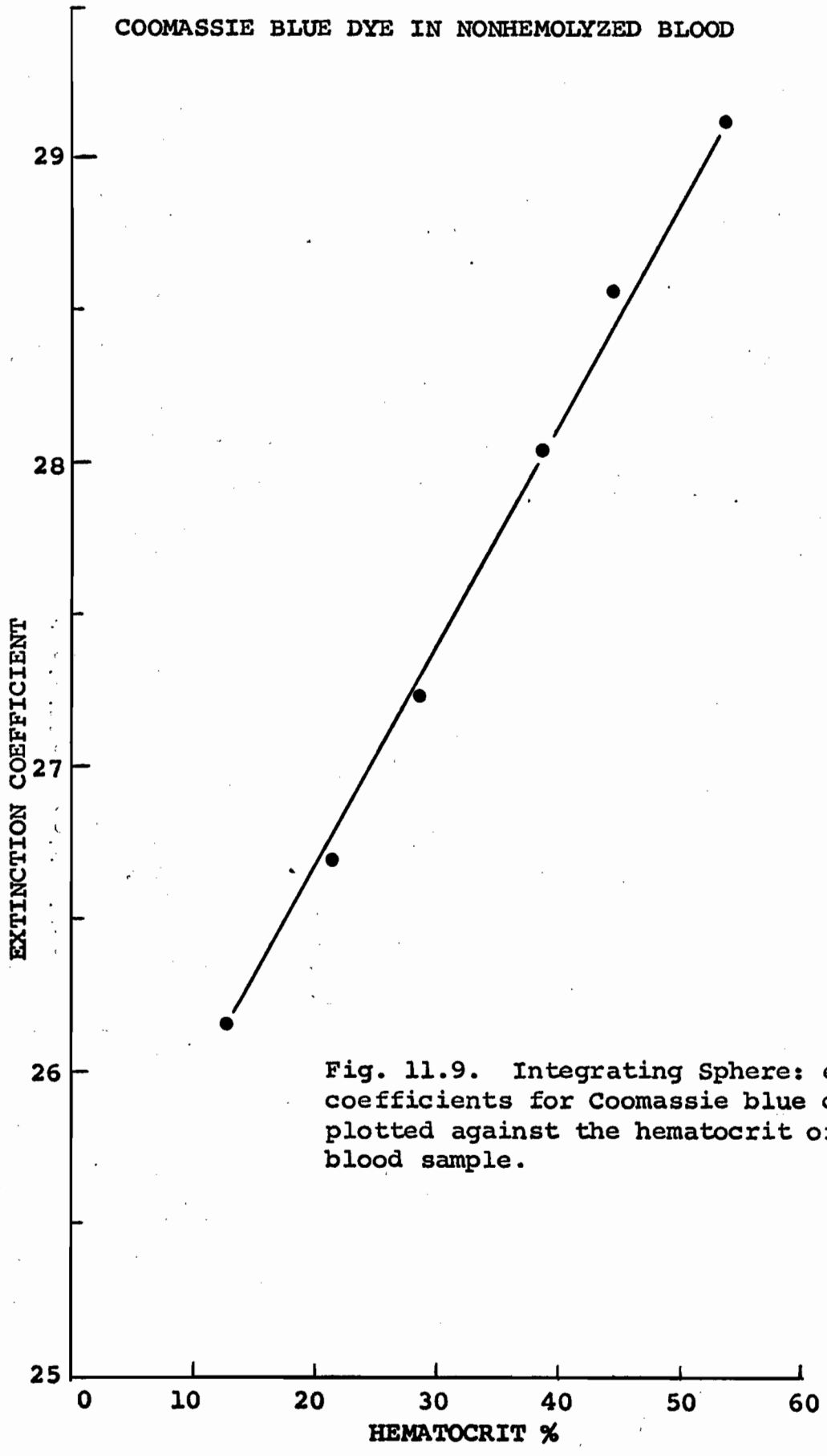

Fig. 11.9. Integrating Sphere: extinction coefficients for Coomassie blue dye are plotted against the hematocrit of the blood sample.

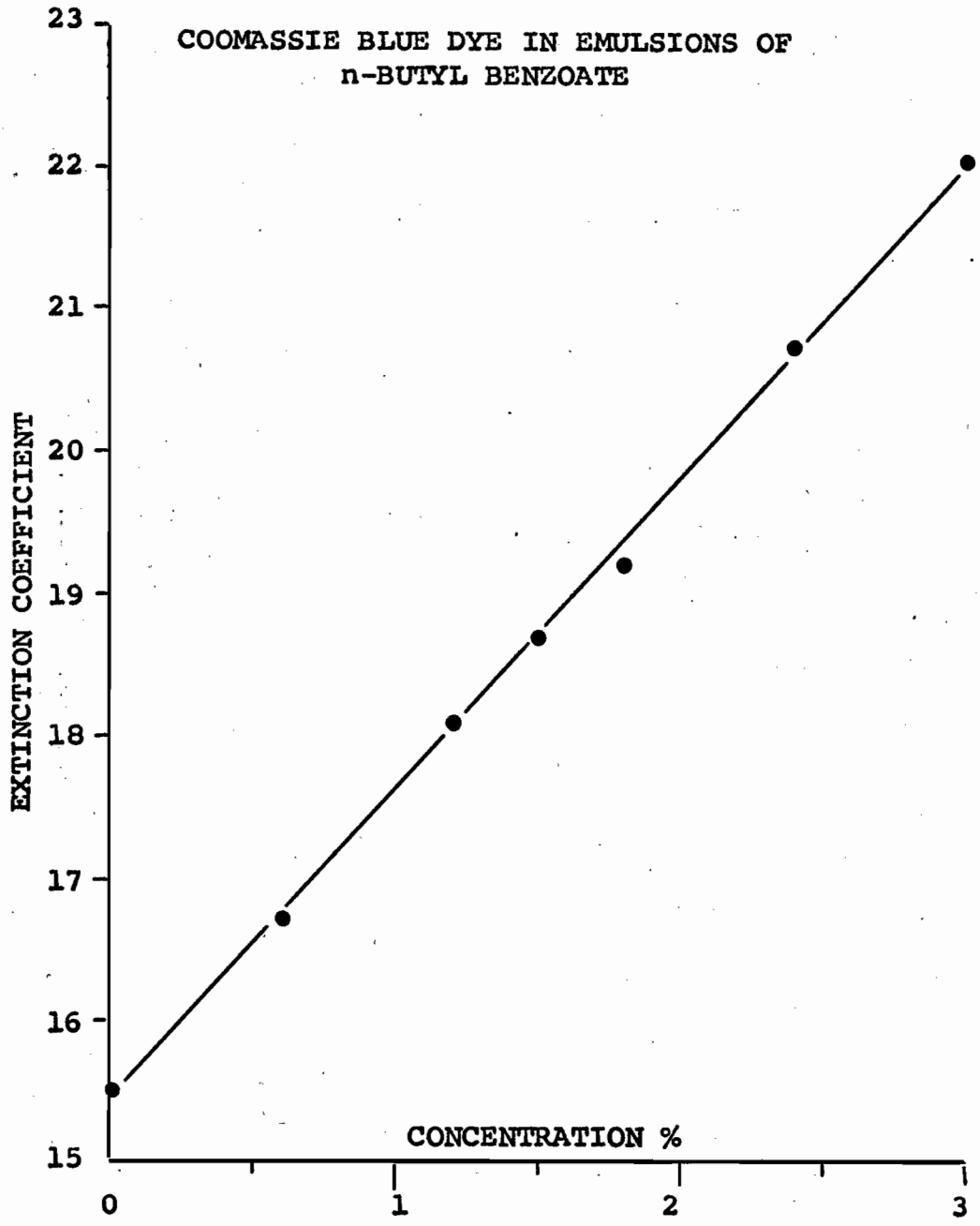

Fig. 11.10. Integrating Sphere: extinction coefficients for Coomassie blue dye are plotted against the concentration of n-butyl benzoate in the emulsions.

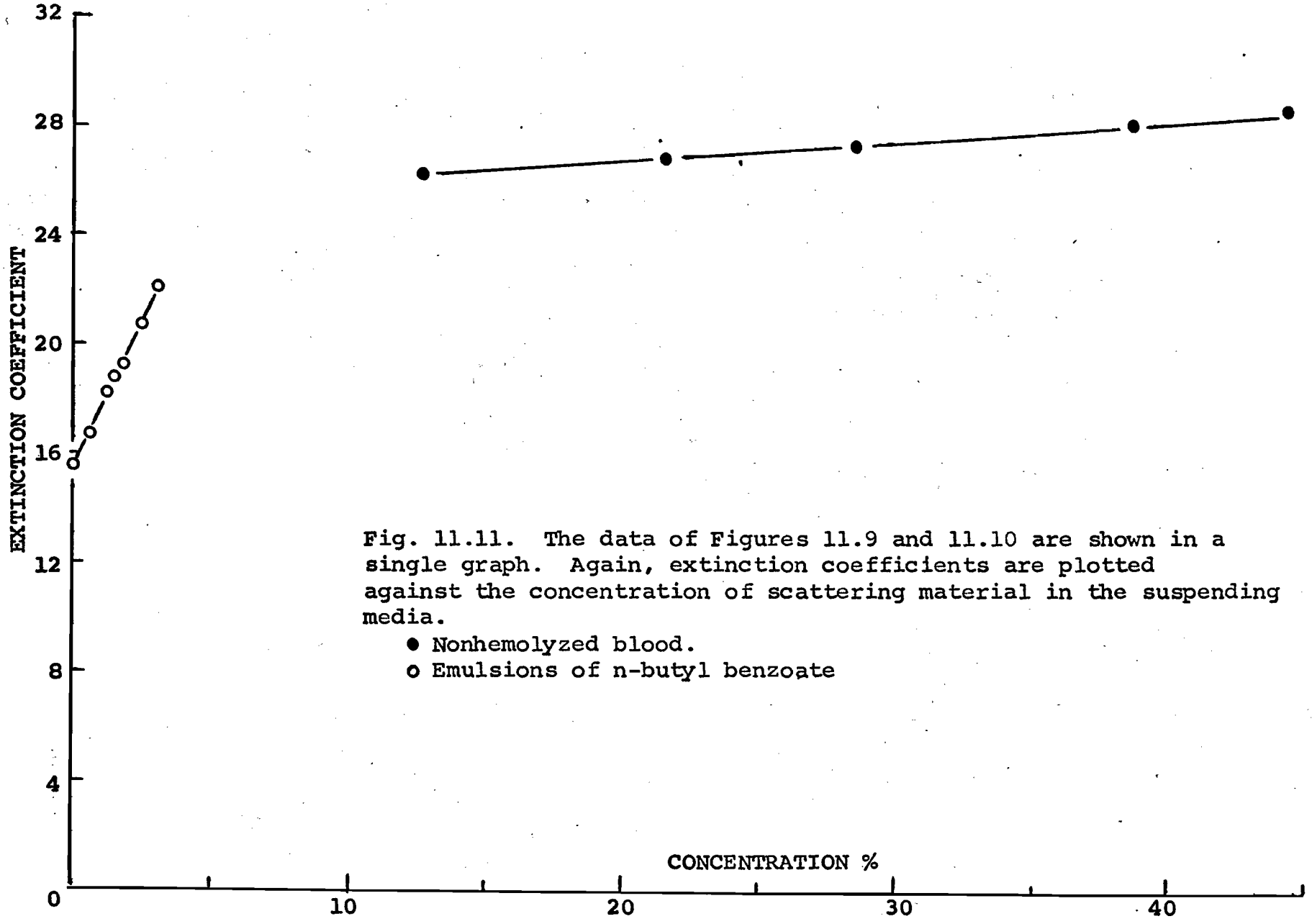

Fig. 11.11. The data of Figures 11.9 and 11.10 are shown in a single graph. Again, extinction coefficients are plotted against the concentration of scattering material in the suspending media.

● Nonhemolyzed blood.

o Emulsions of n-butyl benzoate

was increased. The two apparent differences between these two suspensions are in particle size and light absorption: the red blood cells are about 8 microns in diameter and absorb light; the emulsified droplets are about 1 to 4 microns in diameter and do not absorb light. Perhaps either or both of these factors contribute to the difference in the behaviour of ϵ in blood and in the emulsion.

D. Conclusions

The relationship between optical density and dye concentration in nonhemolyzed blood was linear if monochromatic light is used. Using the cuvette oximeter, this relationship was linear for Coomassie blue dye concentrations up to 150 mg/liter in whole nonhemolyzed blood. This linear relationship was confirmed in the integrating sphere for dye concentrations up to 285 mg/liter in whole blood. In the cuvette oximeter a linear relationship was obtained using both collimated and diffuse incident light for Coomassie blue in nonhemolyzed blood up to 140 mg/liter.

Extinction coefficients for Coomassie blue were higher in nonhemolyzed blood than in clear isotonic saline. In nonhemolyzed blood, there was a trend towards increasing ϵ with increasing hematocrit. Using the integrating sphere, ϵ was clearly shown to be directly related to hematocrit. A

10% change in ϵ was measured when hematocrit was varied from 12% to 60%.

Thus, the use of a constant value for the extinction coefficient of indicator dyes in the estimation of cardiac output introduces a source of error. However, within the normal limits of hematocrit, the error incurred by this assumption amounts to less than 5%. Except in cases of severe anemia or polycythemia, this error is not more than the technical error involved in making up individual calibration curves for each cardiac output estimation in individual subjects.

XII. SUMMARY AND STATEMENT OF CLAIMS TO ORIGINAL CONTRIBUTIONS

A. Summary

A few studies on the transmitting and reflecting properties of nonhemolyzed blood have appeared in the literature. The work was done using conventional spectrophotometric techniques. Using the diffusing plate technique, we confirmed the observations of other investigators on the transmitting properties of nonhemolyzed blood. We reaffirmed the following findings: the validity of Beer's law for hemolyzed blood; the linear relationship between optical density and oxygen content in nonhemolyzed blood at a constant hemoglobin concentration; the nonlinear relationship between optical density and total hemoglobin concentration and sample depth in nonhemolyzed blood. Our results differed in one respect from previous observations; in the present experiments, the lines relating optical density to oxygen content were parallel rather than divergent. This difference was attributed to the collection of a large amount of scattered light - an advantage provided by the diffusing plate technique.

The quantity of scattered light collected is highly dependent on the geometry of the measuring system. Even the diffusing plate technique does not yield absolute values,

but depends, to a much smaller extent than the conventional spectrophotometric techniques do, on the geometrical arrangement and the relative size of the light source, sample chamber, and detector. In order to study the light absorption and scattering of nonhemolyzed blood in terms of a light scattering theory, an integrating sphere, which provides absolute measurements of the quantity of light scattered and transmitted into the forward hemisphere or scattered into the back half space was used.

Due to the high concentration of particles in undiluted blood, multiple scattering occurs. Twersky's theory for the multiple scattering of waves was successfully applied to the light transmission of nonhemolyzed blood. This would be impossible if the lines relating optical density to oxygen content were not parallel.

The successful application of Twersky's theory to nonhemolyzed blood is significant since it enables us to evaluate separately the contributions of absorption and scattering to the total optical density of blood. We were able to show that the relationship between the light absorption by the hemoglobin pigment obeys Beer's law, even when the pigment is encapsulated within the red blood cell. The nonlinearity of the relationship between optical density and the hemoglobin concentration of nonhemolyzed blood is due to the relationship

between scattering and hematocrit. This relationship is parabolic. The appearance of both hemoglobin concentration as well as the fractional volume occupied by the red cells in the equation for optical density derived from Twersky's theory indicates that not only hemoglobin concentration but cell size determine the optical density of nonhemolyzed blood.

The complexity of the relationship between the extinction coefficient of hemoglobin, and thus the oxygen saturation of the hemoglobin, and optical density demonstrates why the previously used oximetric techniques of relating the ratio of the optical density values of nonhemolyzed blood at two wavelengths to oxygen saturation, estimated by a reference method, fails to provide accurate results.

The use of Twersky's theory to obtain an expression for oxygen saturation yielded accurate results, but proved impractical, since it required that the hemoglobin concentration of the sample be known.

We obtained a simple empirical equation to describe the nonlinear relationship between the optical density of nonhemolyzed blood and hemoglobin concentration. Using this equation, expressions for the oxygen saturation of nonhemolyzed blood in a one wavelength system and a two wavelength system were derived, resulting in a method of extimating oxygen saturation with a high degree of accuracy. The method

proved to be independent of both oxygen saturation and hemoglobin concentration. The latter point is of particular importance since the most noticeable drawback of previous oximetric techniques, both transmission and reflection methods, was their inadequacy at low hemoglobin concentrations. Unlike previous oximetric techniques, the method described in Chapter IV does not require calibration against reference techniques. Calibration is analogous to the calibration for the theoretically sound spectrophotometric technique for hemolyzed blood.

Studies of the reflectance of thin layers of nonhemolyzed blood confirmed previous observations that absorption and reflection are inversely related. An important new finding, that reflection and transmission are linearly related at a constant hemoglobin concentration, demonstrated that reflection is exponentially related to the extinction coefficient of hemoglobin. This point has been the subject of some controversy in the field of reflection oximetry.

Studies on Coomassie blue dye in nonhemolyzed blood showed that, provided monochromatic light is used, the relationship between dye concentration and optical density is linear. However, the extinction coefficient of the dye shows a slight increase as the concentration of scattering particles in the suspension is increased.

The successful application of a light scattering theory to nonhemolyzed blood provides us with an explanation for the deviations from Beer's law exhibited by nonhemolyzed blood.

B. Claims to Original Contributions

1. An integrating sphere was used to measure the transmittance and reflectance of undiluted nonhemolyzed blood; this is the first time an absolute method of measurement has been applied to nonhemolyzed blood.

2. An expression was derived from a scattering theory which was developed by Twersky for the multiple scattering of waves in the microwave region of the electromagnetic spectrum to describe the absorbing and scattering properties of nonhemolyzed blood. The use of this theory made it possible to separate the absorption and scattering contributions to the total optical density.

3. Theoretical equations for estimating oxygen saturation in nonhemolyzed blood were derived using this theory.

4. An empirical equation was developed to describe the relationship between optical density and total hemoglobin concentration. The equation is of sufficient general validity that it may be used to describe results obtained

using the diffusing plate technique, conventional spectrophotometric techniques, and the integrating sphere technique, over a wide range of wavelengths and sample depths.

5. This empirical equation was used to obtain equations for estimating oxygen saturation with a high degree of accuracy. The method requires no comparison with reference techniques. It requires only two optical density readings. The accuracy is much better than that obtained using previous oximetric techniques and is independent of hemoglobin concentration and oxygen saturation.

6. Reflectance studies on thin samples of undiluted nonhemolyzed blood permitted the comparison of the transmittance and reflectance of the same sample. The linear relationship between reflectance and transmittance at constant hemoglobin concentration demonstrated that reflectance is exponentially related to the extinction coefficient of hemoglobin.

BIBLIOGRAPHY

1. Abney, W. de W.: Phot. J. 11: 38, 1887; Phot. J. 13: 2, 1888; J. Soc. Chem. Ind. 9: 722, 1890; J. Soc. Chem. Ind. 10: 18, 1891; cited by Weaver (243).

2. Adams, G. A.: Biochem. J. 32: 646, 1938.

3. Adams, G. A., Bradley, R. C., and A. B. Macallum: Biochem. J. 28: 482, 1934

4. Amesz, J., Duysens, L. N. M., and D. C. Brandt: J. Theoret. Biol. 1: 59, 1961.

5. Amy, L.: Rev. d'Optique 16: 81, 1937.

6. Aron, H. and F. Müller: Z. Physiol. Chem. 50: 443, 1906 - 1907.

7. Austin, J. H. and D. L. Drabkin: J. Biol. Chem. 112: 67, 1935 - 1936.

8. Bachem, A. and C. I. Reed: Amer. J. Physiol. 97: 86, 1931.

9. Barcroft, J.: The Respiratory Function of the Blood (2d ed.; Cambridge, England, Cambridge Univ. Press, 1928), pt. 2 (Haemoglobin), pp. 41 - 50.

10. Bardachzi, F.: Z. Physiol. Chem. 49: 465, 1906.

11. Barer, R.: Science 121: 709, 1955.

12. Barer, R., Ross, K. F. A., and S. Tkaczyk: Nature 171: 720, 1953.

13. Bayliss, L. E.: J. Physiol. 179: 1, 1965.

14. Beer, A.: Ann. Phys. Chem. 84: 37, 1851; Ann. Phys. Chem. 86: 78, 1852.

15. Benesch, R., Benesch, R. E., and G. Macduff: Science 144: 68, 1964.

16. Berzon, R. and E. Schubert: Pflueger Arch. Ges. Physiol. 270: 195, 1959 - 1960.

17. Blevin, W. R. and W. J. Brown: J. Opt. Soc. Amer. 51: 129, 1961.

18. Bouguer, P.: Essai d'Optique sur la Gradation de la Lumière, Paris, 1729 (reprinted in Les Maîtres de la Pensée Scientifique, Paris, Gauthier-Villars et Cie., 1921).

19. Bouguer, P.: Optical Treatise on the Gradation of Light, 1760, Middleton, W. E. K., tr., (Toronto, University of Toronto Press, 1961).

20. Brice, B. A., Halwer, M., and R. Speiser: J. Opt. Soc. Amer. 40: 768, 1950.

21. Brinkman, R. and A. J. H. Wildschut: Acta Med. Scand. 94: 459, 1938.

22. Brinkman, R. and W. G. Zijlstra: Arch. Chir. Neerl. 1: 177, 1949; cited by Rodrigo (190).

23. Broch, O. J., Dahl, H., Haarstad, J., and E. Hatletveit: Scand. J. Clin. Lab. Invest. 14: 66, 1962.

24. Buckley, W. R., and F. Grum: Arch. Derm. 89: 110, 1964.

25. Budde, W.: J. Opt. Soc. Amer. 50: 217, 1960.

26. Bunsen, R. and G. R. Kirchoff: cited by Harrison, Lord, and Loofbourow (88).

27. Burke, J. E. and V. Twersky: J. Res. NBS 68D: 500, 1964.

28. Bürker, K.: in Tigerstedt, R., ed., Handbuch der physiologischen Methodik 2: 68, 1911.

29. Butler, W. L.: J. Opt. Soc. Amer. 52: 292, 1962.

30. Butler, W. L. and K. H. Norris: Arch. Biochem. Biophys. 87: 31, 1960.

31. Butterfield, E. E.: Z. Physiol. Chem. 62: 173, 1909.

32. Butterfield, E. E.: Z. Physiol. Chem. 79: 439, 1912.

33. Butterfield, E. E. and F. W. Peabody: J. Exp. Med. 17: 587, 1913.

34. Callier, A.: Phot. J. 49: 200, 1909; cited by Weaver (243).

35. Chandrasekar, S.: Radiative Transfer (London, Oxford University Press, 1950).

36. Chang, T. M. S.: Science 146: 524, 1964; Chang, T. M. S., MacIntosh, F. C., and S. G. Mason: Canad. J. Physiol. Pharmacol. 44: 115, 1966.

37. Channon, H. J., Renwick, F. F., and B. V. Storr: Proc. Roy. Soc. (London) A 94: 222, 1918.

38. Cherbuliez, E.: Etude Spectrophotométrique du Sang Oxycarboné, Paris, 1890; cited by Newcomer (172).

39. Chu, C. and S. W. Churchill: J. Phys. Chem. 59: 855, 1955.

40. Churchill, S. W., Clark, G. C., and C. M. Sliepcevich: Disc. Far. Soc. 30: 192, 1960.

41. Comroe, J. H., Jr. and P. Walker: Amer. J. Physiol. 152: 365, 1948.

42. Cornwall, J. B., Marshall, D. C., and J. Boyes: J. Sci. Instrum. 40: 253, 1963.

43. Crittenden, E. C.: J. Washington Acad. Sci. 13: 69, 1923.

44. Dawson, A. B., Evans, H. M., and G. H. Whipple: Amer. J. Physiol. 51: 232, 1920.

45. Deibler, G. E., Holmes, M. S., Campbell, P. L., and J. Gans: J. Appl. Physiol. 14: 133, 1959.

46. Dempsey, M. E. and R. H. Wilson: J. Lab. Clin. Med. 43: 791, 1954.

47. Drabkin, D. L.: in Glasser, O., ed., Medical Physics (Chicago, Year Book Publishers, 1950), vol. 2, p. 1039.

48. Drabkin, D. L. and J. H. Austin: J. Biol. Chem. 98: 719, 1932.

49. Drabkin, D. L. and J. H. Austin: J. Biol. Chem. 112: 51, 1935 - 1936.

50. Drabkin, D. L. and J. H. Austin: J. Biol. Chem. 112: 105, 1935 - 1936.

51. Drabkin, D. L. and C. F. Schmidt: J. Biol. Chem. 157: 69, 1945.

52. Drabkin, D. L. and R. B. Singer: J. Biol. Chem. 129: 739, 1939.

53. Duntley, S. Q.: J. Opt. Soc. Amer. 32: 61, 1942.

54. Edwards, E. A. and S. Q. Duntley: Amer. J. Anat. 65: 1, 1939.

55. Edwards, E. A., Finklestein, N. A., and S. Q. Duntley: J. Invest. Derm. 16: 311, 1951.

56. Edwards, A. W. T., Isaacson, J., Sutterer, W. F., Bassingthwaighte, J. B., and E. H. Wood: J. Appl. Physiol. 18: 1294, 1963.

57. Elam, J. O., Neville, J. F., Sleator, W., and W. N. Elam: Ann. Surg. 130: 755, 1949.

58. Enson, Y., Briscoe, W. A., Polanyi, M. L., and A. Cournand: J. Appl. Physiol. 17: 552, 1962.

59. Falholt, W.: Scand. J. Clin. Lab. Invest. 15: 67, 1963.

60. Feinberg, H. and Sister Mary Alma: J. Lab. Clin. Med. 55: 784, 1960.

61. Foldy, L. L.: Phys. Rev. 67: 107, 1945.

62. Fox, I. J.: in Wood, E. H., ed., Symposium on Use of Indicator-Dilution Technics in the Study of the Circulation; Salt Lake City, Utah, Jan., 1961 (New York, Amer. Heart Ass., Monograph No. 4, 1962), p. 381.

63. Fox, I. J.: in Wood, E. H., ed., Symposium on Use of Indicator-Dilution Technics in the Study of the Circulation; Salt Lake City, Utah, Jan., 1961 (New York, Amer. Heart Ass., Monograph No. 4, 1962), p. 447.

64. Fox, I. J., Brooker, L. G. S., Heseltine, D. W., Essex, H. E., and E. H. Wood: Mayo Clin. Proc. 32: 478, 1957.

65. Fox, I. J. and E. H. Wood: J. Lab. Clin. Med. 50: 598, 1957.

66. Fox, I. J. and E. H. Wood: Mayo Clin. Proc. 35: 732, 1960.

67. Fox, I. J. and E. H. Wood: in Glasser, O., ed., Medical Physics (Chicago, Year Book Publishers, 1960), vol. 3, p. 155.

68. Fraunhofer, J.: cited by Harrison, Lord, and Loofbourow (88).

69. Friedlich, A., Heimbecker, R., and R. J. Bing: J. Appl. Physiol. 3: 12, 1950 - 1951.

70. Gamgee, A.: Proc. Roy. Soc. (London) 59: 276, 1895 - 1896.

71. Gilford, S. R., Gregg, D. E., Shadle, O. W., Ferguson, T. B., and L. A. Marzetta: Rev. Sci. Instrum. 24: 696, 1953.

72. Gold, E.: Proc. Roy. Soc. (London) A 82: 43, 1909.

73. Goldie, E. A. G.: J. Sci. Instrum. 19: 23, 1942.

74. Gordy, E. and D. L. Drabkin: J. Biol. Chem. 227: 285, 1957.

75. Gregersen, M. I. and J. G. Gibson: Amer. J. Physiol. 120: 494, 1937.

76. Groom, D., Wood, E. H., Burchell, H. B., and R. L. Parker: Mayo Clin. Proc. 23: 601, 1948.

77. Gross, R. E. and R. Mittermaier: Pflueger Arch. Ges. Physiol. 212: 136, 1926.

78. Gurevič, M.: Phys. Z. 31: 753, 1930.

79. Hadley, L. N. and D. M. Dennison: J. Opt. Soc. Amer. 37: 451, 1947.

80. Hall, F. G.: J. Physiol. 80: 502, 1934.

81. Hall, F. G.: J. Biol. Chem. 130: 573, 1939.

82. Haller, A.: Halleri Elementa Physiologiae, Lausanne, 1761, p. 246; cited by Stewart, G. N.: J. Physiol. 15: 1, 1894.

83. Hamburger, H. J.: Z. Biol. 28: 405, 1891.

84. Handforth, C. P.: Lancet 268: 1252, 1955.

85. Harding, R. H., Golding, B., and R. A. Morgen: J. Opt. Soc. Amer. 50: 446, 1960.

86. Hardy, A. C. and O. W. Pineo: J. Opt. Soc. Amer. 21: 502, 1931.

87. Hari, P.: Biochem. Z. 82: 229, 1917.

88. Harrison, G. R., Lord, R. C., and J. R. Loofbourow: Practical Spectroscopy (New York, Prentice-Hall, 1948).

89. Hartel, W.: Das Licht 10: 141, 1940.

90. Hartman, F. W. and R. D. McClure: Ann. Surg. 112: 791, 1940.

91. Hartridge, H.: J. Physiol. 44: 1, 1912.

92. Hartridge, H. and A. V. Hill: J. Physiol. 48: li, 1914.

93. Henriques, V.: Biochem. Z. 56: 230, 1913.

94. Hering, E.: cited by Fox (62).

95. Herschel, W.: cited by Harrison, Lord, and Loofbourow (88).

96. Hickam, J. B. and R. Frayser: J. Biol. Chem. 180: 457, 1949.

97. Hickam, J. B. and R. Frayser: J. Appl. Physiol. 5: 125, 1952 - 1953.

98. Hodkinson, J. R.: Staub 23: 374, 1963.

99. Holling, H. E., MacDonald, I., O'Halloran, J. A., and A. Venner: J. Appl. Physiol. 8: 249, 1955.

100. Holmgren, A. and B. Pernow: Scand. J. Clin. Lab. Invest. 11: 143, 1959.

101. Hoppe-Seyler, F.: Arch. Path. Anat. Physiol. 23: 446, 1862.

102. Horecker, B. L.: J. Biol. Chem. 148: 173, 1943.

103. Huckabee, W. E.: J. Lab. Clin. Med. 46: 486, 1955.

104. Hüfner, G.: Z. Physiol. Chem. 3: 1, 1879.

105. Hüfner, G.: Arch. Physiol. 18: 130, 1894.

106. Hulbert, E. O.: J. Opt. Soc. Amer. 33: 42, 1943.

107. Hurter, F. and V. C. Driffield: J. Soc. Chem. Ind. 9: 455, 1890; J. Soc. Chem. Ind. 10: 20, 1891; J. Soc. Chem. Ind. 10: 98, 1891; J. Soc. Chem. Ind. 10: 100, 1891; cited by Weaver (243).

108. Jacquez, J. A., Kuppenheim, H. F., Dimitroff, J. M., McKeehan, W., and J. Huss: J. Appl. Physiol. 8. 212, 1955; Jacquez, J. A., Huss, J., McKeehan, W., Dimitroff, J. M., and H. F. Kuppenheim: J. Appl. Physiol. 8: 297, 1955.

109. Jacquez, J. A. and H. F. Kuppenheim: J. Appl. Physiol. 7: 523, 1955.

110. Jacquez, J. A. and H. F. Kuppenheim: J. Opt. Soc. Amer. 45: 460, 1955.

111. Johnston, G. W., Holtkamp, F., and J. R. Eve: Clin. Chem. 5. 421, 1959.

112. Jonxis, J. H. P.: Acta Med. Scand. 94: 467, 1938.

113. Jonxis, J. H. P.: Acta Med. Scand. 115: 425, 1943.

114. Jonxis, J. H. P. and J. H. W. Boeve: Acta Med. Scand. 155: 157, 1956.

115. Jope, E. M.: in Roughton, F. J. W. and J. C. Kendrew, ed., Haemoglobin: Barcroft Memorial Conference; Cambridge, England, June, 1948 (London, Butterworths Scientific Publications, 1949), p. 205.

116. Judd, D. B.: Paper Trade J. 106: 5, 1938.

117. Kay, R. H. and R. V. Coxon: J. Sci. Instrum. 34: 233, 1957.

118. Keilin, D. and E. F. Hartree: Proc. Roy. Soc. (London) B 127: 167, 1939.

119. Keilin, D. and E. F. Hartree: Nature 148: 75, 1941.

120. Keilin, D. and E. F. Hartree: Nature 164: 254, 1949.

121. Keilin, D. and E. F. Hartree: Biochim. Biophys. Acta 27: 173, 1958.

122. Kennedy, R. P.: Amer. J. Physiol. 79: 346, 1926 - 1927.

123. Kinsman, J. M., Moore, J. W., and W. F. Hamilton: Amer. J. Physiol. 89: 322, 1929.

124. Klungsøyr, L. and K. Fr. Støa: Scand. J. Clin. Lab. Invest. 6: 270, 1954.

125. Kottler, F.: J. Opt. Soc. Amer. 50: 483, 1960.

126. Kottler, F.: in Wolf, E., ed., Progress in Optics (Amsterdam, North-Holland Publishing Co., 1964), vol. 3, p. 1.

127. Kramer, K.: Klin. Wschr. 12: 1875, 1933.

128. Kramer, K.: Z. Biol. 95: 126, 1934.

129. Kramer, K.: Z. Biol. 96: 61, 1935.

130. Kramer, K. Pflueger Arch. Ges. Physiol. 238: 91, 1937.

131. Kramer, K., Elam, J. O., Saxton, G. A., and W. N. Elam, Jr.: Amer. J. Physiol. 165: 229, 1951.

132. Kramer, K., Graf, K., and W. Overbeck: Pflueger Arch. Ges. Physiol. 262: 285, 1956.

133. Kramer, K. and F. R. Winton: J. Physiol. 96: 87, 1939.

134. Krogh, A.: J. Physiol. 52: 281, 1919.

135. Krogh, A. and I. Leitch: J. Physiol. 52: 288, 1919.

136. Krüger, F.: Z. Biol. 24: 47, 1888; Z. Biol. 26: 452, 1890.

137. Kubelka, P.: J. Opt. Soc. Amer. 38: 448, 1948.

138. Lambert, J. H.: Photometria, sive de mensura et gradibus luminis, colorum, et umbrae, Augsburg, 1760, tr. into German by Andung, E.: in Ostwald, Klassiker der exakten Wissenschaften (Leipzig, W. Engelmann, 1892), nos. 31 - 33; cited by Drabkin (47).

139. Lambertsen, C. J., Bunce, P. L., Drabkin, D. L., and C. F. Schmidt: J. Appl. Physiol. 4: 873, 1952.

140. Latimer, P.: Plant Physiol. 34: 193, 1959.

141. Lax, M.: Rev. Mod. Phys. 23: 287, 1951.

142. Lefevre, P. G. and M. E. Lefevre: J. Gen. Physiol. 35: 891, 1952.

143. Letsche, E.: Z. Physiol. Chem. 76: 243, 1911 - 1912.

144. Levens, A. S.: Nomography (New York, 1948).

145. Loewinger, E., Gordon, A., Weinreb, A., and J. Gross: J. Appl. Physiol. 19: 1179, 1964.

146. Logan, N. A.: J. Opt. Soc. Amer. 52: 342, 1962.

147. Lothian, G. F. and F. P. Chappel: J. Appl. Chem. 1: 475, 1951.

148. Lothian, G. F. and P. C. Lewis: Nature 178: 1342, 1956.

149. MacRae, R. A., McClure, J. A., and P. Latimer: J. Opt. Soc. Amer. 51: 1366, 1961.

150. Mason, H. S., Kahler, H., MacCardle, R. C., and A. J. Dalton: Proc. Soc. Exp. Biol. Med. 66: 421, 1947.

151. Matthes, K.: Arch. Exp. Path. Pharmakol. 176: 683, 1934.

152. Matthes, K.: Arch. Exp. Path. Pharmakol. 179: 698, 1935.

153. Matthes, K. and F. Gross: Arch. Exp. Path. Pharmakol. 191: 369, 1939.

154. Matthes, K. and F. Gross: Arch. Exp. Path. Pharmakol. 191: 381, 1939.

155. Matthes, K. and F. Gross: Arch. Exp. Path. Pharmakol. 191: 391, 1939.

156. Matthes, K. and I. Schleicher: Z. Ges. Exp. Med. 105: 755, 1939.

157. McGregor, M., Sekelj, P. and W. Adam: Circ. Res. 9: 1083, 1961.

158. Mees, C. E. K.: Theory of the Photographic Process (New York, MacMillan, 1942).

159. Meldahl, K. F., and S. L. Ørskov: Skand. Arch. Physiol. 83: 266, 1940.

160. Merkelbach, O.: Schweiz. Med. Wschr. 65: 1142, 1935.

161. Michaelis, L. and S. Granick: J. Amer. Chem. Soc. 67: 1212, 1945.

162. Middleton, W. E. K.: Vision through the Atmosphere (Toronto, The University of Toronto Press, 1952).

163. Mie, G.: Ann. Phys. 4te Folge 25: 377, 1908.

164. Millikan, G. A.: J. Physiol. 79: 152, 1933.

165. Millikan, G. A.: Rev. Sci. Instrum. 13: 434, 1942.

166. Milnor, W. R., Talbot, S. A., McKeever, W. P., Marye, R. B., and E. V. Newman: Circ. Res. 1: 117, 1953.

167. Nahas, G. G.: Amer. J. Physiol. 163: 737, 1950.

168. Nahas, G. G.: Science 113: 723, 1951.

169. Nahas, G. G.: J. Appl. Physiol. 13: 147, 1958.

170. Nahas, G. G. and R. C. Fowler: Amer. J. Physiol. 159: 582, 1949.

171. Nasse, H.: Pflueger Arch. Ges. Physiol. 16: 604, 1878.

172. Newcomer, H. S.: J. Biol. Chem. 37: 465, 1919.

173. Newton, I.: Opticks, London, 1730, reprinted from the 4th ed. (London, G. Bell and Sons, 1931).

174. Nicholson, J. W., III and E. H. Wood: Amer. J. Physiol. 163: 738, 1950.

175. Nicolai, L.: Pflueger Arch. Ges. Physiol. 229: 372, 1932.

176. Nilsson, N. J.: Pflueger Arch. Ges. Physiol. 263: 374, 1956.

177. Nilsson, N. J.: Physiol Rev. 40: 1, 1960.

178. von Noorden, C.: Z. Physiol. Chem. 4: 9, 1880.

179. Otto, J.: Z. Physiol. Chem. 7: 57, 1882 - 1883; Pflueger Arch. Ges. Physiol. 31: 240, 1883; Pflueger Arch. Ges. Physiol. 36: 12, 1885.

180. Pappenheimer, J. R.: J. Physiol. 99: 283, 1941.

181. Polanyi, M. L. and R. M. Hehir: Rev. Sci. Instrum. 31: 401, 1960.

182. Rawson, R. A.: Am. J. Physiol. 138: 708, 1942 - 1943.

183. Rayleigh, J. W. Strutt, 3d Baron: Philosoph. Mag. 41: 447, 1871.

184. Refsum, H. E.: Scand. J. Clin. Lab. Invest. 9: 190, 1957.

185. Refsum, H. E. and B. Hisdal: Scand. J. Clin. Lab. Inves. 10: 439, 1958.

186. Refsum, H. E. and S. L. Sveinsson: Scand. J. Clin. Lab. Invest. 8: 67, 1956.

187. Reichert, E. T. and A. P. Brown: Carnegie Inst. of Washington, Publication No. 116, 1909.

188. Ritter, J. W.: cited by Harrison, Lord, and Loofbourow (88).

189. Roddie, I. C., Shepperd, J. T., and R. F. Whelan: Brit. Heart J. 19: 516, 1957.

190. Rodrigo, F. A.: Amer. Heart J. 45: 809, 1953.

191. Roos, A. and J. A. Rich: J. Lab. Clin. Med. 40: 431, 1952.

192. Roughton, F. J. W., Darling, R. C., and W. S. Root: Amer. J. Med. Sci. 208: 132, 1944.

193. Ryde, J. W.: Proc. Roy. Soc. (London) A 131: 451, 1931.

194. Sabiston, D. C., Khouri, E. M., and D. E. Gregg: Circ. Res. 5: 125, 1957.

195. de Saint Martin, L. G.: Spectrophotométrie du Sang, Paris, 1898; cited by Newcomer (172).

196. Salmon, P., Stish, R., and M. B. Visscher: J. Appl. Physiol. 18: 739, 1963.

197. Sannié, C., Amy, L., and J. M. Sarrat: Rev. d'Optique 16: 86, 1937.

198. Saunderson, J. L.: J. Opt. Soc. Amer. 32: 727, 1942.

199. Schuster, A.: Astrophys. J. 21: 1, 1905.

200. Scott, P. H., Clark, G. C., and C. M. Sliepcevich: J. Phys. Chem. 59: 849, 1955.

201. Sekelj, P.: Amer. Heart J. 48: 746, 1954.

202. Sekelj, P. and A. L. Johnson: J. Lab. Clin. Med. 49: 465, 1957.

203. Sekelj, P., Johnson, A. L., Hoff, H. E., and M. Pratt Schuerch: Amer. Heart J. 42: 826, 1951.

204. Sheppard, S. E. and A. L. Geddes: J. Amer. Chem. Soc. 66. 1995, 1944.

205. Sheppard, S. E. and A. L. Geddes: J. Amer. Chem. Soc. 66: 2003, 1944.

206. Shibata, K.: J. Biochem. 45: 599, 1958.

207. Shibata, K., Benson, A. A., and M. Calvin: Biochim. Biophys. Acta 15: 461, 1954.

208. Sidwell, A. E., Jr., Munch, R. H., Guzman Barron, E. S., and T. R. Hogness: J. Biol. Chem. 123: 335, 1938.

209. Siggaard Andersen, O., Jørgensen, K., and N. Naeraa: Scand. J. Clin. Lab. Invest. 14: 298, 1962.

210. Silberstein, L.: Philosoph. Mag. 4: 1291, 1927.

211. Sinclair, D.: J. Opt. Soc. Amer. 37: 475, 1947.

212. Sinclair, J. D., Sutterer, W. F., Fox, I. J., and E. H. Wood: J. Appl. Physiol. 16: 669, 1961.

213. Smart, C., Jacobsen, R., Kerker, M., Kratohvil, J. P., and E. Matijević: J. Opt. Soc. Amer. 55: 947, 1965.

214. Soret, J. L.: Arch. Sci. Phys. Nat. 61: 322, 1878; cited by Newcomer (172).

215. Squire, J. R.: Clin. Sci. 4: 331, 1940.

216. States, M. N. and J. C. Anderson: J. Opt. Soc. Amer. 32: 659, 1942.

217. Steele, F. A.: Paper Trade J. 100: 37, 1935.

218. Stewart, G. N.: J. Physiol. 15: 1, 1894; J. Physiol. 22. 159, 1897 - 1898; Amer. J. Physiol. 58: 20, 1921; Amer. J. Physiol. 58: 278, 1921.

219. Stott, F. D.: J. Sci. Instrum. 30: 120, 1953.

220. Sumpner, W. E.: Phys. Soc. Proc. 12: 10, 1892; cited by Walsh (241).

221. Taylor, M.: Aust. J. Exp. Biol. 33: 1, 1955.

222. Taylor, S. H. and J. P. Shillingford: Brit. Heart J. 21: 497, 1959.

223. Taylor, S. H. and J. M. Thorp: Brit. Heart J. 21: 492, 1959.

224. Tsao, M. U., Sethna, S. S., Sloan, C. H., and L. J. Wyngarden: J. Biol. Chem. 217: 479, 1955.

225. Twersky, V.: J. Res. NBS 64D: 715, 1960.

226. Twersky, V.: J. Math. Phys. 3: 700, 1962.

227. Twersky, V.: J. Math. Phys. 3: 724, 1962.

228. Twersky, V.: J. Opt. Soc. Amer. 52: 145, 1962.

229. Twersky, V.: in Kerker, M., ed., Interdisciplinary Conference on Electromagnetic Scattering; Potsdam, New York, 1962 (a Pergamon Press Book, New York, MacMillan, 1963), p. 523.

230. Twersky, V.: in Proc. of Symposia in Applied Math. (Providence, R. I., Amer. Math. Soc., 1964), vol. 16, p. 84.

231. Twersky, V.: Personal communication.

232. Van de Hulst, H. C.: Light Scattering by Small Particles (New York, John Wiley & Sons, 1957).

233. Van de Hulst, H. C.: in Kerker, M., ed., Interdisciplinary Conference on Electromagnetic Scattering; Potsdam, New York, 1962 (a Pergamon Press Book, New York, MacMillan, 1963), p. 583.

234. Van Slyke, D. D.: J. Biol. Chem. 33: 127, 1918.

236. Van Slyke, D. D., Hiller, A., Weisiger, J. R., and W. O. Cruz: J. Biol. Chem. 166, 121, 1946.

237. Van Slyke, D. D. and J. M. Neill: J. Biol. Chem. 61: 523, 1924.

238. Vierordt, K.: Die Anwendung des Spectralapparates zur Photometrie der Absorptionsspectren und zur quantitativen chemischen Analyse, Tübingen, 1873; cited by Welker and Williamson (245).

239. Vierordt, K.: Die quantitative Spektralanalyse in ihrer Anwendung auf Physiologie, Chemie und Technilogie, Tübingen; cited by Drabkin (47).

240. da Vinci, Leonardo: Treatise on Painting, Paris, 1661, McMahon, A. P., tr., (Princeton, N. J., Princeton University Press, 1956), vol. 1.

241. Walsh, J. W. T.: Photometry (3d ed.; London, Constable & Co., 1958).

242. Ware, P. F., Polanyi, M. L., Hehir, R. M., Stapleton, J. F., Sanders, J. I., and S. L. Kocot: J. Thorac. Cardiov. Surg. 42: 580, 1961.

243. Weaver, K. S.: J. Opt. Soc. Amer. 40: 524, 1950.

244. Wever, R.: Pflueger Arch. Ges. Physiol. 259: 97, 1954.

245. Welker, W. H. and C. S. Williamson: J. Biol. Chem. 41: 75, 1920.

246. Winegarden, H. M. and H. Borsook: J. Cell. Comp. Physiol. 3: 437, 1933.

247. Wolfe, R. N., DePalma, J. J., and S. B. Saunders: J. Opt. Soc. Amer. 55: 956, 1965.

248. Wollaston, W. H.: cited by Harrison, Lord, and Loofbourow (88).

249. Wood, E. H.: in Glasser, O., ed., Medical Physics (Chicago, Year Book Publishers, 1950), vol. 2, p. 664.

250. Wood, E. H. and J. E. Geraci: J. Lab. Clin. Med. 34: 387, 1949.

251. Wood, E. H., Sutterer, W. F., and L. Cronin: in Glasser, O., ed., Medical Physics (Chicago, Year Book Publishers, 1960), vol. 3, p. 416.

252. Woodward, D. H.: J. Opt. Soc. Amer. 54: 1325, 1964.

253. Wurmser, R.: J. Physique 7: 33, 1926.